Entwicklung und Synthese von γ-Sekretase-Modulatoren zur Behandlung von Morbus Alzheimer

Vom Fachbereich Chemie
der Technischen Universität Darmstadt

zur Erlangung des akademischen Grades eines
Doctor rerum naturalium (Dr. rer. nat.)

genehmigte
kumulative Dissertation

vorgelegt von
Dipl.- Biochem. Nicole Höttecke
aus Lippstadt

Referent: Prof. Dr. Boris Schmidt
Korreferent: Prof. Dr. Harald Kolmar
Korreferent: PD Dr. Andreas Ludwig (RWTH Aachen)

Tag der Einreichung: 16. Dezember 2009
Tag der mündlichen Prüfung: 08. Februar 2010

Darmstadt 2010
D17

Die vorliegende Arbeit wurde unter der Leitung von Herrn Prof. Dr. Boris Schmidt am Clemens Schöpf-Institut für Organische Chemie und Biochemie der Technischen Universität Darmstadt von Oktober 2006 bis Dezember 2009 angefertigt.

Teile dieser Arbeit sind bereits veröffentlicht oder zur Veröffentlichung eingereicht:

1) Stefanie Baumann, Nicole Höttecke, Boris Schmidt, "γ-Secretase as a target for AD", *in* Medicinal Chemistry of Alzheimer Disease, ed. A. Martinez, Research Signpost, **2008**.

2) Nicole Höttecke, Stefanie Baumann *Bioforum* **2008**, *6*, 32-34.
"Alzheimer-Demenz: Ein Pla(qu)e mit Hoffnung auf Besserung?"

3) Nicole Höttecke, Stefanie Baumann, Ali Taghavi, Hannes A. Braun and Boris Schmidt, "Drug Development and Diagnostics for Alzheimer's Disease Up to 2008", *in* Frontiers in Medicinal Chemistry Vol. 4, Ed.: Atta-ur-Rahman, A.B. Reitz, pp. 730-766, Bentham Books **2009**.

4) Stefanie Baumann, Nicole Höttecke, Robert Schubenel, Karlheinz Baumann, Boris Schmidt *Bioorg. Med. Chem. Lett.* **2009**, *19*, 6986-6990.
"NSAID-derived γ-secretase modulators. Part III: Membrane anchoring."

5) Jessica Pruessmeyer, Christian Martin, Franz M. Hess, Nicole Schwarz, Sven Schmidt, Tanja Kogel, Nicole Hoettecke, Boris Schmidt, Antonio Sechi, Stefan Uhlig, Andreas Ludwig *J. Biol. Chem.* Zur Publikation angenommen. (http://www.jbc.org/cgi/doi/10.1074/jbc.M109.059394)
"The disintegrin and metalloproteinase 17 (ADAM17) mediates inflammation-induced shedding of syndecan-1 and -4 by lung epithelial cells."

6) Nicole Höttecke, Andreas Ludwig, Sabine Foro, Boris Schmidt *Neurodegener. Dis.*, Zur Publikation angenommen: 09.12.09. "Improved synthesis of the ADAM10 inhibitor GI254023X."

7) Nicole Höttecke, Matthias Gralle, Maria Angela C. Dani, Karlheinz Baumann, Fred Wouters, Christian Czech, Boris Schmidt *Nature Chem. Biol.*, eingereicht. "The Modulation of Aβ production involves dimerization of APP."

8) Nicole Höttecke, Miriam Liebeck, Karlheinz Baumann, Robert Schubenel, Edith Winkler, Harald Steiner, Boris Schmidt *ChemMedChem*, eingereicht: 02.12.09. "Inhibition of γ-secretase by the CK1 inhibitor IC261 does not depend on CK1."

9) Nicole Höttecke, Andrea Zall, Daniel Kieser, Eva Fuchs, Katrin Schneider, Dirk Steinbacher, Robert Schubenel, Karlheinz Baumann, Boris Schmidt *J.Med.Chem.*, wird im Januar 2010 eingereicht. "NSAID-derived γ-secretase modulators: PartIV: The isosteric replacement of a carboxylic acid on a carbazole scaffold."

Danken möchte ich:

Prof. Dr. Boris Schmidt für die interessante Themenstellung, die Unterstützung und Hilfestellungen während dieser Arbeit. Die zahlreichen Hilfestellungen und die vielen interessanten fachlichen Diskussionen konnten diese Arbeit erst ermöglichen.

PD Dr. Andreas Ludwig für die Finanzierung und Unterstützung während der Synthese des ADAM10 Inhibitors.
Prof. Dr. Kolmar für die Bereitschaft als Korreferent zu fungieren. Und seiner Arbeitsgruppe für die gemessenen HPLCs

Dem BMBF, DFG, TU Darmstadt und RWTH Aachen für die Finanzierung dieser Arbeit.

Meinen Kollegen Steffi, Daniel, Andrea, Thomas, Fabio, Alex, Estella, Azadeh und Ali die immer ein offenes Ohr hatten und mir immer helfend zur Seite gestanden haben. Ohne das gute Verhältnis wären es lange drei Jahre geworden. Meinen Studenten Mille, Katrin, Dirk, Stefan und Norman für eine tolle und lustige Zeit im Labor und deren guten Ergebnisse.
Meinen Kooperationspartnern von Hoffmann-LaRoche Dr. Karlheinz Baumann und Dr. Christian Czech für die Beantwortung all meiner Fragen während meines Aufenthaltes in Basel und der Testung der Substanzen. Robert Schubenel für die tollen zwei Wochen in Basel und die Durchführung des Assays für all unsere Verbindungen.

Der analytischen Abteilung der TU Darmstadt:
Frau Rudolf und Frau Sahinalp für das schnelle Anfertigen der Massenspektren.
Dr. Meusinger, Herrn Runzheimer und Frau Jungk für die schnelle Messung der NMR Aufträge.
Frau Foro für die Durchführung und Auswertung der Röntgenstrukturanalyse sowie der Bestimmung der Elementaranalysen.

Meiner Familie und Freunden für die immerwährende Unterstützung und Aufbauhilfen während dieser Zeit.
Meinem Freund Uwe für die vielen gefahrenen Kilometer während dieser Zeit. Seine uneingeschränkte Unterstützung in jedem Bereich meines Lebens war mir immer eine wichtige Stütze.

Inhaltsverzeichnis:

Abkürzungsverzeichnis:

Aβ	amyloides-β-Peptid
Abb.	Abbildung
AChE	Acetylcholinesterase Hemmer
AD	Alzheimer-Demenz
ADAM	*A disintegrin and metalloproteinase protease*
Ala, A	Alanin
Aph-1	*anterior pharynx defective-1*
APP	amyloides Vorläuferprotein
Arg, R	Arginin
AS	Aminosäuren
Asn, N	Asparagin
Asp, D	Asparaginsäure
BACE	*β-site APP-cleavinge enzyme*
bzw.	beziehungsweise
COX-1	Cyclooxygenase-1
CR	Cystein reiche- Domäne
CSF	*cerebrospinal fluid*
CT	cytoplasmatische Domäne
CTF	*C*-Terminales-Fragment
Cys, C	Cystein
d	Tag
Dis	Disintergrin-Domäne
ED	EGF-*like*- Domäne
et al.	Et alia
FAD	familiäre Alzheimer-Demenz
FDA	*Food and Drug Administration*
Gln, Q	Glutamin
Glu, E	Glutaminsäure
Gly, G	Glycin
GSI	γ-Sekretase-Inhibitor
GSM	γ-Sekretase-Modulator
h	Stunde
HEK	*Human Embryonic Kidney*
His, H	Histidin
HTS	*high-throughput-screening*
IC_{50}	mittlere inhibitorische Konzentration
Ile, I	Isoleucin
kDa	Kilodalton
kg	Kilogramm
Leu, L	Leucin
Lys, K	Lysin
MCT1	Monocarboxylat-Transporter 1

Met, M	Methionin
mg	Milligramm
MMP	Metalloproteinase
MP	Metalloproteinase- Domäne
Nct	Nicastrin
NFTs	Neurofibrilläre Bündel
NGF	Nervenwachstumsfaktor
NMDA	*N*-Methyl-D-Aspartat
NSAIDs	Nichtsteroidale Antirheumatika
NTF	*N*-terminales-Fragment
PDB	Proteindatenbank
Pen-2	*presenilin enhancer-2*
Phe, F	Phenylalanin
PHF	*paired helical filament*
Pro	Propeptid-Domäne
Pro, P	Prolin
PS	Präsenilin
rf	refluxieren
RIP	*Regulated Intra-membrane Proteolysis*
rt	Raumtemperatur
SAR	Struktur-Aktivitäts-Analyse
Ser, S	Serin
SPP	Signalpeptidase
SVMP	*snake venom* Metalloproteinase
Tg	transgen
Thr, T	Threonin
TMD	Transmembran-Domäne
TNFα	Tumornekrosefaktor-α
Trp, W	Tryptophan
Tyr, Y	Tyrosin
Val, V	Valin
x	variable Aminosäure
z.B.	zum Beispiel
Zn	Zink
ZNS	Zentrales Nervensystem

1. Einleitung

1.1 Alzheimer-Demenz

Die Alzheimer-Demenz (AD) ist die am häufigsten vorkommende Form der Demenz und eine verheerende Krankheit, da sie den Betroffenen das Erinnerungsvermögen raubt und mit starken Persönlichkeitsveränderungen verbunden ist. Die Alzheimerkrankheit wurde zum ersten Mal 1906 von Alois Alzheimer als eine „krankhafte Veränderung der Gehirnrinde“ beschrieben. [1-3] In diesen Veränderungen wurden zwei verschiedene Proteinablagerungen identifiziert: extrazelluläre, amyloide Plaques und intrazelluläre, neurofibrilläre Bündel (NFTs) (Abb. 1).

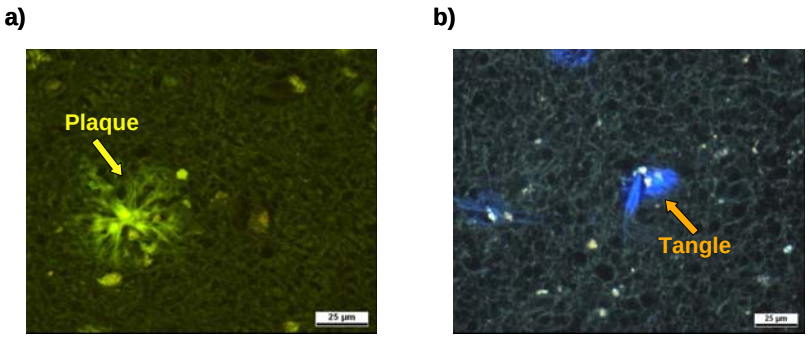

Abb. 1: Histologische Färbungen der **a)** extrazellulären amyloiden Plaques und **b)** intrazellulären neurofibrillären Bündeln, welche als pathologische Ursache der Alzheimer-Demenz angesehen werden. Diese Färbungen wurden in Kooperation mit dem Klinikum Darmstadt angefertigt.

Ein großes Problem stellt die Diagnose von AD dar, da es schwierig ist die Symptome von „normaler“ Vergesslichkeit älterer Menschen zu unterscheiden. Zuverlässig kann die Diagnose Alzheimer-Demenz erst bei einer Autopsie bestätigt werden durch die AD-typische Hirnatrophie und histologischem Nachweis der Plaques und NFTs in der Hirnregion Ammonshorn. Ist die Diagnose gestellt, gibt es verschiedene Ansätze für eine Behandlung, welche jedoch nur die Symptome verbessern, aber nicht die Krankheit selbst heilen können. Verschiedene Wirkstoffklassen werden derzeit auf ihre Wirksamkeit zur Behandlung von AD untersucht, wie zum Beispiel Acetylcholinesterase-Hemmer (AChE), Agonisten der nikotinergen und muskarinergen Rezeptoren, Antioxidantien, Aktivatoren des Neurotrophin-Signalweges, sowie die Verabreichung des Nervenwachstumsfaktors (NGF). Ebenso werden entzündungshemmende Medikamente wie Cyclooxygenase-1 (COX-1) oder COX-2 Inhibitoren untersucht, da Entzündungsvorgänge im Gehirn von AD-Patienten beobachtet werden. Aus dem großen Forschungsinteresse resultieren weltweit bisher etwa 50 Wirkstoffkandidaten für die AD-Therapie und über 500 für Neurodegenerative Erkrankungen im Allgemeinen. Verschiedene Wirkstoffe befinden sich derzeit im fortgeschrittenen Stadium

der Entwicklung, wie z.B. AChE Inhibitoren, NMDA (*N*-Methyl-D-Aspartat) Rezeptor-Antagonisten oder Serotonin-Rezeptor-Agonisten. Außerdem gibt es verschiedene Ansätze zur Immunisierung (z.B. Elan, *Cytos Biotechnology*).[4] Bis 2001 wurde die Bildung von Plaques als die wichtigste Ursache von AD angesehen und somit war bis zu diesem Zeitpunkt deren Reduktion das Hauptziel in der AD-Forschung. Heute werden jedoch zum einen aus Tau Protein bestehende *paired helical filaments* (PHFs) und zum anderen lösliches Aβ (amyloides-β-Peptid) und deren frühen Oligomere als pathologische Ursache angesehen. Durch die Gabe von AChE Inhibitoren wie Galantamin (**1**), Tacrin (**2**), Donepezil (**3**) oder Rivastigmin (**4**) wurden leichte Verbesserungen der kognitiven Fähigkeiten von Patienten in einem frühen Stadium von AD beobachtet (Abb. 1). Diese Inhibitoren verhindern den Abbau des Neurotransmitters Acetylcholin, welcher bei Alzheimer-Patienten nicht mehr gebildet wird. Durch den Acetylcholin-Mangel wird die Übermittelung von Informationen im Gehirn zunächst nur verringert, aber letzten Endes ganz verhindert, was zu einem Absterben der Zellen durch programmierten Zelltod (Apoptose) führt und es resultiert eine AD typische Gehirnatrophie. Die Therapie mit AChE Inhibitoren kann jedoch nur die Symptome im frühen Stadium der Krankheit verringern, die Krankheit selbst jedoch nicht heilen.

Der NMDA-Rezeptor-Antagonist Memantin (**5**) lässt den Eintritt von Ionen in die Zelle wieder zu und hebt somit die schädliche Wirkung des Neurotransmitters Glutamat auf, welche zum Absterben von Nervenzellen führt (Abb. 2). Verbindung **5** wurde als erstes Medikament seiner Klasse für mittlere bis schwere Fälle von AD im Jahre 2002 zugelassen. Aber nichts desto trotz gibt es noch kein Medikament, welches AD heilen kann.

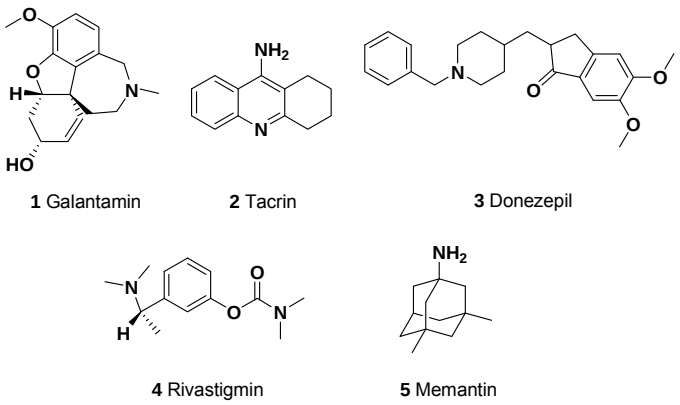

Abb. 2: Wirkstoffe, die derzeit für eine symptomatische Behandlung der Alzheimer-Demenz angewendet werden.

1.1.1 APP Metabolismus

Die Plaques bestehen aus dem amyloiden-β-Peptid (Aβ), welches durch einen „falschen“ Abbau des membranständigen, amyloiden Vorläuferproteins *(*APP) gebildet wird. APP kann auf zwei verschiedenen Wegen abgebaut werden: 1) über den „normalen“, nicht-amyloidogenen Weg und 2) über den amyloidogenen Weg, welcher für die Bildung des pathogenen Aβ verantwortlich ist. (Abb. 3)

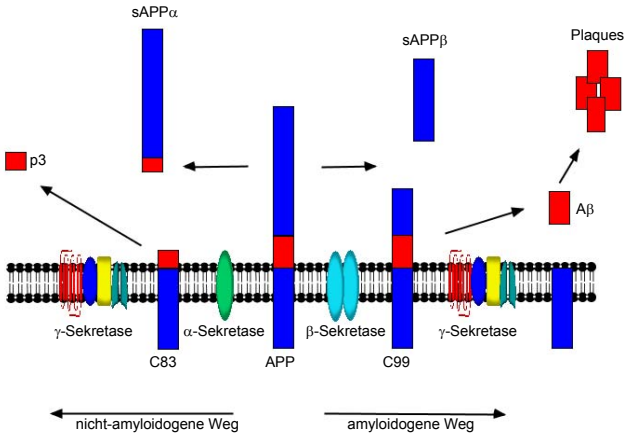

Abb. 3 Abbau des Transmembranproteins APP durch β- und γ-Sekretase führt zu amyloiden Plaques.

Bei dem nicht-amyloidogenen Weg, der bei gesunden Menschen einen Anteil von etwa 90% ausmacht, wird APP zunächst von der α-Sekretase, einer membrangebundenen Metalloprotease, in der Aβ-Sequenz geschnitten, was zu dem löslichen Fragment sAPPα und dem membrangebundenen Fragment C83 führt.[5] Bei anschließender Spaltung von C83 durch die γ-Sekretase, einer membrangebundenen Aspartylprotease, wird das nicht zur Aggregation neigende Peptid p3 freigesetzt. Wird APP jedoch sequentiell von den beiden Aspartylproteasen β- und γ-Sekretase abgebaut, dann entsteht pathogenes Aβ. Die β-Sekretase (*β-site APP-cleavinge enzyme* oder BACE-1) generiert ein extrazelluläres Fragment (sAPPβ) und ein intrazelluläres, membrangebundenes Fragment C99, aus dem nach Spaltung durch die γ-Sekretase Aβ-Peptide unterschiedlicher Länge entstehen. Die häufigsten Aβ-Peptide sind $Aβ_{38}$, $Aβ_{40}$ und $Aβ_{42}$, welche aus 38, 40 bzw. 42 Aminosäuren (AS) bestehen.[6] Für die Aggregation gilt: je länger ein Aβ-Fragment ist, desto besser und schneller kann es sich zusammenlagern. Hierbei werden besonders die frühen Oligomere von aggregiertem Aβ als pathologische Ursache angesehen, woraus folgt, dass die Bildung von $Aβ_{38}$ eher unbedenklich und $Aβ_{42}$ toxisch ist. Um die Entstehung von Aβ zu verhindern, könnte nun z.B. die α-Sekretase aktiviert oder die β- bzw. γ-Sekretase inhibiert werden. Da

die α-Sekretase bei diversen Entzündungsmechanismen eine wichtige Rolle spielt, ist eine Aktivierung mit Risiken behaftet. Die β-Sekretase *(β-site APP-cleaving enzyme*, BACE) existiert in zwei Isoformen BACE-1 und 2, welche eine wichtige Rolle in der Myelinisierung von Nervenzellen übernehmen,[3] die jedoch in AD-Patienten weitgehend abgeschlossen ist. Bisher konnten aber nur wenige oral verfügbare und damit für klinische Studien geeignete Inhibitoren erhalten werden. Auch eine vollständige Inhibition der γ-Sekretase würde, ähnlich wie bei BACE, unerwünschte Nebenwirkungen verursachen. Neben APP spaltet die γ-Sekretase nämlich weitere Transmembranproteine vom Typ-1 wie Notch, welches für die Zellproliferation und -differenzierung notwendig ist, sowie *E*- und *N*-Cadherin, CD44, ErbB4, LRP und Nectin-1.[7] Diese unerwünschte Totalinhibition kann jedoch durch eine allosterische Regulation umgangen werden. So genannte γ-Sekretase-Modulatoren (GSM) regulieren den APP-Metabolismus derart, dass vermehrt $A\beta_{38}$ und weniger pathologisches $A\beta_{42}$ gebildet wird. Aus diesem Grund ist die Modulation der γ-Sekretase ein interessantes Ziel in der Therapie der Alzheimer-Demenz.

1.2 γ-Sekretase

Die γ-Sekretase ist ein membranständiger Enzymkomplex, der aus vier Proteinen zusammengesetzt ist: Präsenilin (PS), Nicastrin (Nct), *anterior pharynx defective-1* (Aph-1) und *presenilin enhancer-2* (Pen-2).[8] (Abb. 4) Jedes dieser Proteine in dem Enzymkomplex ist für die Aktivität notwenig, da nur der komplette Enzymkomplex Aktivität zeigt.

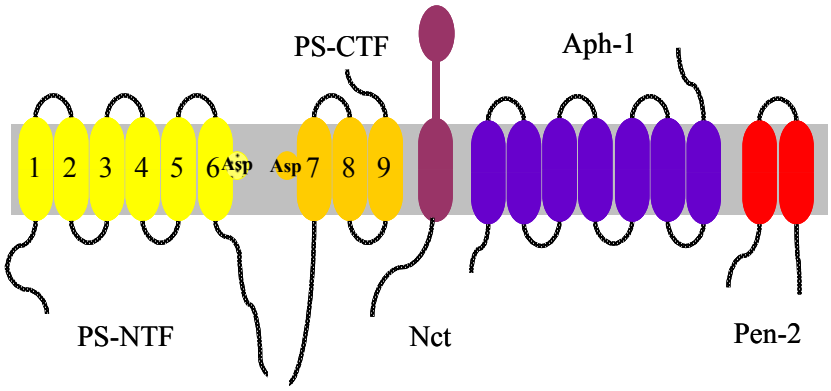

Abb. 4: Der membrangebundene Enzymkomplex der γ-Sekretase besteht in der aktiven Form aus vier Untereinheiten, welche alle für die Aktivität des Enzyms wichtig sind.

Die beiden Präseniline (PS1 und PS2) kontrollieren die Aktivität der γ-Sekretase und Mutationen in den codierenden Genen auf Chromosom 14 bzw. 1 führen zu familiären, d.h. vererbbaren Formen der AD (FAD). Die γ-Sekretase Aktivität hingegen beruht zum größten Teil auf der Aktivität von PS1.[9-10] Diese membranständige Aspartylprotease besteht aus 9 Transmembrandomänen (TMD) und zwei Aspartaten, welche als katalytisches Homodimer agieren und sich auf den Transmembrandomänen 6 (Asp^{257}) und 7 (Asp^{385}) befinden.[11-12] Mutationen dieser beiden AS in Mäusen hatten einen kompletten Aktivitätsverlust der γ-Sekretase zur Folge.[13] Obwohl PS für die Aktivität der γ-Sekretase verantwortlich ist, führte eine Überexpression von PS zu keinem erhöhten Level der Spaltprodukte NTF bzw. CTF (*N*-terminale bzw. *C*-terminale Fragmente), die für die Aktivität der γ-Sekretase notwendig sind.[14] Es muss somit eine Aktivierung von dem, als Holoprotein vorliegenden PS durch zusätzliche Untereinheiten (Nct, Aph-1, Pen-2) erfolgen, die Endoproteolyse. Diese wird durch einen Schnitt in dem großen cytoplasmatischen Loop zwischen TMD 6 und 7 ausgeführt, was zu dem aktiven Homodimer führt: einem 30 kDa großen NTF und einem 20 kDa großen CTF.[15] Das Verhältnis der Untereinheiten wurde durch Fällung und anschließenden massenspektroskopischen Untersuchungen mit 1:1:1:1 bestimmt (Abb. 4).[16] Nct wurde als erstes Protein aus dem γ-Sekretase-Komplex identifiziert.[17] Es ist ein großes Typ-1 Transmembranprotein (130 kDa), welches in einer „reifen“ und einer „unreifen“ Form

vorliegen kann, die sich durch den Grad der Glykosylierung unterscheiden.[18] Nct besitzt eine große extrazelluläre *N*-terminale und eine kleine intrazelluläre *C*-terminale Domäne. In ihrer nur teilweise glykosylierten, „unreifen" Form kann Nct an das PS-Holoprotein binden und unterstützt deren spätere Endoproteolyse und ist somit wichtig für die γ-Sekretase Aktivität.[19-20] Die große extrazelluläre Domäne ist für die Substraterkennung sowie für den Substrateintritt in den Komplex notwendig, indem es mit dem *N*-Terminus des Substrats interagiert.[19]

Aph-1, ein 30 kDa großes Protein mit 7-Transmembranen-Domänen, welches mit Nct einen Subkomplex bildet, ist für die Stabilisierung des PS-Holoproteins notwendig.[19, 21-22]

Pen-2, ein zwei Membrandomänenprotein mit 101 AS, ist für die Stabilität des PS-Nct Subkomplexes verantwortlich.[23] Seine *C*-terminale Domäne induziert die Entstehung des katalytisch aktiven PS Homodimers, die Endoproteolyse, und stabilisiert anschließend die beiden entstehenden Fragmente (PS-NTF and PS-CTF).[19, 24]

Der Mechanismus für die Zusammenlagerung des γ-Sekretase-Komplexes wurde von Zhou *et al.* durch das folgende Modell vorgeschlagen: Zuerst formt das „unreife" Nicastrin einen Unterkomplex mit Aph-1 welcher in das endoplasmatische Retikulum eintreten soll. Dort wird ein dreigliedriger Übergangszustand mit dem PS-Holoprotein gebildet. In diesem Übergangszustand wird Nct vollständig glykosyliert und gelangt in den Golgi-Apparat. Beim Eintritt von Pen-2 in den Komplex wird die Endoproteolyse von PS induziert wodurch der aktive γ-Sekretase-Komplex vorliegt.[19] Durch die Endoproteolyse liegt das PS als katalytisches Homodimer in Form des NTF und des CTFs vor, welches je ein katalytisch aktives Aspartat trägt. Der Spaltungsmechanismus der γ-Sekretase ist identisch mit dem jeder anderen Aspartylprotease (Abb. 5).[25]

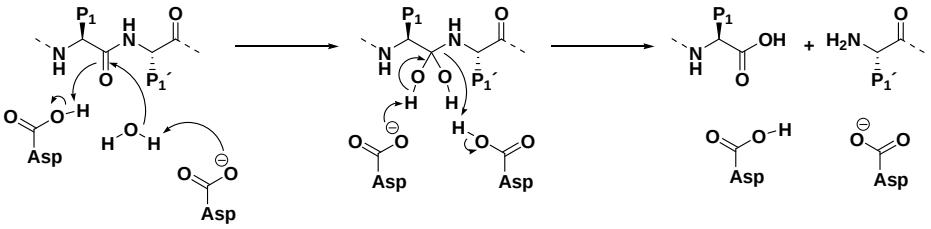

Abb. 5: Spaltungsmechanismus einer Aspartylprotease.

Eine Besonderheit dieses Spaltungsmechanismus ist das Vermögen der γ-Sekretase das Substrat APP in der hydrophoben und daher wasserarmen Membran zu spalten, ein Vorgang der jedoch Wasser benötigt.[26] Dieser Mechanismus wird „*Regulated Intra-membrane*

Proteolysis“ (RIP) genannt und benötigt einen Transport von Wassermolekülen in die hydrophobe Membran, in der wenig Wasser verfügbar ist.[27] Damit die Spaltung auch in der Membran stattfinden kann scheint im Inneren des Komplexes eine hydrophile aktive Tasche vorzuliegen, die das Wasser für die Spaltung des Substrates bereithält.[26, 28]

Es wurden noch weitere Proteine identifiziert die mit dem aktiven γ-Sekretase Komplex assoziiert sind, wie z.B. CD147, das einen regulativen Effekt auf die γ-Sekretase zu haben scheint. Weitere Bindungspartner wurden durch Aufreinigung entdeckt, wie GSK-3, Phospholipase D1 und TMP21.[19, 29]

Da verschieden lange Aβ-Peptide gebildet werden, scheint die γ-Sekretase keine spezielle Sequenz für die Spaltung des Substrates APP zu besitzen. Für das Auftreten der verschiedenen Aβ Spezies wurde von Lichtenthaler *et al.* ein Modell postuliert, in dem das Substrat in α-helicaler Kornformation gespalten wird.[30] Die Windung einer α-Helix setzt sich aus 3.6 Aminosäuren (AS) zusammen, was zur Folge hat, dass sich die AS 40, 43, 46 und 49 auf der einen Seite der α-Helix befinden und 42, 45 und 48 auf der gegenüberliegenden Seite. Abhängig von der Orientierung des Substrates zu dem katalytischen Zentrums des Enzyms entstehen die verschiedenen Aβ Spezies. Das Auftreten von $A\beta_{38}$ zusammen mit $A\beta_{42}$ lässt sich durch die Windung in einer α-Helix von 3.6 AS erklären, wobei hier zum Ausgleich erst nach der vierten AS geschnitten wird. Am häufigsten werden $A\beta_{38}$, $A\beta_{40}$ und $A\beta_{42}$ gebildet, wobei $A\beta_{42}$, welches in Zellen einen Anteil von 5 bis 10% ausmacht, das toxischste ist, da es am meisten zu der Aggregation zu Plaques neigt. Es werden auch Aβ Spezies mit 19, 37, 39 sowie 43 bis 48 AS gebildet, jedoch in so geringem Maße, dass sie keine Rolle in der Pathologie von AD spielen.[31] Es gibt aber bislang keine Präzedenzfälle für die Spaltung α-helicaler Substrate durch Aspartyl-Proteasen.

Multhaup *et al.* beschrieb 2007 einen neuartigen Mechanismus, welcher die Entstehung der verschiedenen Aβ-Spezies erklärt. Sie beschrieben, dass zwei APP-Proteine eine Dimerisierung über die AS Gly^{29} und Gly^{32}, ein GxxxG-Motiv, eingehen und dass diese sterische Barriere die Spaltung durch die γ-Sekretase zu dem unerwünschten, pathologischen $A\beta_{42}$ hin verschiebt (Abb. 6).[32]

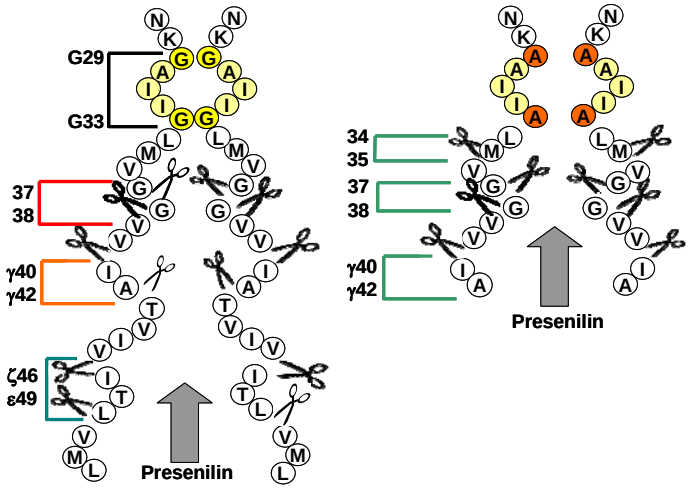

Abb. 6 Dimerisierung des Substrates über das von Multhaup et al. beschriebene GxxxG-Motiv.

Mutationen der beiden Glycine zu Asparagin, G29A und G32A, zeigten wieder einen „normalen“ Abbau von APP zu $A\beta_{38}$, wo hingegen der Austausch durch Isoleucin oder Leucin zu einer drastischen Verringerung von dem $A\beta_{total}$ führt.[33] Es wird vermutet, dass die Aβ-Produktion an die Dimerisierung von C99 gekoppelt ist (Abb. 7). Auch Notch trägt ein solches GxxxG-Motiv, jedoch kann Notch auch als Monomer umgesetzt werden.[34]

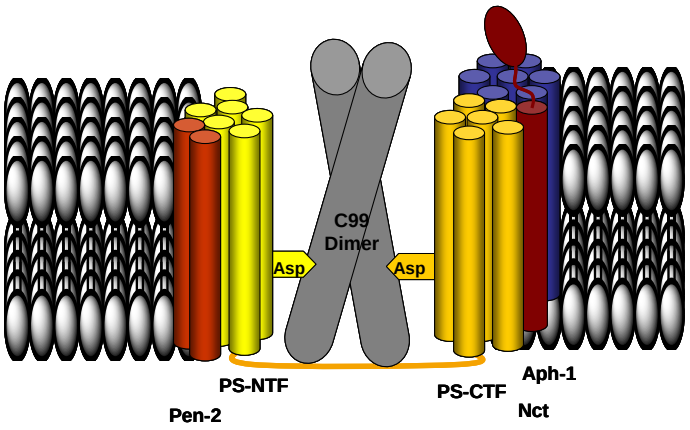

Abb. 7 Schematischer Aufbau des γ-Sekretase-Komplexes und des Substrates C99, welches als Dimer gespalten wird.

1.2.1 Inhibition der γ-Sekretase

Eine Inhibition der γ-Sekretase hat eine Reduktion aller Aβ-Spezies zur Folge, wodurch AD verhindert werden könnte. Eine solche vollständige Inhibition würde aber auch die Spaltungsrate der anderen Substrate mit wichtigen neuronalen Eigenschaften verringern. Die γ-Sekretase scheint durch die große Anzahl an Substraten das „Proteasom der Membran" zu sein, wodurch das Risiko von unerwünschten Nebenwirkungen bei der Inhibition deutlich erhöht wird.[35] Insbesondere ein Eingriff in den Stoffwechselweg von Notch, welches für die embryonale Entwicklung und die Zelldifferenzierung wichtig ist, lassen die γ-Sekretase zu einem anspruchsvollen und schwierigen *Target* für die AD Behandlung werden. Dies wird verdeutlicht durch die Tatsache, dass sich PS -/- Knockout-Mäuse nicht über den Status eines Embryos hinaus entwickelt haben, was jedoch durch einen Einsatz von embryonalen Stammzellen behoben werden konnte.[36] Der intrazelluläre Transport von Notch in die Neuronen des menschlichen ZNS (Zentrales Nervensystem) wird durch eine PS-Inhibition deutlich gesenkt, was zu Einbußen in der neuronalen Morphologie führt. Diese Probleme können von Wirkstoffen mit einem großen therapeutischen Fenster (dem Verhältnis der therapeutischen Dosis, d.h. das Maß der γ-Sekretase Inhibition im Vergleich zu der toxischen Dosis, in diesem Falle der Notch-Inhibiton) umgangen werden.[37] Falls dieses zu klein sein sollte könnten diese Wirkstoffe jedoch noch Anwendungsgebiete in der Tumortherapie und bei Bluthochdruck finden. Neuesten Untersuchungen zur Folge würde aber schon eine 30%ige Reduktion der Aβ-Sekretion eine kognitive Beeinträchtigung verbessern,[38-39] wobei auch eine bis zu 15%ige Inhibition von Notch ohne Nebenwirkungen verlaufen würde.[36, 39]
In den letzten Jahren wurde allerdings der Forschungsschwerpunkt von der Inhibition zu der Modulation der γ-Sekretase gerichtet. Ein Modulator verändert nur den APP Schnitt der γ-Sekretase, um mehr erwünschtes $A\beta_{38}$ und weniger toxisches $A\beta_{42}$ zu generieren, ohne die Spaltung der anderen Substrate zu beeinflussen.
Für die Inhibitoren- bzw. Modulatorenentwicklung wäre eine Röntgenkristallstrukturanalyse des Enzyms nützlich, da sie das strukturbasierte Wirkstoffdesign ermöglichen würde. Es gelang bislang nicht den Komplex zu kristallisieren aufgrund der Membranlokalisation des γ-Sekretase-Komplexes sowie der notwendigen Lipidstabilisierung. Allerdings existiert eine Cryoelektronen-mikroskopische Aufnahme von der γ-Sekretase mit einer Auflösung von 12Å.[39-41] Diese weist auf verschiedene, kleine Vertiefungen in der Oberfläche des Komplexes zu sowohl der cytosolischen als auch der extrazellulären Seite der Membran hin, bei ansonsten gleichmäßiger Oberfläche. Diese Vertiefungen können im Rahmen der Messgenauigkeit als Hohlräume gedeutet werden durch die die entstehenden

Spaltungsprodukte den Komplex verlassen können. Eine große Einhöhlung wird als laterale Eintrittsstelle des Substrates spekuliert.[40-41]

Die meisten selektiven γ-Sekretase Inhibitoren (GSIs) wurden durch Hochdurchsatz-Screenings (*high-throughput-screening*, HTS) identifiziert.[42-43] Es wurden bereits verschiedene Mechanismen für die Inhibition beschrieben.[44] Die meisten GSI binden direkt an das aktive Zentrum oder verändern dieses durch allosterische Wechselwirkungen.[45] Die Bindungsstelle der Sulfonamid abgeleiteten GSIs wurde auf PS1 an den AS Lys^{172}, Tyr^{281} und Lys^{282} identifiziert.[46] Manche Inhibitoren wirken gar nicht direkt auf die γ-Sekretase sondern die Inhibition ist nur eine Begleiterscheinung, wie z.B. bei der Stoffklasse der Isocumarine. Ebenso können Inhibitoren der Signalpeptidase (SPP) auch die γ-Sekretase inhibieren, welche ein ähnliches aktives Zentrum wie SPP zu haben scheint.[47]

1.2.1.1 Peptidische Inhibitoren

Die Entwicklung von GSIs begann mit peptidischen PS1 Inhibitoren wie Mercks L-685,458 (**6**), welcher die γ-Sekretase mit einem IC_{50} von 17 nM inhibiert (Abb. 8).[48] Aufgrund der lipophilen Phenylalanine in der Sequenz von **6** wurde das Vorhandensein einer lipophile Bindungstasche (P2, P1, P1´, P2´, P4´ und P7´) in der Nähe der Schnittstelle angenommen und später durch verschiedene Studien auch belegt.[30] Dieser Befund deutet darauf hin, dass **6** als ein Übergangszustandsanalogon der $A\beta_{40}$- und $A\beta_{42}$-Schnittstelle agiert. (Abb. 8) Durch Biotinylierung (**6**) mit anschließender Photolyse in der Gegenwart von löslicher γ-Sekretase wurde ein 20 kDa großes Fragment mit L-852,505 (**7**) ermittelt, welches durch Antikörper-Nachweis als PS1-CTF identifiziert werden konnte. Photolyse von L-852,646 (**8**), ein Benzophenon-substituiertes L-852,505 Derivat, lieferte interessanterweise das 34 kDa große PS1-NTF, was darauf hindeutet, dass **7** sowohl mit dem PS-NTF als auch dem PS-CTF interagiert.

Ein ähnlicher Übergangszustandsinhibitor III-31-C (**9**), basierend auf einem Hydroxyethylharnstoff-Motiv, zeigt eine Aktivität <300 nM.[49] Durch Immobilisierung von **9** gelang eine Isolierung und Identifizierung der γ-Sekretase Untereinheiten PS-CTF, PS-NTF sowie Nicastrin. Dieses gelang jedoch nur mit dem isolierten Komplex und konnte mit der aktiven Form nicht reproduziert werden. Mit der Hilfe von Brij-35 und dem Detergenz CHAPSO gelang eine Isolierung des aktiven Komplexes, welcher in seiner inhibierten Form erfolgreich zusammen mit seinen Substraten C83 und C99 gefällt werden konnte. Dieses ließ auf weitere Inhibitor-Bindungsstellen schließen, welche sich nicht mit dem aktiven Zentrum überschneiden.

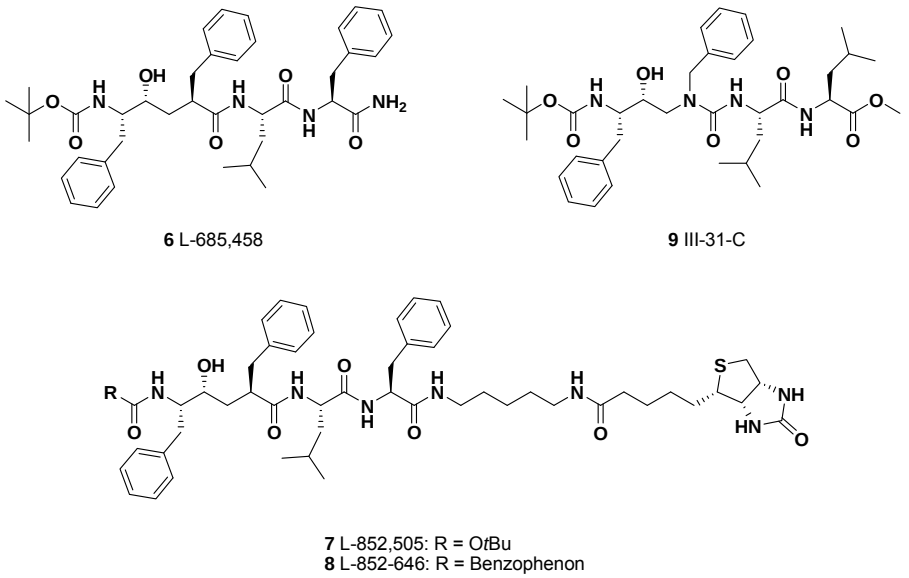

Abb. 8: Peptidische γ-Sekretase-Inhibitoren.

1.2.1.2 Semi-peptidische Inhibitoren

Eine Struktur-Aktivitäts-Analyse des viel versprechenden *N*-Dichlorphenylalanin-Grundgerüstes identifizierte den semi-peptidischen Inhibitor DAPT (**10**). (Abb. 9) Für dessen Aktivität (IC_{50} = 20 nM, in HEK Zellen) ist sowohl das Difluorbenzylessigsäure- als auch das Phenylglycin-Motiv verantwortlich.[50-51] **10** zeigte eine hohe Effizienz *in vivo* nach 3h bei einer Dosis von 100 mg/kg, sowohl bei subkutaner (50% $A\beta_{Kortikal}$-Reduktion) als auch bei oraler (40% $A\beta_{Kortikal}$-Reduktion) Verabreichung.[52] Ein Nachteil ist, dass DAPT die Blut-Hirn-Schranke nicht überwinden kann, was für die Behandlung einer Erkrankung des zentralen Nervensystems (ZNS) als notwendig erachtet wird.[53-55] Tatsächlich wurden im Hirn von Mäusen keine DAPT-Konzentration detektiert. Überraschenderweise konnte aber ein Absetzphänomen (Rebound-Effekt) beobachtet werden, dessen Ursache bisher nicht eindeutig erklärt werden konnte. In einer vorklinischen Studie wurde zusätzlich eine *in vivo*-Toxizität ermittelt, was auf das Eingreifen in den Notch Signalweg zurückzuführen ist. **10** inhibiert den Notch-Signalweg sogar um das 100-1000-fache selektiver als den APP-Abbau, wodurch eine klinische Studie unmöglich wurde. Durch Derivatisierung des DAPT-Grundgerüstes (Einführen eines rotationsgehinderten Caprolactam Gerüstes sowie einer stereoselektiven Einführung einer Hydroxylgruppe) wurde der potente Inhibitor LY-411575 (**11**) bei *in vivo* Untersuchungen identifiziert. **11** zeigte eine 20-fach gesteigerte Aktivität gegenüber DAPT mit einem IC_{50}< 1 nM. Nach oraler Verabreichung des weniger potenten Diastereomers wurde bei einer Dosis von 1 mg/kg eine Halbierung des $A\beta_{Kortikal}$-

und $A\beta_{Plasma}$-Levels nach 3h in Tg2576 Mäusen beobachtet.[56] Die Selektivität von **11** bezüglich des APP Abbaus (IC_{50} ($A\beta_{40}$) = 0.082 nM) und des Notch Abbaus (IC_{50} = 0.39 nM) lässt auf ein kleines therapeutisches Fenster schließen, was eine klinische Studie dieser Stoffklasse eigentlich ausschließt. Eine 15-tägige Studie von dem weniger potenten LY 450139 (**12**), welches aber eine geringfügig verbesserte APP-Selektivität zeigt, in C57BL/6 und TgCRND8 APP überexprimierenden Mäusen bei einer Dosis von 1-10 mg/kg/d zeigte eine Aβ-Reduktion, jedoch wurden als Nebenwirkungen die Rückbildung des Thymus und des Darmepithels beobachtet.[57] Trotz des kleinen therapeutischen Fensters und der beobachteten Nebenwirkungen wurde **12** in einer klinischen Studie getestet. In der Studie IIb, an der sich 51 AD Patienten beteiligten, wurden verschiedene Nebenwirkungen, wie Dünndarmverschluss, blutiger Stuhl und Durchfall beobachtet. Am Ende dieser Studie konnte in keiner der Gruppen eine kognitive oder funktionale Verbesserung festgestellt werden.[58]

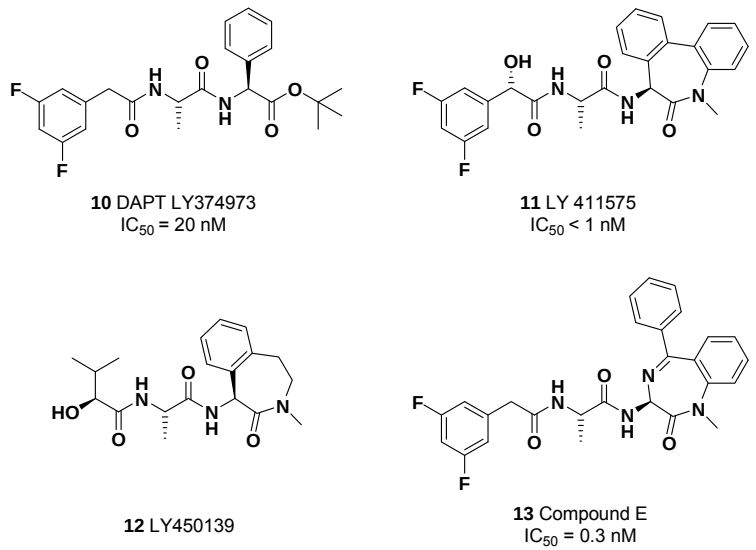

Abb. 9: Semipeptidische γ-Sekretase-Inhibitoren.

Trotz großem Forschungsaufwand bleibt der Inhibitionsmechanismus dieser Stoffklasse noch unklar. Unter anderem wurden auch Photoaffinitätsuntersuchungen mit *cross-linking* Einheiten wie z.B. Benzophenon, Phenyldiazerin und Biotin an **10**, **11** und der potenten Verbindung Compound E (**13**) durchgeführt. Diese reduzierten die Aβ-Sekretion stark und zeigten eine Nähe zum aktiven Zentrum der γ-Sekretase; **10** markierte hierbei das PS-CTF im Gegensatz zu **11** und **13**, welche eher an das PS-NTF binden. Ein kompetitiver Assay von DAPT mit **11** bzw. **13** zeigte jedoch dass die beiden Bindungsstellen sich überlappen. Anscheinend ist der *C*-terminale Teil von **11**/**13** für die Erkennung der Bindungsstelle verantwortlich. Ein weiterer Unterschied ist, dass **11**/**13** ebenso die membranständige

Signalpeptidase (SPP) beeinflussen, welche große Ähnlichkeiten mit der γ-Sekretase hat, im Gegensatz zu **10**.

In einem spekulativen Mechanismus wird vermutet, dass die PS-Bindungstasche dipeptidische Inhibitoren bindet, welche Difluorbenzol-, Phenylglycin- oder Caprolactam-Motive tragen, wobei das Caprolactam-Motiv wohl eher selektiv für die SPP ist. Zuerst scheinen diese Substanzen an die Difluorphenyl-Bindungsstelle auf dem PS zu binden und anschließend wird ein stabiler Komplex ausgebildet. Dieser Komplex ist dann in der Lage auch an die zweite Bindungstasche zu binden, wodurch dann die Aktivität der γ-Sekretase inhibiert wird.[59]

1.2.1.3 Nicht-peptidische Inhibitoren

Neben den peptidischen und semi-peptidischen Inhibitoren wurden verschiedene Grundgerüste als moderate Inhibitoren entdeckt, die ein Sulfonamid-Motiv tragen, wie unter anderen Fenchylamin (**14**) oder das Aminoalkohol-Derivat (**15**). Brystol-Myer Squibb beschrieb potente Acetamid-Derivate, wie BMS-299897 (**16**), die die γ-Sekretase in einem Zellassay im nanomolaren Bereich inhibieren (Abb. 10).[36, 60-61] Im Gegensatz zu den Inhibitoren aus der DAPT-Gruppe konnte mit **16** neben der Verringerung der Aβ-Konzentration im Gehirn auch eine vergleichbare Verringerung im CSF von jungen Mäusen in einer Dosis- und Zeit-abhängigen Weise gezeigt werden. Untersuchungen bezüglich der Inhibition des Notch Signalweges (IC_{50} = 105.9 nM) zeigten eine 15-fach selektivere Inhibition des APP Abbaus (IC_{50} = 7.1 nM). Weitere Untersuchungen zeigten diese gesteigerte Aktivität auch bei Sulfonamiden verschiedener Grundgerüste, wie z.B. dem Tetrahydrochinolin (**17**) ebenso wie bei Sulfon-Grundgerüsten z.B. mit Cyclohexyleinheit, (**18**) die bizyclische Ringe tragen (**19**) oder auch Heterozyklen (**20**).[62-64]

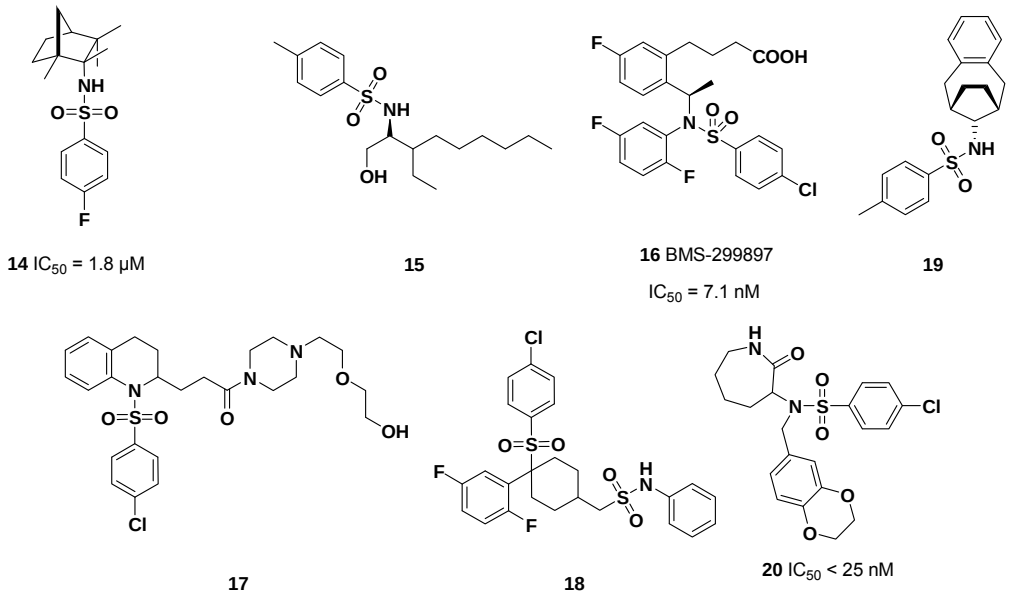

Abb. 10: Nicht-peptidische γ-Sekretase-Inhibitoren.

Gleevec (**21**) war eine der ersten Substanzen, die selektiv nur den APP Abbau inhibieren und Notch auch bei einer >10-fachen Konzentration des IC_{50} für Aβ von ~75 µM nicht beeinflusst.[65] (Abb. 11) Es wird vermutet, dass **21** an der ATP Bindungsstelle bindet, da nach ATP-Verabreichung die Aktivität der γ-Sekretase zurückgewonnen werden konnte. Dieses ist auf die höhere Bindungsaffinität von ATP zurückzuführen, welches Gleevec verdrängt. Aufgrund dieses Befunds wird vermutet, dass die γ-Sekretase mit seinem γ-Phosphatrest an ein Acetamid von ATP bindet.[66]

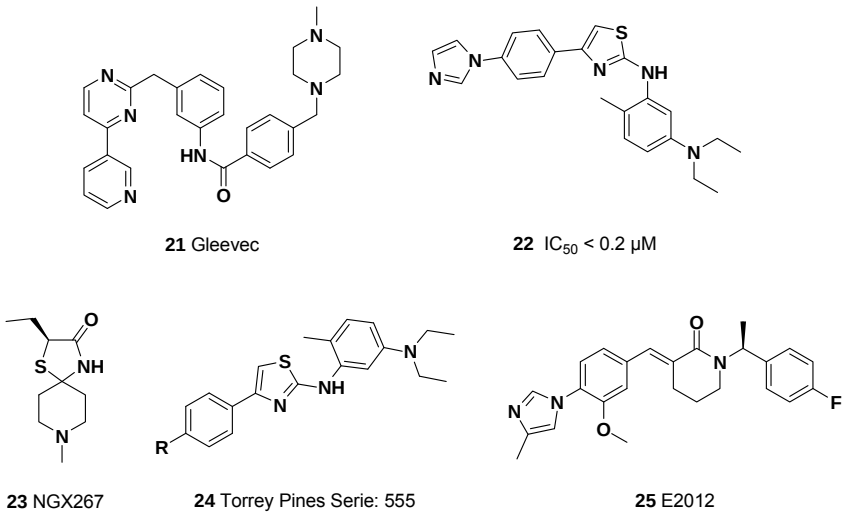

Abb. 11: Selektive Inhibitoren, die nur den APP Abbau durch die γ-Sekretase verhindern und den Abbau der anderen Substrate wie Notch nicht beeinflussen.

Die Strukturklasse der Aminothiazole (z.B. **22**) wurde von Torrey Pines Therapeutics beschrieben, die die $A\beta_{40}/A\beta_{42}$ Bildung mit einer Konzentration von ~30 nM reduzieren konnten.[67] Jedoch wurde nur das Thiazolon-Derivat NGX267 (**23**) soweit entwickelt, dass es in die klinische Testung gebracht werden konnte. Vorklinische Studien deuten auf eine zweifache Wirkung von **23** hin: Zum einen wird der muskarinerge Rezeptor stimuliert, was die Wirkung des Neurotransmitters Acetylcholin nachahmt und so den Mangel kompensiert, der bei AD auftritt. Zum anderen wurde eine $A\beta_{42}$ senkende Aktivität in Mäusen und Hasen ermittelt.[68-69] In der klinischen Phase I wurde eine Doppelblindstudie mit verschiedenen Dosierungen (10 mg, 23 mg, 30 mg, 35 mg) und Placebo mit 90 gesunden Männern im Alter zwischen 18 und 55 durchgeführt. Es konnte eine cholinerge Stimulation ohne nennenswerte Nebenwirkungen beobachtet werden.[70] Die Substanzentwicklung für AD-Therapie wurde 2009 eingestellt.

Zusätzlich zu **23** entwickelte Torrey Pines NGX97555 (keine Struktur veröffentlicht), ebenfalls aus der Serie 555 (**24**), die in einer vorklinischen Studie untersucht wird. Es wird eine allosterische Modulation des γ-Sekretase-Komplexes in SY5Y Zellen vermutet, welche die Schnittstelle von $A\beta_{40}$ (IC_{50} = 64 nM) und $A\beta_{42}$ (IC_{50} = 10 nM) zu $A\beta_{37/38}$ hin verschiebt, ohne Notch-Spaltung oder E-Cadherin-Spaltung zu beeinflussen. Durch diese Eigenschaft kann **24** auch als γ-Sekretase-Modulator eingeordnet werden. Eine 3-Tages Studie in Tg-Mäusen ermittelte eine minimale Dosis für die $A\beta_{42}$-Reduktion mit 25-50 mg/kg.

Zusammen mit Eisai hat Torrey Pines einen weiteren Entwicklungskandidaten in der vorklinischen Studie.[71] E2012 (**25**) zeigte jedoch in einem hochdosierten, 13 wöchigem Untersuchung Nebenwirkungen in Form von Trübungen der Linse in den Augen von Ratten. Dieses hatte zur Folge, dass die FDA die gleichzeitig durchgeführte Phase I Studie im Februar 2007 unterbrochen hat. Im April 2008 wurde diese wieder aufgenommen, nachdem umfangreiche Untersuchungen abgeschlossen waren: Eine 13 wöchige einmalige Verabreichung der höchsten Dosis an Affen; und eine 4-wöchige hochdosierte Verabreichung an Ratten.[70] Ergebnisse aus der klinischen Phase II werden erst im April 2010 erwartet. [1-2]

1.2.2 Modulation der γ-Sekretase

In 2005 beschrieb MerckSharp&Dohme einen selektiven GSM (**26**), welcher eine Carbonsäurefunktion trägt (Abb. 12).[72] Diese Carbonsäure scheint in dieser Modulatorklasse für die Verschiebung der Aβ-Schnittstelle notwendig zu sein. Interessanterweise wurde nur eine Verschiebung in den Aβ-Konzentrationen der verschieden Spezies ermittelt, wodurch der $A\beta_{Total}$-Spiegel unbeeinflusst blieb. Die Notwendigkeit dieser Carbonsäurefunktion wurde später durch weitere Beispiele (z.B. **27**, **28**) bestätigt.[73-75]

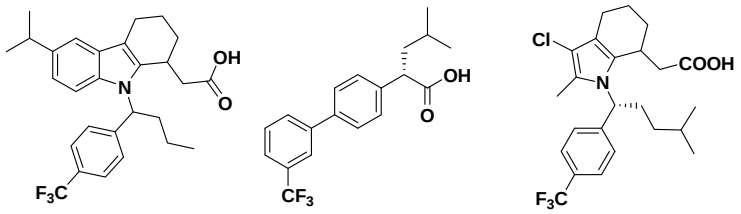

26 **27** **28**

Abb. 12: Modulatoren der γ-Sekretase, die die Aβ-Sekretion vom pathologischen $A\beta_{42}$ verringert und dem unbedenklichen $A\beta_{38}$ erhöht.

1.2.2.1 Nichtsteroidale Antirheumatika

Im Gehirn von AD-Patienten wurden Entzündungsvorgänge sowie deren Mediatoren wie z.B. Cytokine und Chemokine entdeckt.[76] Aufgrund dieser Entdeckung wurden Hypothesen entwickelt, die einen Zusammenhang zwischen den Entzündungsvorgängen und der Alzheimer-Demenz herstellen. Eine dieser Hypothesen schlägt vor, dass die Neurodegeneration in AD erst die Antwort auf die Entzündungen im Gehirn darstellt. Diese Entzündungen sollen erst die Bildung von Plaques und NFTs und die anschließende Aggregation auslösen, welche wiederum eine Immunreaktion auslösen soll. Durch diese Hypothese wären aber chronische Entzündungsvorgänge im Gehirn eine grundsätzliche Vorraussetzung für AD. Genetische Untersuchungen unterstützen diese Hypothese, da Polymorphismus der codierenden Gene von Entzündungsmediatoren wie TNFα (Tumornekrosefaktor-α) oder Interleukinen das Risiko von AD erhöht.[77]

Es konnte gezeigt werden, dass entzündungshemmende Wirkstoffe, die sogenannten nichtsteroidalen Antirheumatika (NSAIDs), wie *R*-Flurbiprofen (**29**), Sulindac-S (**30**) oder Ibuprofen (**31**) den Fortgang von AD hemmen können. (Abb. 13) **29** z.B. zeigt eine selektive $A\beta_{42}$-Sekretion senkende Aktivität (IC_{50} = 34 μM) und erhöht gleichzeitig die nicht-toxische $A\beta_{38}$-Konzentration im Gehirn, wodurch **30** als GSM eingeordnet wird.[78-79] Interessanterweise wurde bei der maximalen, nicht-toxischen Konzentration eine um 70 -80%

verminderte $A\beta_{42}$-Sekretion beobachtet, wobei der $A\beta_{40}$-Spiegel nicht beeinflusst wird. Jedoch zeigen nicht alle dieser NSAIDs eine Modulation. Naproxen (**32**) und Aspirin (**33**) beeinflussen die Aβ-Bildung gar nicht und z.B. Carprofen (**35**) inhibiert die Bildung aller Aβ-Spezies.[78] Untersuchungen in Zellen zeigten, dass die NSAID-abgeleiteten GSMs selektiv den APP-Abbau der γ-Sekretase inhibieren und keinen Effekt auf die anderen Substrate (wie z.B. Notch) der γ-Sekretase ausüben.[78, 80-84]

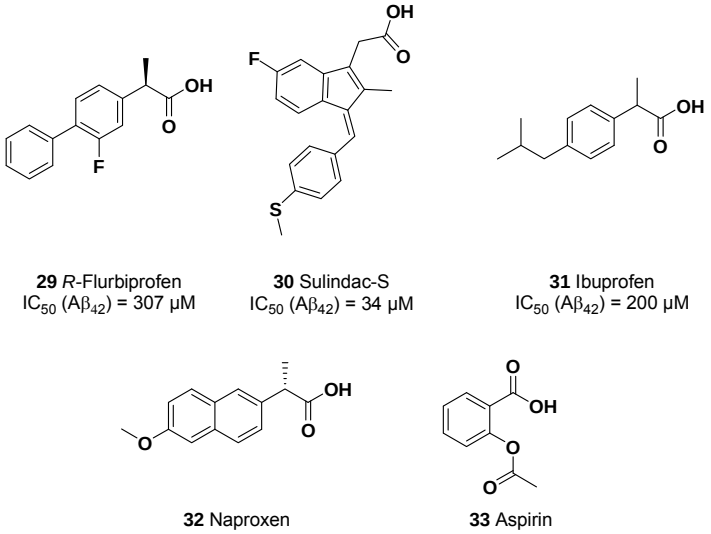

29 *R*-Flurbiprofen
IC_{50} ($A\beta_{42}$) = 307 µM

30 Sulindac-S
IC_{50} ($A\beta_{42}$) = 34 µM

31 Ibuprofen
IC_{50} ($A\beta_{42}$) = 200 µM

32 Naproxen

33 Aspirin

Abb. 13: Ausgewählte NSAIDs beeinflussen die γ-Sekretase in Form von Modulatoren (**29 -31**), was hingegen auf andere Substanzen dieser Klasse nicht zutrifft (**32 -33**).

In einer chronischen Studie mit hochdosiertem Ibuprofen (**31**) über 6 Monaten in Tg2576-Mäusen, wurde eine Reduktion von sowohl den Entzündungsvorgängen als auch der Bildung von Plaques ermittelt.[85] In weiteren Untersuchungen mit Ibuprofen in Tiermodellen konnte eine um 50% verminderte Plaquefläche beobachtet werden, ebenso wie eine um 30- 40% verminderte Aβ-Konzentration.

2008 endete die klinische Phase III Studie des NSAIDs **29** (Flurizan®) ohne signifikante, kognitive Verbesserungen.[58] Es wurde eine relativ hohe Dosierung von 2x 800 mg/d gewählt, da das Überwinden der Blut-Hirn-Schranke und somit die Verfügbarkeit im Gehirn weniger als 5% beträgt.[86]

1.2.3 Vorarbeiten

Photoaffinitätsstudien mit einer GSM-Photoprobe (**34**) des NSAID-Derivats *R*-Flurbiprofen (**29**) zeigten, dass **34** nicht an den γ-Sekretase-Komplex bindet,[87] sondern an das Substrat APP. (Abb. 14) Die Markierung wurde an den Aminosäuren 29 -36 (= 625 -632 APP695) von Aβ lokalisiert, dies entspricht der von Multhaup *et al.* beschriebenen Dimerisierungsregion.[32] Schmidt *et al.* haben GSMs entwickelt, die als Grundgerüst das NSAID Carprofen (**35**) aufweisen, welches selbst ein moderater GSI ist. Für eine Modulation sind zwei Funktionalitäten notwendig: eine Carbonsäure, die vermutlich mit dem Substrat interagiert und ein langer lipophiler Rest, welcher für die Orientierung des Modulators (z.B. **36**) in der Membran verantwortlich zu sein scheint.[88] Des Weiteren gelang der Aktivitäts-Transfer auf Carbazolderivate (**37**), die im Gegensatz zu Carprofen kein stereogenes Zentrum aufweisen und mit einem IC_{50} ($A\beta_{42}$) von 11 µM nahezu equipotent sind.[89]

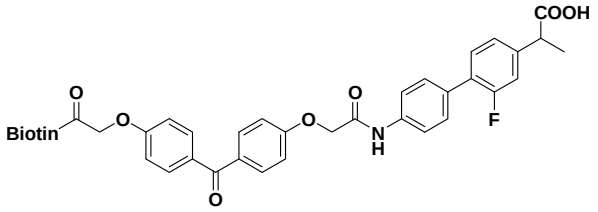

34 Flurbiprofen-Benzophenon-Biotin

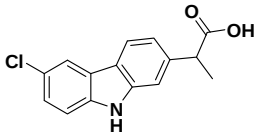

35 Carprofen

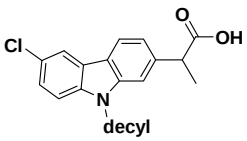

36 BSc3041
IC_{50} ($A\beta_{42}$) = 3 µM

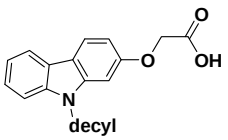

37 BSc3032
IC_{50} ($A\beta_{42}$) = 11 µM

Abb. 14: γ-Sekretase-Modulatoren (**34**, **36**, **37**) aus der Gruppe von Prof. Boris Schmidt, TU Darmstadt.

1.3 ADAM10

ADAM10 gehört zu der Klasse der „*a disintegrin and metalloproteinase protease*“ (ADAM)-Enzyme. Diese Enzymklasse kann in zwei Kategorien eingeordnet werden: die membrangebundenen Enzymen (ADAM) und diejenigen, die ein zusätzliches Thrombospondin Motiv tragen.[90]

1.3.1 Aufbau

ADAM10 oder auch MDAM und Kuzbanian genannt, ist ein 84.1 kDa (748 AS) großes,[90] in der Zellmembran verankertes Enzym welches aus sieben verschiedenen Domänen aufgebaut ist: Propeptid- (Pro), Metalloproteinase- (MP), Disintegrin- (Dis), Cystein-reiche- (CR), EGF-*like*- (ED), Transmembran- (TMD) und der cytoplasmatischen (CT) Domäne (Abb. 15).[91]

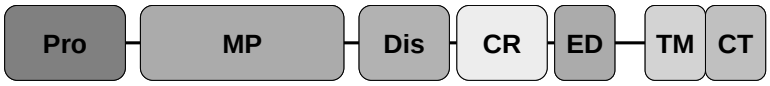

Abb. 15: Schematischer Aufbau von ADAM10.

Dieser Aufbau ist dem der Zink-abhängigen *snake venom* Metalloproteinase (SVMP) sehr ähnlich. Da aber der Spaltungsmechanismus durch ADAM10 noch nicht zufriedenstellend aufgeklärt wurde, wird angenommen, dass er ähnlich zu dem der *snake venom*-Metalloproteinasen verläuft. Ebenso wie die SVMPs liegt ADAM10 als Zymogen vor und ist somit bis zu der Abspaltung der Propeptid-Domäne nicht katalytisch aktiv. Dieses wird durch ein Cystein sichergestellt, welches in der Nähe des *C*-terminalen Endes der Propeptid-Domäne lokalisiert ist und an das für die Katalyse notwendige Zink-Atom koordiniert.[91] Dieser Mechanismus wird als „Cystein-*switch*“ bezeichnet.[92]

1.3.1.1 Metalloproteinase-Domäne

Nach dem „Cystein-*switch*“ liegt das aktive Zentrum nun in seiner aktiven Form vor. Auch hier wird die Verwandtschaft mit den SVMPS deutlich, welche auf der Metalloproteinase Domäne die Konsensus-Sequenz: **HE**XG**H**NL**G**XX**H**D tragen. Dieses Motiv ist bis auf eine Aminosäure, Austausch an Stelle 7: L gegen F, auch in ADAM10 zu finden: 383**HE**VG**H**NF**G**SP**H**D394.[93] Die drei His (H) sind für die Koordination des katalytisch aktiven Zink-Atoms verantwortlich und zwei von diesen His liegen auf der so genannten „*active site helix*“, welche auch die katalytisch aktive Glu (E) trägt. Diese Helix erstreckt sich bis zum Gly (G), wo ein scharfer *Loop* die Koordination des dritten His ermöglicht (Abb. 16Abb. 16).[94-95]

Da ADAM10 noch nicht in vollständiger Form kristallisiert werden konnte, ist in Abbildung 15 lediglich das katalytische Zentrum von ADAM17 dargestellt, welches das am meisten homologe ADAM Enzym zu ADAM10 ist und sich von diesem nur in den variablen Aminosäuren unterscheidet (405**HE**LG**H**NF**G**AE**H**D416) (Abb. 16, PDB: 3e8r).[96]

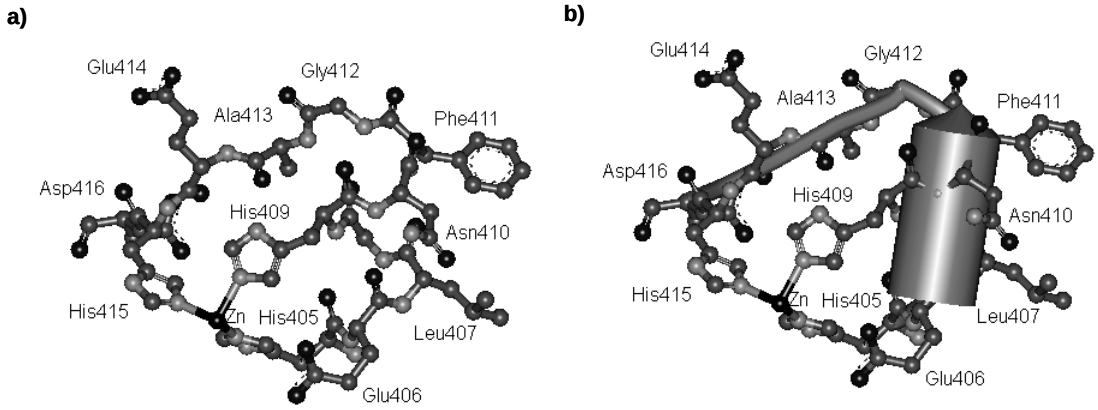

Abb. 16: a) Aktives Zentrum von ADAM17, welches große Ähnlichkeit zu ADAM10 aufweist. **b)** Schematisch dargestellte Sekundärstruktur des aktiven Zentrums von ADAM17, die die Koordination der drei Histidin-Reste an das Zink sicherstellt.

Durch das katalytisch aktive Zink-Atom wird Wasser koordiniert und dissoziiert zu der reaktiven Spezies Zn-OH, (Abb. 17a) welche das Carbonyl-Kohlenstoff im Peptidrückgrad des Substrates nukleophil angreift, anschließend entsteht ein tetraedrisches Intermediat (Abb. 17b). Dieser Vorgang wird durch Deprotonierung durch das katalytisch aktiven Aspartat unterstützt. Die so entstehende negative Ladung am Sauerstoff wird durch das Zink-Atom kompensiert. Der Bindungswechsel vom Zink zurück zum Carbonyl setzt das Amin-Fragment frei, welches von dem als Base fungierendem Aspartat protoniert wird.

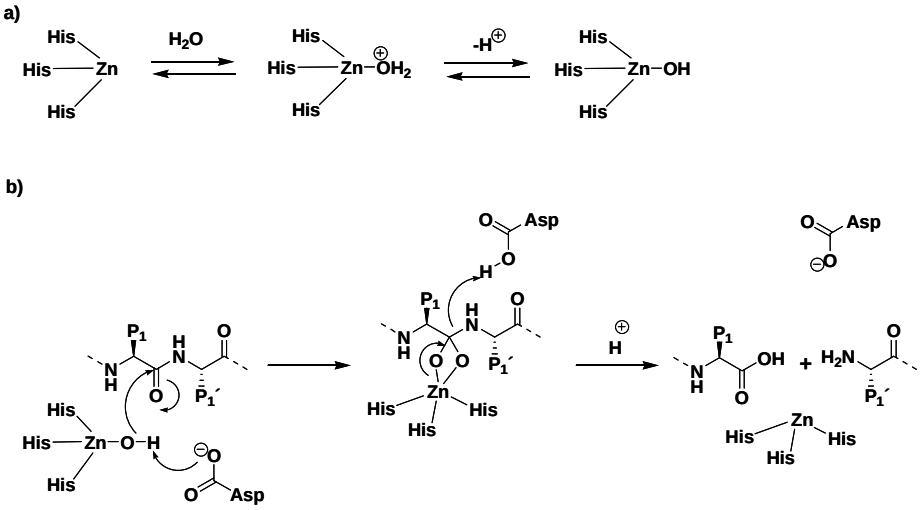

Abb. 17: Spaltungsmechanismus einer Zink-abhängigen Metalloproteinase.

1.3.1.2 Disintegrin-Domäne

Bisher konnten nur die Disintegrin- und die Cystein-reiche Domäne kristallisiert werden (Abb. 18a, PDB:2ao7). Die Disintegrin-Domäne ist vermutlich für die Substraterkennung notwendig, bisher ist jedoch nicht klar, wie das Substrat genau gebunden wird. Auch hier wird wieder durch die Verwandtschaft zu den SVMPs (Gruppe PIII) ein ähnlicher Mechanismus vermutet. Der Bindungsloop der ADAM10 ist 13 Aminosäuren lang (524CRDDSDCAREGIC536) und trägt am *C*-Terminus einen wichtigen Cysteinrest (Abb. 18b).[91] Es werden zwei Bindungsmechanismen diskutiert: 1) Interaktion des Cysteinrestes auf dem Bindungsloop mit einem weiteren Cystein am Substrat unter Ausbildung einer neuen Disulfidbrücke oder 2) eine Umlagerung von bereits existierenden Disulfidbrücken.

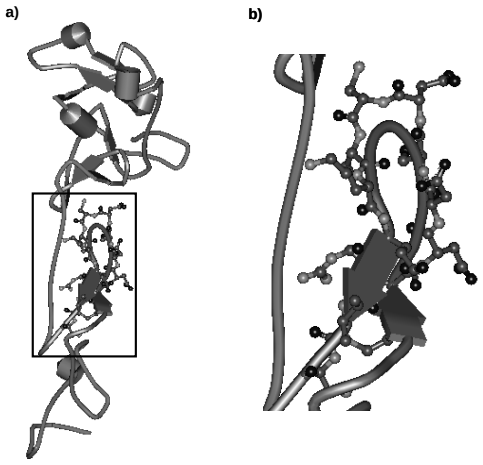

Abb. 18: a) Disintegrin- und Cystein-reiche Domäne mit dem Bindungsloop aus 13 Aminosäuren (**b**), der vermutlich für die Substratbindung verantwortlich ist.

1.3.2 Funktion

ADAM10 weist unterschiedliche Funktionen auf. 1) Im Gegensatz zu den SVMPs, welche die Bindung zwischen Zellen und ihrer extrazellulären Matrix zerstören, unterstützt ADAM10 die Zell-Zell-Interaktionen durch Wechselwirkung mit den Integrinen-Rezeptoren, welche in der Zellmembran lokalisiert sind. Es wird vermutet, dass durch diese Interaktion Signale in die Zelle übermittelt werden.[97-98]

2) Zusätzlich wird ADAM10 u.a. auch zu den *Sheddases* gezählt, die die extrazellulären Domänen von Transmembranproteinen abspalten und somit lösliche Ectodomänen in den extrazellulären Raum entlässen, wo diese als Mediatoren wirken.[99] Da die ADAM10 ein großes Substratspektrum besitzt können verschiedene Stoffwechselwege aktiviert werden wie z.B. Wachstumsfaktoren und Zytokine (Immunabwehr) oder der nicht-amyloidogene Weg bei AD, aber auch pathologische Stoffwechselwegen wie Krebs.

1.3.3 Lokalisierung

ADAM10 ist nahezu in allen Geweben des Körpers zu finden. Am meisten wird es aber in Neuronen, Blutgefäßen, Leukozyten (weiße Blutkörperchen) aber auch in Tumorzellen gebildet. Die zahlreichen physiologischen Eigenschaften der ADAM10 sind zum Einen äußerst wichtig für Entwicklungs- und Reparaturprozesse im Körper und zum Anderen können sie vor Krankheiten schützen (z.B. im Zentralen Nervensystem, ZNS) andererseits können auch Krankheiten ausgelöst werden (z.B. Entzündungsprozesse).

Im ZNS wird ADAM10 in Astrocyten (Blutzufuhr für Nervenzellen), Mikrogliazellen (Abbau von Zellresten) und Neuronen gebildet. ADAM10, sowie ADAM9/17, zeigen im ZNS unter Anderem Aktivität als α-Sekretase und sind dadurch mit der Alzheimer-Demenz verbunden.[100-101] Durch die Aktivität der α-Sekretase kann APP vermehrt über den nicht amyloidogenen Weg abgebaut werden. Hierbei wird APP in der Aβ Sequenz (zwischen Lys^{16} und Leu^{17}) gespalten und verhindert somit das Freiwerden von toxischem $A\beta_{42}$.[102] Das entstandene membrangebundene sAPPα, dessen Bildung durch NSAIDs erhöht werden kann, scheint zusätzlich noch eine neuroprotektive Wirkung zu haben.[99, 103] Eine Aktivierung der α-Sekretase wäre also eine Möglichkeit um das Entstehen von Aβ zu reduzieren, wenn ADAM10 nicht auch an Entzündungsmechanismen beteiligt wäre. Das *Shedding* in anderen Geweben des Körpers von ADAM10 und 17 setzt außerdem noch proinflammatorische Mediatoren wie TNFα und dessen Rezeptor, Interleukin-6-Rezeptor, membrangebundene Chemokine oder auch verschiedene Adhäsionsmoleküle frei, die die Aktivierung und Rekrutierung von Leukozyten zur Folge haben. Diese Mediatoren werden mit verschiedenen

chronischen Krankheiten in Verbindung gebracht, wie zum Beispiel Multiple Sklerose oder rheumatische Arthritis. Ebenso werden ADAM10 und 17 mit dem Wachstum von Krebszellen in Verbindung gebracht, da durch *shedding* Wachstumsfaktoren frei werden, die das Wachstum von Krebszellen zur Folge haben.

1.3.4 Inhibition von ADAM10

Bisher wurden verschiedene Inhibitoren für Metalloproteinasen entwickelt, welche häufig am Grundgerüst eine Hydroxamsäure tragen. Das Scheitern der klinischen Studien von Bastimastat (**38**) oder Marimastat (**39**) ist durch unspezifische Hemmung verschiedener Metalloproteinasen, u.a. ADAM10, 17, MMP1, 3, 9 und 13, zu erklären (Abb. 19).[104-106] INCB3619 (**40**) wurde 1992 als selektiver Inhibitor des ErbB4 *sheddings* beschrieben, inhibiert jedoch sowohl ADAM10 (IC_{50} = 22 nM) als auch ADAM17 (IC_{50} = 14 nM).[90, 107]

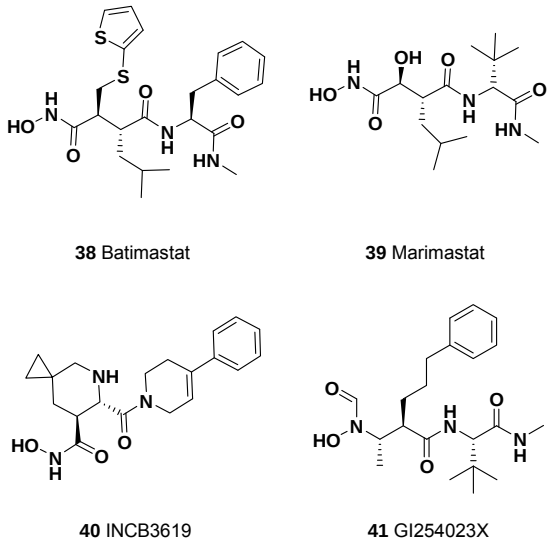

Abb. 19: Inhibitoren von ADAM10.

Die Entwicklung des selektiven Inhibitors GI254023X (**41**) wurde 2000 in einem Patent von GlaxoSmith&Kline beschrieben. Dieser Inhibitor ist um den Faktor 100 selektiver für die Inhibition von ADAM10 (IC_{50} = 5.3 µM) im Vergleich zu der verwandten ADAM17 (IC_{50} = 541 µM).[106]

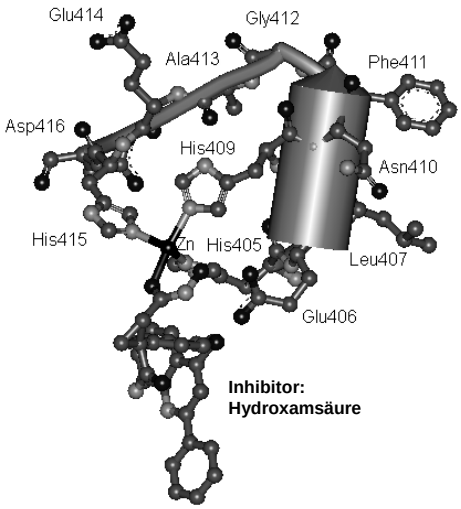

Abb. 20: Der Inhibitor, der eine Hydroxamsäure trägt, koordiniert mit dieser das katalytisch aktive Zink-Atom und verhindert somit die Aktivierung von Wasser, was notwendig ist für die Peptidspaltung.

Die Hydroxamsäurefunktion koordiniert an dem katalytisch aktiven Zink-Atom und verhindert so die Aktivierung von Wasser, was zu einer Peptidspaltung führen würde (Abb. 20).

Die selektive Inhibition von ADAM10 wäre also eine gute Möglichkeit das Wachstum von verschiedenen Krebsarten wie Prostata- oder Darmkrebs zu reduzieren sowie zur Behandlung von chronischen Entzündungskrankheiten. Da die Inhibition im ZNS jedoch gegenteilige Auswirkungen hätte, wie z.B. den Abbau von APP über den nicht-amyloidogenen Weg zu reduzieren, müsste beim Einsatz von Inhibitoren darauf geachtet werden, dass diese die Blut-Hirn-Schranke nicht überschreiten können, dies ist z.B. bei den Hydroxamsäuren, durch den hohen Anteil an polaren Gruppen, vermutlich der Fall.

2 Zielsetzung

Die Entwicklung von Wirkstoffen zur Behandlung von Morbus Alzheimer ist ein interessantes Ziel der Medizinischen Chemie. Die Anzahl der Erkrankungen an Alzheimer-Demenz wird in den nächsten Jahrzehnten zunehmen, bedingt durch den Anstieg des Altersdurchschnitts sowie der Lebenserwartung der Bevölkerung in der Bundesrepublik Deutschland.

Ein interessantes *Target* für die Entwicklung von Wirkstoffen ist die γ-Sekretase, da diese das Protein ($A\beta_{42}$) freisetzt, welches durch Aggregation zu einem der charakteristischen pathologischen Ursachen der Alzheimer-Demenz führt: den amyloiden Plaques.

Da eine vollständige Inhibition der γ-Sekretase pathologische Nebenwirkungen zur Folge hat, besteht die Aufgabenstellung dieser Arbeit in dem Design und der Synthese von γ-Sekretase-Modulatoren. Diese verschieben nur die Schnittstelle des Enzyms von $A\beta_{42}$ zum nicht-pathologischen $A\beta_{38}$ ohne die unerwünschten Nebenwirkungen der Vollinhibition.

Neben den amyloiden Plaques sind auch Entzündungsvorgänge in Gehirnen von Patienten mit Alzheimer-Demenz beobachtet worden. Entzündungsvorgänge sind unter Anderem mit der Aktivität der zwei Metalloproteinasen ADAM10 und ADAM17 verbunden. Diese beiden Enzyme werden auch als *Sheddasen* bezeichnet, da sie Transmembranproteine schneiden und einen löslichen Teil, die Ectodomäne, in den extrazellulären Raum abgeben. Zu diesen Ectodomänen gehören auch proinflammatorische Mediatoren, die chronische Entzündungen auslösen können. Aus diesem Grund soll ein Inhibitor von ADAM10 synthetisiert werden, um Entzündungsvorgänge im menschlichen untersuchen Körper zu können.

3 Kumulativer Teil der Dissertation

3.1 Interessante *Targets* in der Alzheimer-Demenz Forschung und Ansätze einer Diagnostik für eine Früherkennung der Alzheimer-Demenz.

Der Inhalt dieses Kapitels wurde bereits veröffentlicht:

Nicole Höttecke, Stefanie Baumann, Ali Taghavi, Hannes A. Braun and Boris Schmidt, "Drug Development and Diagnostics for Alzheimer's Disease Up to 2008", *in* Frontiers in Medicinal Chemistry Vol. 4, Ed.: Atta-ur-Rahman, A.B. Reitz**,** pp. 730-766, Bentham Books **2009**.
Mit freundlicher Genehmigung von *Bentham Science Publishers Ltd.*

Verschiedene Medikamente sind bereits für die Behandlung der Alzheimer-Demenz zugelassen, wie z.B. AChE Inhibitoren und NMDA-Rezeptor-Antagonisten. Diese Medikamente können jedoch nur die Symptome der Alzheimer-Demenz verringern, die Krankheit selbst jedoch nicht heilen. Eine Immunisierung gegen Aβ wird zurzeit von verschiedenen Firmen untersucht, und könnte eine viel versprechende Therapiemöglichkeit darstellen.

Eine Inhibition der β-Sekretase, dem Enzym, das den amyloidogenen Weg des APP Metabolismus initialisiert, und eine Inhibition bzw. Modulation der γ-Sekretase, welche die zur Aggregation neigenden Aβ-Spezies generiert, sind weitere interessante *Targets* für eine Behandlung der Alzheimer-Demenz.

Das Phänomen, das ausgewählte Cholesterol-senkende Medikamente das Risiko an AD zu erkranken senken, wird weiter untersucht. Ebenso wird die Beobachtung untersucht, bei der Mäuse, die Trinkwasser mit einem höheren Kupfer-Gehalt trinken, weniger Aβ bilden als die Kontrollgruppe.

Ein weiterer wichtiger Schwerpunkt in der AD-Forschung ist die Früherkennung von AD. Bis heute kann eine AD-Diagnose erst nach dem Tod des Patienten durch eine Autopsie eindeutig bestätigt werden. Die AD-Diagnose besteht im Nachweis von Plaques und NFTs im Gehirn von Patienten in Kombination mit der AD-typischen Hirnatrophie. Diese so genannten Biomarker im Gehirn von lebenden AD-Patienten nachzuweisen und damit eine eindeutige Diagnose bereits zu Lebzeiten des Patienten zu erhalten ist bis heute sehr schwierig. Es wird an Substanzen geforscht die selektiv an NFTs oder Plaques binden und durch z.B. Positronen-Emissions-Tomographie nachgewiesen werden können.

Drug Development and Diagnostics for Alzheimer's Disease Up to 2008

Nicole Höttecke, Stefanie Baumann, Ali Taghavi, Hannes A. Braun and Boris Schmidt *

Clemens Schöpf-Institute for Organic Chemistry and Biochemistry, TU Darmstadt, Petersenstr. 22, D-64287 Darmstadt, Germany

Abstract: The exact cause of Alzheimer's disease is still unknown; despite the dramatic progress in understanding. Most gene mutations associated with Alzheimer's disease point to the amyloid precursor protein and amyloid β. The α-, β- and γ-secretases execute the amyloid precursor protein processing. Significant progress has been made in the selective inhibition and modulation of these proteases, regardless of the availability of structural information. Peptidic and nonpeptidic leads were identified and several drug candidates are 2008 in clinical trials. Successful trials demand either large cohorts or reliable biological surrogate markers for Alzheimer's disease. Therefore, several radio markers are under investigation to support such clinical trials by PET-imaging. Here we summarize the developments until 2006 and highlight the important developments until 2008.

Key Words: Alzheimer's disease, secretase, copper, aspartic protease, cholesterol, imaging.

INTRODUCTION

Alzheimer's disease (AD), the most common dementia, affects nearly 2% of the population in industrialized countries. This epidemic neurodegenerative disorder claims millions of victims per year, not just erasing the memory of the patient, but effecting severe social implications. The AD prevalence equals 5.5% above 60 years of age and increases for elderly people [1, 2]. The onset of Alzheimer's disease is usually after 65 years of age, though earlier onset is not uncommon. As age advances, the incidence increases rapidly and roughly doubles every 5 years [1]. Age is the dominant risk factor overruling even the positive impacts of nutrition (low-fat diets), nutritional supplements after onset [3-5]. The previously reported risk reducing effects of higher education were not confirmed in more recent surveys. The socio-economic impact of AD, the care needed for disabled and chronically wasting patients, the consequences for patients, relatives and caretakers alike is a major social and financial issue for the coming decades. Current annual AD related expenditures total $83.9 billion in the US [6]. 14 Million Americans are likely to be stricken by 2050 [7]. Despite all efforts, the exact cause of Alzheimer's disease is still unknown, but the pathways towards and away from Alzheimer's disease become better understood [8]. The process results in neuron and synapse degeneration, reduction of brain regions, memory loss and ultimately in death. There is progress in the definite diagnosis of AD prior to a post-mortem diagnosis. Additional problems arise from other causes of memory loss

*Corresponding author: E-mail: schmidt_boris@t-online.de

(e.g. vascular dementia). Several steps in the process offer potential for intervention, these include the amyloid cascade and plaque-related proteins [9], hyperphosphorylated tau protein [10, 11], zinc, copper and aluminium cations [12-14].

ESTABLISHED THERAPIES AND NOVEL APPROACHES

Some 500 compounds are in development to treat neurodegenerative diseases. At least 10% of these are related to AD [15, 16]. The targets derive from a whole range of sometimes well-known receptors and enzymes: GSK-3, PDE 4 and muscarinic M1. nACh modulators, AChE inhibitors, NMDA modulators, 5-HT agonists and several vaccination projects (e.g. Elan, Cytos Biotechnology) are in advanced stages of research or development. 2 trial failures were reported from 2006-2008 alone: Flurizan and Alzhamed. The early rush on fibril formation inhibition resulted in a number of potent inhibitors thereof. However, the activities were confined to *in vitro* experiments or limited by poor DMPK properties, which excluded further development [17,18]. More recently, this resulted in enhanced activities to interfere with the formation of tau derived paired helical filaments. Methylene blue actually entired phase II trials [19-21]. Few drug candidates (e.g. SKF74652, **1** [22], Scheme **1**) went beyond animal testing and convincing clinical data are still wanted. Furthermore, the view on Aβ toxicity has changed dramatically. Plaques were seen as the true culprit and their removal was one of the therapy goals until 2001. Now, soluble Aβ and early oligomers have to take the blame for the Aβ associated effects. Thus mature Aβ plaques may rather rest in peace.

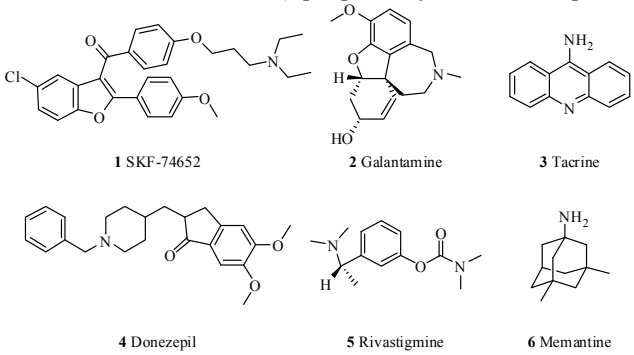

1 SKF-74652 **2** Galantamine **3** Tacrine

4 Donezepil **5** Rivastigmine **6** Memantine

Scheme 1: Current drugs for therapeutic intervention. (**2**-**6**).

Cholinesterase inhibitors [23-26] produce small improvements in cognitive and global assessments [27, 28], but galantamine (**2**), tacrine (**3**), donepezil (**4**) and rivastigmine (**5**) do not address the severe mortality in the final stages of AD. 565 patients with mild to moderate Alzheimer's disease entered a 12-week run-in period in which they were randomly allocated to donepezil or placebo. There were no significant benefits for the 486 patients who completed the 2nd period until the primary endpoints: entry to institutional care and progression of disability [25]. This outcome contradicts a previous report: the chosen AChEI was not cost effective, with benefits below minimally relevant thresholds [6]. Tacrine is losing ground to the other 3 AChE inhibitors because of hepatotoxic effects [29].

The message of these studies is obvious: better drugs are needed to treat Alzheimer's disease!

Memantine hydrochloride (**6**), first made in 1960 by Ely Lilly as an antidiabetic agent, protects neurons against overactivation of *N*-methyl-D-aspartate receptors and was approved for the treatment of moderate to severe Alzheimer's disease in 2002 as first of its class [6]. Previous attempts utilizing this non-competitive antagonism failed. This was due to CNS side effects such as hallucinations. Memantine hydrochloride was tested in a 28 weeks trial at 20 mg/day against placebo, indicating a significant cognitive improvement. The current strategy to use memantine hydrochloride in combination therapy with the AChEI donezepil was concluded from the outcome of a 24 week trial against placebo. The combinations halted or slowed further decline, but the magnitude of these effects was modest [30]. Furthermore, these results have become questionable in the light of the recent extended donezepil trials.

VACCINATION

Immunization therapies against Aβ hold high potential and are under investigation by several companies [31]. The most advanced companies in this field: Elan Corp plc and Wyeth-Ayerst Laboratories suffered a setback of their joined clinical development of AN-1792 in March 2002 [32, 33]. The phase IIa trials were abandoned after observation that four out of 372 patients displayed clinical signs consistent with inflammation in the central nervous system. The alarming and unexplained brain-shrinkage of 6% on average and the lack of cognitive improvement backed the decision to end the trial, but all patients were monitored until December 2002 [34]. Unfortunately, just 13 patients were monitored afterwards, although a small group displayed significant improvements in brain volume and cognitive abilities [35]. These positive results suggest further studies with improved epitopes or different vaccination strategies. Aβ vaccination reduces not only extra-and intracellular Aβ accumulation, but is accompanied by the clearance of early tau pathology. The tau pathology is reduced by the proteasome and depends on tau phosphorylation. Hyperphosphorylated tau aggregates remained unaffected by this antibody treatment [35]. On the contrary, the clearance of tau aggregates was reported for immunotherapy and DAPT treatment. However, Aβ deposits were cleared within 3 days after injection, versus 5 days it took for the reduction of tau lesions [36-39].

Thus, a causal therapy is still in utter demand, as no existing therapy effectively stops or even cures the disease. The incidence of early-onset Alzheimer's disease in Down syndrome patients indicated chromosome 21 as a likely hotspot for gene location. Mutations linked to early-onset Alzheimer's disease afflicted families in London and Sweden and additional polymorphisms, that either cause or further AD, provided some insight into the biological pathways and the involvement of the amyloid precursor protein (APP) [40]. The genetic background of AD is quite heterogeneous; a large number of gene associations have been made with localisations on almost every chromosome [41]. Replicated or confirmed associations are few: the late-onset AD is linked to the ε4-allele of APOE, but its presence is neither necessary nor sufficient to cause the disease, but there is a dose-dependent relation to the age of onset, which results in up to 16x enhanced risk [42]. Another cluster of mutations is located on chromosome 14, on the gene encoding for presenilin 1 [43]. Mouse models expressing mutated human APP and presenilin 1 display many symptoms of AD, although no model represents the full range of pathologies of the human disease. Particularly, the inflammation processes in humans and mice do not adequately relate to each other [44]. The observed loss of neurons (mice [45]) is accompanied by plaque formation consisting of amyloid β-peptide in the human prefrontal cortices. But there is mounting evidence for a second pool of insoluble Aβ in cholesterol enriched low-density membranes, where it moderates membrane fluidity [46].

A rational approach to a successful, causal therapy is based on the detailed understanding of Aβ formation, deposition and the inflammatory consequences. Decisive functions were assigned to the amyloid precursor protein (APP) and its degrading aspartic proteases β-secretase and the presenilins. A simplified APP processing is depicted in Scheme 2. The up to 771 amino acid long APP occurs in 3 isoforms: APP695, APP751, and APP771, this includes a signalling sequence, a large extramembraneous sequence and the crucial membrane spanning domain followed by a short cytoplasmic tail. The non-pathological cleavage occurs between Lys^{687}-Leu^{688} (resp. K16L17 in Scheme 2) by the α-secretase, which belongs to the ADAM family and is suspected to be TACE or ADAM10.

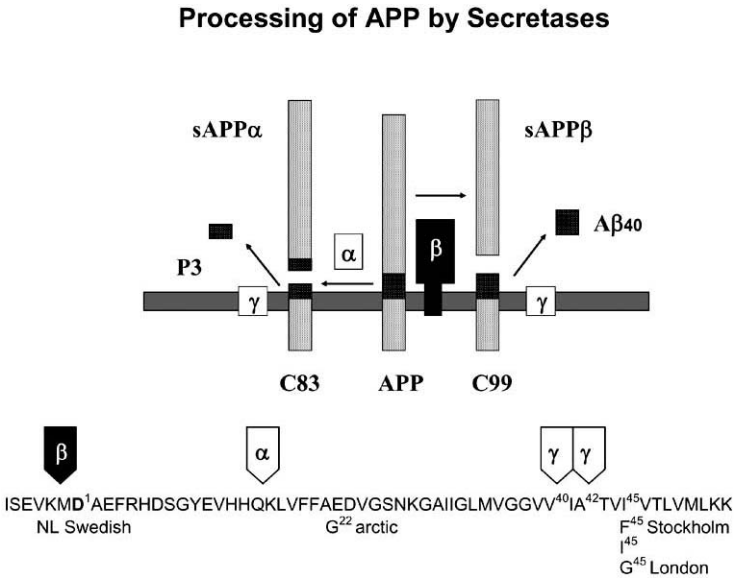

Scheme 2. APP amino acid sequence close to the cleavage sites and point mutations in Aβ numbering.

This dominating event leaves just 10% of the APP behind for the β-secretase, produces α-APP and ultimately leads to the fragments p3 and C83. The α-secretase is sensitive to membrane cholesterol levels and can thus be modulated [47, 48]. The most relevant point mutations for Aβ formation are K670-M671->NL and V717->F (Stockholm or Indiana), which cause familial Alzheimer's dementia (FAD). The molecular basis of these point mutations is explained by their modulation of the secretases. The rate limiting β-secretase usually cleaves between the Met^{671}-Asp^{672} residues, but prefers the preceding amino acids Asn^{670}-Leu^{671} of the Swedish mutation over Lys^{670}-Met^{671}. The V717F mutation accelerates cleavage after Ala^{714}, which leads to the notorious Aβ42, the decisive factor in plaque formation. The released *C*-terminal fragment interacts in the cytoplasm with an adapter protein, Fe65, and finally induces apoptosis in H4-cells [49]. It seemed to be an obvious target to address Aβ deposits directly, either by inhibition of plaque formation or by enhanced plaque degradation. Several companies pursued strategies related to "plaque busters" [50, 51], but clinical data for this mode of action are still lacking and there is mounting evidence that the plaques are not the real culprit, e.g. AD does not correlate well with total plaque load. Both soluble Aβ and *early fibrils* are now commonly blamed to be toxic, particularly in the presence of copper cations (see copper section below). This hypothesis has its merits and is hard to falsify *in vivo* as neither copper nor *early fibrils* are detectable at the necessary resolution. Fortunately, there is evidence for a common mechanism in amyloidogenic diseases, which may hold the key to Aβ, tau and PrP^{Sc} [52].

β-SECRETASE

β-Secretase was identified as an aspartic protease despite the initial lack of selective inhibitors [53]. The key features of an aspartic protease were confirmed: the flexible flap region, which is crucial for substrate docking. The kinetics of statine-based inhibitors revealed stepwise mechanism with structural reorganisation and activity modulation [54]. The two states: open and closed, contribute to selectivity and activity of the enzyme [7]. Two β-secretases are known BACE1 (ASP2 or memapsin2) and BACE2 with high homology, but subtle differences in the active site and an additional disulfide bridge for BACE1 [55, 56]. BACE2 causes additional cleavages close to Phe^{20}, which are reminiscent of α-secretase activity [57]. BACE1 is anchored to the membrane *via* its transmembrane domain (455-480) and may be active as a dimer [58]. BACE1 has a propeptide domain, which is cleaved by furin-like proteases to form mature enzyme. The *C*-terminal transmembrane domain of BACE1 is not strictly required for activity, but the localization of both enzyme and substrate in the same membrane enhances kinetics and specificity. The *C*-terminal truncation seems to influence enzyme kinetics even in the absence of membranes. BACE1 maturation requires cysteine bridge formation (Cys^{216}/Cys^{420}, Cys^{278}/Cys^{443}, Cys^{330}/ Cys^{380}), *N*-glycosylation and propeptide removal. Cystein mutants undergo impaired maturation, but obtain catalytic activity. The Cys^{330}/Cys^{380} bridge was found to be the most important [59]. Crucial for assay development and animal models: BACE1 -/- knockout mice are fertile and healthy, and display reduced Aβ levels [55, 60, 61]. Selectivity issues arise not only by other aspartic proteases, but by the homologous BACE2, which displays a less pathogenic APP cleavage pattern and a distinctly different localization [62]. The Aβ protein is released by a subsequent proteolysis at Val^{711}-Ile^{712} or Ala^{713}-Thr^{714} by the intramembrane protease: γ-secretase, resulting in $Aβ_{40}$ and $Aβ_{42}$. A detailed analysis of BACE distribution, structure, species variation, degradation and properties was published recently [63]. BACE inhibition is not the only way to modulate the BACE dependent APP cleavage. High levels of ceramide or improved raft association can extend the half life of BACE1 (16h) [62, 64-67]. The myelination of nerve cells is regulated by BACE but this process does not cause an obstacle for therapeutic intervention in adults [68, 69].

β-SECRETASE INHIBITORS

Several inhibitors for β-secretase were identified in cellular assays, but more often than not, the true nature of the inhibition mechanism was not reported. Broad spectrum protease inhibitors such as pepstatin **7**, known aspartic protease inhibitors from Renin and HIV protease programs, or cocktails thereof had little inhibitory effect and gave misleading results. To this date several reviews on secretase inhibition were published [62, 66, 67, 7073]. Several peptide-based inhibitors were patented or published immediately after the disclosure of BACE-inhibitor complex X-ray structures [62, 71, 74] (Figs. **1** and **2** show fragments of a homodimeric structure). The active BACE1 used for co-crystallisation lacked the transmembrane and intracellular domains and some flexible *N*-terminal regions were not resolved. The high affinity complex of Glu-Val-Asn-Ψ(Leu-Ala)-Ala-Glu-Phe (**8**, OM99-2, K_i = 1.6 nM) and β-secretase resulted in complete inhibition of β-secretase activity and allowed crystallisation and structure determination at 1.9 Å resolution (PDB: 1FKN, Figs. **1** and **2**) [70, 75].

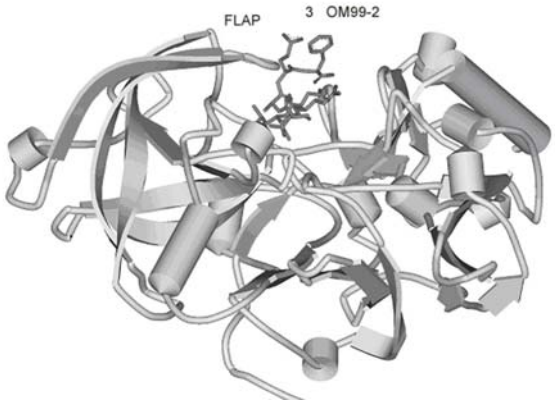

Figure 1. BACE complexed to M99-2 (**8**)

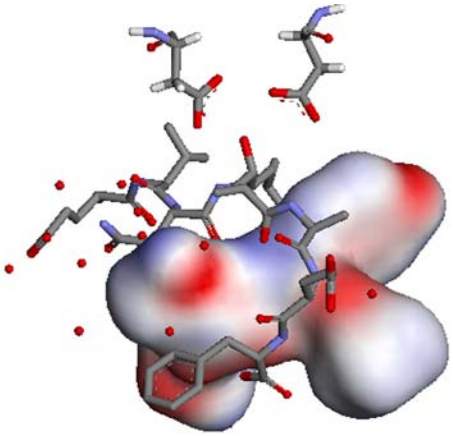

Figure 2. BACE complexed to OM99-2 (**8**)

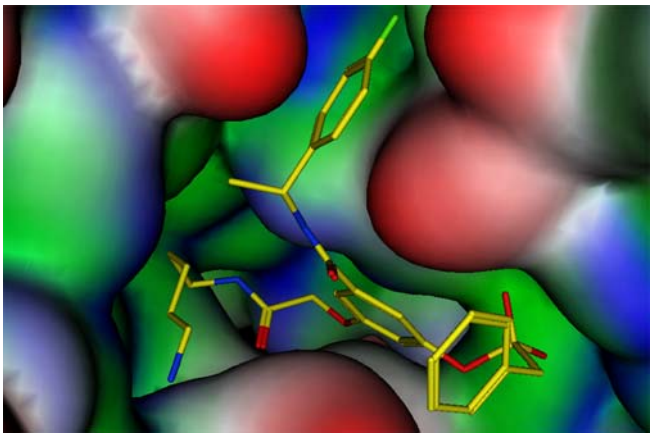

Figure 3. Isophthalamide 18 (yellow) and (b) resorcylate 27 (yellow) above the flap. MOE 2004.10 GaussConolly surface green: hydro-phobic, blue: hydrophilic (PDB: 1W51, 1TQF)

The inhibitor is located in the active site as intended by design and the hydroxyethylene is coordinated by four hydrogen bonds to the two catalytic aspartates. Further 10 hydrogen bonds are established between OM99-2 (**8**), the binding pocket and the flap region. Despite the analogies to other aspartic proteases, there are significant differences in the side chain preferences. S4, S3' are hydrophilic and readily accessible by water. The hydrophilic S4', which holds the phenylalanine, is located at the surface and contributes little to binding. The subsite specificity was revealed by the cleavage rates of combinatorial substrate mixtures and selective inhibitors. This resulted in Glu-Leu-Asp-Ψ(Leu--Ala)-Val-Glu-Phe (**9**, OM00-3, $K_i = 0.31$ nM), which is still the most potent inhibitor of β-secretase. The hydroxyl group of OM00-3 (**9**) is coordinated by the two active site aspartates Asp^{32} and Asp^{228} through four hydrogen bonds (PDB: 1M4H) [74]. Although very similar to OM99-2 (**8**, Glu-Val-Asn-Ψ(Leu-Ala)-Ala-Glu-Phe), the P3, P2, and P2' residues are exchanged, resulting in a more linear and extended conformation at either end. The replacement of the P2' alanine by valine facilitates binding and allows reorientation of the P3' glutamate and the P4' phenylalanine. This shifts the *C*-terminal residue towards the surface of the enzyme and exposes it to the solvent [72]. The structure activity relationship of BACE inhibitors was comprehensively reviewed in 2008 by E. Silvestri [72].

The crystal structure of free BACE (1SGZ) revealed a part of the flap to be locked in an "open" position [74]. The structure is essentially the same as BACE1 bound to an inhibitor, but the flap positions differ by 4.5 Å at the tips. The open position of the flap is stabilized by two intraflap hydrogen bonds and is anchored by a new hydrogen bond involving Tyr^{71} in a novel orientation. The resulting gorge may contribute to sequence and shape selection. A gatekeeper function was evident from the unusually small substituent Ala in P2' (**8**, 1FKN). Thr^{72} forms the narrowest point (6.5 Å in apo BACE) between the flap and Arg^{235}, Ser^{328}, and Thr^{329} on the opposite side and thus contributes to the specificity of BACE. This gatekeeper blocks the access of peptides carrying larger residues in this position, although pocket P1' provides more than enough space for a significantly larger residue [76-80]. The small interaction of the *C*-terminal end of the octapeptides OM99-2 (**8**) and OM00-3 (**9**) with the enzyme inspired the design of shorter peptidic inhibitors (**10**-**13**). Different peptidic inhibitors featuring the hydroxyethylene moiety and flanked by multitude of amino acid residues were published (Schemes **3** and **4**) [81]. Remarkably, the compact P1'-Ala of potent inhibitors has never been replaced by a sterically more demanding group. Several scaffolds are known to provide inhibitors for aspartic proteases.

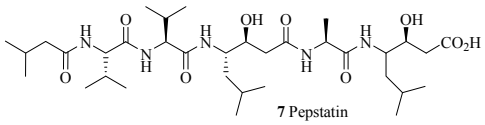

7 Pepstatin

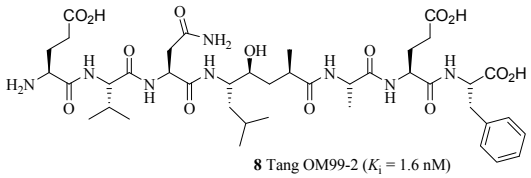

8 Tang OM99-2 (K_i = 1.6 nM)

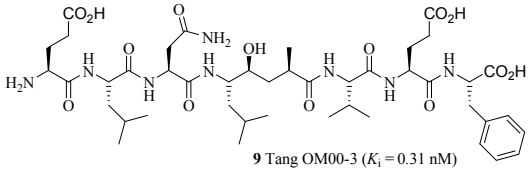

9 Tang OM00-3 (K_i = 0.31 nM)

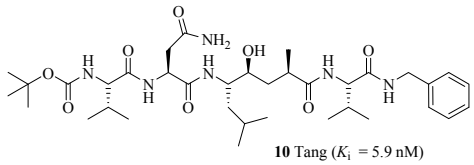

10 Tang (K_i = 5.9 nM)

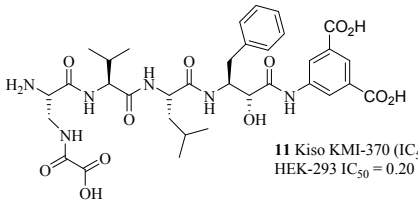

11 Kiso KMI-370 (IC_{50} = 3.4 nM, HEK-293 IC_{50} = 0.20 μM)

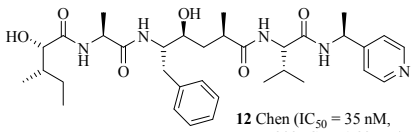

12 Chen (IC_{50} = 35 nM, HEK-293 IC_{50} =1.23 μM)

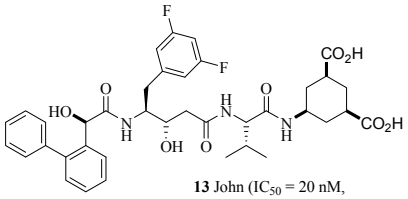

13 John (IC_{50} = 20 nM, HEK-293 IC_{50} > 10000 nM)

Scheme 3. BACE inhibitors I.

Accordingly, statines, norstatines, hydroxyethylamines and hydroxyethylureas can be employed as transition state mimetics, yet with dramatic differences in potency. The inhibitor **11** (KMI-370, IC_{50} = 3.4 nM) featured a short *C*-terminal end with a dicarboxylic acid and displayed high activity *in vitro* and *in vivo* (BACE1-HEK293 cells EC_{50} = 0.20 μM) [81, 82]. Chen *et al.* synthesized (Phe-Ala)-based pentapeptide mimetics like **12** (IC_{50} = 35 nM) and came to similar conclusions [83, 84]. The SAR of these two series postulated a benzyl or a 3,5-difluorobenzyl residue to occupy the P1 position as realized in compound **13** [85]. A good part of the peptidic heritage was replaced by an isophthalamide [86, 87], which functions as the *N*-terminus in the compounds **14-21**. The switch from the statine core to the hydroxyethylene isostere allowed the replacement of the carboxylic acids by smaller groups and resulted in the compact inhibitors (**16-19**) with a reduced molecular mass and fewer hydrogen bond donors.

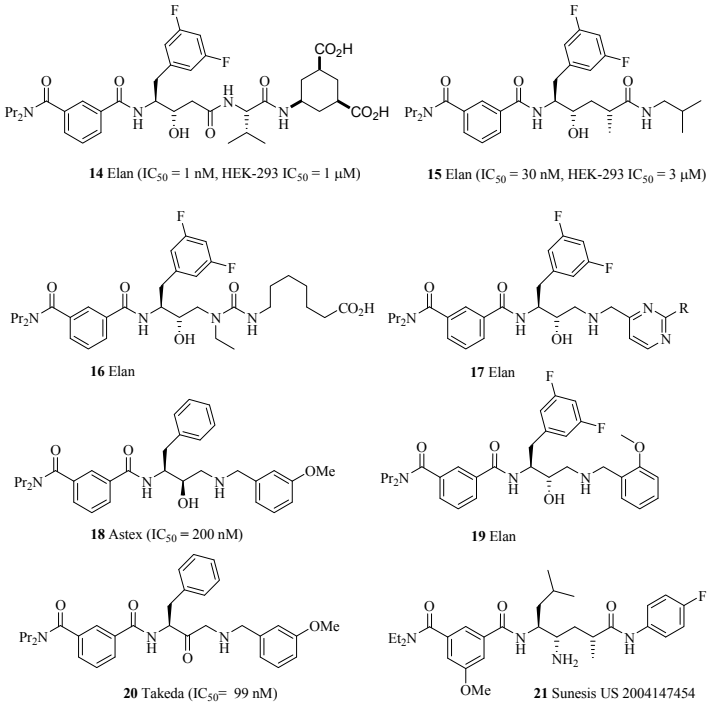

Scheme 4. BACE inhibitors II.

The Elan compounds (13-19) have lost a good part of their peptidic origin, which is mandatory to obtain sufficient oral absorption and blood brain barrier penetration [88]. Significant information was revealed by a novel BACE complexed to a transition state mimetic [89]. Soaking of apo BACE crystals (PDB: 1W50) with small peptidomimetics, which were known to be moderate inhibitors in FRET or cellular assays, resulted in the incorporation of 18 in the active site (PDB: 1W51, Fig. 3a). This peptide mimetic features the isophthalamide to mimic the S2-S4 section and was claimed to have an IC_{50} = 200 nM. Some 750 close analogues were revealed in patents by Takeda (20) [90], Glaxo [91-93], Upjohn Pharmacia [86, 94], Elan (19) [95-97], Astex [98] and a Sunesis employee
(**21**) [99, 100]. But the amino alcohol **18** held a little surprise, despite the *R*-configuration of the alcohol it was far more potent than its *S*-configured diastereomer or the parent ketone and thus contradicted previous SAR of the absolute configuration. The neighbouring amine receives a proton from the catalytic Asp^{228} and places its benzyl substituent in the S2´ pocket. One of the *N*-propyl groups of the isophthalamide occupies the S3 pocket and is directed towards the phenyl ring in the S1 pocket. The phenyl rings in both the S1 and the S2' pocket interact with Tyr^{71}. The *C*-terminal methoxyphenyl is positioned in the S2' pocket. This success in high-throughput crystallography enabled ASTEX to license out this programme to GSK in 2003. However, there is a caveat associated with the depicted BACE inhibitors featuring the phthalamide moiety. Almost all are good substrates for the PGP-transporter and thus do not reach the required brain concentrations for BACE inhibition.

Despite all efforts by the pharmaceutical companies and academic groups, non-peptidic leads for BACE inhibition are still few. The FRET assays of soluble BACE deliver false positive hits to such a degree, that it is mandatory to profile potential hits in a reliable secondary assay, such as a radioligand displacement [101]. This progress in assay development allowed identifying peptidic and non-peptidic leads. Takeda reported a tetraline (22, Scheme 5), which is not an obvious scaffold for protease inhibition and is likely to stem from high-throughput screening efforts [102]. The activity is poor (IC_{50} = 1 μM) and the mode of action was not confirmed. Neurologic's diacid (24) [103] is unlikely to be an easy lead for AD. Latifolin (23), isolated from the heartwood of Dalbergia sissoo, was reported to inhibit the Aβ synthesis with an IC_{50} of 180 μM, again a rather weak and unsecured activity [104]. Vertex reported [105] the biphenylpiperazine (25) as BACE inhibitor (IC_{50} = 3 μM) and it was docked into the BACE structure by Park and Lee [106, 107]. An unfortunate error "improved" it to 3 nM, which makes the outcome of this docking very questionable. Yet similar biphenylated amines (26) were revealed by Actelion [79, 108-110]. MSD undertook the rational design [107, 111, 112] of BACE inhibitors like many others [113]

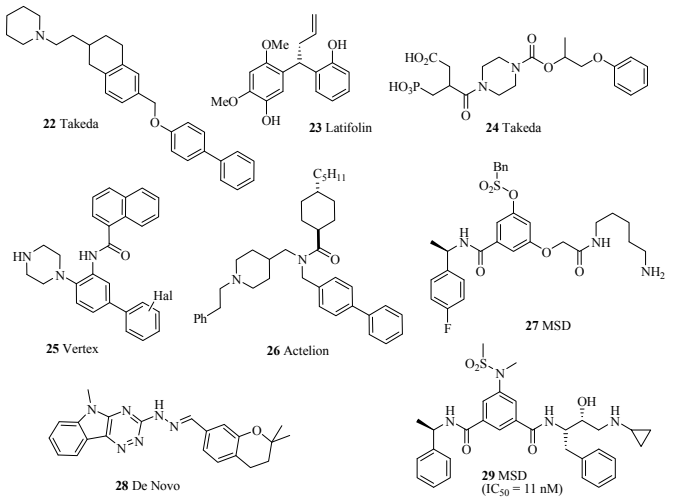

Scheme 5. Non-peptidic BACE inhibitors.

But more innovation was obtained by an *Automated Ligand Identification System* (ALIS): a novel resorcylic acid scaffold [109]. The amino pentyl derivative **27** was obtained after subtle modifications of the lead structure and displayed a moderate inhibition of BACE 1 (IC_{50} = 1.4 μM) and good selectivity towards cathepsin D (IC_{50} > 500 μM). A modified BACE 1 (K75A, E77A) was used for co-crystallisation with **27** (PDB: 1TQF, Fig. **3b**), which occupies the S1-S4 subsites. Quite unusually, the S' sites and the active site have no direct contact with the inhibitor. The acetamide is engaged in a hydrogen bond to the catalytic water, which is placed between the two aspartates. The 4-fluorophenyl moiety wedges the novel S3 subpocket open and the aminopentyl coils back into the S1 pocket. The S1 and S3 substituents may be linked together to result in macrolactams with reduced rotational freedom, which may hold the key for improved activity [114]. Extension towards the active site, occupation of P1 by a phenyl group and placement of a cyclopropyl in P1' improved the inhibition to 11 nM for **29** and retained 500-fold selectivity towards cathepsin D [115-118]. The compound was co-crystallized with BACE, but there was no entry in the PDB by 11/2004. DeNovo reported several scaffolds and mimetics: sulfonamides, 1-piperazinylpropan-2-ols and the triazine **28**, which may offer additional imaging of Aβ fibrils [73]. The implication of BACE1 Cathepsin D similarity were analyzed by L. Marinelli recently [119].

γ-SECRETASE

Paradoxical: despite being the secretase reported first, the identity of γ-secretase was long subject to debate and the detailed structure is still unknown. The close relation to the Notch pathway, which is important in embryonic development, became less hazy over the years. Notch 1, an integral membrane receptor, is processed by proteases upon ligand binding. The intramembraneous cleavage is similar to the APP cleavage and requires PS1. The released intracellular domain migrates to the nucleus, where it finally activates Notch target genes [120]. The crossover to the Notch pathway hampered attempts towards PS-/- knockout animals, which do not pass the embryonic state, but embryonic stem cells may fill part of the gap [121]. The intracellular trafficking of Notch in human CNS neurons is reduced by PS1 inhibitors and results in dramatic changes in neurite morphology. Maybe the Notch dysregulation causes the neuritic dystrophy observed in AD brain tissue [122]. Several other substrates are known to be cleaved by γ-secretase, which seems to be the "proteasome of the membrane" [8]. The relevance of the presenilin cofactors: Pen-2, Aph-1, Nicastrin is well established [123], and even isoforms of these cofactors have been studied at detail [124], but the Nicastrin association to FAD was questioned recently [125]. Cell free γ-secretase assays are still an art, despite the progress in kinetics and feasibility [126, 127]. Substrate optimisation was crucial for both β-secretase and γ-secretase assays [128]. The localisation of the active site within the membrane and the cleavage within the membrane anchor of C99 turns γ-secretase inhibition into a rather slippery fish. Currently, there is only one related enzyme: the signal peptide peptidase, which shares a number of the features and problems, but is inserted into the membrane by 7 transmembrane helices [129]. A proposal for the arrangement of the transmembrane helices has been made, but it does not explain the observed cleavage pattern [130]. Moreover, the importance of the cytoplasmic tail is not acknowledged in this model; two sequences of this tail are required for ER-retention and Nicastrin binding [131, 132]. The active site of γ-secretase is still subject to debate, but replacements of both Asp^{257} and Asp^{385} within the transmembrane regions of PS1 (and the analogue replacements in PS2) inhibit γ-secretase activity [133, 134]. Furthermore, these Asp^{257} modifications significantly inhibited the Notch pathway. The Notch pathway may be a druggable target on its own; applications in oncology were claimed already [135].

γ-SECRETASE INHIBITORS

Non-peptidic inhibitors of γ-secretase are known from the patents by Elan/Eli Lilly, Bristol Myers Squibb and DuPont. Peptidic PS1 inhibitors, like Merck's L-685,458 (**30**) [136-138] are still the most potent inhibitors [139-146]. Lipophilic di- and tripeptides with bulky *N*-terminal protection are common inhibitors for β-secretase and γ-secretase. Lacking specificity and the inhibition of serine and cysteine proteases makes the use of these aldehydes rather cumbersome, because the general protease inhibition results in complex concentration activity relationships. Obviously, this structural motif serves just a tool for assay development and labelling [147, 148], e.g. difluoro ketones were used to block endoproteolysis of PS1 and to distinguish γ-secretase and the Notch receptor [129]. The inhibition by several difluoro ketones supported the point mutation analysis and confirmed the phenylalanine scan of APP [149]. This scan strongly supported a unique α-helical presentation of the C99 fragment to the γ-secretase. Initial attempts of α-helix induction by γ-amino isobutyric acid (Aib) were not convincing [150, 151]. Yet, a surprising activity of an all *D*-tridecapeptide: Boc-VGAibVVIAibTVAIbVIAib-OMe (cell free IC_{50} = 0.14 nM) was reported by Wolfe *et al*. [152] A more druglike tetrapeptide mimetic Boc-Ψ(*Phe*-Phe)-*Leu*-*Val*-OMe displayed a cellular IC_{50} of 0.4 μM [129].

A giant leap forward was obtained by the serendipitous identification of Merck's L-685,458 (**30**, Scheme **6**). This potent inhibitor (IC_{50} = 17 nM), which bears lipophilic moieties, was part of several studies which indicate lipophilic binding pockets (P2, P1, P1', P2', even P4' and P7') next to the cleavage site [153]. The inversion of the hydroxyethylene moiety reduced the inhibition 270fold. Labelling studies were conducted, linking biotin and photo reactive fragments *N*- or *C*-terminally to the core structure to furnish L-852,505 (**32**) and L-852,646 (**33**).

Labelled probes with a biotin moiety were isolated and identified by streptavidin enzyme linked conjugates. Both attachments of photo reactive benzophenones (L-852,646 (**33**), L-852,505 (**32**) retained potent inhibition (IC_{50} < 1 nM for γ-secretase).

Photolysis of **32** in presence of solubilized γ-secretase-complex provided a protein of 20 kDa, which was identified to be PS 1-CTF by western blot. Control experiments revealed binding to wt PS1 but not to PS1ΔE9 was found [154]. Comparative studies with **33** delivered a 34 kDa protein, which was identified to be PS1-NTF.

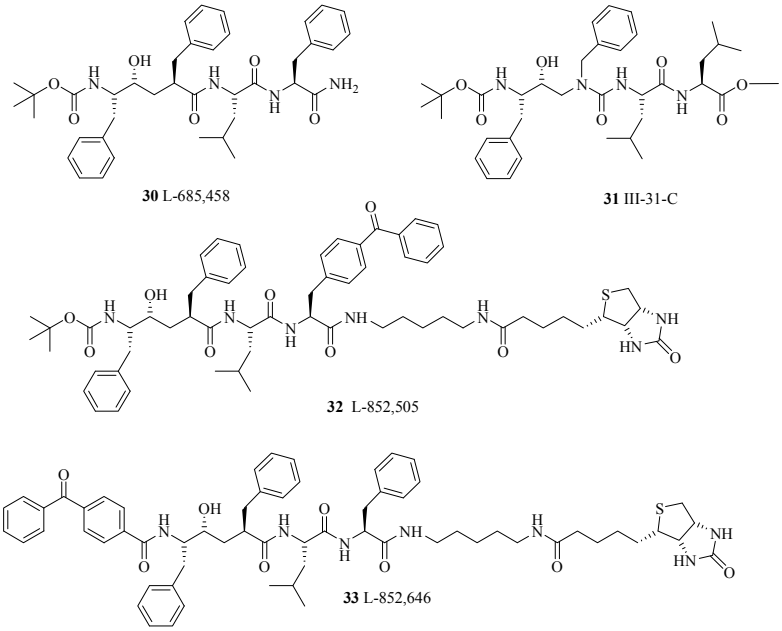

Scheme 6. γ-Secretase inhibitors I.

Further investigation of III-31-C (**31**, IC_{50} < 300 nM), with a hydroxyurea transition state motif, on affi-gel 102 led to the identification of PS1-CTF, PS1-NTF and Nicastrin [155].

Disappointingly, all strategies to free active γ-secretase from the affinity gel failed. This is probably due to the high binding affinity of **31** to the target protein complex and partially due to the deep and narrow binding site, which requires strong denaturing conditions to break up the binding interactions.

The co-precipitation of the inhibited γ-secretase with its substrates C83 and C99 gave rise to speculations about additional binding sites, where the substrate is recognized prior to transfer to the active site. These speculations are in accordance with the observed promiscuous nature of the cleavage, as they assign the specific recognition to other domains [156-158].

To this day very little structural information is available for the γ-secretase complex. Therefore selective, non-peptidic γ-secretase inhibitors had to be provided by HTS efforts.

DAPT (**35**), a promising inhibitor, was developed by Elan in 2001. DAPT, based on a *N*-dichlorophenylalanine lead, and the phenylglycine and the difluoro phenylacetic acid have been pegged as the crucial functionalities for activity [159]. DAPT is not a prodrug, despite the labile tertiary butyl ester, which may be cleaved at the low pH of the gut. The even more labile cyclopropyl methyl ester **36** displayed similar activity [160]. Replacements of the ester by amides were tolerated, but primary alcohols were almost inactive [161]. The subcutaneous application to mice in a dosage of 100 mg/kg resulted in a 50% reduction of cortical Aβ levels within 3 hours. A 40% Aβ reduction was observed at the dosage of 100 mg/kg orally, again after 3 hours, but no brain levels of DAPT were reported for the latter study. Moreover, there is evidence for the slow removal of tau lesions under DAPT treatment [162]. There were several reports of *in vivo* toxicity, mainly because DAPT affects the Notch pathway at higher levels (100-1000x) [134]. A biotinylated DAPT-based photo affinity label (DAPT-BB) was used to investigate the competition of sulindac-*S* (a NSAID) and L-685,458 (**30**) for the active site of PS1. DAPT-BB binds to the PS1-CTF. There was no competitive replacement by Sulindac-*S* up to 100 μM. The displacement of DAPT-BB by L-685,458 (**30**) depended on the Chapso concentration: full displacement at 0.25% Chapso, but only partial displacement at 1% [163].

Further improvement and variation of the crucial functionalities of DAPT resulted in caprolactam **37** (LY411575), which is still the gold standard in the field and in LY450139 (**38**). DAPT, **37**, and **38** were attached with a cross-linking moiety, like benzophenon or phenyldiazirine, as well as with biotin, in azide/alkyle fusion processes. A strong Aβ secretion reduction shows affinity towards γ-secretase and subsequent photoaffinity experiments resulted in identification of PS1-NTF as a target of **37** and **38**, compared to the PS1-CTF targeting DAPT [164]. **37** halved plasma and cortical Aβ levels in young mice already at the oral dosage of 1 mg/kg and therefore **37** and its lesser active diastereomer were administered [165] orally to C57BL/6 and TgCRND8 APP mice for 15 days at 1-10 mg/kg per day. This resulted in the reduction of Aβ levels but also in atrophy of the thymus and deterioration of the intestinal epithelium. Only a 5-fold higher selectivity of APP ($A\beta_{40}$ IC_{50} = 0.082 nM) than Notch (Notch IC_{50} = 0.39 nM) was determined in cellular assays: This small toxicity window will be a crucial issue for clinical trials. Curiously, the Aβ lowering abilities of DAPT like compounds are not effected by their sometimes poor blood brain barrier penetration.

Nevertheless, E. Siemer *et al.* continued in clinical investigations and reported phase I and II studies of LY450139 (**38**), a less potent but APP cleavage selective γ-secretase inhibitor. A 74% reduced $A\beta_{total}$ with constant Aβ levels in cerebrospinal fluid (CSF) at an oral dosage of 40 mg/d after 14 days was observed in phase I. Similar data were reported in Phase II, with 70 AD patients: 38% plasma Aβ reduction with unchanged CSF levels and a secondary effect of Barrett oesophagus were observed. Fleisher *et al.* reported Phase IIb results: They investigated 51 AD patients over a 14 weeks period with randomized doses (100 mg, 140 mg) or a placebo. The study reported reduced plasma $A\beta_{40}$ by 58% for the 100 mg group and 65% for the 140 mg group, but no significant reduction of CSF $A\beta_{40}$ (100 mg = 20%, 140 mg = 11%, Placebo = 6%). Three additional secondary effects to the Barrett oesophagus of Phase II were observed: 1) small bowel obstruction, 2) haemoglobin positive stool, and 3) diarrhoea. All in all no differences were seen in cognitive or functional measures of any group [166, 167].

Thus inhibition of APP processing in the periphery or enhanced clearance of peripheral Aβ by neprelysin [168] and other degrading enzymes [169] may hold a key for causal treatment.

Bristol Myers Squibb and Merck [170, 171] disclosed 1000 derivatives of 4-Chloro-*N*-(2,5-difluorophenyl)-benzenesulfonamides **39**. 500 of these were reported to be very good inhibitors of γ-secretase activity. The activity clustered around the core structure **39**, with a wide variation of the substituent R to modulate bioavailability. Less active sulfonamides (**40**, IC_{40} = 2 μMol, Scheme **7**) were reported by Amgen and MSD, which featured similar bicycloalkane skeletons. They share the arylsulfonamide moiety with **39**, but lack the crucial *N*-alkyl extension [172]. DuPont's hybrid structure **41** [173] bears both signatures of a dipeptide based SAR and a lead, which was identified from a matrix metalloproteinase (MMP) programme. Removal of the central amide bond of the parent dipeptide, the replacement of the hydroxamic acid by an amide and the introduction of a caprolactam provided good activity and removed some of the problems associated with dipeptide leads. The potent compounds (IC_{50} = 20-90 nM) were related to DAPT-like compounds and hybrids of the two series. The difluorophenacyl-caprolactam derivative **42**, stemming from a Scios/DuPont cooperation, proved to be the most potent compound (IC_{50} = 0.3 nM) [174, 175].

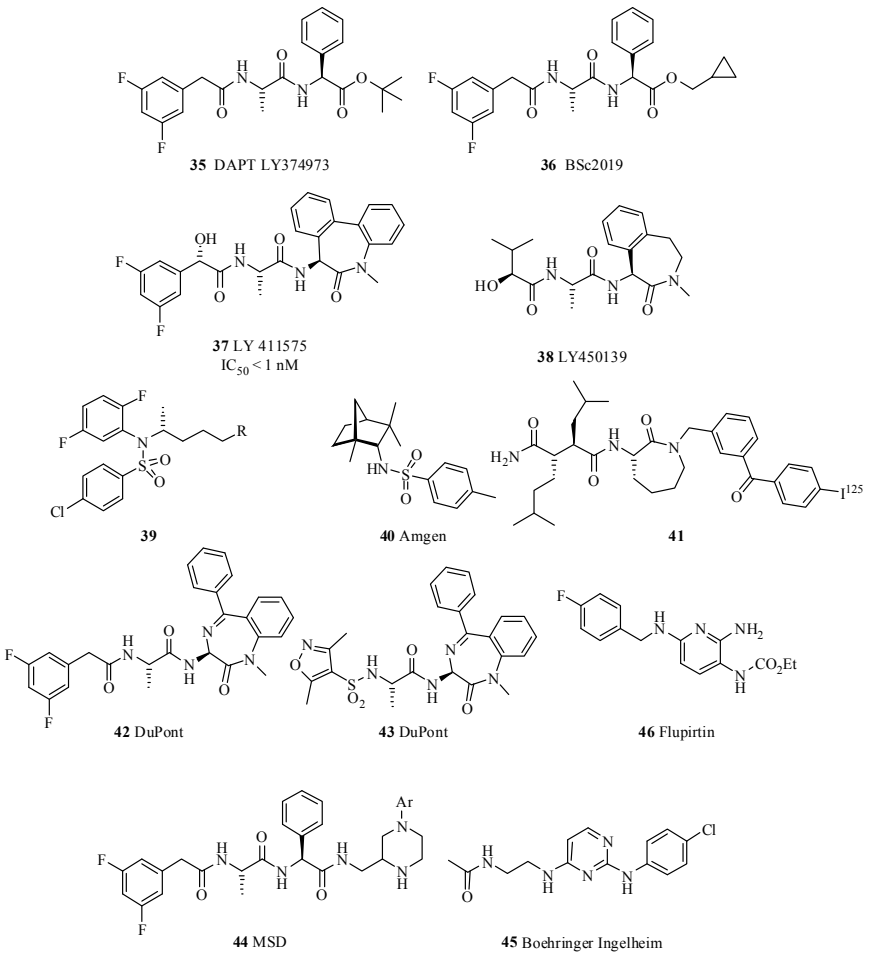

Scheme 7. γ-Secretase inhibitors II.

DuPont Pharmaceuticals, which was taken over by Bristol-Myers Squibb, went on to elaborate the caprolactam motif and described a large number of derivatives in a patent family. Some effort was dedicated to modify the *N*-terminus in order to avoid patent infringement of Elan patents and resulted in the oxazolylsulfonamide **43** [176]. Another straightforward attempt to bypass Elan claims is generalized in compound **44.** Moreover, this series was claimed to be inactive on Notch signalling [177, 178]. Several other compounds or claims exist for hybrid structures of **36** and **41**. A common feature is an aza caprolactam, which places the phenyl groups in a defined, twisted arrangement. Additional residues can be attached to the amide and the glycine is commonly exchanged for small spirocyclic amino acids or amide excision peptidomimetics. Unfortunately, activities for these compounds were not reported yet. Boehringer-Ingelheim [179] disclosed diamino pyrimidines (**45**) as non-peptidic inhibitors of γ-secretase with an $IC_{50} = 4$ to 1000 nM. The patent application is written in German and the most active compound is therefore hidden well. But the BI lead resembles flupirtin (**46**), which displayed beneficial effects on the cognitive function in humans [180, 181]. MSD bypassed the BMS claims for sulfonamide (**39**) by introduction of a cyclohexyl linker (**47**, Scheme **8**). The seven-membered lactam reappeared in several MSD structures like **48** or **49** [182], but the insufficient Notch selectivity put an end to the promising candidate **48** [183, 184]. Elans *N*-bicyclic sulfonamide (**50**) was shown to inhibit Aβ production ($IC_{50} < 100$ nM) even in a cell assay (293sw cells) [185]. Replacement of the sulfonamide moiety by acetamide or sulfones resulted in derivatives like BMS-299897 (**51**) [186] or Scherings *N*-arylsulfonyl heterocyclic amines (**52**) ($IC_{50} = 1$ nM to 1 μM) [187]. BMS-299897 reduces Aβ in brain, CSF and plasma of young mice with a 15-fold higher APP selectivity *in vitro* (APP $IC_{50} = 7.1$ nM, Notch $IC_{50} = 105.9$ nM) in a dose and time dependent manner.

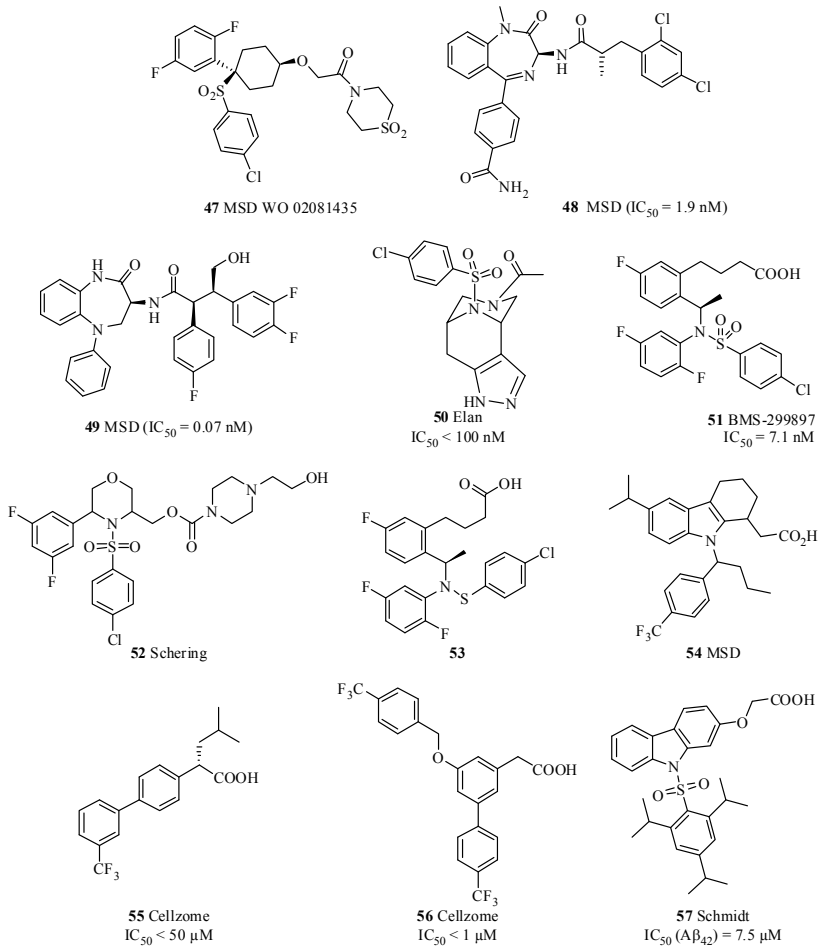

Scheme 8. γ-Secretase inhibitors III.

Mutational studies identified three amino acids (L172, T281, L282) at transmembrane domain 3 (TMD), to be crucial for selective γ-secretase inhibition by sulfonamides like ELN318463 (**53**) and BMS-299897 (**51**). Zhou *et al.* showed a 6.4-fold reduced inhibition by **53** in a L282I mutant, what indicates a direct contact between **53** and L282. L172 and T281 in contrast have only an indirect influence on the inhibition potency [188]. These results implicate a mediation of γ-secretase activity by TMD 3.

MSD reported a selective γ-secretase modulator (GSM) (54), which reduces $A\beta_{42}$ levels with no effect on $A\beta_{40}$ and an increase of $A\beta_{38}$ levels but constant $A\beta_{total}$ levels. It seems the carboxylic acid is crucial for desired modulation. (no data shown) [189, 190]. The carboxylic acid is also a motif in Cellzome´s S-enantiomers of α-substituted arylacetic acids
(**55**) or biphenylacetic acids (**56**) and the most potent modulator of the series **56** displays an IC_{50} < 1 µM in SKN neuroplast cells [191]. *N*-Sulfonylated and *N*-alkylated carbazolyloxy acetic acids have been presented as potent modulators of γ-secretase [6]. Introduction of lipophilic substituents: arylsulfone or alkyl, turned 2-carbazolyloxyacetic acids into potent γ-secretase modulators (e.g. **57** IC_{50} ($A\beta_{42}$) = 7.5 µM).

NON-STEROIDAL ANTI-INFLAMMATORY DRUGS (NSAIDS)

Negative outcomes have been reported for the nonsteroidal anti-inflammatory drugs prednisone, diclofenac, rofecoxib and naproxen [192]. But promising results were obtained with some COX-1 inhibitors [193-195], both *in vitro* and in a prospective, population-based cohort study of 6989 patients [196]. These convincing clinical results are still in need of a sound rational and experimental validation. The proof of concept is still missing, despite the rapid progress. Potential modes of action were hinted or reported several times, but there is much heat and little light: "Non-steroidal anti-inflammatory drugs may lower amyloidogenic $A\beta_{42}$" by inhibition of Rho/ROCK [197]. Yet the Rho/ROCK inhibitors were applied at concentrations several magnitudes higher than the required IC_{50} for Rho/ROCK inhibition. In summary, just few NSAIDs (**58-61**, Scheme **9**) display the desired effect, and if they do so, by modulation of γ-secretase.

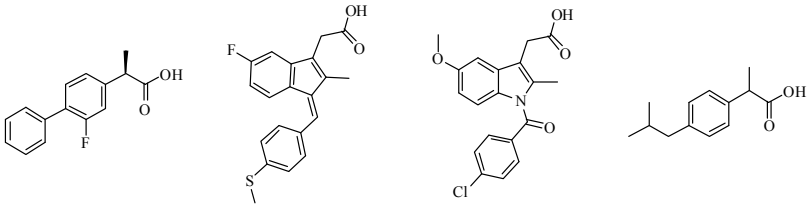

58 *R*-Flurbiprofen
IC_{50} ($A\beta_{42}$) = 307 μM

59 Sulindac sulfide
IC_{50} ($A\beta_{42}$) = 34 μM

60 Indomethacin
$A\beta_{42}$ IC_{50} = 25-50 μM

61 Ibuprofen
IC_{50} ($A\beta_{42}$) = 200 μM

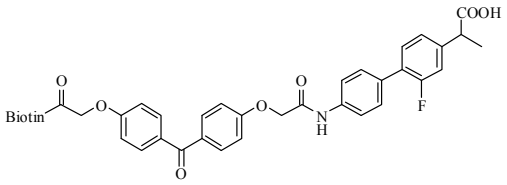

62 Flurbiprofen-benzophenone-biotin

Scheme 9. NSAIDs effect on Aβ levels [28, 29].

Flurbiprofen **58** (10 and 25 mg/kg/d) elicits non-selective reductions in both $A\beta_{1-40}$ and $A\beta_{1-42}$ plasma levels, but was found to be toxic. It produced small reductions in $A\beta_{1-40}$ in the cortex at 25 mg/kg/d, but did not affect Aβ levels in the hippocampus or CSF. Contrary to previous reports, sulindac sulfide (**59**) and ibuprofen (**61**) were found to be neither toxic nor efficacious at doses up to 50 mg/kg/d [198]. The striking discrepancies between these results and the previous reports by Eriksen [193, 194] and Weggen [199] may be explained by the different methods used to extract brain Aβ: alkaline guanidine solution versus 70% formic acid. The kinetics of Aβ formation in the presence of the two NSAIDs and the displacement of an active site directed inhibitor support allosteric, non-competitive modes of action of Sulindac sulfide (**59**) and (*R*)-Flurbiprofen (**58**) [200] at low concentrations. This results in selective inhibition of $A\beta_{42}$ production. However, both NSAIDs shift their mode of action from modulation to complete, non-selective inhibition of γ-secretase at high concentrations. This remarkable pharmacological behaviour may be explained by the stabilisation of dimeric or multimeric enzyme.

The *R*-enantiomere of flurbiprofen **58** (Flurizan®) lowered Aβ brain levels in murine models. A 12 month phase II study, with a dosage of 800 mg twice a day, indicated that 48%, of the patients, with a high drug concentration in blood (> 75 g/mL), had benefits in cognitive and behavioural appearance. Two of three study endpoints were achieved. However, the phase III clinic trial with more than 2400 patients failed in 2008 [155]. "The study did not achieve statistical significance on either of its primary endpoints cognition and activities of daily living" (Myriad Homepage). The lacking efficacy may be assigned to the poor blood brain barrier penetration of (*R*)-flurbiprofen, which is < 5%. Nevertheless, NSAID derivatives belong to an interesting class of modulators. Kukar *et al.* recently reported photoaffinity investigations with flurbiprofen-benzophenone-biotin (**62**), these studies concluded a direct binding of **62** to APP, Aβ and APP-CTF; but no targeting of this GSM to the γ-secretase-complex itself [201]. By contrast Weggen *et al.* and Page *et al.* identified sulinduc sulfide resistant mutants of PS1 at PS1 transmembrane domains: L166P (TMD3), M233V (TMD5) and the extracellular (P117L) [202]. These studies suggest a binding of the modulator to PS1 itself. Further investigations are required to determine the binding sites of individual NSAIDs and non-NSAID derived modulators. Eisai in partnership with Torrey Pines Therapeuticals developed E2012, a novel, more potent γ-secretase-modulator than Flurizan. The definite structure of E2012 is unknown, but a derivative of TorreyPines NGX555-series is depicted in Scheme **10**.

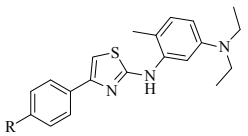

63 NGX555-series

Scheme 10. Torrey Pines NGX555-series.

Lenticular opacity was observed in rats during a 13-week high-dosage safety preclinical trial some side effects. The ongoing phase I study was immediately suspended by the FDA in February 2007. However, the phase I study was resumed in April 2008 after additional safety studies: a 13-weeks safety study in monkeys, a single dose application at maximum dosage and a 4-week high dosage study in rats. (Torrey Pines Homepage)

INDIRECT APPROACHES- OR: DO OUR SOULS RESIDE IN FAT?

Brain cholesterol accounts for up to 25% of total body cholesterol and is turned over within a few months. Individuals on a high-cholesterol diet are at increased risk to develop AD, but the cholesterol brain levels were unaffected in animal models. Some cholesterol lowering drugs such as pravastatin and lovastatin resulted in reduced risk for AD in retrospective trials. Paradoxically, prospective trials resulted in a rather confusing situation with contradicting outcome, most prospective trials failed to confirm a risk reduction for AD [202-205]. Simvastatin does not reduce risk and pravastatin exerts the effect regardless of the blood-brain barrier (BBB) crossing [206, 207]. The answer is not simple; both simvastatin and lovastatin pass the BBB in the prodrug form, prior to hydrolysis to the active acids, and can be detected in the CSF. The rationale for this activity is still subject to debate, but three important observations may hold the clue for an explanation: 1.) hypercholesterolemia results in increased levels of extractable total Aβ in mice 2.) BACE1 was found to be associated to cholesterol stabilized rafts [207] in the plasma membrane and 3.) activity of the benign α-secretase is inversely related to cholesterol levels [208]. The relevance of these different, yet concerted modes of actions remains to be established in humans, but transgenic mice respond to hypercholesterolemia by reduction of soluble Aβ [209]. The pleiotropic, non-lipid-related activities may be caused by the inhibition of the isoprenoid synthesis downstream of HMG-CoA reductase, interfering with RAS and thus cell signalling [210]. A specific inhibitor of squalene synthase can inhibit the cholesterol biosynthesis, but does not block the isoprenoid pathway leading to dolichol and ubiquinone. The potential of such inhibitors was published for the cholesterol-lowering BM15.766 (**64**, Scheme **11**), which resulted in halved Aβ brain loads. The plasma Aβ levels correlated well with the plasma cholesterol [202], but the brain cholesterol went down by a meagre 11-13%, which may be explained by uncorrected cholesterol determination. RPR107393 (**65**) and its *R*- and *S*-enantiomers are potent inhibitors of rat liver microsomal squalene synthase (IC_{50} = 0.6 to 0.9 nM) and modulate Aβ levels in transgenic mice [13, 211].

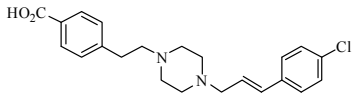

64 BM15.766

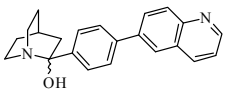

65 RPR107393

Scheme 11. Cholesterol lowering drugs with impact on Aβ levels.

COPPER AND CHELATORS

The copper enhanced Aβ associated toxicity stimulated investigations of dietary copper and copper homeostasis in mice and men [212, 213]. The initial hypothesis had to be revised, as increased copper levels (0.25 g $CuSO_4 \cdot 5\ H_2O$/L) in drinking water turned out to decrease Aβ levels in transgenic APP mice. A potential mode of action may be present in the reduced superoxide dismutase 1 activity. Metal chelators were frequently investigated to moderate copper levels in brain tissue, which were thought to be responsible for Aβ toxicity. However, in most *in vitro* studies, the copper concentrations required to observe the effect were magnitudes higher than found *in vivo*. Studies in 20 patients with clioquinol **66** (Scheme **12**), a metal chelator that crosses the blood-brain barrier readily and has similar affinity for zinc and copper ions, indicated interesting results. But the lack of a control group in the study left ample room for other explanations, e.g. inflammation stimulus [214]. However, recent data from animal models support a benign impact of clioquinol on copper homeostasis. Clioquinol was found to mediate copper uptake and counteract copper efflux activities of APP [215]. The improved selectivity of the quinol towards copper was addressed by Prana Biotechnology [216], who submitted a multitude of clioquinol analogues to a catalase type assay in the presence of Aβ. Several inhibitors (**66-69**) were profiled in rats and the DMPK properties were communicated in a patent application.

The clinical trials of PBT1 (**67**) were abandoned in phase II. Prana Biotechnology reported manufacturing problems as the major reason for the step, as PBT1 was contaminated by process derived impurities which ruled out further investigation. The modified and improved follow up compound PBT2 completed double blinded phase II trials (12 weeks, oral, 50 or 250 mg/day) in September 2007. There were no clinically adverse findings, the higher dosage reduced $A\beta_{40}$ and $A\beta_{42}$ concentrations in cerebrospinal fluid (CSF). There was no significant effect on tau CSF levels. Efficacy of PBT2 could not be determined because of the small number of patients (**74**), but there were significant improvements at 250 mg/d in the category fluency test [217-219].

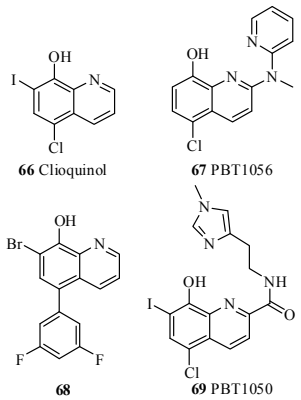

Scheme 12. Clioquinols.

DIAGNOSTICS - MARKERS FOR AD

The ongoing quest for a diagnostic tool for Alzheimer's disease has recently made great progress. Early stages of Alzheimer's Disease, at a point where no clinical symptoms have occurred yet, may be detected with the help of technologies, such as measuring the cerebrospinal fluid (CSF) for biomarkers like total tau (T-tau), phospho-tau (P-tau) and $A\beta_{1-42}/A\beta_{1-40}$ [217-219]; magnetic resonance imaging (MRI) measuring hippocampal and entorhinal cortex atrophy [220, 221]; fluoro-deoxy-glucose (FDG) positron emission tomography (PET) determining regional abnormalities in glucose and oxygen metabolism [222]. However, the large variation in the distribution and severity of both neurophathological changes and neurochemical abnormalities among AD cases renders it very difficult for a single biomarker to provide accurate results with high enough sensitivity and specificity. Today, a passably true diagnostic can only be achieved through combining methods, i.e. clinical assessment/ cognitive testing in conjunction with neuroimaging technologies measuring markers such as structural and/ or metabolic changes [223]. Radiotracers do not suffer from the severe drawback of biomarkers that demands CSF fluid sampling which excludes fragment sampling in large clinical trials. Moreover, a radiotracer may be more accurate as it directly measures the hallmarks of the disease senile plaques (SPs) and neurofibrillar tangles (NFTs). Today, a combination of Aβ imaging and ^{18}F-fluorodeoxyglucose PET promises greater accuracy for distinguishing patients with mild AD from elderly controls [223]. Although being the hallmarks of AD, both amyloid and tau proteins occur in over one hundred different related diseases. Therefore, a tremendous value would be added to an early diagnostic marker that can differentiate AD from other forms of dementia. Lack of such differentiation may cause false diagnosis leading to wrong and deleterious "treatment" of patients. Furthermore, misdiagnoses can result in false negatives in clinical trials, preventing a promising drug to reach the market, thus entailing major losses, both for the pharmaceutical company and for patients in hope for a cure. This chapter will present the current status of *in vivo* amyloid PET ligands investigated in humans.

The "proof of concept" for human *in vivo* amyloid imaging was conducted with ^{18}FFDDNP (**70**) [224], ^{11}C-PIB (**71**) [225], and ^{11}C-SB13 (**73**) [226]. To date, several new radiotracers have been investigated in human AD patients by means of PET (Scheme **13**).

1 [^{18}F] 1,1-dicyano-2-[6-(dimethylamino)-2-naphtalenyl] propene (^{18}FFDDNP) (**70**) [224].

2 *N*-methyl [^{11}C] 2-(4´-methylaminophenyl)-6-hydroxy-benzothiasole (^{11}C-PIB) (**71**) [225].

3 2-(3-[^{18}F] fluoro-4-(methylamino)phenyl)benzo[*d*]thiazol-6-ol (^{18}F 3'-F-PIB, **72**) [227].

4 4-*N*-methyl[^{11}C] amino-4´-hydroxystilbene (^{11}C-SB13) (**73**) [226].

5 2-(2-[-dimethylaminothizol-5-yl]ethenyl)-6-(2-[fluoro]benzoxazole) (^{11}C-BF-227, **74**) [228].

6 trans-4-(*N*-methylamino)-4´-(2-[2-(2-[^{18}F]fluoro-ethoxy)-ethoxy]-ethoxy)-stilbene (^{18}F-BAY94-9172, **76**) [229].

7 ([S-methyl-[^{11}C]]*N*,*N*-dimethyl-4-(6-(methylthio)imidazo[1,2-a]pyridine-2-yl)aniline) (^{11}C-MeS-IMPY, **77**) [230, 231].

^{18}FFDDNP **70** demonstrated a high signal intensity within the hippocampus, amygdala and entorhinal cortex, which are associated to areas with high levels of NFT deposition [232]. Slightly less ligand retention was observed in the frontal cortical areas, which are associated with high SP load. This demonstrates certain specificity towards NFTs. Furthermore, the signal intensity from the NFT regions showed a correlation to the cognitive status [224]. In addition, with as little as 9% increase in binding compared to controls, (**70**) was able to distinguish all AD cases from control. However, the inconvenient 2-hour scan time makes it difficult to reproduce results with the same precision and prevents the tracer from becoming applied on a widespread clinical scope.

With an estimated 500 human injections, ^{11}C-PIB (**71**) is the best studied radioligand. **71** has two binding sites: a high-affinity binding site with B_{max} of 1,407 pmol/g and K_d value of 2.5 nM, and a low-affinity binding site with B_{max} of 13 nM and K_d of 250 nM [233]. **71** also demonstrates an excellent brain uptake and rapid washout. **71** shows an

80% increase in cortical binding in AD compared to controls, with a measuring time of approx. 20 minutes. A recent 2-year follow-up PET study has shown that the amyloid load in an AD brain reaches a plateau, all the while a decline in cerebral glucose metabolism and cognitive deterioration can be observed [225, 234]. The plateau indicates a different time course for the amyloid load in relation to the functional activity in the brain, possibly indicating the predromal stage of AD. This assumption was also supported by a study conducted with 17 mild cognitive impairment (MCI) patients. Seven patients who showed a high Aβ load (according to **71** retention) converted to AD. Interestingly, non of the ten patients with low Aβ load developed AD [235, 236]. Furthermore, excellent correlation of episodic memory and **71** retention in MCI patients was found while demonstrating poor correlation for AD patients [237]. In recent studies, the Pittsburgh Probe (**71**) was able to discriminate AD from frontotemporal dementia (FTD) [238-240]. At brain tissue autopsy, Aβ burden did not correlate with the poor cognitive status the late patient exhibited [241]. Contrary to **70**, **71** binds solely to Aβ plaques (at tracer concentrations). The above-mentioned results, in combination with the findings from **70** trials suggest that amyloid detection may be a suitable target for early, preclinical detection of AD. NFT detection correlates better with the cognitive decline in later stages of the disease. Moreover, this idea is consistent with the amyloid hypothesis, classing NFT formation as a downstream event of large SP depositions [242, 243]. These results suggest that a diagnostic radiotracer for Aβ may provide us with a tool for early MCI detection of dementia. The **71** probe mainly suffers from two major drawbacks: its unspecific binding to white matter that makes it difficult to analyze the images. Second, and more critical, is the short half-life (20.4 min) of the ^{11}C radioisotope, restricting measurements to places with an on-site cyclotron affording immediate injection into patients. Recently, an ^{18}F analogue, with a half-life of 109.8 min, namely ^{18}F 3'-F-PIB (**72**), was developed by GE Healthcare and investigated in humans. With an injected activity of 185 MBq, the tracer showed a higher specific binding in the cortical regions, e.g. in the frontal and lateral temporal as well as the posterior cingulated cortex, than compared to healthy controls. Although, a 20% higher white matter uptake was observed, this probe is suggested to be a valuable radiotracer due to its advantageously longer decay time of the ^{18}F radioisotope and the high cortical uptake.

Structural analogues to **71** are the stilbene based ligands. The first stilbene ligand investigated in humans, ^{11}C-SB13 (**73**), showed uptake and retention patterns very similar to **71** [226]. All AD patients could be identified after a 2-hour scan. An increased **73** uptake was observed in the frontal and posterior temporal-inferior parietal association cortices in the AD patients but not in the controls. However, **71** also differentiated from control in the temporal cortex of AD patients. When tried in normal rat brain, **73**, with it's moderate lipophilicity (LogP = 2.36), showed a good brain penetration and washout after an i*v* injection [244] and demonstrated a B_{max} value of 14-45 pmol/mg protein with a K_d of 2.4 nM [245].

^{11}C-BF-227 (**74**) (K_i value of 4.3 nM to $A\beta_{1-42}$ fibrils) was designed to improve BBB penetration and clearance from brain tissue [228]. The logP value was measured to 1.75 which is lower than that for **73**, but higher than **71**. The higher lipophilicity might be the reason for the slower clearance of **74** compared to **71**. A higher lipophilicity also causes high nonspecific binding in the brain. Furthermore, compounds with higher lipophilicity bind better to plasma protein and therefore undergo a more rapid metabolism by the liver resulting in reduced brain uptake. The measured *in vivo* binding of **74** to Aβ deposits is lower than that for **71**. A possible explanation is that **74** binds preferentially to dense amyloid fibrils and less strong to the diffuse plaques containing fewer Aβ fibrils. This might result in more specific diagnosis of amyloid deposition in AD patients compared to normal aging or other forms of dementia. **74** also accommodates an ^{18}F radioisotope, which is subject of ongoing investigations. However, much more research and improvements are necessary before this ligand becomes a serious competitor to **71** or other ligands tested in humans.

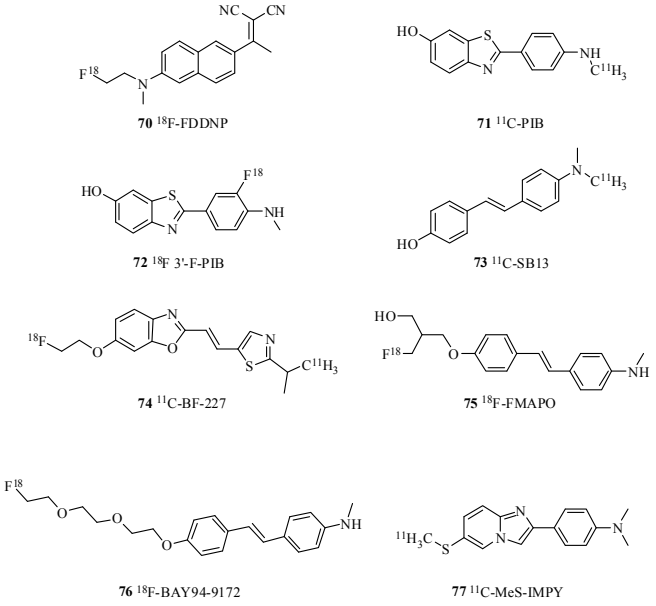

Scheme 13. AD imaging probes.

Two approaches have been adopted to circumvent the inherent lower lipophilicity of the ^{18}F-labeled ligands [246]. An additional hydroxy group was added onto a stilbene analogue affording ^{18}F-FMAPO (**75**). Measured in a transgenic mouse model, **75** demonstrated an excellent brain penetration (5.55 and 9.75% dose/g at 2 min) with rapid brain washout [247]. B_{max} was in the range of 10-20 pmol/mg in tissue. The ligand displayed high binding affinities for Aβ plaques in AD brain homogenates K_i =5.0+- 1.2 nM. However, this compound has not yet been tested in human clinical trials.

A second approach to achieve better lipophilicity was to adopt various lengths of polyethylene glycol (PEG) tails. There are many publications evaluating these compounds *in vitro* and *in vivo*. Also, one such ligand has been investigated in humans. ^{18}F-BAY949172 (**76**) has been shown to bind to Aβ plaques (K_i = 6.7±0.3 nM), but not to Pick bodies, Lewy Bodies, or glial cytoplasmic inclusions [229]. Tangle binding was observed at higher dosages only. For a radiotracer to be useful for clinical practice, it must allow for short scanning time to reduce PET camera traffic. The decay half-life must be long enough to allow centralized production with subsequent distribution to multiple PET sites in order to improve access to Aβ imaging in a cost-efficient manner. **76** was measured 90 minutes after injection and it was able to distinguish AD from frontotemporal dementia. After 30 min of scan acquisition only, a binding distribution identical to **71** and its long decay half-life from ^{18}F, **76** clearly has favourable results compared to the ones reported in **71** PET studies. However, **71** has a higher degree of neocortical binding, approx. 70% compared to 57% in **76** (9% for **70**) [248]. The metabolic rate of **76** is similar to that of **71** [249]. Also, some troublesome radiometabolites (TR) of **76** cross the BBB due to their lipophilic nature and contribute to background brain radioactivity. Only lipophilic and non-charged molecules can cross the BBB. Therefore, TR can be avoided by designing "smart radio-ligands". A "smart radioligand" carries the radioisotope on a group that when metabolized becomes a charged species too polar to cross the BBB.

A respective study was conducted with ^{11}C-MeS-IMPY (**77**) [231]. Two analogues, one with the radiotracer on the thiomethyl group **77** and the other with the radiotracer on the *N*,*N*-dimethylamine group (MeS-IMPY-C^{11}), were prepared and investigated. Interestingly, **77** demonstrated a superior washout of radioactivity to both MeS-IMPY-C^{11} and **71**. This effect was assigned to the lower amount of TR in the brain. On the other hand, studies also indicated three major radiometabolites in various tissue compartments, all of which with less lipophilicity than the ligand itself. However, once the intact ligand entered the brain, it was protected from further metabolism [231]. Results from the clinical trials are underway and it remains to be seen if this compound is as promising in human clinical trials.

OUTLOOK

Despite the tremendous progress in the field, a γ-secretase inhibitor free of Notch activity is still in utter demand. The selective inhibition of γ-secretase by NSAIDs is pointing in the right direction: allosteric modulation of the active site, which can be identified by additional cleavage sites mediated by PS1. Confirmed, non-peptidic γ-secretase inhibitors are few and still have to reveal their true potential. Several compounds and vaccinations are entering phase II clinical trials and demand improved AD diagnostics. Actually, the vaccination may outpace the other therapies on the way to market. Dietary copper is unlikely to be a remedy for late stage AD, but may offer inexpensive prevention.

REFERENCES

[1] WHO, *The World Health Report 2001 Mental Health: New Understanding, New Hope*, **2001**.

[2] Polvikoski, T.; Sulkava, R.; Myllykangas, L.; Notkola, I. L.; Niinisto, L.; Verkkoniemi, A.; Kainulainen, K.; Kontula, K.; Perez-Tur, J.; Hardy, J.; Haltia, M. Prevalence of Alzheimer's disease in very elderly people: a prospective neuropathological study. *Neurology,* **2001**, *56*, 1690-6.

[3] Gil Gregorio, P.; Ramirez Diaz, S.P.; Ribera Casado, J.M. Dementia and Nutrition. Intervention study in institutionalized patients with Alzheimer disease. *J. Nutr. Health Aging.,* **2003**, *7*, 304-8.

[4] Thorsett, E.D.; Latimer, L.H. Therapeutic approaches to Alzheimer's disease. *Curr. Opin. Chem. Biol.,* **2000**, *4*, 377-382.

[5] Grant, W.B. Dietary links to Alzheimer's disease: 1999 update. *J. Alzheimer's Dis.,* **1999**, *1*, 197-201.

[6] Cummings, J.L. Alzheimer's disease. *N. Engl. J. Med.,* **2004**, *351*, 56-67.

[7] Chou, K.C. Insights from modeling the tertiary structure of human BACE2. *J. Proteome Res.,* **2004**, *3*, 1069-72.

[8] Mattson, M.P. Pathways towards and away from Alzheimer's disease. *Nature,* **2004**, *430*, 631-9.

[9] Czech, C.; Adessi, C. Disease modifying therapeutic strategies in Alzheimer's disease targeting the amyloid cascade. *Curr. Neuropharmacol.,* **2004**, *2*, 295-307.

[10] Mandelkow, E.-M.; Mandelkow, E. Tau in Alzheimer's disease. *Trends Cell Biol.,* **1998**, *8*, 425-427.

[11] Augustinack, J.C.; Schneider, A.; Mandelkow, E.-M.; Hyman, B.T. Specific tau phosphorylation sites correlate with severity of neuronal cytopathology in Alzheimer's disease. *Acta Neuropathol.,* **2002**, *103*, 26-35.

[12] Ritchie, C.W.; Bush, A.I.; Mackinnon, A.; Macfarlane, S.; Mastwyk, M.; MacGregor, L.; Kiers, L.; Cherny, R.; Li, Q.X.; Tammer, A.; Carrington, D.; Mavros, C.; Volitakis, I.; Xilinas, M.; Ames, D.; Davis, S.; Beyreuther, K.; Tanzi, R.E.; Masters, C.L. Metal-protein attenuation with iodochlorhydroxyquin (clioquinol) targeting Aβ amyloid deposition and toxicity in Alzheimer disease: a pilot phase 2 clinical trial. *Arch. Neurol.,* **2003**, *60*, 1685-91.

[13] Bush, A.I.; Masters, C.L.; Tanzi, R.E. Copper, β-amyloid, and Alzheimer's disease: Tapping a sensitive connection. *PNAS,* **2003**, 11193-1194.

[14] Altmann, P. Aluminium induced disease in subjects with and without renal failure - does it help us understand the role of aluminium in Alzheimer's disease? *Alum. Alzheimer's Dis.,* **2001**, 1-36.

[15] Fischer, F.; Matthisson, M.; Herrling, P. List of Drugs in Development for Neurodegenerative Disease. *Neurodegener. Dis.,* **2004**, *1*, 50.

[16] Kwon, M.-O.; Fischer, F.; Matthisson, M.; Herrling, P. List of Drugs in Development for Neurodegenerative Disease. *Neurodegener. Dis.,* **2004**, *1*, 113-152.

[17] Luond, R.M.; Banziger, M.; Frey, P. Preparation of piperidine and piperazine derivatives as inhibitors of the Aβ fibril formation. WO0047571, 2000.

[18] Goldsbury, C.S.; Wirtz, S.; Muller, S.A.; Sunderji, S.; Wicki, P.; Aebi, U.; Frey, P. Studies on the in Vitro Assembly of $A\beta_{1-40}$: Implications for the Search for Aβ Fibril Formation Inhibitors. *J. Struct. Biol.,* **2000**, *130*, 217-231.

[19] Larbig, G.; Pickhardt, M.; Lloyd, D.G.; Schmidt, B.; Mandelkow, E. Screening for inhibitors of tau protein aggregation into Alzheimer paired helical filaments: a ligand based approach results in successful scaffold hopping. *Curr. Alzheimer Res.,* **2007**, *4*, 315-323.

[20] Pickhardt, M.; Larbig, G.; Khlistunova, I.; Coksezen, A.; Meyer, B.; Mandelkow, E.-M.; Schmidt, B.; Mandelkow, E. Phenylthiazolyl-Hydrazide and Its Derivatives Are Potent Inhibitors of τ-Aggregation and Toxicity in Vitro and in Cells. *Biochemistry,* **2007**, *46*, 10016-10023.

[21] Bulic, B.; Pickhardt, M.; Khlistunova, I.; Biernat, J.; Mandelkow, E.M.; Mandelkow, E.; Waldmann, H. Rhodanine-based tau aggregation inhibitors in cell models of tauopathy. *Angew. Chem. Int. Ed. Engl.,* **2007**, *46*, 9215-9.

[22] Howlett, D.R.; George, A.R.; Owen, D.E.; Ward, R.V.; Markwell, R.E. Common structural features determine the effectiveness of carvedilol, daunomycin and rolitetracycline as inhibitors of Alzheimer βamyloid fibril formation. *Biochem. J.,* **1999**, *343*, 419-423.

[23] Courtney, C.; Farrell, D.; Gray, R.; Hills, R.; Lynch, L.; Sellwood, E.; Edwards, S.; Hardyman, W.; Raftery, J.; Crome, P.; Lendon, C.; Shaw, H.; Bentham, P. Long-term donepezil treatment in 565 patients with Alzheimer's disease (AD2000): randomised double-blind trial. *Lancet,* **2004**, *363*, 2105-15.

[24] Jacobsen, J.S. Alzheimer's disease: an overview of current and emerging therapeutic strategies. *Curr. Top. Med. Chem.,* **2002**, *2*, 343-352.

[25] Ikeda, S.; Yamada, Y.; Ikegami, N. Economic Evaluation of Donepezil Treatment for Alzheimer's Disease in Japan. *Dementia Geriatr. Cognit. Disord.,* **2002**, *13*, 33-39.

[26] Carlson, M.C.; Brandt, J.; Steele, C.; Baker, A.; Stern, Y.; Lyketsos, C.G. Predictor index of mortality in dementia patients upon entry into long-term care. *J. Gerontol. A Biol. Sci. Med. Sci.,* **2001**, *56*, M567-70.

[27] AD2000 Collaborative Group, Long-term donepezil treatment in 565 patients with Alzheimer's disease (AD2000): randomised double-blind trial. *Lancet,* **2004**, *363*, 2105-2115.

[28] Schneider, L.S. AD2000: donepezil in Alheimer's disease. *The Lancet,* **2004**, *363*, 2100-2001.

[29] Witt, A.; Macdonald, N.; Kirkpatrick, P. Fresh from the pipeline: memantine hydrochloride. *Nat. Rev. Drug Discov.,* **2004**, *3*, 109-110.

[30] Bachmann, M.F.; Tissot, A.; Ortmann, R.; Lueoend, R.; Staufenbiel, M.; Frey, P. Vaccine compositions containing amyloid β 1-6 antigen epitopes conjugated with virus-like particles. WO 2004016282, 2004.

[31] Schenk, D.; Games, D.; Seubert, P. Immunotherapy with β-amyloid peptide as a potential treatment for Alzheimer's disease. *Neurosci. News,* **2000**, *3*, 46-51.

[32] Nicoll, J.A.R.; Wilkinson, D.; Holmes, C.; Steart, P.; Markham, H.; Weller, R.O. Neuropathology of human Alzheimer disease after immunization with amyloid-bold β peptide: a case report. *Nat. Med.,* **2003**, *9*, 448 - 452.

[33] Greenberg, S.M.; Bacskai, B.J.; Hyman, B.T. Alzheimer disease's double-edged vaccine. *Nat. Med.,* **2003**, *9*, 389 - 397.

[34] Abbott, A. Doctors seek lost data on Alzheimer's vaccine. *Nature,* **2004**, *430*, 715.

[35] Oddo, S.; Billings, L.; Kesslak, J.P.; Cribbs, D.H.; LaFerla, F.M. Aβ Immunotherapy Leads to Clearance of Early, but Not Late, Hyperphosphorylated Tau Aggregates via the Proteasome. *Neuron,* **2004**, *43*, 32132.

[36] Saunders, A.M. Gene identification in Alzheimer's disease. *Pharmacogenomics,* **2001**, *2*, 239-249.

[37] Holmes, C. Genotype and phenotype in Alzheimer's disease. *Br. J. Psychiatry.,* **2002**, *180*, 131-4.

[38] Tanzi, R.E.; Bertram, L. New frontiers in Alzheimer's disease genetics. *Neuron,* **2001**, *32*, 181-4.

[39] Hardy, J. The Alzheimer family of diseases: many etiologies, one pathogenesis? *PNAS,* **1997**, *94*, 2095-7.

[40] Hardy, J.; Myers, A.; Wavrant-De Vrieze, F. Problems and solutions in the genetic analysis of late-onset Alzheimer's disease. *Neurodegener. Dis.,* **2004**, *1*, 213-7.

[41] Bertram, L.; Tanzi, R.E. Dancing in the dark? The status of late-onset Alzheimer's disease genetics. *J. Mol. Neurosci.,* **2001**, *17*, 127.

[42] Fraser, P.E.; Yang, D.-S.; Yu, G.; Lévesque, L.; Nishimura, M.; Arawak, S.; Serpell, L.C.; Rogaev, E.; George-Hyslop, P.S. Presenilin structure, function and role in Alzheimer disease. *BBA-Mol. Basis Dis.,* **2000**, *1502*, 1-15.

[43] Janus, C.; Westaway, D. Transgenic mouse models of Alzheimer's disease. *Physiol. Behav.,* **2001**, *73*, 873 886.

[44] Schmitz, C.; Rutten Bart, P.F.; Pielen, A.; Schafer, S.; Wirths, O.; Tremp, G.; Czech, C.; Blanchard, V.; Multhaup, G.; Rezaie, P.; Korr, H.; Steinbusch Harry, W.M.; Pradier, L.; Bayer Thomas, A. Hippocampal neuron loss exceeds amyloid plaque load in a transgenic mouse model of Alzheimer's disease. *Am. J. Pathol.,* **2004**, *164*, 1495-502.
[45] Eckert, G.P.; Kirsch, C.; Leutz, S.; Wood, W.G.; Muller, W.E. Cholesterol modulates amyloid β-peptide's membrane interactions. *Pharmacopsychiatry,* **2003**, *36 Suppl 2*, S136-43.
[46] Moss, M.L.; White, J.M.; Lambert, M.H.; Andrews, R.C. TACE and other ADAM proteases as targets for drug discovery. *Drug Discov. Today,* **2001**, *6*, 417-426.
[47] Kinoshita, A.; Whelan, C.M.; Smith, C.J.; Berezovska, O.; Hyman, B.T. Direct visualization of the γ-secretase-generated carboxyl-terminal domain of the amyloid precursor protein: association with Fe65 and translocation to the nucleus. *J. Neurochem.,* **2002**, *82*, 839-847.
[48] Kinoshita, A.; Whelan, C.M.; Berezovska, O.; Hyman, B.T. The γ-secretase-generated carboxyl-terminal domain of the amyloid precursor protein induces apoptosis via Tip60 in H4 cells. *J. Biol. Chem.,* **2002**, *277h*, 28530-28536.
[49] Soto, C. Plaque busters: strategies to inhibit amyloid formation in Alzheimer's disease. *Mol. Med. Today,* **1999**, *5*, 343-350.
[50] Kayed, R.; Glabe, C.G. Immunogens and corresponding antibodies specific for high molecular weight aggregation intermediates common to amyloids formed from proteins of differing sequence. WO 2004024090, 2004.
[51] Kayed, R.; Head, E.; Thompson, J.L.; McIntire, T.M.; Milton, S.C.; Cotman, C.W.; Glabe, C.G. Common structure of soluble amyloid oligomers implies common mechanism of pathogenesis. *Science,* **2003**, *300*, 486-9.
[52] Capell, A.; Steiner, H.; Willem, M.; Kaiser, H.; Meyer, C.; Walter, J.; Lammich, S.; Multhaup, G.; Haass, C. Maturation and pro-peptide cleavage of γ-secretase. *J. Biol. Chem.,* **2000**, *275*, 30849-54.
[53] Marcinkeviciene, J.; Luo, Y.; Graciani, N.R.; Combs, A.P.; Copeland, R.A., Mechanism of inhibition of β-site amyloid precursor protein-cleaving enzyme (BACE) by a statine-based peptide. *J. Biol. Chem.,* **2001**, *276*, 23790-23794.
[54] Leung, D.; Abbenante, G.; Fairlie, D.P. Protease Inhibitors: Current Status and Future Prospects. *J. Med. Chem.,* **2000**, *43*, 305-341.
[55] Farzan, M.; Schnitzler, C.E.; Vasilieva, N.; Leung, D.; Choe, H. BACE2, a β-secretase homolog, cleaves at the β–site and within the amyloid-β region of the amyloid-β precursor protein. *PNAS,* **2000**, *97*, 9712-7.
[56] Yan, R.; Munzner, J.B.; Shuck, M.E.; Bienkowski, M.J. BACE2 functions as an alternative α-secretase in cells. *J. Biol. Chem.,* **2001**, *276*, 34019-27.
[57] Westmeyer, G.G.; Willem, M.; Lichtenthaler, S.F.; Lurman, G.; Multhaup, G.; Assfalg-Machleidt, I.; Reiss, K.; Saftig, P.; Haass, C. Dimerization of β-site β-amyloid precursor protein-cleaving enzyme. *J. Biol. Chem.,* **2004**, *279*, 53205-12.
[58] Fischer, F.; Molinari, M.; Bodendorf, U.; Paganetti, P. The disulphide bonds in the catalytic domain of BACE are critical but not essential for amyloid precursor protein processing activity. *J. Neurochem.,* **2002**, *80*, 1079-1088.
[59] Luo, Y.; Bolon, B.; Kahn, S.; Bennett, B.D.; Babu-Khan, S.; Denis, P.; Fan, W.; Kha, H.; Zhang, J.; Gong, Y.; Martin, L.; Louis, J.-C.; Yan, Q.; Richards, W.G.; Citron, M.; Vassar, R. Mice deficient in BACE1, the Alzheimer's β-secretase, have normal phenotype and abolished β-amyloid generation. *Nat. Neurosci.,* **2001**, *4*, 231-232.
[60] Vassar, R. The β-secretase, BACE: a prime drug target for Alzheimer's disease. *J. Mol. Neurosci.,* **2001**, *17*, 157-70.
[61] Gruninger-Leitch, F.; Schlatter, D.; Kung, E.; Nelbock, P.; Dobeli, H. Substrate and inhibitor profile of BACE β-secretase and comparison with other mammalian aspartic proteases. *J. Biol. Chem.,* **2002**, *277*, 4687-4693.
[62] Roggo, S. Inhibition of BACE, a Promising Approach to Alzheimer's Disease Therapy. *Curr. Top. Med. Chem.,* **2002**, *2*, 359-70.
[63] Dominguez, D.-I.; Hartmann, D.; De Strooper, B. BACE1 and Presenilin: Two Unusual Aspartyl Proteases Involved in Alzheimer's Disease. *Neurodegener. Dis.,* **2004**, *1*, 168-174.
[64] Wolfe, M.S.; Haass, C. The role of presenilins in γ-secretase activity. *J. Biol. Chem.,* **2001**, *276*, 54135416.
[65] Ishiura, S. New developments in amyloid secretases. *Dementia Jpn.,* **2000**, *14*, 236-239.
[66] Schmidt, B. Aspartic Proteases Involved in Alzheimer's Disease. *Chem. Bio. Chem.,* **2003**, *4*, 366-378.
[67] John, V.; Beck, J.P.; Bienkowski, M.J.; Sinha, S.; Heinrikson, R.L. Human β-secretase (BACE) and BACE inhibitors. *J. Med. Chem.,* **2003**, *46*, 4625-30.
[68] Grosch, H.-W.; Kunzel, U.; Hummel, M.; Henseler, M.; Sandhoff, K.; Hasilik, A. Trafficking and processing of cathepsin D. *Biomed. Health Res.,* **1997**, *13*, 229-233.
[69] Haass, C. Take five-BACE and the γ-secretase quartet conduct Alzheimer's amyloid β-peptide generation. *EMBO J.,* **2004**, *23*, 483-488.
[70] Hong, L.; Turner, R.T.; Koelsch, G.; Shin, D.; Ghosh, A.K.; Tang, J. Crystal structure of memapsin 2 (β secretase) in complex with an inhibitor OM00-3. *Biochemistry,* **2002**, *41*, 10963-7.
[71] Hong, L.; Koelsch, G.; Lin, X.; Wu, S.; Terzyan, S.; Ghosh, A.K.; Zhang, X.C.; Tang, J. Structure of the protease domain of memapsin 2 (β-secretase) complexed with inhibitor. *Science,* **2000**, *290*, 150-153.
[72] Silvestri, R. Boom in the development of non-peptidic β-secretase (BACE1) inhibitors for the treatment of Alzheimer's disease. *Med. Res. Rev.,* **2008**.
[73] Limongelli, V.; Marinelli, L.; Cosconati, S.; Braun, H.A.; Schmidt, B.; Novellino, E. Ensemble-Docking Approach on BACE-1: Pharmacophore Perception and Guidelines for Drug Design. *Chem. Med. Chem.,* **2007**, *3*, 667-678.
[74] Hong, L.; Tang, J. Flap position of free memapsin 2 (β-secretase), a model for flap opening in aspartic protease catalysis. *Biochemistry,* **2004**, *43*, 4689-95.
[75] Hong, L.; Turner, I.R.T.; Koelsch, G.; Ghosh, A.K.; Tang, J. Memapsin 2 (β-secretase) as a therapeutic target. *Biochem. Soc. Trans.,* **2002**, *30*, 530-4.
[76] Tung, J.S.; Davis, D.L.; Anderson, J.P.; Walker, D.E.; Mamo, S.; Jewett, N.; Hom, R. K.; Sinha, S.; Thorsett, E.D.; John, V. Design of substrate-based inhibitors of human β-secretase. *J. Med. Chem.,* **2002**, *45*, 259-62.
[77] Shuto, D.; Kasai, S.; Kimura, T.; Liu, P.; Hidaka, K.; Hamada, T.; Shibakawa, S.; Hayashi, Y.; Hattori, C.; Szabo, B.; Ishiura, S.; Kiso, Y. KMI-008, a novel β-secretase inhibitor containing a hydroxymethylcarbonyl isostere as a transition-state mimic: design and synthesis of substrate-based octapeptides. *Bioorg. Med. Chem. Lett.,* **2003**, *13*, 4273-6.
[78] Tamamura, H.; Kato, T.; Otaka, A.; Fujii, N. Synthesis of potent β-secretase inhibitors containing a hydroxyethylamine dipeptide isostere and their structure-activity relationship studies. *Org. Biomol. Chem.,* **2003**, *1*, 2468-2473.

[79] Brady, S.F.; Singh, S.; Crouthamel, M.C.; Holloway, M.K.; Coburn, C.A.; Garsky, V. M.; Bogusky, M.; Pennington, M.W.; Vacca, J.P.; Hazuda, D.; Lai, M.T. Rational design and synthesis of selective BACE-1 inhibitors. *Bioorg. Med. Chem. Lett.,* **2004**, *14*, 601-4.
[80] Ghosh, A.K.; Bilcer, G.; Harwood, C.; Kawahama, R.; Shin, D.; Hussain, K.A.; Hong, L.; Loy, J.A.; Nguyen, C.; Koelsch, G.; Ermolieff, J.; Tang, J. Structure-based design: potent inhibitors of human brain memapsin 2 (β-secretase). *J. Med. Chem.,* **2001**, *44*, 2865-8.
[81] Chen, S.H.; Lamar, J.; Guo, D.; Kohn, T.; Yang, H.C.; McGee, J.; Timm, D.; Erickson, J.; Yip, Y.; May, P.; McCarthy, J. P3 cap modified Phe*-Ala series BACE inhibitors. *Bioorg. Med. Chem. Lett.,* **2004**, *14*, 245-50.
[82] Lamar, J.; Hu, J.; Bueno, A.B.; Yang, H.C.; Guo, D.; Copp, J.D.; McGee, J.; Gitter, B.; Timm, D.; May, P.; McCarthy, J.; Chen, S.H. Phe*-Ala-based pentapeptide mimetics are BACE inhibitors: P2 and P3 SAR. *Bioorg. Med. Chem. Lett.,* **2004**, *14*, 239-43.
[83] Hu, B.; Fan, K.Y.; Bridges, K.; Chopra, R.; Lovering, F.; Cole, D.; Zhou, P.; Ellingboe, J.; Jin, G.; Cowling, R.; Bard, J. Synthesis and SAR of bis-statine based peptides as BACE 1 inhibitors. *Bioorg. Med. Chem. Lett.,* **2004**, *14*, 3457-3460.
[84] Hom, R.K.; Fang, L.Y.; Mamo, S.; Tung, J.S.; Guinn, A.C.; Walker, D.E.; Davis, D. L.; Gailunas, A.F.; Thorsett, E.D.; Sinha, S.; Knops, J.E.; Jewett, N.E.; Anderson, J.P.; John, V. Design and synthesis of statine-based cell-permeable peptidomimetic inhibitors of human β-secretase. *J. Med. Chem.,* **2003**, *46*, 1799-802.
[85] Hom, R.K.; Gailunas, A.F.; Mamo, S.; Fang, L.Y.; Tung, J.S.; Walker, D.E.; Davis, D.; Thorsett, E.D.; Jewett, N.E.; Moon, J.B.; John, V. Design and synthesis of hydroxyethylene-based peptidomimetic inhibitors of human β-secretase. *J. Med. Chem.,* **2004**, *47*, 158-64.
[86] Maillaird, M.; Hom, C.; Gailunas, A.; Jagodzinska, B.; Fang, L.Y.; John, V.; Freskos, J.N.; Pulley, S.R.; Beck, J.P.; Tenbrink, R.E. Preparation of substituted amines to treat Alzheimer's disease. WO 0202512, 2002.
[87] Beck, J.P.; Gailunas, A.; Hom, R.; Jagodzinska, B.; John, V.; Maillaird, M. Compounds to treat Alzheimer's disease. WO 0202520, 2002.
[88] Patel, S.; Vuillard, L.; Cleasby, A.; Murray, C.W.; Yon, J. Apo and Inhibitor Complex Structures of BACE (β-secretase). *J. Mol. Biol.,* **2004**, *343*, 407-416.
[89] Uchikawa, O.; Aso, K.; Koike, T.; Tarui, N.; Hirai, K. Preparation of benzamide derivatives as β-secretase inhibitors. WO 2004014843, 2004.
[90] Demont, E.H.; Faller, A.; MacPherson, D.T.; Milner, P.H.; Naylor, A.; Redshaw, S.; Stanway, S.J.; Vesey, D.R.; Walter, D.S. Preparation of hydroxethylamine derivatives for the treatment of Alzheimer's disease. WO 2004050619, 2004.
[91] Pulley, S.R.; Beck, J.P.; Tenbrink, R.E.; Jacobs, J.S. Preparation of macrocycles useful in the treatment of Alzheimer's disease. WO 2002100399, 2002.
[92] Reeder, M.R. Processes for the synthesis of amino acid-related benzyl epoxides used in the production of pharmaceutical agents. WO 2002085877, 2002.
[93] Tenbrink, R.; Maillard, M.; Warpehoski, M. Preparation of substituted hydroxyethylamines as β-secretase inhibitors. WO 0350073, 2003.
[94] Fang, L.Y.; Hom, R.; John, V.; Maillaird, M. Preparation of substituted amines for treating Alzheimer's disease. WO 0202505, 2002.
[95] Fang, L.Y.; John, V. Compounds to treat Alzheimer's disease. WO 0202506, 2002.
[96] Fobian, Y.M.; Freskos, J.N.; Jagodzinska, B. A preparation of 1,3-diamino-2-hydroxypropane derivatives as β-secretase enzyme inhibitors. WO 2004022523, 2004.
[97] Vuillard, L.M.M.; Patel, S.J.; Yon, J.R.; Cleasby, A.; Hamilton, B.J.; Shah, A. Crystal structure of human _-secretase mutants and drug discovery applications. WO 2004011641, 2004.
[98] Yang, W. Preparation of amino carboxamide derivatives as aspartyl protease inhibitors. WO 2004147454, 2004.
[99] Brockhaus, M.; Doebeli, H.; Grueninger, F.; Huguenin, P.; Kitas, E.A.; Nelboeck-Hochstetter, P. Fluorescence and competitive radioligand binding assays for identifying β-secretase inhibitors and for screening agents for treatment of Alzheimer's disease and cerebrovascular amyloidosis. WO 2003125257, 2003.
[100] Brockhaus, M.; Doebeli, H.; Grueninger, F.; Huguenin, P.; Kitas, E.A.; Nelboeck-Hochstetter, P. Assay for identifying β-secretase inhibitors. WO 20030125257, 2003.
[101] Miyamoto, M.; Matsui, J.; Fukumoto, H.; Tarui, N. Preparation of 2-[2-amino- or 2-(*N*-heterocyclyl) ethyl]-6-(4-biphenylylmethoxy)-tetralin derivatives as β-secretase inhibitors. WO 0187293, 2001.
[102] Qiao, L.; Etcheberrigaray, R. Preparation of phosphinylmethyl and phosphorylmethyl succinic and glutaric acid analogs as β-secretase inhibitors useful in the treatment of Alzheimer's disease. WO 2002096897, 2002.
[103] Ramakrishna, N.V.S.; Kumar, E.K.S.V.; Kulkarni, A.S.; Jain, A.K.; Bhat, R.G.; Parikh, S.; Quadros, A.; Deuskar, N.; Kalakoti, B.S. Screening of natural products for new leads as inhibitors of β-amyloid production: Latifolin from Dalbergia sissoo. *Ind. J. Chem. Sect. B. Org. Chem. Incl. Med. Chem.,* **2001**, *40B*, 539-540.
[104] Bhisetti, G.R.S.J.O.; Murcko, M.A.; Lepre, C.A.; Britt, S.D.; Come, J.H.; Deninger, D.D.; Wang, T. Preparation of β-carbolines and other inhibitors of BACE-1 aspartic proteinase useful against Alzheimer's and other BACE-mediated dieseases. WO 2002088101, 2002.
[105] Park, H.; Lee, S. Determination of the active site protonation state of β-secretase from molecular dynamics simulation and docking experiment: implications for structure-based inhibitor design. *J. Am. Chem. Soc.,* **2003**, *125*, 16416-22.
[106] Boss, C.; Bur, D.; Fischli, W.; Jenck, F.; Weller, T. Preparation of piperidines for the treatment of central nervous system disorders. WO 2004009549, 2004.
[107] Boss, C.; Bur, D.; Fischli, W.; Jenck, F.; Weller, T. Preparation of substituted 3- and 4-(aminomethyl) piperidines for use as β-secretase inhibitors in the treatment of Alzheimer's disease. WO 2004002483, 2004.
[108] Coburn, C.A.; Stachel, S.J.; Vacca, J.P. Preparation of phenylcarboxamide derivatives as β-secretase inhibitors for the treatment of Alzheimer's disease. WO 2004043916, 2004.
[109] Coburn, C.A.; Stachel, S.J.; Vacca, J.P. Preparation of macrocyclic β-secretase inhibitors for treatment of Alzheimer's disease. WO 2004062625, 2004.
[110] Holloway, M.K.; Culberson, J.C.; Shpungin, J.; Munshi, S.; Coburn, C.A.; Stachel, S.J.; Jones, K.G.; Loutzenhiser, E.; Gregro, A.R.; Lai, M.-T.; Crouthamel, M.-C.; Pietrak, B. L. Evaluating scoring functions for docking and designing β-secretase inhibitors. *Abstracts of Papers, 228th ACS National Meeting, Philadelphia, PA, United States, August 22-26,* **2004**.
[111] Rajamani, R.; Reynolds, C.H. Modeling the protonation states of the catalytic aspartates in β-secretase. *J. Med. Chem.,* **2004**, *47*, 5159-66.
[112] Tounge, B.A.; Reynolds, C.H. Calculation of the Binding Affinity of β-Secretase Inhibitors Using the Linear Interaction Energy Method. *J. Med. Chem.,* **2003**, *46*, 2074-2082.
[113] Coburn, C.A.; Stachel, S.J.; Li, Y.-M.; Rush, D.M.; Steele, T.G.; Chen-Dodson, E.; Holloway, M.K.; Xu, M.; Huang, Q.; Lai, M.-T.; DiMuzio, J.; Crouthamel, M.-C.; Shi, X.-P.; Sardana, V.; Chen, Z.; Munshi, S.; Kuo, L.; Makara, G.M.; Annis, D.A.; Tadikonda, P.K.; Nash, H.M.; Vacca, J.P. Identification of a Small Molecule Nonpeptide Active Site β-Secretase Inhibitor That Displays a Nontraditional Binding Mode for Aspartyl Proteases. *J. Med. Chem.,* **2004**, *47*, 6117-6119.

[114] Stachel, S.J.; Coburn, C.A.; Steele, T.G.; Jones, K.G.; Loutzenhiser, E.F.; Gregro, A.R.; Rajapakse, H.A.; Lai, M.-T.; Crouthamel, M.-C.; Xu, M.; Tugusheva, K.; Lineberger, J.E.; Pietrak, B.L.; Espeseth, A.S.; Shi, X.-P.; Chen-Dodson, E.; Holloway, M.K.; Munshi, S.; Simon, A.J.; Kuo, L.; Vacca, J.P. Structure-Based Design of Potent and Selective Cell-Permeable Inhibitors of Human β-Secretase (BACE-1) *J. Med. Chem.,* **2004**, *47*, 6447-6450.
[115] Willems, H. Preparation of piperazines as β-amyloid converting enzyme (BACE) inhibitors for the treatment of Alzheimer's disease. WO 2004020422, 2004.
[116] Willems, H.; Gordon, R. Protected amino acid derivatives for the treatment of Alzheimer's disease. GB 2392443, 2004.
[117] Willems, H.; Harris, W.; John, D.E. A preparation of triazinoindole derivatives as inhibitors of β-secretase (BACE), useful in the treatment of Alzheimer's disease. WO 2004063196, 2004.
[118] Willems, H.; Harris, W.H. Preparation of *N*-sulfonyl amino acid derivatives for the treatment of Alzheimer's disease. WO 2004020402, 2004.
[119] De Strooper, B.; Annaert, W. Where notch and Wnt signaling meet: the presenilin hub. *J. Cell Biol.,* **2001**, *152*, F17-F19.
[120] Herreman, A.; Serneels, L.; Annaert, W.; Collen, D.; Schoonjans, L.; De Strooper, B. Total inactivation of γ-secretase activity in presenilin-deficient embryonic stem cells. *Nat. Cell Biol.,* **2000**, *2*, 461-2.
[121] Figueroa, D.J.; Morris, J.A.; Ma, L.; Kandpal, G.; Chen, E.; Li, Y.M.; Austin, C.P. Presenilin-dependent γ-secretase activity modulates neurite outgrowth. *Neurobiol. Dis.,* **2002**, *9*, 49-60.
[122] Kopan, R.; Ilagan, M.X. γ-Secretase: proteasome of the membrane? *Nat. Rev. Mol. Cell Biol.,* **2004**, *5*, 499-504.
[123] Shirotani, K.; Edbauer, D.; Prokop, S.; Haass, C.; Steiner, H. Identification of distinct γ-secretase complexes with different APH-1 variants. *J. Biol. Chem.,* **2004**, *279*, 41340-5.
[124] Cousin, E.; Hannequin, D.; Mace, S.; Dubois, B.; Ricard, S.; Genin, E.; Brun, C.; Chansac, C.; Pradier, L.; Frebourg, T.; Brice, A.; Campion, D.; Deleuze, J.F. No replication of the association between the Nicastrin gene and familial early-onset Alzheimer's disease. *Neurosci. Lett.,* **2003**, *353*, 153-5.
[125] Edbauer, D.; Winkler, E.; Regula, J.T.; Pesold, B.; Steiner, H.; Haass, C. Reconstitution of γ-secretase activity. *Nat. Cell Biol.,* **2003**.
[126] Turner, R.T.; Loy, J.A.; Nguyen, C.; Devasamudram, T.; Ghosh, A.K.; Koelsch, G.; Tang, J. Specificity of memapsin 1 and its implications on the design of memapsin 2 (β-secretase) inhibitor selectivity. *Biochemistry,* **2002**, *41*, 8742-6.
[127] Farmery, M.R.; Tjernberg, L.O.; Pursglove, S.E.; Bergman, A.; Winblad, B.; Naslund, J. Partial Purification and Characterization of γ-Secretase from Post-mortem Human Brain. *J. Biol. Chem.,* **2003**, *278*, 24277-24284.
[128] Weihofen, A.; Binns, K.; Lemberg, M.K.; Ashman, K.; Martoglio, B. Identification of signal peptide peptidase, a presenilin-type aspartic protease. *Science,* **2002**, *296*, 2215-8.
[129] Lichtenthaler, S.F.; Wang, R.; Grimm, H.; Uljon, S.U.; Masters, C.L.; Beyreuther, K. Mechanism of the cleavage specifity of Alzheimer's disease γ-secretase identified by phenylalanine-scanning mutagenesis of the transmembrane domain of the amyloid precursor protein. *PNAS,* **1999**, *96*, 3053-3058.
[130] Kaether, C.; Capell, A.; Edbauer, D.; Winkler, E.; Novak, B.; Steiner, H.; Haass, C. The presenilin *C*-terminus is required for ER-retention, nicastrin-binding and γ-secretase activity. *Embo J.,* **2004**, *23*, 473848.
[131] Wolfe, M.S.; Xia, W.; Ostaszewski, B.L.; Diehl, T.S.; Kimberly, W.T.; Selkoe, D.J. Two transmembrane aspartates in presenilin-1 required for presenilin endoproteolysis and γ-secretase activity. *Nature,* **1999**, *398*, 513-7.
[132] Kimberly, W.T.; Xia, W.; Rahmati, T.; Wolfe, M.S.; Selkoe, D.J. The Transmembrane Aspartates in Presenilin 1 and 2 Are Obligatory for γ-Secretase Activity and Amyloid β-Protein Generation. *J. Biol. Chem.,* **2000**, *275*, 3173-3178.
[133] Paris, D.; Mullan, M.J. Anti-angiogenic and anti-tumoral properties of β- and γ-secretase inhibitors. WO 2004073630, 2004.
[134] Kan, T.; Tominari, Y.; Rikimaru, K.; Morohashi, Y.; Natsugari, H.; Tomita, T.; Iwatsubo, T.; Fukuyama, T. Parallel synthesis of DAPT derivatives and their γ-secretase-inhibitory activity. *Bioorg. Med. Chem. Lett.,* **2004**, *14*, 1983-1985.
[135] Shearman, M.S.; Beher, D.; Clarke, E.E.; Lewis, H.D.; Harrison, T.; Hunt, P.; Nadin, A.; Smith, A.L.; Stevenson, G.; Castro, J.L. L-685,458, an Aspartyl Protease Transition State Mimic, Is a Potent Inhibitor of Amyloid β-Protein Precursor γ-Secretase Activity. *Biochemistry,* **2000**, *39*, 8698-704.
[136] Nadin, A.J.; Stevenson, G.I. Preparation of peptides as γ-secretase inhibitors. WO 0177144, 2001.
[137] Nadin, A.; Owens, A.P.; Castro, J.L.; Harrison, T.; Shearman, M.S. Synthesis and γ-secretase activity of APP substrate-based hydroxyethylene dipeptide isosteres. *Bioorg. Med. Chem. Lett.,* **2003**, *13*, 37-41.
[138] Nadin, A.; López, J.M.S.; Neduvelil, J.G.; Thomas, S.R. A stereocontrolled synthesis of 2*R*-benzyl-5*S*tert-butoxycarbonylamino-4*R*-(tert-butyldimethylsilanyloxy)-6-phenyl-hexanoic acid (Phe-Phe hydroxyethylene dipeptide isostere). *Tetrahedron,* **2001**, *57*, 1861-1864.
[139] Moore, C.L.; Leatherwood, D.D.; Diehl, T.S.; Selkoe, D.J.; Wolfe, M.S. Difluoro Ketone Peptidomimetics Suggest a Large S1 Pocket for Alzheimer's γ-Secretase: Implications for Inhibitor Design. *J. Med. Chem.,* **2000**, *43*, 3434-3442.
[140] Wolfe, M.S. __Secretase inhibitors as molecular probes of presenilin function. *J. Mol. Neurosci.,* **2001**, *17*, 199-204.
[141] Campbell, W.A.; Iskandar, M.K.; Reed, M.L.; Xia, W. Endoproteolysis of presenilin in vitro: inhibition by γ-secretase inhibitors. *Biochemistry,* **2002**, *41*, 3372-9.
[142] Petit, A.; Bihel, F.; Alves da Costa, C.; Pourquie, O.; Checler, F.; Kraus, J.-L. New protease inhibitors prevent γ-secretase-mediated production of Aβ40/42 without affecting Notch cleavage. *Nat. Cell Biol.,* **2001**, *3*, 507-511.
[143] Zhang, L.; Song, L.; Terracina, G.; Liu, Y.; Pramanik, B.; Parker, E. Biochemical Characterization of the γ-Secretase Activity That Produces β-Amyloid Peptides. *Biochemistry,* **2001**, *40*, 5049-5055.
[144] Berezovska, O.; Jack, C.; McLean, P.; Aster, J.C.; Hicks, C.; Xia, W.; Wolfe, M.S.; Kimberly, W.T.; Weinmaster, G.; Selkoe, D.J.; Hyman, B.T. Aspartate mutations in presenilin and γ-secretase inhibitors both impair Notch1 proteolysis and nuclear translocation with relative preservation of Notch1 signaling. *J. Neurochem.,* **2000**, *75*, 583-593.
[145] Wolfe, M.S.; Xia, W.; Moore, C.L.; Leatherwood, D.D.; Ostaszewski, B.; Rahmati, T.; Donkor, I.O.; Selkoe, D.J. Peptidomimetic probes and molecular modeling suggest that Alzheimer's γ-secretase is an intramembrane-cleaving aspartyl protease. *Biochemistry,* **1999**, *38*, 4720-7.
[146] Wolfe, M.S.; Citron, M.; Diehl, T.S.; Xia, W.; Donkor, I.O.; Selkoe, D.J. A Substrate-Based Difluoro Ketone Selectively Inhibits Alzheimer's γ-Secretase Activity. *J. Med. Chem.,* **1998**, *41*, 6-9.
[147] Doerfler, P.; Shearman, M.S.; Perlmutter, R.M. Presenilin-dependent γ-secretase activity modulates thymocyte development. *PNAS,* **2001**, *98*, 9312-9317.
[148] Roncarati, R.; Sestan, N.; Scheinfeld, M.H.; Berechid, B.E.; Lopez, P.A.; Meucci, O.; McGlade, J.C.; Rakic, P.; D'Adamio, L. The γ-secretase-generated intracellular domain of β-amyloid precursor protein binds Numb and inhibits Notch signaling. *PNAS,* **2002**, *99*, 7102-7107.
[149] Das, C.; Wolfe, M.S.; Tsai, J.-Y.; Diehl, T.S. Designed helical peptides as γ-secretase inhibitors. *Abstracts of Papers, 223rd ACS National Meeting, Orlando, FL, United States, April 7-11,* **2002**, MEDI-011.
[150] Wolfe, M.S. Helical peptidomimetics as inhibitors of β-amyloid production, and therapeutic use thereof. WO 2003068168, 2003.

[151] Bihel, F.; Das, C.; Bowman, M.J.; Wolfe, M.S. Discovery of a Subnanomolar Helical D-Tridecapeptide Inhibitor of γ-Secretase. *J. Med. Chem.,* **2004**, *47*, 3931-3933.
[152] Bakshi, P.; Wolfe, M.S. Stereochemical Analysis of (Hydroxyethyl)urea Peptidomimetic Inhibitors of γ-Secretase. *J. Med. Chem.,* **2004**, *47*, 6485-6489.
[153] McLendon, C.; Xin, T.; Ziani-Cherif, C.; Murphy, M.P.; Findlay, K.A.; Lewis, P.A.; Pinnix, I.; Sambamurti, K.; Wang, R.; Fauq, A.; Golde, T.E. Cell-free assays for γ-secretase activity. *FASEB J.,* **2000**, *14*, 2383-6.
[154] Esler, W.P.; Kimberly, W.T.; Ostaszewski, B.L.; Ye, W.; Diehl, T.S.; Selkoe, D.J.; Wolfe, M.S. Activity dependent isolation of the presenilin-γ-secretase complex reveals nicastrin and a γ substrate. *PNAS,* **2002**, *99*, 2720-5.
[155] Kukar, T.L.; Ladd, T.B.; Bann, M.A.; Fraering, P.C.; Narlawar, R.; Maharvi, G.M.; Healy, B.; Chapman, R.; Welzel, A.T.; Price, R.W.; Moore, B.; Rangachari, V.; Cusack, B.; Eriksen, J.; Jansen-West, K.; Verbeeck, C.; Yager, D.; Eckman, C.; Ye, W.; Sagi, S.; Cottrell, B.A.; Torpey, J.; Rosenberry, T.L.; Fauq, A.; Wolfe, M.S.; Schmidt, B.; Walsh, D.M.; Koo, E.H.; Golde, T.E. Substrate-targeting γ-secretase modulators. *Nature,* **2008**, *453*, 925-9.
[156] Dovey, H.F.; John, V.; Anderson, J.P.; Chen, L.Z.; de Saint Andrieu, P.; Fang, L.Y.; Freedman, S.B.; Folmer, B.; Goldbach, E.; Holsztynska, E.J.; Hu, K.L.; Johnson-Wood, K.L.; Kennedy, S.L.; Kholodenko, D.; Knops, J.E.; Latimer, L.H.; Lee, M.; Liao, Z.; Lieberburg, I. M.; Motter, R.N.; Mutter, L.C.; Nietz, J.; Quinn, K.P.; Sacchi, K.L.; Seubert, P.A.; Shopp, G.M.; Thorsett, E.D.; Tung, J.S.; Wu, J.; Yang, S.; Yin, C.T.; Schenk, D.B.; May, P.C.; Altstiel, L.D.; Bender, M.H.; Boggs, L.N.; Britton, T.C.; Clemens, J.C.; Czilli, D.L.; Dieckman-McGinty, D.K.; Droste, J.J.; Fuson, K.S.; Gitter, B.D.; Hyslop, P.A.; Johnstone, E.M.; Li, W.Y.; Little, S.P.; Mabry, T.E.; Miller, F.D.; Audia, J.E. Functional γ-secretase inhibitors reduce β-amyloid peptide levels in brain. *J. Neurochem.,* **2001**, *76*, 173-81.
[157] Audia, J.E.; Britton, T.C.; Droste, J.J.; Folmer, B.K.; Huffman, G.W.; Varghese, J.; Latimer, L.H.; Mabry, T.E.; Nissen, J.S.; Porter, W.J.; Reel, J.K.; Thorsett, E.D.; Tung, J.S.; Wu, J.; Eid, C.N.; Scott, W.L. Methods and compounds for inhibiting β-amyloid peptide release and/or its synthesis. WO 6191166, 2001.
[158] Audia, J.E.B.T.C.; Droste, J.J.; Folmer, B.K.; Huffman, G.W.; John, V.; Latimer, L.H.; Mabry, T.E.; Nissen, J.S.; Porter, W.J.; Reel, J.K.; Thorsett, E.D.; Tung, J.S.; Eid, C.N.; Scott, W.L. Preparation of *N*(phenylacetyl)di- and tripeptide derivatives for inhibiting β-amyloid peptide release. WO 9822494, 1998.
[159] Larbig, G.; Zall, A.; Schmidt, B. Inhibitors Designed for Presenilin 1 utilizing by Means of Aspartic Acid Activation. *Helv. Chim. Acta,* **2004**, *87*, 2334-2340.
[160] Garofalo, A.W.; Wone, D.W.G.; Phuc, A.; Audia, J.E.; Bales, C.A.; Dovey, H.F.; Dressen, D.B.; Folmer, B.; Goldbach, E.G.; Guinn, A.C.; Latimer, L.H.; Mabry, T.E.; Nissen, J.S.; Pleiss, M.A.; Sohn, S.; Thorsett, E.D.; Tung, J.S.; Wu, J. A Series of C-Terminal Amino Alcohol Dipeptide Aβ Inhibitors. *Bioorg. Med. Chem. Lett.,* **2002**, *12*, 3051-3053.
[161] Hutton, M.; Lewis, J.; Dickson, D.; Yen, S.H.; McGowan, E. Analysis of tauopathies with transgenic mice. *Trends Mol. Med.,* **2001**, *7*, 467-470.
[162] Hadland, B.K.; Manley, N.R.; Su, D.-M.; Longmore, G.D.; Moore, C.L.; Wolfe, M.S.; Schroeter, E.H.; Kopan, R. γ-Secretase inhibitors repress thymocyte development. *PNAS,* **2001**, *98*, 7487-7491.
[163] Fuwa, H.; Takahashi, Y.; Konno, Y.; Watanabe, N.; Miyashita, H.; Sasaki, M.; Natsugari, H.; Kan, T.; Fukuyama, T.; Tomita, T.; Iwatsubo, T. Divergent Synthesis of Multifunctional Molecular Probes To Elucidate the Enzyme Specificity of Dipeptidic γ-Secretase Inhibitors. *ACS Chem. Biol.,* **2007**, *2*, 408-418.
[164] Wong, G.T.; Manfra, D.; Poulet, F.M.; Zhang, Q.; Josien, H.; Bara, T.; Engstrom, L.; Pinzon-Ortiz, M.; Fine, J.S.; Lee, H.J.; Zhang, L.; Higgins, G.A.; Parker, E.M. Chronic treatment with the γ-secretase inhibitor LY-411,575 inhibits β-amyloid peptide production and alters lymphopoiesis and intestinal cell differentiation. *J. Biol. Chem.,* **2004**, *279*, 12876-82.
[165] Fleisher, A.S.; Raman, R.; Siemers, E.R.; Becerra, L.; Clark, C.M.; Dean, R.A.; Farlow, M.R.; Galvin, J.E.; Peskind, E.R.; Quinn, J.F.; Sherzai, A.; Sowell, B.B.; Aisen, P.S.; Thal, L.J. Phase 2 safety trial targeting amyloid-β production with a γ-secretase inhibitor in Alzheimer disease. *Arch. Neurol.,* **2008**, *65*, 1031-8.
[166] Iwata, N.; Saido, T.C. Catabolism of β-amyloid peptide in brain. *Dementia Jpn.,* **2000**, *14*, 80-88.
[167] Iwata, N.; Tsubuki, S.; Takaki, Y.; Watanabe, K.; Sekiguchi, M.; Hosoki, E.; Kawashima-Morishima, M.; Lee, H.-J.; Hama, E.; Sekine-Aizawa, Y.; Saido, T.C. Identification of the major $A\beta_{1-42}$-degrading catabolic pathway in brain parenchyma: Suppression leads to biochemical and pathological deposition. *Nat. Med.,* **2000**, *6*, 143-150.
[168] Abraham, C.R.; McGraw, W.T.; Slot, F.; Yamin, R. a1-antichymot rypsin inhibits Aβ degradation in vitro and in vivo. *Ann. N.Y. Acad. Sci.,* **2000**, *920*, 245-248.
[169] Smith, D.W.; Munoz, B.; Srinivasan, K.; Bergstrom, C.P.; Chaturvedula, P.V.; Deshpande, M.S.; Keavy, D.J.; Lau, W.Y.; Parker, M.F.; Sloan, C.P.; Wallace, O.B.; Wang, H.H. Preparation of sulfonamide derivs. as amyloid β production inhibitors useful in treating or preventing diseases related to Aβ. WO 2000050391, 2000.
[170] Rishton, G.M.; Retz, D.M.; Tempest, P.A.; Novotny, J.; Kahn, S.; Treanor, J.J.S.; Lile, J. D.; Citron, M. Fenchylamine Sulfonamide Inhibitors of Amyloid Peptide Production by the γ-Secretase Proteolytic Pathway: Potential Small-Molecule Therapeutic Agents for the Treatment of Alzheimer's Disease. *J. Med. Chem.,* **2000**, *43*, 2297-2299.
[171] Belanger, P.C.; Collins, I.J.; Hannam, J.C.; Harrison, T.; Lewis, S.J.; Madin, A.; McIver, E.G.; Nadin, A.J.; Neduvelil, J.G.; Shearman, M.S.; Smith, A.L.; Sparey, T.J.; Stevenson, G.I.; Teall, M.R. Synthesis of sulfonamido-substituted bridged bicycloalkyl derivatives as γ-secretase inhibitors. WO 20010170677, 2001.
[172] Olson, R.E.; Maduskuie, T.P.; Thomas, L.A. Preparation of succinoylaminoazepinones and related compounds as inhibitors of Aβ-peptide production. WO 0007995, 2000.
[173] Seiffert, D.; Bradley, J.D.; Rominger, C.M.; Rominger, D.H.; Yang, F.; Meredith, J.E., Jr.; Wang, Q.; Roach, A.H.; Thompson, L.A.; Spitz, S.M.; Higaki, J.N.; Prakash, S.R.; Combs, A.P.; Copeland, R.A.; Arneric, S.P.; Hartig, P.R.; Robertson, D.W.; Cordell, B.; Stern, A.M.; Olson, R.E.; Zaczek, R. Presenilin1 and -2 are molecular targets for γ-secretase inhibitors. *J. Biol. Chem.,* **2000**, *275*, 34086-91.
[174] Thompson, L.A. Amino lactam sulfonamides as inhibitors of Aβ protein production. WO 0127091, 2001.
[175] Thompson, L.A.; Han, A.Q. Preparation of amino lactam sulfonamides as inhibitors of Aβ-protein production. WO 0127108, 2001.
[176] Teall, M.R. γ-secretase inhibitors. WO 20020013315, 2002.
[177] Fuchs, K.; Romig, M.; Mendla, K.; Briem, H.; Fechteler, K. Preparation of novel imidazopyridines as β-amyloid formation inhibitors. WO 2002014313, 2002.
[178] Himmelsbach, F.; Fuchs, K.; Briem, H.; Fechteler, K.; Kostka, M.; Dorner-Ciossek, C.; Bornemann, K.; Klinder, K. Preparation of diaminopyrimidines as inhibitors of β-amyloid formation or its release. WO 2003032994, 2003.
[179] Otto, M.; Cepek, L.; Ratzka, P.; Doehlinger, S.; Boekhoff, I.; Wiltfang, J.; Irle, E.; Pergande, G.; Ellers-Lenz, B.; Windl, O.; Kretzschmar, H.A.; Poser, S.; Prange, H. Efficacy of flupirtine on cognitive function in patients with CJD: A double-blind study. *Neurology,* **2004**, *62*, 714-8.
[180] Churcher, I.; Williams, S.; Kerrad, S.; Harrison, T.; Castro, J.L.; Shearman, M.S.; Lewis, H.D.; Clarke, E.E.; Wrigley, J.D.; Beher, D.;

Tang, Y.S.; Liu, W. Design and synthesis of highly potent benzodiazepine γ-secretase inhibitors: preparation of (2*S*,3*R*)-3-(3,4-difluorophenyl)-2-(4-fluorophenyl)-4-hydroxy-*N*((3*S*)-1-methyl-2-oxo-5-phenyl-2,3-dihydro-1*H*-benzo[e][1,4]-diazepin-3-yl)butyramide by use of an asymmetric Ireland-Claisen rearrangement. *J. Med. Chem.,* **2003**, *46*, 2275-8.

[181] Churcher, I.; Ashton, K.; Butcher, J.W.; Clarke, E.E.; Harrison, T.; Lewis, H.D.; Owens, A.P.; Teall, M.R.; Williams, S.; Wrigley, J.D.J. A new series of potent benzodiazepine γ-secretase inhibitors. *Bioorg. Med. Chem. Lett.,* **2003**, *13*, 179-183.

[182] Lewis, H.D.; Perez Revuelta, B.I.; Nadin, A.; Neduvelil, J.G.; Harrison, T.; Pollack, S.J.; Shearman, M.S. Catalytic site-directed γ-secretase complex inhibitors do not discriminate pharmacologically between Notch S3 and β-APP cleavages. *Biochemistry,* **2003**, *42*, 7580-6.

[183] Bowers, S.; Garofalo, A.W.; Hom, R.K.; Konradi, A.W.; Mattson, M.N.; Neitzel, M.L.; Semko, C.M.; Truong, A.P.; Wu, J.; Xu, Y.-Z. Preparation of bridged *N*-cyclic sulfonamide compounds as inhibitors of γ-secretase. WO 2007022502, 2007.

[184] Konradi, A.W.; Mattson, M.N.; Semko, C.M.; Ye, X.M. Preparation of bridged *N*-bicyclic sulfonamides as inhibitors of γ-secretase. WO 2007024651, 2007.

[185] Barten, D.M.; Guss, V.L.; Corsa, J.A.; Loo, A.; Hansel, S.B.; Zheng, M.; Munoz, B.; Srinivasan, K.; Wang, B.; Robertson, B.J.; Polson, C.T.; Wang, J.; Roberts, S.B.; Hendrick, J.P.; Anderson, J.J.; Loy, J.K.; Denton, R.; Verdoorn, T.A.; Smith, D.W.; Felsenstein, K.M. Dynamics of β-Amyloid Reductions in Brain, Cerebrospinal Fluid, and Plasma of β-Amyloid Precursor Protein Transgenic Mice Treated with a γ-Secretase Inhibitor. *J. Pharmacol. Exp. Ther.,* **2005**, *312*, 635-643.

[186] Josien, H.B.; Clader, J.W.; Bara, T.A.; Xu, R.; Li, H.; Pissarnitski, D.; Zhao, Z. Preparation of substituted *N*-arylsulfonylheterocyclic amines as γ-secretase inhibitors. WO 2006004880, 2006.

[187] Zhao, B.; Yu, M.; Neitzel, M.; Marugg, J.; Jagodzinski, J.; Lee, M.; Hu, K.; Schenk, D.; Yednock, T.; Basi, G. Identification of γ-secretase inhibitor potency determinants on presenilin. *J. Biol. Chem.,* **2008**, *283*, 2927-38.

[188] Beher, D.; Bettati, M.; Checksfield, G.D.; Churcher, I.; Doughty, V.A.; Oakley, P.J.; Quddus, A.; Teall, M.R.; Wrigley, J.D. Preparation of tetrahydrocarbazole-1-alkanoic acids for the treatment of Alzheimer's disease and related conditions. WO 2005013985, 2005.

[189] Wilson, F.; Reid, A.; Reader, V.; Harrison, R.J.; Sunose, M.; Hernandez-Perni, R.; Major, J.; Boussard, C.; Smelt, K.; Taylor, J.; Leformal, A.; Cansfield, A.; Burckhardt, S. Preparation of biphenylacetic acids as γ–secretase modulators for the treatment of Alzheimer's disease. WO 2006045554, 2006.

[190] Ramsden, N.; Wilson, F. Use of *S*-enantiomers of γ-substituted aryl acetic acids for the prevention of alzheimer's disease. WO 2006048219, 2006.

[191] Narlawar, R.; Perez Revuelta, B.I.; Baumann, K.; Schubenel, R.; Haass, C.; Steiner, H.; Schmidt, B. *N*-Substituted carbazolyloxyacetic acids modulate Alzheimer associated γ-secretase. *Bio. Med. Chem. Lett.,* **2007**, *17*, 176-82.

[192] Serradji, N.; Bensaid, O.; Martin, M.; Kan, E.; Dereuddre-Bosquet, N.; Redeuilh, C.; Huet, J.; Heymans, F.; Lamouri, A.; Clayette, P.; Dong, C.Z.; Dormont, D.; Godfroid, J.J. Structure-activity relationships in platelet-activating factor (PAF). 10. From PAF antagonism to inhibition of HIV-1 replication. *J. Med. Chem.,* **2000**, *43*, 2149-54.

[193] Weggen, S.; Eriksen, J.L.; Das, P.; Sagi, S.A.; Wang, R.; Pietrizik, C.U.; Findlay, K.A.; Smith, T.E.; Murphy, M.P.; Bulter, T.; Kang, D.E.; Marquez-Sterling, N.; Golde, T.E.; Koo, E.H. A subset of NSAIDs lower amyloidogenic $A\beta_{42}$ independently of cyclooxygenase activity. *Nature,* **2001**, *414*, 212-216.

[194] Weggen, S.; Eriksen, J.L.; Sagi, S.A.; Pietrzik, C.U.; Golde, T.E.; Koo, E.H. Aβ42-lowering Nonsteroidal Anti-inflammatory Drugs Preserve Intramembrane Cleavage of the Amyloid Precursor Protein (APP) and ErbB-4 Receptor and Signaling through the APP Intracellular Domain. *J. Biol. Chem.,* **2003**, *278*, 3074830754.

[195] in 't Veld, B.A.; Ruitenberg, A.; Hofman, A.; Launer, L.J.; van Duijn, C.M.; Stijnen, T.; Breteler, M.M.B.; Stricker, B.H.C. Nonsteroidal Antiinflammatory Drugs and the Risk of Alzheimer's Disease. *N. Engl. J. Med.,* **2001**, *345*, 1515-1521.

[196] Zhou, Y.; Su, Y.; Li, B.; Liu, F.; Ryder, J.W.; Wu, X.; Gonzalez-DeWhitt, P.A.; Gelfanova, V.; Hale, J.E.; May, P.C.; Paul, S.M.; Ni, B. Nonsteroidal Anti-Inflammatory Drugs Can Lower Amyloidogenic $A\beta_{42}$ by Inhibiting Rho. *Science,* **2003**, *302*, 1215-1218.

[197] Lanz, T.A.; Hosley, J.D.; Adams, W.J.; Merchant, K.M. Studies of Aβ pharmacodynamics in the brain, cerebrospinal fluid, and plasma in young (plaque-free) Tg2576 mice using the _-secretase inhibitor N2[(2S)-2-(3,5-difluorophenyl)-2-hydroxyethanoyl]-N1-[(7S)-5-methyl-6-oxo-6,7-dihydro-5Hdibenzo[b,d]azepin-7-yl]-L-alaninamide (LY-411575). J. Pharmacol. Exp. Ther., 2004, 309, 49-55.

[198] Eriksen, J.L.; Sagi, S.A.; Smith, T.E.; Weggen, S.; Das, P.; McLendon, D.C.; Ozols, V.V.; Jessing, K.W.; Zavitz, K.H.; Koo, E.H.; Golde, T.E. NSAIDs and enantiomers of flurbiprofen target g-secretase and lower $A\beta_{42}$ in vivo. *J. Clin. Invest.,* **2003**, *112*, 440-449.

[199] Beher, D.; Clarke, E.E.; Wrigley, J.D.J.; Martin, A.C.L.; Nadin, A.; Churcher, I.; Shearman, M.S. Selected Non-steroidal Anti-inflammatory Drugs and Their Derivatives Target γ-Secretase at a Novel Site: Evidence for an allosteric mechanism. *J. Biol. Chem.,* **2004**, *279*, 43419-43426.

[200] Geerts, H. Drug evaluation: (R)-flurbiprofen-an enantiomer of flurbiprofen for the treatment of Alzheimer's disease. *IDrugs,* **2007**, *10*, 121-33.

[201] Page, R.M.; Baumann, K.; Tomioka, M.; Perez-Revuelta, B.I.; Fukumori, A.; Jacobsen, H.; Flohr, A.; Luebbers, T.; Ozmen, L.; Steiner, H.; Haass, C. Generation of $A\beta_{38}$ and $A\beta_{42}$ is independently and differentially affected by familial Alzheimer disease-associated presenilin mutations and γ-secretase modulation. *J. Biol. Chem.,* **2008**, *283*, 677-83.

[202] Eckert, G.P.; Wood, W.G.; Muller, W.E. Statins: drugs for Alzheimer's disease? *J. Neural. Transm.,* **2005**, *112*, 1057-71.

[203] Cucchiara, B.; Kasner, S.E. Use of statins in CNS disorders. *J. Neurol. Sci.,* **2001**, *187*, 81-89.

[204] Fassbender, K.; Simons, M.; Bergmann, C.; Stroick, M.; Lutjohann, D.; Keller, P.; Runz, H.; Kuhl, S.; Bertsch, T.; Von Bergmann, K.; Hennerici, M.; Beyreuther, K.; Hartmann, T. Simvastatin strongly reduces levels of Alzheimer's disease β-amyloid peptides $A\beta_{42}$ and $A\beta_{40}$ in vitro and in vivo. *PNAS,* **2001**, *98*, 5856-5861.

[205] Simons, M.; Keller, P.; Dichgans, J.; Schulz, J.B. Cholesterol and Alzheimer's disease: Is there a link? *Neurology,* **2001**, *57*, 1089-1093.

[206] Riddell, D.R.; Christie, G.; Hussain, I.; Dingwall, C. Compartmentalization of β-secretase (Asp2) into low-buoyant density, noncaveolar lipid rafts. *Curr. Biol.,* **2001**, *11*, 1288-1293.

[207] Kojro, E.; Gimpl, G.; Lammich, S.; Marz, W.; Fahrenholz, F. Low cholesterol stimulates the nonamyloidogenic pathway by its effect on the α-secretase ADAM 10. *PNAS,* **2001**, *98*, 5815-5820.

[208] George, A.J.; Holsinger, R.M.D.; McLean, C.A.; Laughton, K.M.; Beyreuther, K.; Evin, G.; Masters, C.L.; Li, Q.-X. APP intracellular domain is increased and soluble Aβ is reduced with diet-induced hypercholesterolemia in a transgenic mouse model of Alzheimer disease. *Neurobiol. Dis.,* **2004**, *16*, 124132.

[209] Eckert, G.P.; Kirsch, C.; Leutz, S.; Wood, W.G.; Muller, W.E. Cholesterol modulates amyloid β-peptide's membrane interactions. *Pharmacopsychiatry,* **2003**, *36 Suppl 2*, S136-43.

[210] Refolo, L.M.; Pappolla, M.A.; LaFrancois, J.; Malester, B.; Schmidt, S.D.; Thomas-Bryant, T.; Tint, G.S.; Wang, R.; Mercken, M.; Petanceska, S.S.; Duff, K.E. A cholesterol-lowering drug reduces β-amyloid pathology in a transgenic mouse model of Alzheimer's disease. *Neurobiol. Dis.,* **2001**, *8*, 890-9.

[211] Bayer, T.A.; Schaefer, S.; Simons, A.; Kemmling, A.; Kamer, T.; Tepest, R.; Eckert, A.; Schuessel, K.; Eikenberg, O.; Sturchler-pierrat, C.; Abramowski, D.; Staufenbiel, M.; Multhaup, G. Dietary Cu stabilizes brain superoxide dismutase 1 activity and reduces amyloid Aβ production in APP23 transgenic mice. *PNAS,* **2003**, *100*, 14187-14192.
[212] Regland, B.; Lehmann, W.; Abedini, I.; Blennow, K.; Jonsson, M.; Karlsson, I.; Sjoegren, M.; Wallin, A.; Xilinas, M.; Gottfries, C.-G. Treatment of Alzheimer's Disease with Clioquinol. *Dement. Geriatr. Cogn.,* **2001**, *12*, 408-414.
[213] Melov, S.`… and C is for Clioquinol' - the AβCs of Alzheimer's disease. *Trends. Neurosci.,* **2002**, *25*, 1214.
[214] Treiber, C.; Simons, A.; Strauss, M.; Hafner, M.; Cappai, R.; Bayer, T.A.; Multhaup, G. Clioquinol mediates copper uptake and counteracts copper efflux activities of the amyloid precursor protein of Alzheimer's disease. *J. Biol. Chem.,* **2004**, *279*, 51958-64.
[215] Barnham, K.J.; Gautier, E.C.L.; Kok, G.B.; Krippner, G. Preparation of 8-hydroxyquinolines for treatment of neurological conditions. WO 2004007461, 2004.
[216] Lannfelt, L.; Blennow, K.; Zetterberg, H.; Batsman, S.; Ames, D.; Harrison, J.; Masters, C.L.; Targum, S.; Bush, A.I.; Murdoch, R.; Wilson, J.; Ritchie, C.W. Safety, efficacy, and biomarker findings of PBT2 in targeting Aβ as a modifying therapy for Alzheimer's disease: a phase IIa, double-blind, randomised, placebo-controlled trial. *Lancet Neurol.,* **2008**, *7*, 779-786.
[217] Marksteiner, J.; Hinterhuber, H.; Humpel, C. Cerebrospinal fluid biomarkers for diagnosis of Alzheimer's disease: β-amyloid(1-42), tau, phospho-tau-181 and total protein. *Drugs Today,* **2007**, *43*, 423-431.
[218] Brys, M.; Mosconi, L.; De Santi, S.; Rich, K.; de Leon, M.J. Cerebrospinal fluid biomarkers for mild cognitive impairment. *Aging Health,* **2006**, *2*, 111-121.
[219] Parnetti, L.; Lanari, A.; Silvestrelli, G.; Saggese, E.; Reboldi, P. Diagnosing prodromal Alzheimer's disease: Role of CSF biochemical markers. *Mech. Ageing Dev.,* **2006**, *127*, 129-132.
[220] Mosconi, L.; Sorbi, S.; de Leon, M.J.; Li, Y.; Nacmias, B.; Myoung, P.S.; Tsui, W.; Ginestroni, A.; Bessi, V.; Fayyazz, M.; Caffarra, P.; Pupi, A. Hypometabolism exceeds atrophy in presymptomatic early-onset familial Alzheimer's disease. *J. Nucl. Med.,* **2006**, *47*, 1778-1786.
[221] Devanand, D.P.; Pradhaban, G.; Liu, X.; Khandji, A.; De Santi, S.; Segal, S.; Rusinek, H.; Pelton, G.H.; Honig, L.S.; Mayeux, R.; Stern, Y.; Tabert, M.H.; de Leon, M.J. Hippocampal and entorhinal atrophy in mild cognitive impairment: prediction of Alzheimer disease. *Neurology,* **2007**, *68*, 828-36.
[222] Strassner, B. Coherences between cerebral glucose metabolism (F-18-FDG-PET), genetic marker (APOE) and biomarkers (TAU and β -Amyloid in liquor cerebrospinalis) in patients with Alzheimer's disease (AD) and patients with (mild cognitive impairment MCI). 2008.
[223] Ng, S.; Villemagne, V.L.; Berlangieri, S.; Lee, S.-T.; Cherk, M.; Gong, S.J.; Ackermann, U.; Saunder, T.; Tochon-Danguy, H.; Jones, G.; Smith, C.; O'Keefe, G.; Masters, C.L.; Rowe, C.C. Visual assessment versus quantitative assessment of ^{11}C-PIB PET and ^{18}F-FDG PET for detection of Alzheimer's disease. *J. Nucl. Med.,* **2007**, *48*, 547-552.
[224] Shoghi-Jadid, K.; Small Gary, W.; Agdeppa Eric, D.; Kepe, V.; Ercoli Linda, M.; Siddarth, P.; Read, S.; Satyamurthy, N.; Petric, A.; Huang, S.-C.; Barrio Jorge, R. Localization of neurofibrillary tangles and β-amyloid plaques in the brains of living patients with Alzheimer disease. *Am. J. Geriatr. Psychiatry,* **2002**, *10*, 24-35.
[225] Klunk, W.E.; Engler, H.; Nordberg, A.; Wang, Y.; Blomqvist, G.; Holt, D.P.; Bergstrom, M.; Savitcheva, I.; Huang, G.-f.; Estrada, S.; Ausen, B.; Debnath, M.L.; Barletta, J.; Price, J.C.; Sandell, J.; Lopresti, B.J.; Wall, A.; Koivisto, P.; Antoni, G.; Mathis, C.A.; Langstrom, B. Imaging brain amyloid in Alzheimer's disease with Pittsburgh compound-B. *Ann. Neurol.,* **2004**, *55*, 306-319.
[226] Verhoeff Nicolaas, P.L.G.; Wilson Alan, A.; Takeshita, S.; Trop, L.; Hussey, D.; Singh, K.; Kung Hank, F.; Kung, M.-P.; Houle, S. In-vivo imaging of Alzheimer disease β-amyloid with [^{11}C]SB-13 PET. *Am. J. Geriatr. Psychiatry,* **2004**, *12*, 584-95.
[227] Mathis, C.; Lopresti, B.; Mason, N.; Price, J.; Flatt, N.; Bi, W.; Ziolko, S.; DeKosky, S.; Klunk, W. Comparison of the amyloid imaging agents [F-18]3'-F-PIB and [C-11]PIB in Alzheimer's disease and control subjects. In **2007**, Vol. *48*, pp 56P-b.
[228] Kudo, Y.; Okamura, N.; Furumoto, S.; Tashiro, M.; Furukawa, K.; Maruyama, M.; Itoh, M.; Iwata, R.; Yanai, K.; Arai, H. 2-(2-[2-dimethylaminothiazol-5-yl]ethenyl)-6-(2-[fluoro]ethoxy)benzoxazole: a novel PET agent for in vivo detection of dense amyloid plaques in Alzheimer's disease patients. *J. Nucl. Med.,* **2007**, *48*, 553-561.
[229] Rowe, C.; Ackerman, U.; Browne, W.; Mulligan, R.; Pike, K.L.; O'Keefe, G.; Tochon-Danguay, H.; Chan, G.; Berlangieri, S.U.; Jones, G.; Dickinson-Rowe, K.L.; Kung, H.P.; Zhang, W.; Kung, M.P.; Skovronsky, D.; Dyrks, T.; Hall, G.; Krause, S.; Friebe, M.; Lehman, L.; Lindemann, S.; Dinkelborg, L.M.; Masters, C.L.; Villemagne, V.L. Imaging of amyloid beta in Alzheimer's disease with 18F-BAY94-9172, a novel PET tracer: proof of mechanism. *Lancet Neurol.,* **2008**, *7*, 129-135.
[230] Seneca, N.; Cai, L.; Liow, J.-S.; Zoghbi Sami, S.; Gladding Robert, L.; Hong, J.; Pike Victor, W.; Innis Robert, B. Brain and whole-body imaging in nonhuman primates with [^{11}C]MeS-IMPY, a candidate radioligand for β-amyloid plaques. *Nucl. Med. Biol.,* **2007**, *34*, 681-9.
[231] Cai, L.; Liow, J.-S.; Zoghbi, S.S.; Cuevas, J.; Baetas, C.; Hong, J.; Shetty, H.U.; Seneca, N.M.; Brown, A.K.; Gladding, R.; Temme, S.S.; Herman, M.M.; Innis, R.B.; Pike, V.W. Synthesis and Evaluation of N-Methyl and S-Methyl 11C-Labeled 6-Methylthio-2-(4'-N,N-dimethylamino)phenylimidazo[1,2a]pyridines as Radioligands for Imaging β-Amyloid Plaques in Alzheimer's Disease. *J. Med. Chem.,* **2008**, *51*, 148-158.
[232] Braak, H.; Braak, E. Staging of Alzheimer's disease-related neurofibrillary changes. *Neurobiol. Aging,* **1995**, *16*, 271-8; discussion 278-84.
[233] Klunk, W.E.; Lopresti, B.J.; Ikonomovic, M.D.; Lefterov, I.M.; Koldamova, R.P.; Abrahamson, E.E.; Debnath, M.L.; Holt, D.P.; Huang, G.-f.; Shao, L.; DeKosky, S.T.; Price, J.C.; Mathis, C.A. Binding of the positron emission tomography tracer pittsburgh compound-B reflects the amount of amyloid-β in Alzheimer's disease brain but not in transgenic mouse brain. *J. Neurosci.,* **2005**, *25*, 10598-10606.
[234] Engler, H.; Forsberg, A.; Almkvist, O.; Blomquist, G.; Larsson, E.; Savitcheva, I.; Wall, A.; Ringheim, A.; Langstrom, B.; Nordberg, A. Two-year follow-up of amyloid deposition in patients with Alzheimer's disease. *Brain,* **2006**, *129*, 2856-66.
[235] Forsberg, A.; Engler, H.; Almkvist, O.; Blomquist, G.; Hagman, G.; Wall, A.; Ringheim, A.; Langstrom, B.; Nordberg, A. PET imaging of amyloid deposition in patients with mild cognitive impairment. *Neurobiol Aging,* **2008**, *29*, 1456-65.
[236] Kemppainen, N.M.; Aalto, S.; Wilson, I.A.; Naagren, K.; Helin, S.; Brueck, A.; Oikonen, V.; Kailajaervi, M.; Scheinin, M.; Viitanen, M.; Parkkola, R.; Rinne, J.O. PET amyloid ligand [^{11}C]PIB uptake is increased in mild cognitive impairment. *Neurology,* **2007**, *68*, 1603-1606.
[237] Pike Kerryn, E.; Savage, G.; Villemagne Victor, L.; Ng, S.; Moss Simon, A.; Maruff, P.; Mathis Chester, A.; Klunk William, E.; Masters Colin, L.; Rowe Christopher, C. Beta-amyloid imaging and memory in non-demented individuals: evidence for preclinical Alzheimer's disease. *Brain,* **2007**, *130*, 2837-44.
[238] Rabinovici, G.D.; Furst, A.J.; O'Neil, J.P.; Racine, C.A.; Mormino, E.C.; Baker, S.L.; Chetty, S.; Patel, P.; Pagliaro, T.A.; Klunk, W.E.; Mathis, C.A.; Rosen, H.J.; Miller, B.L.; Jagust, W.J. ^{11}C-PIB PET imaging in Alzheimer disease and frontotemporal lobar degeneration. *Neurology,* **2007**, *68*, 1205-12.
[239] Engler, H.; Santillo Alexander, F.; Wang Shu, X.; Lindau, M.; Savitcheva, I.; Nordberg, A.; Lannfelt, L.; Langstrom, B.; Kilander, L. In vivo amyloid imaging with PET in frontotemporal dementia. *Eur. J. Nucl. Med. Mol. Imaging,* **2008**, *35*, 100-6.

[240] Drzezga, A.; Grimmer, T.; Henriksen, G.; Stangier, I.; Perneczky, R.; Diehl-Schmid, J.; Mathis Chester, A.; Klunk William, E.; Price, J.; DeKosky, S.; Wester, H.-J.; Schwaiger, M.; Kurz, A. Imaging of amyloid plaques and cerebral glucose metabolism in semantic dementia and Alzheimer's disease. *Neuroimage,* **2008**, *39*, 619-33.
[241] Nordberg, A. Amyloid imaging in Alzheimer's disease. *Neuropsychologia,* **2008**, *46*, 1636-41.
[242] Fein, J.A.; Sokolow, S.; Miller, C.A.; Vinters, H.V.; Yang, F.; Cole, G.M.; Gylys, K.H. Co-localization of amyloid beta and tau pathology in Alzheimer's disease synaptosomes. *Am. J. Pathol.,* **2008**, *172*, 16831692.
[243] Oddo, S.; Caccamo, A.; Kitazawa, M.; Tseng, B.P.; LaFerla, F.M. Amyloid deposition precedes tangle formation in a triple transgenic model of Alzheimer's disease. *Neurobiol. Aging,* **2003**, *24*, 1063-1070.
[244] Ono, M.; Wilson, A.; Nobrega, J.; Westaway, D.; Verhoeff, P.; Zhuang, Z.-P.; Kung, M.-P.; Kung Hank, F. ^{11}C-labeled stilbene derivatives as Abeta-aggregate-specific PET imaging agents for Alzheimer's disease. *Nucl. Med. Biol.,* **2003**, *30*, 565-71.
[245] Kung, M.-P.; Hou, C.; Zhuang, Z.-P.; Skovronsky, D.; Kung Hank, F. Binding of two potential imaging agents targeting amyloid plaques in postmortem brain tissues of patients with Alzheimer's disease. *Brain Res.,* **2004**, *1025*, 98-105.
[246] Henriksen, G.; Yousefi Behrooz, H.; Drzezga, A.; Wester, H.-J. Development and evaluation of compounds for imaging of β-amyloid plaque by means of positron emission tomography. *Eur. J. Nucl. Med. Mol. Imaging,* **2008**, *35 Suppl 1*, S75-81.
[247] Zhang, W.; Oya, S.; Kung, M.-P.; Hou, C.; Maier, D.L.; Kung, H.F. F-18 stilbenes as PET imaging agents for detecting β-amyloid plaques in the brain. *J. Med. Chem.,* **2005**, *48*, 5980-5988.
[248] Rowe, C.C.; Ng, S.; Ackermann, U.; Gong, S.J.; Pike, K.; Savage, G.; Cowie, T.F.; Dickinson, K.L.; Maruff, P.; Darby, D.; Smith, C.; Woodward, M.; Merory, J.; Tochon-Danguy, H.; O'Keefe, G.; Klunk, W.E.; Mathis, C.A.; Price, J.C.; Masters, C.L.; Villemagne, V.L. Imaging β-amyloid burden in aging and dementia. *Neurology,* **2007**, *68*, 1718-1725.
[249] Lopresti, B.J.; Klunk, W.E.; Mathis, C.A.; Hoge, J.A.; Ziolko, S.K.; Lu, X.; Meltzer, C.C.; Schimmel, K.; Tsopelas, N.D.; DeKosky, S.T.; Price, J.C. Simplified quantification of Pittsburgh Compound B amyloid imaging PET studies: a comparative analysis. *J. Nucl. Med.,* **2005**, *46*, 1959-1972.

3.2 Die γ-Sekretase als ein interessantes *Target* für die Behandlung der Alzheimer-Demenz

Der Inhalt dieses Kapitels wurde bereits veröffentlicht:
Stefanie Baumann, Nicole Höttecke, Boris Schmidt, "γ-Secretase as a target for AD", *in* Medicinal Chemistry of Alzheimer Disease, ed. A. Martinez, Research Signpost, **2008**.
Mit freundlicher Genehmigung von Research Signpost/Transworld Research.

Nicole Höttecke, Stefanie Baumann *Bioforum* **2008**, *6*, 32-34. "Alzheimer-Demenz: Ein Pla(qu)e mit Hoffnung auf Besserung?"

Die γ-Sekretase ist ein interessantes *Target* in der Behandlung der Alzheimer-Demenz, da das zur Aggregation neigende amyloide-β-Peptid freigesetzt wird. Diese Aspartylprotease ist ein in der Membran eingelagerter Enzymkomplex, der in der aktiven Form aus vier Untereinheiten besteht. Durch die Membranständigkeit dieses Komplexes hat die γ-Sekretase den ungewöhnlichen Spaltungsmechanismus einer „*regulated intermembrane proteolysis*", da für eine Spaltung der Substrate in der lipophilen Membran ein Wasseraustausch mit dem extrazellullären Raum oder dem Cytosol notwendig ist.
In den letzten Jahren wurde eine Vielzahl verschiedener γ-Sekretase-Inhibitoren identifiziert, welche in klinischen Test aber zum Teil schwere Nebenwirkungen zeigten. Diese Nebenwirkungen sind auf die gleichzeitige Inhibition des Notch-Stoffwechsel, eines weiteren Substrates der γ-Sekretase, zurückzuführen. Da Notch auch eine wichtige Rolle in der Zelldifferenzierung spielt können bei dauerhafter Inhibition des Notch Stoffwechselweges toxische Nebenwirkungen auftreten. Seit 2001 ist der Forschungsschwerpunkt eher auf einer Modulation der γ-Sekretase fokussiert, bei der das Schnittmuster der γ-Sekretase von dem toxischen $A\beta_{42}$ zu dem ungefährlichen $A\beta_{38}$ hin verschoben wird.

Transworld Research Network 37/661 (2), Fort P.O., Trivandrum-695 023, Kerala, India

Medicinal Chemistry of Alzheimer's Disease, 2008: ISBN: 978-81-7895-342-7 Editor: Ana Martínez Gil

γ-Secretase as a target for AD

Stefanie Baumann, Nicole Höttecke, Raj Narlawar and Boris Schmidt
Clemens Schöpf-Institute for Organic Chemistry and Biochemistry, Technische Universität Darmstadt, Petersenstrasse 22, D-64287 Darmstadt, Germany

8

Abstract

Most gene mutations associated with Alzheimer's disease point to the metabolism of amyloid precursor protein as potential cause. The β- and γ-secretases are two executioners of amyloid precursor protein processing resulting in amyloid β. Significant progress has been made in the selective inhibition of γ-secretase, regardless of structural information for γsecretase. Several peptidic and non-peptidic leads were identified and several drug candidates are in clinical trials for Alzheimer´s disease. This review focuses on the developments in the field of γ-secretase inhibition and modulation since 2003.

Correspondence/Reprint request: Dr. Boris Schmidt, Clemens Schöpf-Institute for Organic Chemistry and Biochemistry, Technische Universität Darmstadt, Petersenstrasse 22, D-64287 Darmstadt, Germany E-mail: Schmidt_Boris@t-online.de

1. Introduction

Alzheimer's disease (AD) is the most common progressive and currently irreversible form of dementia with symptoms like memory loss, personality changes, impaired judgment, disorientation and loss of language skills. Despite great efforts to understand the causes, there remains the challenge to develop novel agents for AD therapy. Approved drugs such as acetylcholinesterase inhibitors or *N*-methyl-*D*-aspartate (NMDA) receptor antagonists offer symptomatic treatment and delay memory impairment but they do not address the basic pathology of the disease which is deposition of extracellular amyloid plaques and formation of intracellular neurofibrillary tangles (NFT) in the brain.

The aggregation of β-amyloid (Aβ) peptide, which is the major component of these amyloid plaques, exerts a decisive role in the neuropathology of AD. The Aβ peptides, which differ in length from 38 to 42 amino acids, are generated from the amyloid precursor protein (APP, chromosome 21) by processing of two aspartic proteases: β-(BACE-1) and γ-secretase. Both secretases have multiple substrates and cause different APP cleavages. The membrane localization of both enzymes is crucial for selectivity, as cell free conditions shift the cleavage pattern or result in additional cleavage sites. Usually 90% of APP is degraded by the α-secretase pathway and only 10% by the consecutive cleavages of β- and γ-secretase, which results in aggregation of insoluble extracellular Aβ deposits of approximately 4 kDa. Neither the pathological consequences of deposited or soluble Aβ are established beyond doubt, nor does plaque formation adequately correlate to the progress of AD. A definite proof of the Aβ hypothesis is still missing for humans. Furthermore γ-secretase inhibition may be utilized to control cell proliferation, and thus be a target for oncology.

Herein, we report the relevance of γ-secretase involved in AD and give an overview of the research efforts in this field. γ-Secretase inhibitors and modulators are presented as well as their mode of action, if available.

1.1 Established therapies for AD and novel approaches

Current pharmacological approaches related to AD treatment include antioxidant therapy, acetylcholine esterase (AChE) inhibitors, nicotinic and muscarinic agonists, nerve growth factor (NGF), low molecular lipophilic activators of the neurotrophic factor signaling pathway, anti-inflammatory drugs such as cyclooxygenase-1 (COX-1) and COX-2 inhibitors, drugs which interfere with Aβ formation and deposition, as well as food dietary components. Approximately 500 compounds are in development for the treatment of neurodegenerative diseases and at least 10% of these are related to AD. The targets derive from a whole range of receptors and enzymes like β-and γ-secretase, glycogen synthase kinase 3 (GSK-3), phosphodiesterase 4 (PDE 4) and the muscarinic M1 receptor.

nACh modulators, AChE inhibitors, nMDA receptor antagonists, 5-HT agonists and several vaccination projects (e.g. Elan, Cytos Biotechnology) are in advanced **1.1** stages of development [1]. Plaque formation was seen as a major cause for AD and their removal was one of the therapy goals until 2001. Today, Tau derived paired helical filaments (PHFs), soluble Aβ and its low molecular weight oligomers (Aβ*56) are seen as the main causes of Aβ pathology. AChE inhibitors like galantamine, tacrine, donepezil and rivastigmine (**Scheme 1**) produce small improvements in cognitive abilities of patients in the early stages of AD by suppressing the hydrolysis

of acetylcholine, an essential neurotransmitter which is diminished in AD, but they do not address the severe mortality in the final stages nor did they improve upon the primary endpoint of clinical trials: hospitalisation. Memantine hydrochloride (**Scheme 1**), a nMDA receptor antagonist, is able to modulate the influx of Calcium ions, which forms the basis of neuronal excitotoxicity; it was approved for the treatment of moderate to severe AD in 2002 as first of its class. Nevertheless, a causal therapy is still in demand, since no approved therapy effectively stops or cures AD.

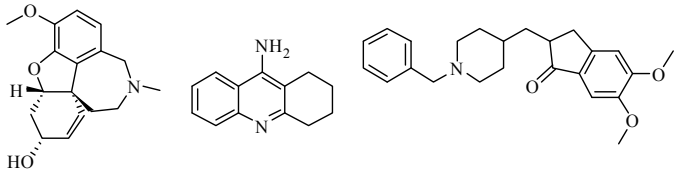

1 Galantamine **2** Tacrine **3** Donezepil

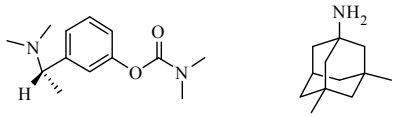

4 Rivastigmine **5** Memantine

Scheme 1. Current used drugs for symptomatic therapies.

1.2 APP processing

Amyloid plaques are processed *via* two different pathways: the amyloidogenic and the non-amyloidogenic pathway.

The non-amyloidogenic pathway involves membrane located α-secretase (**Figure 1**) [2]. The α−secretase belongs to the family of metalloproteases, e.g. Adam10, and cleaves APP within the Aβ sequence at amino acid 17 [3]. Non-amyloidogenic processing of APP generates p3 peptides which do not aggregate and do not display amyloid associated pathology. Amyloidogenic processing of APP results in the production of Aβ and involves sequential cleavage by β- and γ-secretase (**Figure 1**). This requires trafficking of APP from the membrane to the endosomes and finally to the lysosomes [4]. β-Secretase, recently identified as the β-site APP-cleaving enzyme (BACE-1) [5], cleaves APP thereby generating an extracellular soluble fragment called s-APPβ and an intracellular *C*-terminal fragment called C99. Subsequently, γ-secretase cleaves C99 at amino acids 38, 40 or 42 thereby generating Aβ peptides of various lengths.

Figure 1. APP processing by β- and γ-secretase leads to aggregated amyloid plaques and is called the amyloidogenic way. Initial cleavage by α- and subsequently γ-secretase represents the non-amyloidgenic way by generating p3 instead of Aβ.

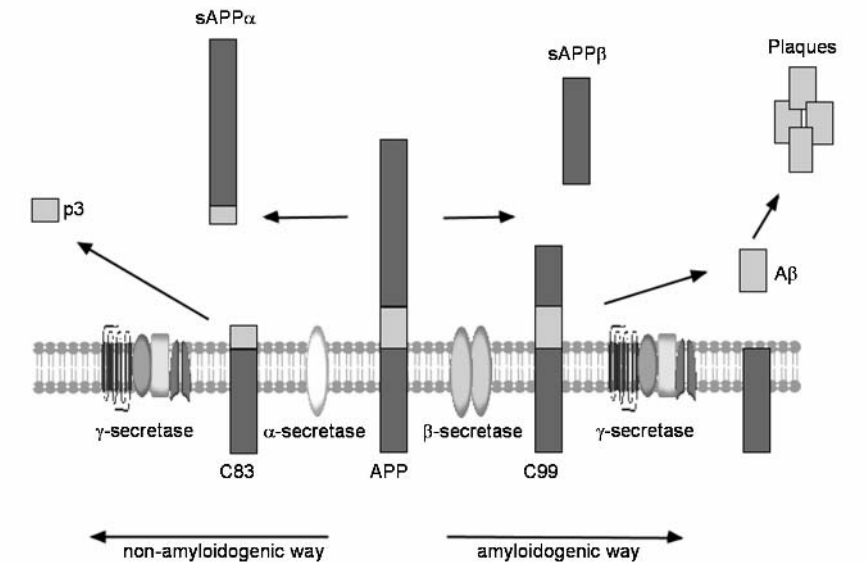

1.3 BACE and its inhibitors

Cleavage of the APP by BACE-1 is the first step in the generation of Aβ . *In vitro* and *in vivo* experiments confirmed that this enzyme is mainly responsible for initiating the amyloidogenic processing of APP [6]. Particularly, brains of BACE knockout mice had no detectable levels of Aβ and did not show accumulation of APP *C*-terminal fragments (CTF) C99 and C89 [7]. Brains of BACE transgenic mice are characterized by increased levels of Aβ and amassing of the CTF [6]. BACE was identified as an aspartic protease [8]. The key features are the mobile flap region and the flexible 10s loop, which are crucial for substrate docking [9]. The kinetics of statine-based inhibitors revealed a two state mechanism with structural reorganisation and activity modulation [8,10]. The two states: open and closed, contribute to selectivity and activity of the enzyme [8,11]. The flexibility of free and inhibitor bound BACE was investigated *in silico* and revealed several novel aspects of BACE, which are useful for structure-based, computer-aided inhibitor design [8,12]. The protonation states of the two active site residues Asp32 and Asp228 were calculated by several groups with different results [8,12-15]. Two β-secretases are known: BACE1 (ASP2 or memapsin 2) and BACE2 (ASP1 or memapsin 1) with high homology, yet subtle differences in the active site and an additional disulfide bridge for BACE1 [8,16]. BACE2 causes additional cleavages close to Phe20, which are reminiscent of α-secretase activity [17,18]. BACE1 is anchored to the membrane via its transmembrane domain (TMD, 455-480) and under native conditions BACE exists as a homodimer [19]. Several reviews on secretase inhibition of BACE have been published [8,20-23] as well as modelling studies [9].

2. γ-Secretase complex

γ-Secretase mediates the critical step in the liberation of Aβ from the membrane. γ-Secretase has an unusual cleavage mechanism, as the proteolysis takes place within a hydrophobic environment. Thereby different lengths of Aβ peptides are generated, indicating a lack of sequence specificity.

Lichtenthaler *et al*. reported an α -helical model for substrate cleavage [24]. It is postulated that one turnof α-helix contains around 3.6 residues and thus one site of the α-helix carries the amino acids 40, 43, 46 and 49 and the opposite of the α-helix the residues 42, 45 and 48. The cleavage depends on the substrate orientation in the catalytic core. Cleavage at every third residue does not correspond to a whole turn and therefore compensational cleavage after a fourth residue is necessary which explains the existence of $A\beta_{38}$ beside $A\beta_{42}$. γ-Secretase recognizes substrate α-helical substrates in topographically distinct manner and interacts with them from opposite directions and cleaves at multiple sites [25]. γ-Secretase is conformation specific since it selectively cleaves α-helical substrates [24].

The major forms of Aβ generated by γ-secretase are $A\beta_{38}$, $A\beta_{40}$ and $A\beta_{42}$ [26]. $A\beta_{42}$, which is toxic due its trend to aggregate and thereby forming plaques, corresponds to approximately 5-10% of the total amount of Aβ secreted by cultured cells under normal conditions. Other Aβ peptides of 19, 37–39 and 43–48 amino acids were also identified but these represent only minor species [27]. The longer the peptides, the more insoluble they are and hence they are more prone to aggregate and thus seed amyloid deposition. γ-Secretase also mediates the release of the APP intracellular domain (AICD) by cleaving at the ε-site, located nine amino acids close to the $A\beta_{40}$ cleavage site [28]. The relationship between γ- and ε-cleavage has been discovered recently by the isolation of $A\beta_{49}$, which is the *N*-terminal product of ε-cleavage and thus may be a precursor of Aβ. γ-Secretase processes the APP transmembrane domain from its *C*-terminal end by sequential steps and each cleavage occurs on the same side of the α-helix. Biochemical and genetic studies have demonstrated that presenilin (PS), nicastrin (Nct), anterior pharynx defective-1 (Aph-1) and presenilin enhancer-2 (Pen-2) form the enzymatically active core of the γ-secretase complex (**Figure 2**) [29].

Evidence indicates that PS comprises the catalytic moiety of the complex, while the other identified subunits are necessary for proper maturation and sub-cellular localization of the active enzyme complex [30]. Consistent with that hypothesis is that PS knockout mice exhibit significant reduction in β-amyloid production [31].

PS1 is a 9 (or 10) transmembrane (TM) aspartyl protease which possesses two highly conserved aspartic residues as a catalytic dimer. These essential amino acids are parts of a hydrophilic loop between TM6 and TM7, which reaches into the cytoplasmatic region of the plasma membrane. Consequently, substrate proteolysis takes place within the hydrophobic environment of the plasma membrane and represents an unusual cleavage mechanism [32].

The influence of detergents on γ-secretase activity in rat brain isolates has been investigated by Frånberg *et al.* [33] γ-Secretase showed the highest activity at 0.4% of CHAPSO, a zwitterionic detergent that protects the native state of proteins, resulting in approximately four times more AICD than in absence of the detergent. 1% CHAPSO solubilized a substantial amount of the γ-secretase components but lowered the activity. Diluting the sample to 0.4% restored the activity. The production of AICD was time dependent: γ-secretase was still active after 16 h incubation at 37°C. Beside the detergent concentration, the protein concentration was considered: concentrations higher than 1 mg/ml led to a decrease in the relative amount of soluble active γ-secretase in 1% CHAPSO. Therefore, a detergent: protein ratio of at least 10:1 should be used for efficient solubilization.

Figure 2. γ-Secretase is an aspartyl protease and requires the correct assembling of the tetrameric subunits Aph-1, Nct, PS and Pen-2.

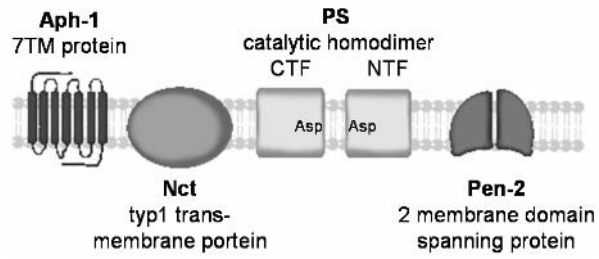

2.1 Presenilins

The presenilins (PS1 and PS2) control the activity of γ-secretase and are involved in the processing of APP and the production of Aβ [34]. Mutations in the genes of PS1/2 (Chromosome 14, 1) account for the majority of the cases of inherited familial AD. Aβ levels were dramatically decreased in animal models lacking the expression of PS1 but not PS2 [35]. This indicates that among the two presenilins, PS1 exerts the major role in regulating the activity of γ-secretase and hence Aβ secretion. PS1 is an aspartyl protease and its topology is characterized by 9 or 10-membrane spanning domains. The sixth and seventh domains bear the aspartate residues (D257 and D385) which are crucial for the production of Aβ, as a mutation on either of these residues abolishes the Aβ generation [36,37].

Nevertheless, PS1 alone is not able to coordinate all the processes that lead to its own activation [38]. It has been reported that overexpression of PS1 does not lead to increased levels of its *N*- and *C*-terminal fragments [39]. Therefore, there must be additional limiting factors (Nct, Aph-1, Pen-2) which control the endoproteolysis of PS1.

2.2 Nicastrin

Nicastrin (Nct) was the first protein of the γ-secretase complex to be identified [40]. It is a large type-1 transmembrane protein (~ 130 kDa) and exists in an immature and a mature form which differ in their glycosylation [41]. It has a large extracellular *N*-terminal and a short intracellular domain. In its partial glycosylated, immature form it is able to bind to PS where it is crucial for PS endoproteolysis and thus for γ-secretase activity [42]. This was confirmed by the experiments carried out with transition-state analogue inhibitors which bind specifically to active PS. These experiments showed that nicastrin co-purifies with the active form of PS1. This indicates that it is an integral part of the active γ-secretase complex [43]. The extracellular domain of Nicastrin interacts with the *N*-terminal region of the substrate and enables them to reach the complex [42].

2.3 Anterior pharynx-defective phenotype-1 and presenilin enhancer-2

Anterior pharynx-defective phenotype 1 (Aph-1) and presenilin enhancer 2 (Pen-2) were isolated as part of the γ-secretase complex in two different experiments carried out in *C. elegans* [44,45]. Aph-1 and Pen-2 are required for Notch signalling and Aβ formation. Aph-1, a 30 kDa and 7 TM protein, forms a subcomplex with Nicastrin and is required for stabilization of PS holoprotein [42].

Pen-2 is a short two-membrane domain spanning protein and it has approximately 101 amino acids. Pen-2 knockout affects the activity of the γ-secretase complex by altering the Notch-mediated signalling pathway and the processing of APP [44]. The physiological significance of Aph-1 in the γ-secretase complex is to stabilize the PS-Nicastrin subcomplex [46].

The *C*-terminal domain of Pen-2 induces the endoproteolysis of PS which is crucial for the development of the active heterodimer and also stabilizes the resulting *C*- and *N*-terminal fragments afterwards [47]. It was revealed that, in absence of PS, Pen-2 is destabilized and degraded in the endoplasmic reticulum (ER) as an ubiquitinylated protein [48].

2.4 Assembling

An assembling model was proposed by Zhou *et al*. Initially Nicastrin, in its partially glycosylated "immature" mode, forms a subcomplex with Aph-1 and this subcomplex is suggested to enter the ER. Together with PS holoprotein a trimeric intermediate complex is formed. This is followed by complete glycosylation of Nicastrin in the Golgi/transGolgi network and entry of Pen-2 into the complex induces the PS endoproteolysis to the active γ-secretase complex (**Figure 3**)[42].

Endoproteolysis of PS results in the formation of a *N*-terminal (NTF) and a *C*-terminal (CTF) fragment. These two fragments contain one of the two critical aspartic residues and remain associated forming a heterodimer which comprises the active PS [49]. PS1 activity resides in its ability to cleave APP within the plasma membrane at the 38-, 40- and 42- sites of the Aβ sequence. This process is known as "Regulated Intra-membrane Proteolysis" (RIP). It requires the exchange of water molecules, which are excluded from the hydrophobic lipid bilayer of the cell membrane [50].

Figure 3. Simplistic model of the γ-secretase complex with dimeric substrate C99.

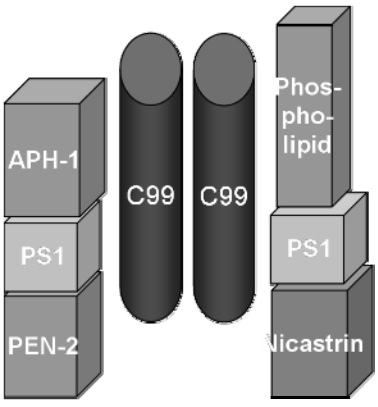

2.5 Binding partners

Purification of endogenous γ-secretase complex from detergent solubilized HeLa cell membranes showed an additional integral subunit, the membrane protein CD147. CD147 was found to have a regulatory effect on γ-secretase activity [51]. Apart from CD147, other transient or weak binding partners of the γ-secretase complex, such as GSK-3, phospholipase D1 (PLD1) and TMP21 also have been reported [42]. Although the presence of these binding partners is crucial for the activity of γ-secretase, none of these proteins have been detected in purified samples of the complex. In addition to APP, the γ-secretase complex processes numerous other type I TM proteins including fragments of Notch, E-cadherin, N-cadherin, CD44, ErbB4, LRP and nectin-1, which are involved in many physiological and pathological functions [52].

2.6 Mode of action

Multhaup *et al.* revealed new mechanistic aspects of γ-secretase cleavage [53]. They reported the dimerization of two APP-TMSs, via G29 and G33 as a hinge for substrate dimerization, to be essential for $A\beta_{40}$ and $A\beta_{42}$ production. This hinge is a sterical hindrance for γ–secretase processing and shifts the cleavage to the pathological Aβ (**Figure 4**). The mutations G29A and G32A resolve this hindrance and favour the "normal" cleavage to $A\beta_{38}$ and $A\beta_{37}$.

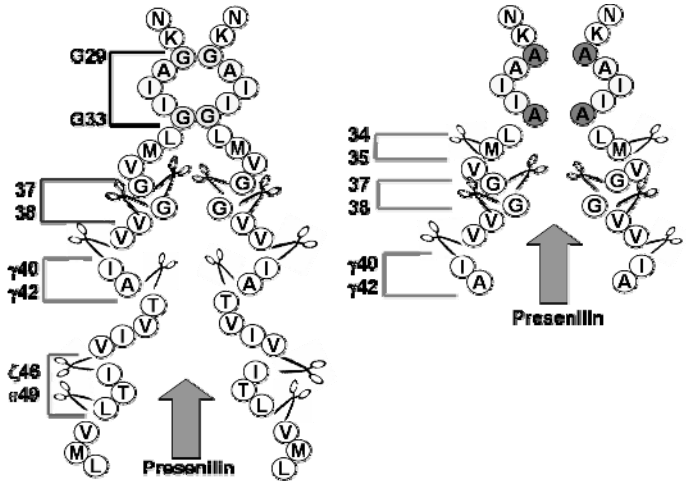

Figure 4. Sterical hindrance for secretase processing by a G29, G33 cross point (see Multhaup) [53].

3. Inhibition of γ-secretase

γ-Secretase inhibitors must reduce Aβ secretion sufficiently to alleviate the cause of AD, but must neither totally abolish secretion nor the processing of other proteins, which have important roles in neuronal structure and function. In addition to βAPP, several substrates are known to be cleaved by γ-secretase, which seems to be the "proteasome of the membrane" [54]. Generally, such multiple substrates increase the risk for toxic side effects by γ-secretase inhibition. In fact, the close relation to the Notch pathway, which is important in embryonic development, makes γ-secretase a rather challenging and risky drug target. The crossover to the Notch pathway hampered attempts towards PS -/- knockout animals, which did not pass the embryonic state, but embryonic stem cells may fill part of the gap [55]. The intracellular trafficking of Notch in human CNS neurons is reduced by PS1 inhibitors, and results in dramatic changes in neurite morphology. A great task will be the determination of a therapeutic window between efficacy and unacceptable toxicity [56]. If a safe therapeutic window cannot be defined, there may remain an option to use γ-secretase inhibitors in oncology. Several other substrates must be considered in addition to APP and Notch: the Notch ligands Delta and Jagged, apoER2 lipoprotein receptor, the low-density lipoprotein receptor-related protein, ErbB4 receptor tyrosine kinase, CD44, p75 neurotrophin and β-subunits of voltage-gated sodium channels [57,58]. Advances in the last years indicate the right direction: γ-secretase modulators that modify APP processing without generating unacceptable side effects.

Special features of the γ-secretase complex hinder crystallisation and thus crystallographic analysis of the enzyme, which is a major obstacle for rational structure-based drug design. Therefore, docking and molecular modelling studies are available for BACE, but not for γ-secretase. One crude model was recently proposed by Fraering *et al.* [59]. The information available on inhibitor binding sites has improved but is still limited. Hence, most of the selective γ-secretase inhibitors were discovered by high-throughput-screening (HTS) efforts. However, during the last decade a number of potent γ-secretase inhibitors were successfully developed [60,61].

Wolfe *et al.* explored the mechanisms of different γ-secretase inhibitors in detail [62]. Most of them bind directly to the active site or alter it through an allosteric interaction. Some inhibitors, e.g. the isocoumarins and the *Aib* containing helical peptides, do not block Aβ-production by affecting the active site of the protease, thus they do not target γ-secretase directly. Signal Peptide Peptidase (SPP) inhibitors can inhibit γ-secretase too, showing that SPP and γ-secretase have similar active sites and are likely to share the proteolytic mechanism [63].

Compounds inhibiting the production of all Aβ species without selectivity are called γ-secretase inhibitors (GSIs), while compounds selectively reducing the secretion of the pathological $A\beta_{42}$ are called γ-secretase modulators (GSMs). Inverse γ-secretase modulators either downregulate $A\beta_{38}$ production without affecting $A\beta_{40/42}$ or increase $A\beta_{42}$ production.

3.1 Peptidic, semi-peptidic and non peptidic γ-secretase inhibitors and modulators

Peptidic PS1 inhibitors, like Merck's L-685,458 (**6, Scheme 2**) display potent γ-secretase inhibition ($IC_{50} = 17$ nM) [64]. The all-lipophilic sequence with 3 phenylalanines was somewhat anticipated, as several studies had indicated the lipophilic binding pockets (P_2, P_1, P_1', P_2', even P_4' and P_7') in proximity to the cleavage site [24]. It was suggested that compound **6** acts as a direct transition-state analogue of the $A\beta_{40}$ and $A\beta_{42}$ cleavage sites. The core structure of **6** was linked to biotin and photoreactive fragments attached *N*- or *C*-terminally leading to L-852,505 (**7**) and L-852,646 (**8**), which were suitable for labelling studies. Despite the attachment of the photoreactive benzophenones, **7** and **8** retained potent inhibition ($IC_{50} < 1$ nM for γ-secretase). Biotin was used to facilitate the isolation and identification of the reversibly labelled adducts via their streptavidin-enzyme linked conjugates. Photolysis in the presence of solubilized γ-secretase provided a protein of 20 kDa linked to L-852,505 (**7**) after isolation on a biotin-specific streptavidin-agarose gel, followed by partial digestion. This fragment was shown to be the *C*-terminal fragment of PS1 (PS1-CTF) by specific antibodies. Binding to wild-type PS1 was negative in a control experiment. Yet binding to the deletion construct PS1Δ E9, which lacks the cytosolic E9 loop, was positive [65]. Useful information resulted from the photolysis of L-852,646 (**8**) in the presence of solubilized γ-secretase. This resulted in the isolation of a 34 kDa fragment, which was assigned to be an *N*-terminal fragment of PS1. A similar transition-state motif, the hydroxyethylurea **9** (III-31-C) [66], was utilised for activity based affinity purification. Immobilisation of **9** ($IC_{50} < 300$ nM) on affigel 102 allowed isolation and identification of PS1-CTF, PS1-NTF and Nicastrin from solubilized γ-secretase preparations [67]. Initial attempts to free active γ-secretase from the affinity gel failed. Yet, a delicate combination of Brij-35 and CHAPSO resulted in the isolation of active γ-secretase. The co-precipitation of the inhibited γ-secretase with its substrates C83 and C99 gave rise to speculations about additional binding sites, where the substrate is recognised prior to transfer to the active site.

Semi-peptidic inhibitors have also been comprehensively utilized in a range of discoveries from the Elan group [68]. DAPT (**10**, $IC_{50} = 20$ nM; HEK) was developed from a *N*-dichlorophenylalanine lead and structure activity relationships

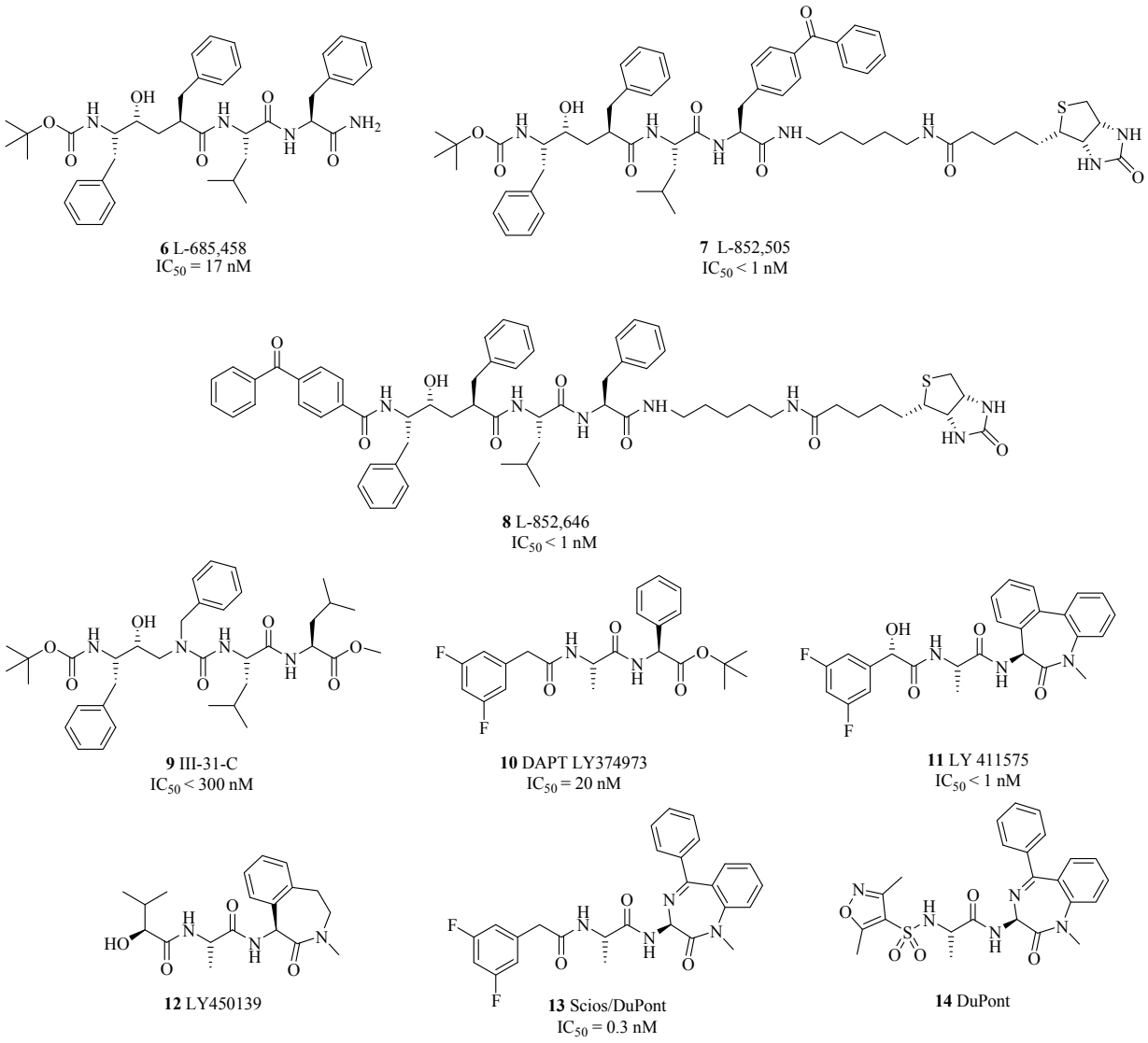

Scheme 2. Peptidic and semi-peptidic γ-secretase inhibitors.

(SAR) studies revealed difluorophenylacetic acid and phenylglycine to be crucial for activity [69]. DAPT has demonstrated robust efficacy *in vivo* at relatively high doses. The subcutaneous application to mice in a dosage of 100 mg/kg resulted in a 50% reduction of cortical Aβ levels within 3 hours. A 40% Aβ reduction was observed at the dosage of 100 mg/kg orally, again after 3 hours, but no brain levels of DAPT were reported for the latter study [70]. A setback came from several preclinical studies, which revealed *in vivo* toxicity, mainly because DAPT effects the Notch pathway at higher levels (100 – 1000 fold) [8,71,72].

Extensive *in vivo* studies have been carried out with the more potent dibenzoazepine-type analogue LY-411575 (**11**, DBZ). The stereoselective placement of the hydroxyl group and the locked spatial arrangement of two phenyl rings in a caprolactam increased the activity 20fold (IC_{50} < 1 nM). Oral dosing of 1 mg/kg of **11** to 3 to 5 month-old Tg2576 mice halved plasma and cortical Aβ levels within 3 hours [73]. A lesser active diastereomer was administered orally to C57BL/6 and TgCRND8 APP mice for 15 days at 1-10 mg/kg per day and resulted in reduction of Aβ levels [74]. This was accompanied by atrophy of the thymus and deterioration of the

intestinal epithelium. The Notch/APP selectivity was determined in cellular assays: IC_{50} ($A\beta_{40}$) = 0.082 nM, Notch IC_{50} = 0.39 nM. This small toxicity window and the high potency made DAPT and LY-411575 unlikely candidates to enter clinical trials. Nevertheless, E. Siemers *et al*. went on and reported the results of the phase I and phase II studies of the γ-secretase inhibitor LY450139 (**12**), which is less potent than **11** [75]. LY450139 (**12**) is moderately selective for APP cleavage over the Notch pathway. The oral application of **12** to healthy volunteers resulted in reduced plasma levels of $A\beta_{total}$ to 74.3% of the initial baseline at 40 mg/d after 14 days. The sampling time point was crucial, as a single dose resulted in significant reduction of $A\beta_{total}$ 3-6 h after dosage but also in recovery and overshoot within 12 h. However, cerebrospinal fluid (CSF) levels were constant. Furthermore the results of phase IIa were reported [76]: The application of 30-40 mg/d over 6 weeks to AD 70 patients led to 38% plasma Aβ reduction: again no changes in CSF were observed. Moreover, there appeared one severe case of Barrett oesophagus, but biopsy excluded Notch mediated processes. Recently, the results of the phase IIb clinical study of LY450139 were reported at the 2nd International Conference on Prevention of Dementia by Fleisher *et al.* (Washington, 2007), testing the effect of LY450139 on 51 participants with AD for 14 weeks with randomized doses (100 mg, 140 mg) or a placebo. Three adverse events were observed during this clinical study: 1) small bowel obstruction, 2) haemoglobin positive stool, and 3) diarrhoea. The study recorded reduced plasma $A\beta_{40}$ by 58.2% for the 100 mg group and 64.6% for the 140 mg group, but no significant reduction of CSF $A\beta_{40}$ (100 mg = 20%, 140 mg = 11%, Placebo = 6%). During this trial a $t_{1/2}$ of 2.59 h with a T_{max} of 1.68 h at 140 mg was observed. No differences were seen in cognitive or functional measures of any group.

DuPont Pharmaceuticals and Scios described a highly potent difluorophenacyl-caprolactam derivative (**13**, IC_{50} = 0.3 nM) [77]. **13**, better known as Compound E is a potent, selective, non-transition state and non-competitive inhibitor of γ-secretase and Notch processing. Bristol-Meyers Squibb and DuPont continued to elaborate this caprolactam motif. Some efforts were dedicated to modify the *N*-terminus to create non-infringing structures to the Elan patents. The synthesis of oxazolylsulfonamide **14** is one such example [78].

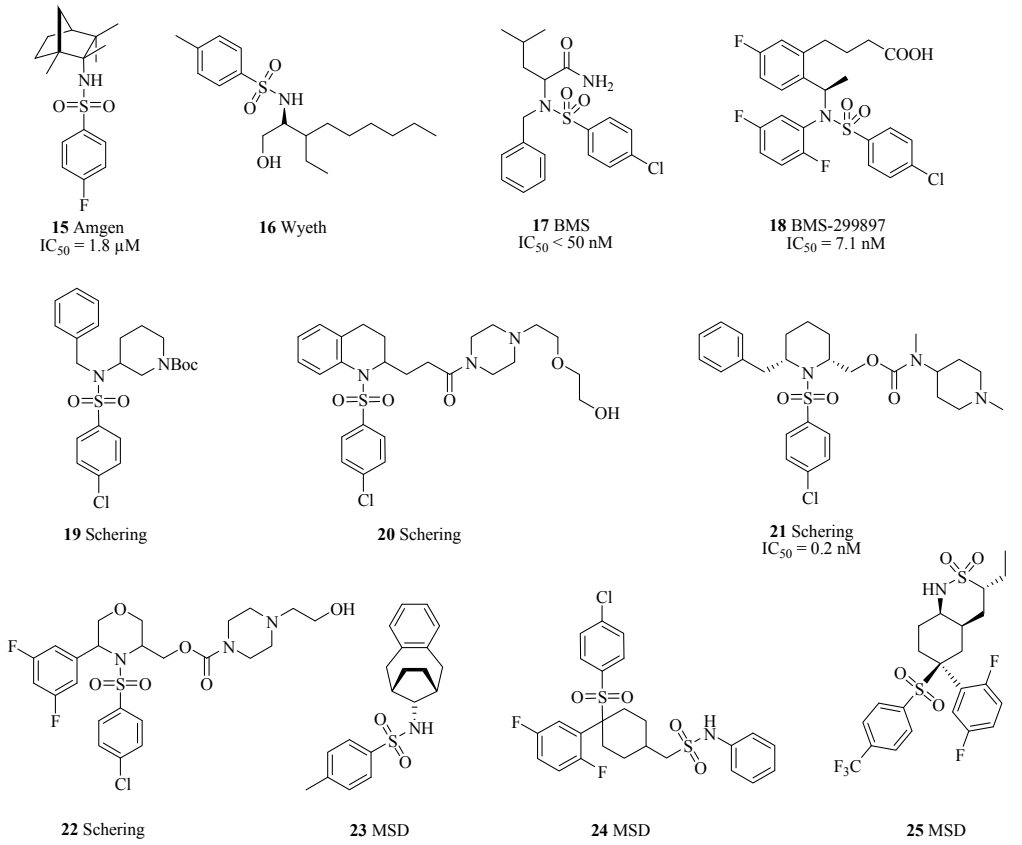

Scheme 3. Non-peptidic γ-Secretase inhibitors I.

Despite tremendous research efforts, the molecular mechanism of DAPT and Co. still remain unclear. Fuwa *et al.* presented the synthesis of multifunctional probes for the identification and characterization of molecular domains in γ-secretase or signal peptide peptidase (SPP). A photoaffinity as cross-linking unit like benzophenone or phenyldiazirine and biotin as reporter were attached to DAPT, **11** and **13** via the azide/alkyne fusion process. The affinity probes displayed strong inhibition of Aβ secretion comparable to the parent compounds, suggesting affinity towards γ-secretase. Photoaffinity labelling experiments revealed that **11** and **13** directly target PS1 *N*-terminal fragments (NTF), while DAPT targets *C*-terminal fragments (CTF) of PS1. A competition assay was performed and the results suggest that the binding site for **11** and **13** is functionally overlapping with the DAPT binding site. The *C*-terminal structure of these compounds might determine the final target region in PS1 and the mode of action on γ-secretase activity. Furthermore, **11** and **13** directly and specifically target signal peptide peptidase while DAPT does not. The authors proposed a speculative mode of binding: PS1 harbours a binding pocket for dipeptidic γ-secretase inhibitors that is composed for difluorobenzene, phenylglycine and caprolactam binding sites. The phenylglycine and caprolactam binding sites reside on PS1 CTF and PS1 NTF, while the caprolactam binding site resides on SPP. DAPT, **11** and **13** initially bind to the difluorobenzene binding site in PS1 and subsequently the compounds target the secondary site, forming a stable complex with γ-secretase, eventually inhibiting the proteolytic activity. The authors argue, that these results do not allow a final conclusion as they cannot rule out an allosteric effect caused by affinity ligands [79].

Apart from the previously described peptidic and semi-peptidic inhibitors, lipophilic scaffolds based on sulfonamide moieties have been explored in recent discoveries. The Amgen group exploited fenchylamine sulfonamides as moderately potent inhibitors (e.g. **15**, IC_{50} = 1.8 μM, HEK293-cells) (**Scheme 3**) [80]. Wyeth/Arqule reported sulfonamides (**16**) which were prepared from amino alcohols [81]. Acetamide derivatives such as **17** have been reported by BMS. Compound **17** displayed potent inhibition of Aβ secretion with an IC_{50} < 50 nM in H4-cells. BMS-299897 (**18**) [56] was found to reduce Aβ in brain, cerebrospinal fluid (CSF) and plasma in young transgenic mice in a dose and time dependent manner with a significant correlation between brain and CSF Aβ levels. Transgenic mice were used to examine potential side effects related to Notch inhibition which is a crucial issue with γ-secretase inhibitors. **18** was 15-fold more effective and selective at preventing the cleavage of APP than of Notch *in vitro* (APP IC_{50} = 7.1 nM, Notch IC_{50} = 105.9 nM). No changes in the maturation of CD8+ thymocytes or of intestinal goblet cells were observed in mice treated with 18. In a series of closely related disclosures, the Schering-Plough group employed a variety of sulfonamides, such as piperidine **19**, tetrahydroquinoline **20** (IC_{50} = 30-535 nM, DKF167 cells expressing C99) and the 2,6-disubstituted piperidine **21** (IC_{50} = 0.2 nM). Replacement of the sulfonamides by a sulfone moiety resulted in corresponding series. Substituted *N*-arylsulfonyl heterocyclic amines (**22**) displayed IC_{50} values in the range of 1 nM to 1 μM [82]. The Merck group employed an unusual bicyclo-[4.2.1]-sulfonamide scaffold characterized by the toluyl sulfonamide **23** [83]. Other aryl cyclohexyl sulfones like **24** (IC50 < 100 nM, SH-SY5Y cells) [84] and **25** [no data shown] were also claimed by Merck Sharp & Dohme (MSD) as γ-secretase inhibitors [85,86].

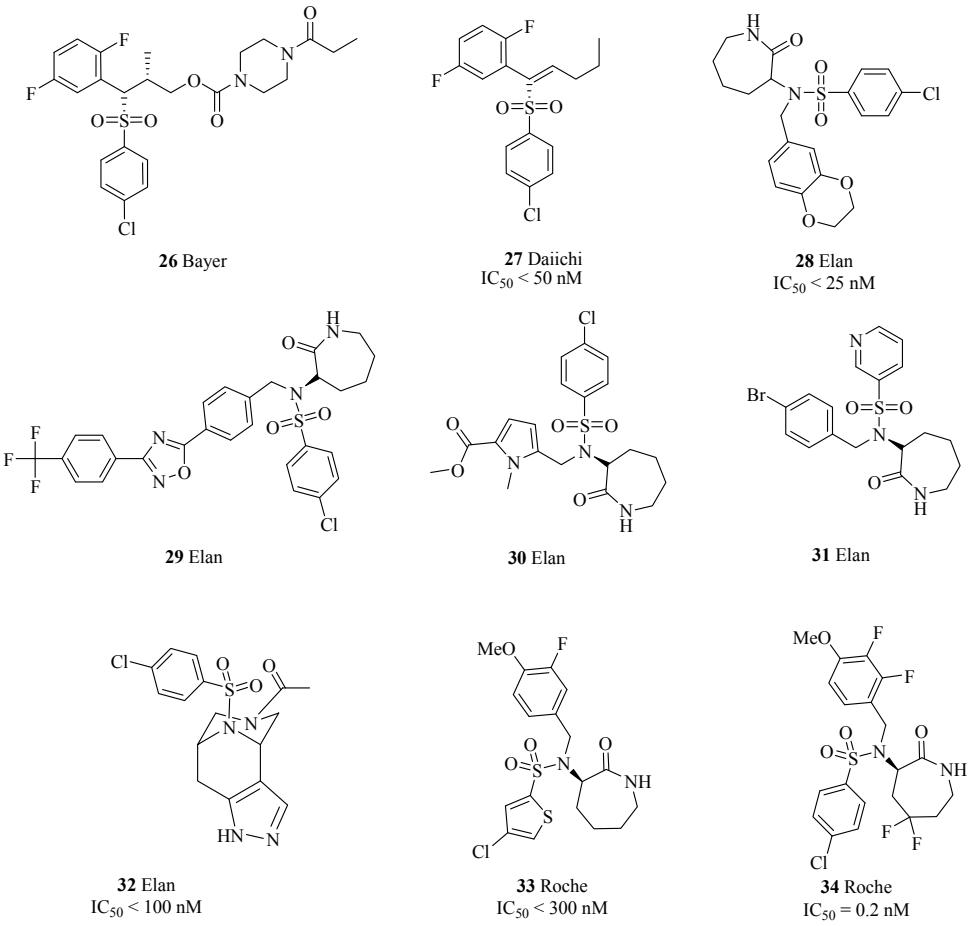

Scheme 4: Non-peptidic γ-Secretase inhibitors II.

Following this initial discovery of cyclohexyl sulfones, additional compounds such as 26 (**Scheme 4)** have been claimed by the Bayer AG [87]. Various related sulfones were claimed by Daiichi Pharm Co. (e.g. 27, IC_{50} < 50 nM, H4-cells). The Elan patent application reported three general synthetic schemes and about 700 tabulated examples [88]. Selected *N*-(oxoazepanyl) benzenesulfonamides showed promising activities, for example, compound **28** inhibits γ-secretase with an IC_{50} within the range of 0.1-25 nM. However, the activities of compound **29** and **30** are not reported. Another related Elan patent described the synthesis of *N*-substituted heterocyclic sulfonamides like **31** as potent inhibitors of Aβ synthesis with minimal inhibition of Notch signalling [89]. Furthermore, Elan identified bridged N-bicyclic sulfonamides for γ-secretase inhibition [90, 91]. Compound **32** exhibited an IC_{50} value for Aβ secretion of less than 100 nM in 293sw cells.

Roche presented sulfonamides (e.g. **33**) and preferred compounds display IC_{50} values < 0.3 μM [92]. Related fluoro-substituted 2-oxo-azepanes were prepared as γ-secretase inhibitors for the treatment of AD or cancer. Synthesis and activities in HEK293 are given as well as formulations as tablets and capsules. Preferred compounds exert an IC_{50} of < 10 nM, e.g. compound **34** inhibits Aβ secretion with an IC_{50} of 2 nM [93]. Additionally, Roche presented malonamide derivatives (**35**), where several compounds display IC_{50} values of <10 nM (**Scheme 5**) [88,94]. Roche's 1,4-benzoxazepin-3-one **36** was prepared by a cyclocondensation of (formylaryloxy)-alkanoic acid, amines and isonitrile [95]. Compound **36** inhibits γ-secretase with an IC_{50} value of 0.18 (no units given). Astra Zeneca claimed novel

molecular probes for the detection, characterisation and localization and isolation of γ-secretase. They presented biotinylated and bodipy-labeled compounds (e.g. **37**) and determined the inhibition of $A\beta_{40}$ production in HEK cells, but did not reveal assay data [96]. Gleevec (**38**) inhibits Aβ production but not Notch cleavage [97]. Recently, Fraering *et al*. reported IC_{50} values for $A\beta_{40}$, $A\beta_{42}$ and AICD generation of ~75 μM. Generation of the *N*-terminal intracellular domain-Flag (NICD) was not inhibited, even at >10-fold concentrations. The authors proposed a potential nucleotide-binding domain on γ-secretase, because ATP was able to recover the γ-secretase activity inhibited by a Gleevec formulation. There is strong support for this hypothesis: γ-secretase binds to ATP acrylamide resin through the γ-phosphate [98].

Torrey Pines Therapeutics (formerly named Neurogenetics) disclosed a large number of aminothiazole derivatives (e.g. **39**) with $A\beta_{42}/A\beta_{40}$-lowering activities at concentrations of about 30 μM [99]. The compounds derived from α-halogenated ketones and appropriate thioureas or ureas. Approximately 60 of these structures were claimed to display good inhibition (activity < 0.2 μM). Furthermore, Torrey Pines delivered interesting news: the results of the phase I study for the company's lead AD candidate, NGX267 (**40**), were presented by M. Murphy (Salzburg 2007, 8th International Conference on Alzheimer's and Parkinson's Diseases). **40** is a muscarinic or M1 receptor agonist which has also been linked to a decrease in $A\beta_{42}$-production. The double-blind, placebo-controlled, multiple-dose trial enrolled 90 healthy males, between the ages of 18 and 55, in sequential cohorts. Doses of 10, 20, 30, and 35 mg were evaluated. Evidence of cholinergic stimulation was detected by increase in salivary flow, and there were no clinically notable adverse events. NGX267 or (*S*)-2-ethyl-8-methyl-1-thia-4,8-diazaspiro-[4.5]-decan-3-one is identical with AF267b, claimed by Abraham Fisher [100]. Preclinical data support a dual mechanism of action. NGX267 has been shown to stimulate M1 receptors in a mode analogous to acetylcholine. Additionally, NGX267 lowered brain levels of $A\beta_{42}$ in studies in mice and rabbits [101]. Furthermore, the company has two preclinical candidates targeted for the treatment of AD in the pipeline: first, the follow-on M1 agonist, NGX292, a desmethyl derivative of NGX267. Second, NGX97555 (structure not disclosed), a γ-secretase modulator presented by S. Wagner in Salzburg 2007. According to the working hypothesis, series555 compounds bind to, and allosterically modulate, the γ-secretase complex, causing a shift in the γ-site cleavage preference from $A\beta_{40/42}$ to $A\beta_{37/38}$, without inhibiting the overall catalytic activity of the complex. The changed ratio of Aβ isoforms and Aβtotal (IC_{50} ($A\beta_{42}$) = 10 nM, IC_{50} ($A\beta_{40}$) = 64 nM, SY5Y cells), and the retained Notch and E-cadherin processing supports classification of NGX97555 as a γ-secretase modulator. Similar Aβ isoform changes have been observed *in vivo*. A 3-day oral dosing revealed the minimum efficacious dose of 25-50 mg/kg to lower brain $A\beta_{42}$ in Tg mice. NGX97555 is likely to be a close analogue of the very lipophilic compound **39** (**Scheme 5**) and Pen-2 has been advanced as a potential binding site. The unusually high lipophilicity (clogP = 6.8) makes **39** and analogues thereof to potent binders to protein aggregates such as tau derived PHFs and Aβ fibrils. These poor pharmacokinetic properties in combination with the metabolically labile and notorious hepatotoxic arythiazole fragment (Pfizer disclosed two clinical trials failures) will be severe obstacles in the further clinical development of analogues.

Substituted thiazolamides (**41**), which resemble the Torrey Pines compounds, were coupled to a redox chemical delivery system (RCDS) and may feature enhanced pharmacokinetic properties [102]. A dihydropyridine RCDS was introduced to improve the blood brain barrier (BBB) permeation. The compounds exhibited EC_{50} values ranging from 0.1 to 1.0 μM in cell free assays. Compound **41** displayed an ED_{50} value of 0.2 μM for $A\beta_{total}$ in cellular assays using APP transfected HEK293 cells. An application by Pfizer contains 7 general synthetic schemes and more than 350 tabulated imidazolylamides, e.g. **42**, inhibiting the generation of Aβ-peptide (no data shown) [103].

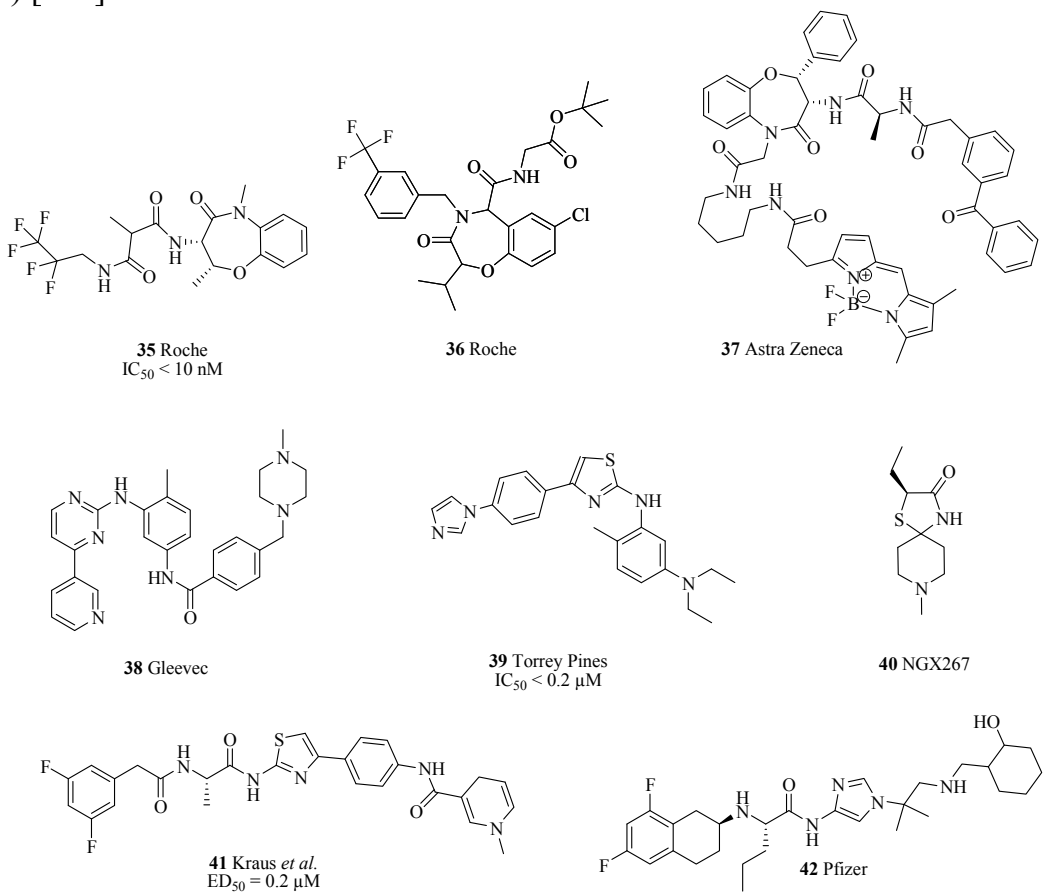

Scheme 5. Non-peptidic γ-Secretase inhibitors III.

A selective GSM (**43, Scheme 6**) was reported by MSD [104]. The carboxylic acid seems to be important to achieve the desired ratio of $A\beta_{38}/A\beta_{40}/A\beta_{42}$. This modulation is distinctly different from inhibition as the Aβtotal load may be unaffected. Tetrahydroindole derivatives like **44** and **45** [105] as well as arylacetic acids (e.g. **46**) [106] developed by MSD were tested using a cell-based (human SH-SY5Y cells) assay. These compounds exhibit selective inhibition (modulation) of $A\beta_{42}$ production. The IC_{50} values of the most potent compounds are at least 2-fold lower than for $A\beta_{40}$, typically at least 5-fold lower and in the preferred cases 50-fold lower (data not shown). Closely related *S*-enantiomers of α-substituted aryl acetic acids and biphenylacetic acids (**47** and **48**) have been reported by Cellzome. Potent modulators (e.g. **48**) display an $IC_{50} < 1$ μM in SKN neuroplast cells [107,108].

N-Sulfonylated and *N*-alkylated carbazolyloxyacetic acids have been presented as potent modulators of γ-secretase [109]. Introduction of a lipophilic substituent, which may vary from arylsulfone to alkyl, turned 2-carbazolyloxyacetic acids into potent

γ-secretase modulators (e.g. **49**, IC_{50} ($A\beta_{42}$) = 7.5 μM). This resulted in the selective reduction of $A\beta_{42}$ and an increase of the less aggregatory $A\beta_{38}$ fragment. Introduction of an electron donating group at position 6 and 8 of *N*-substituted carbazolyloxyacetic acids either decreased the activity or inversed modulation. The most active compounds displayed activity in the low micromolar range and little or no effect on the γ-secretase cleavage at the ε-site. Furthermore, *N*-sulfonylated and *N*-alkylated carprofen derivatives displayed modulatory effects on γ-secretase. The introduction of a lipophilic substituent transformed the COX-2 inhibitor carprofen into a potent γ-secretase modulator (e.g. **50**, IC_{50} ($A\beta_{42}$) = 2.9 μM). Several compounds selective reduced $A\beta_{42}$ secretion and increased $A\beta_{38}$ secretion.

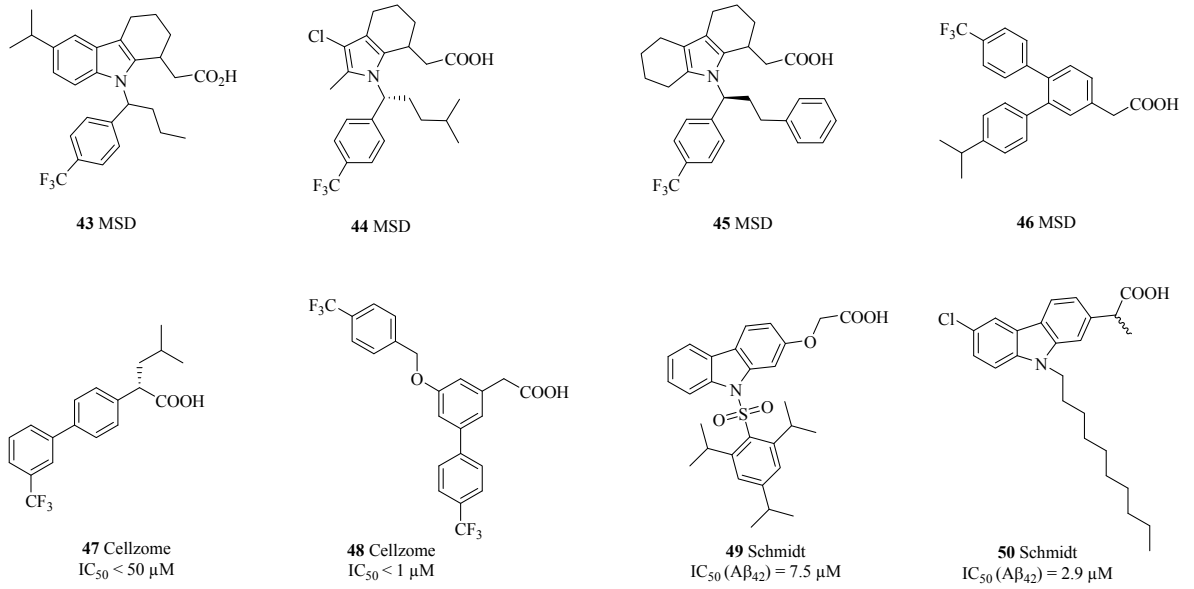

Scheme 6. Non-peptidic γ-secretase inhibitors IV.

The lipophilic substituents cause amphiphilic properties of the carboxylic acids, which may interact with membranes. The authors favour the *N*-alkylated derivatives for the investigation of potential membrane interactions, as they allow the incorporation of phospholipids analogues and membrane disrupting fragments. If affected at all, the ε–cleavage of γ-secretase was inhibited at much higher compound concentrations than those determined to be modulatory at the γ-site. The compounds are therefore expected to have little or no impact on γ-secretase mediated signalling via the AICD or via intracellular domains of other γ-secretase substrates. However, the interaction site of these compounds has not been reported yet.

3.2 Non-steroidal anti-inflammatory drugs as γ-secretase modulators

Brains of AD patients show a number of pathological abnormalities such as a profound loss of synapses, profuse reactive glyosis, microglial proliferation and ultimately indication of inflammatory processes [110]. Increasing evidence suggests that a large number of inflammatory mediators are elements of the AD neuropathology. Several inflammatory factors were identified in the brains of AD patients which include activated complement proteins, cytokines, chemokines, acute phase reactants, proteases and their inhibitors, proteoglycans, growth factors and various other enzymes. Due to these observations, different inflammation based hypothesis for AD have been proposed. One of these postulates that neurodegeneration in AD brain is secondary to an inflammatory response to plaques and NFTs rather than to these hallmarks themselves. Moreover, inflammation initiates the formation of plaques and NFTs and their progressive accumulation, which in sequence activates immune reactions that force a self-sustaining "auto destructive" process. Thus, these hypotheses propose that in both circumstances chronic inflammation has a fundamental role in AD pathogenesis. This hypothesis is further supported by several genetic studies indicating that polymorphisms of inflammatory genes (i.e., interleukin (IL)-1α; IL-1β; tumour necrosis factor (TNF)-α; α2-macroglobulin, a1-antichimotrypsin) increase the risk of AD [111]. Epidemiological studies demonstrated that use of non-steroidal anti-inflammatory drugs (NSAIDs) may delay or prevent the onset of AD. They slow AD progression and reduce the severity of cognitive symptoms [112,113]. The duration of the treatment is critical for the outcome as long-term treatment is more beneficial compared to short-term treatment [112]. Moreover, the type of NSAIDs is crucial for the outcome e.g. ibuprofen, sulindac, indomethacin offer the best protection, whereas naproxen does not. This provided the rationale for clinical trials of different NSAIDs in AD patients.

3.2.1 APP metabolism by NSAIDs

It is well documented that NSAIDs can modulate the secretion of s-APPβ in different neuronal cell lines, astrocytes and neurons *via* a protein kinase C (PKC)-mediated mechanism [114]. Weggen *et al*. reported three NSAIDs which display selective Aβ42-lowering activity in a variety of stable transfected cell lines [115]. Two structurally closed compounds, sulindac sulfide and indomethacin lowered Aβ42 secretion (IC_{50} = 25-50 μM), whereas ibuprofen lowered Aβ42 secretion with an IC_{50} of around 250 μM. At maximal non-toxic concentrations, 70–80% Aβ42 secretion inhibition was observed without significant reduction of Aβ40 levels. Interestingly, this activity was not associated with all NSAIDs and negative results were observed with other commonly prescribed NSAIDs such as naproxen and Aspirin® as they did not affect either Aβ40 or Aβ42 levels [115]. Later Eriksen *et al.* identified other NSAIDs with Aβ42-lowering activity such as fenoprofen **55**, flurbiprofen **51** and meclofenamic acid **56** (**Scheme 7**) [116].

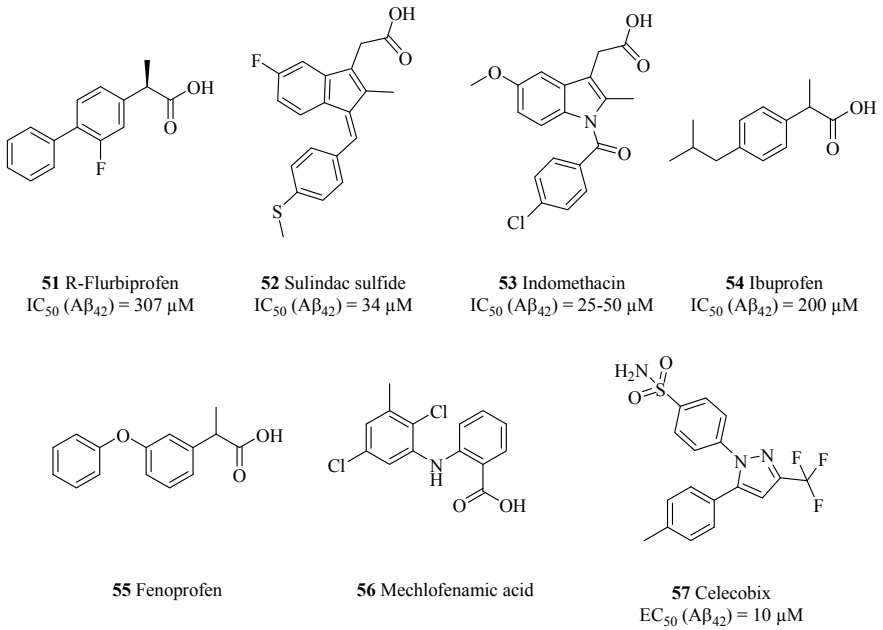

51 R-Flurbiprofen
IC_{50} ($Aβ_{42}$) = 307 μM

52 Sulindac sulfide
IC_{50} ($Aβ_{42}$) = 34 μM

53 Indomethacin
IC_{50} ($Aβ_{42}$) = 25-50 μM

54 Ibuprofen
IC_{50} ($Aβ_{42}$) = 200 μM

55 Fenoprofen

56 Mechlofenamic acid

57 Celecobix
EC_{50} ($Aβ_{42}$) = 10 μM

Scheme 7. NSAIDs that modulate γ-secretase activity.

Some cyclooxygenase-2 (COX-2) specific inhibitors, including celecoxib **57** and other structurally related compounds such as the peroxisome proliferator-activated receptor-γ (PPAR-γ) antagonist fenofibrate **58** were found to increase Aβ42 levels selectively [117,118]. Furthermore, cell based studies with Aβ42-lowering compounds have revealed that γ-secretase modulators do not affect the cleavage of other γ-secretase substrates such as Notch and others [115,118-122]. Assays with APP-transfected cell lines revealed that Aβ42-lowering NSAIDs do not change APP expression, turnover, internalization or release of the APP ectodomain. Significantly, in contrast to the conventional γ-secretase inhibitors NSAIDs do not cause accumulation of APP *C*-terminal fragments [115,118,121]. Some NSAIDs may display their Aβ-lowering effect by inhibiting the small GTP-binding protein Rho and its effector, Rho associated kinase (Rock) [123]. Remarkable, some NSAIDs shift the *in vitro* β-APP metabolism towards shorter and less fibrillogenic forms of the Aβ peptides. Ibuprofen **54**, sulindac **52** and indomethacin **53** (**Scheme 7**) modulate APP metabolism to explicitly generate

less Aβ42 and more soluble Aβ38 by interfering directly with the activities of γ-secretase. Furthermore, treatment with sulindac sulfide **52**, indomethacin **53** and ibuprofen **54** did neither impair γ-secretase-mediated Notch receptor cleavage and NICD formation nor the generation of the ICDs of APP and the ErbB-4 receptor [115,118,119,122]. This consistently unaffected ICD-generation of several γ-secretase substrates indicate that γ-secretase modulators and improved compounds may avoid the toxicity associated with γ-secretase inhibitors. Substantial progress has been made to determine the mechanism of action of Aβ42-lowering compounds. However, several arguments rule out any involvement of COX in the Aβ42-lowering activity such as: only a few NSAIDs display Aβ42-lowering activity, whereas all NSAIDs inhibit COX [115], the Aβ42-lowering activity of sulindac sulfide was not impaired in COX-1/2-deficient cells [115], and NSAID derivatives have been reported which lower Aβ42 devoid of their COX inhibitory activity [116,121,124,125]. Peretto *et al.* reported novel cyclopropylated flurbiprofen analogues with potent and selective inhibitory activity on Aβ42 [125].

Compared to flurbiprofen, the compounds **59, 60** (**Scheme 8**) exert improved potency on Aβ42-secretion. Moreover, introduction of the cyclopropyl substituent at the alpha position caused almost complete loss of COX-1 inhibition. In rats, compounds **59, 60** showed good oral bioavailability and long elimination half-life. Short-term studies in transgenic mice showed that compounds **59, 60** decreased plasma Aβ42 concentrations significantly. Carprofen **61**, a COX-2 inhibitor approved for the use in dogs, cows and horses is a weak inhibitor of γ-secretase. The geminal dimethyl derivatives of carprofen and flurbiprofen (**62, 63**) display 40% and 67% inhibition of Aβ42 production respectively in HEK cells at 100 μM concentration [126].

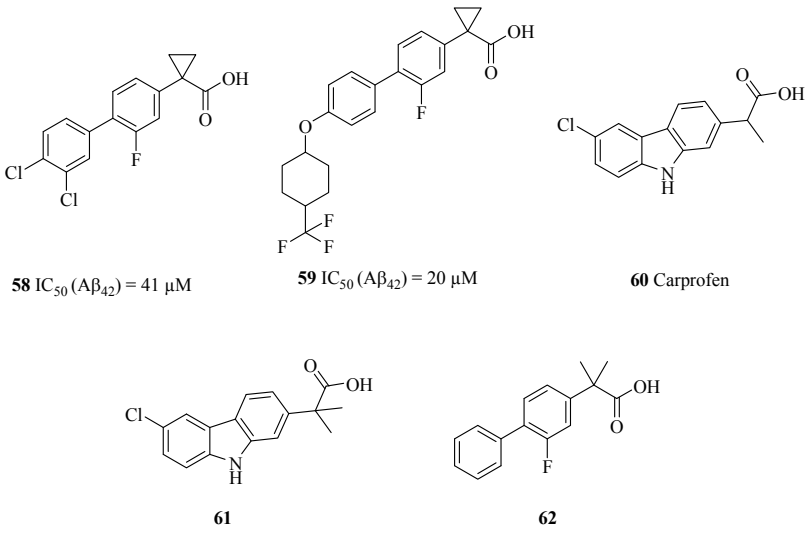

Scheme 8. NSAIDs derivatives that modulate γ-secretase activity.

3.2.2 Long-term and short term treatment studies with Aβ42-lowering NSAIDs

Several long-term and short-term treatment studies in APP-transgenic mouse models of AD have been performed with Aβ42-lowering NSAIDs. Even before the Aβ42-lowering activity of certain NSAIDs was reported, Lim *et al.* demonstrated that chronic treatment with high doses of ibuprofen for 6 months strongly reduced both amyloid pathology and inflammatory responses in Tg2576 mice [127]. In animals treated with ibuprofen, the total number and area of Aβ plaques was reduced by 50% while the soluble and insoluble Aβ in the brain was reduced by 30–40%. This was accompanied by reductions in the number of plaque-associated activated microglia cells and lowered levels of pro-inflammatory markers. Indomethacin was found to reduce amyloid pathology in Tg2576 mouse model but celecoxib and nimesulide did not show significant reductions in amyloid pathology [128,129]. Short-term treatments have demonstrated that Aβ42-lowering NSAIDs can lower Aβ42 levels in the brains of young, plaque-free APP-transgenic mice. In the initial experiments, 3-month-old Tg2576 mice were orally dosed for 3 days with 50 mg/kg/day of ibuprofen or naproxen [115]. Treatment with ibuprofen resulted in a 39% decrease in SDS-soluble Aβ42 without any changes in Aβ40 levels, whereas naproxen displayed no effect. Further short term studies have confirmed *in vivo* Aβ42-lowering activity for sulindac sulfide, indomethacin and flurbiprofen [67]. Only a few clinical trials with NSAIDs in AD patients have been conducted to date. A slowing of the cognitive decline was observed in the first trial with indomethacin [130]. Severe side effects caused by the long-term use of NSAIDs hamper the clinical use of NSAIDs, especially in elderly AD patients. Another promising strategy may be the application of specific NSAID enantiomers devoid of COX-1/2 inhibition. A particular interesting compound is the (*R*)-enantiomer of flurbiprofen, which lacks COX-1 inhibitory activity, but is equipotent in reducing Aβ42 *in vitro* and *in vivo* compared to (*S)*-flurbiprofen [116,121]. Recently, a phase II clinical trial with (*R*)-flurbiprofen (**51**, Flurizan®, developed by Myriad Pharmaceuticals) with duration of 12 months has been completed. According to the company website, a significant fraction of study participants with mild AD who took 800 mg of (*R*)-flurbiprofen twice daily declined less than did patients on placebo. As measured by the MMSE test, 42 percent of patients on (*R*)-flurbiprofen remained stable or even improved compared to 14 percent of patients on placebo. On the ADAS-Cog set of tests and other test batteries, one in four patients on (*R*)-flurbiprofen stayed stable or improved slightly, while none of the patients on placebo did. If the two ongoing phase 3 trials replicate these data, (*R*)-flurbiprofen would appear to be able to not only slow a person's decline but also halt progression of the disease, at least for a period of time. So far, this was true in some but not all people. Last year, the company reported that patients who responded to (*R*)-flurbiprofen also had fewer psychiatric complications. However, a related (*R*)-flurbiprofen dosage of 5 mg/kg per day was reported to interfere with COX-2 mRNA synthesis [131]. Thus AD therapy with (*R*)-flurbiprofen may cause an increase of thrombotic events. This potential cardiovascular risk still requires evaluation against the therapeutic benefit in AD.

4. Models for γ-secretase modulation

Until now, there is no satisfactory explanation for the binding site of the γ-secretase-modulators. To solve this dilemma the authors suggest two models for modulation versus inhibition (**Figure 5**). Potent active site directed inhibitors display modulatory action at concentrations below their IC_{50} concentration. This supports two binding sites (**Figure 5a**) of the active complex where one site is responsible for substrate recognition, the other for cleavage [132]. This observation is in accordance with the activity of partial PS1 Asp mutants by C. Haass and H. Steiner [36]. The hypothesis is that occupation of one site only results in a tilt of the dimeric substrate, which is subsequently cleaved at the $A\beta_{38}$ site. On the contrary the occupation of both sites is predicted to result in full γ-secretase inhibition. The distance between the two sites is an important aim of ongoing investigation for future studying. In the second model (**Figure 5b**) it is hypothesized, that GSMs such as NSAIDs do not target the γ-secretase-complex directly but rather bind to its substrate APP, thereby changing the cleavage pattern. The dimerization of APP may be influenced by this NSAIDs binding. A further possibility for the inhibition of APP cleavage was reported by D´Adamio *et al*. [133]. They discovered BRI2 and BRI3, type II membrane proteins, which inhibit the production of Aβ from APP. BRI2 interacts with APP and regulates the processing of APP resulting in reduced Aβ and AICD levels. 17 amino acids of BRI2 corresponding to the NH_2-terminal portion of Aβ, have been found to be essential for this interaction.

a)

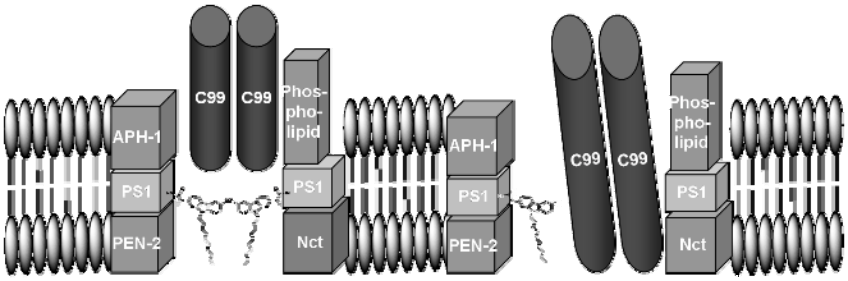

b)

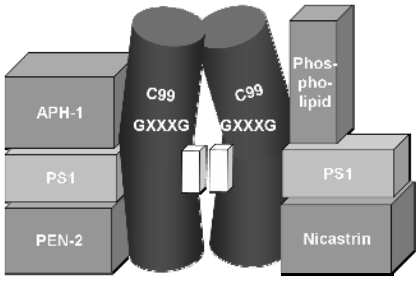

Figure 5. **a**) Simplistic model of the secretase modulation by occupation of one or two sites in the γ-secretase complex. Low inhibitor concentrations result in single occupation of the binding site, which tilts dimeric C99 substrate to result in a novel cleavage pattern. **b**) Substrate binding of GSMs leads to modulation.

5. Outlook

The availability of peptidic and peptidomimetic inhibitors for γ-secretase inhibitors made a huge impact on the research area. But these potent compounds come with costly price tags: oral availability cost of goods and blood-brain barrier penetration impose severe obstacles on drug development. Finally, the first results of brain penetrating secretase inhibitors in phase I or II were reported. Despite the extremely rapid progress in the field, there are no reports of a brain penetrating secretase inhibitor free of undesired activities in phase III in AD treatment. The selective modulation of γ-secretase by NSAIDs is pointing in the right direction: allosteric modulation of the active site, which can be identified by additional cleavage sites of PS1. Models for the mode of action of GSMs have been suggested, but the ultimate proof of concept for γ-secretase inhibition has not been revealed yet. However, the Notch associated anti-proliferative effects stimulated major companies (MSD and others) to switch the GSI programmes to oncology.

6. References

1. Schmidt, B., Narlawar R., Braun H.A. 2005. Current Medicinal Chemistry, 12, 1677.
2. Parvathy, S., Karran E.H., Turner A.J., Hooper N.M. 1998. FEBS letters, 431, 63.
3. Nunan, J., Small David H. 2002. Essays Biochem., 38, 37.
4. Perez, R.G., Soriano S., Hayes J.D., Ostaszewski, B., Xia, W., Selkoe, D.J., Chen, X., Stokin, G.B., Koo, E.H.. 1999. J. Biol. Chem., 274, 18851.
5. Vassar, R., Bennett B.D., Babu-Khan S., Kahn, S., Mendiaz, E.A., Denis, P., Teplow, D.B., Ross, S., Amarante, P., Loeloff, R., Luo, Y., Fisher, S., Fuller, J., Edenson, S., Lile, J., Jarosinski, M.A., Biere, A.L., Curran, E., Burgess, T., Louis, J.C., Collins, F., Treanor, J., Rogers, G., Citron, M. 1999. Science, 286, 735.
6. Bodendorf, U., Danner S., Fischer F., Stefani, M., Sturchler-Pierrat, C., Wiederhold, K.H., Staufenbiel, M., Paganetti, P. 2002. J. Neurochem., 80, 799.
7. Pastorino, L., Ikin A.F., Lamprianou S., Vacaresse, N., Revelli, J.P., Platt, K., Paganetti, P., Mathews, P.M., Harroch, S., Buxbaum, J.D. 2004, Molecular and Cellular Neuroscience, 25, 642.
8. Capell, A., Steiner H., Willem M., Kaiser, H., Meyer, C., Walter, J., Lammich, S., Multhaup, G., Haass, C. 2000, J. Biol. Chem., 275, 30849.
9. Limongelli, V., Marinelli L., Cosconati S., Braun, H.A., Schmidt, B., Novellino, E. 2007. ChemMedChem, 3, 667.
10. Marcinkeviciene, J., Luo Y., Graciani N.R., Combs A.P., Copeland R.A. 2001. J. Biol. Chem., 276, 23790.
11. Leung, D., Abbenante G., Fairlie D.P. 2000. J. Med. Chem., 43, 305.
12. Gorfe, A.A., Caflisch A. 2005. Structure (Camb), 13, 1487.
13. Park, H., Lee S. 2003. J. Am. Chem. Soc., 125, 16416.
14. Rajamani, R., Reynolds C.H. 2004. J. Med. Chem., 47, 5159.
15. Polgar, T., Keserue G.M. 2005. J. Med. Chem., 48, 3749.
16. Chou, K.C. 2004. J. Proteome Res., 3, 1069.
17. Farzan, M., Schnitzler C.E., Vasilieva N., Leung D., Choe H. 2000, PNAS, 97, 9712.
18. Yan, R., Munzner J.B., Shuck M.E., Bienkowski M.J. 2001. J. Biol. Chem., 276, 34019.
19. Westmeyer, G.G., Willem M., Lichtenthaler S.F., Lurman, G., Multhaup, G., Assfalg-Machleidt, I., Reiss, K., Saftig, P., Haass, C. 2004. J. Biol. Chem., 279, 53205.
20. Roggo, S. 2002. Curr. Top. Med. Chem., 2, 359.
21. Ishiura, S. 2000. Dementia Jpn., 14, 236.
22. John, V., Beck J.P., Bienkowski M.J., Sinha S., Heinrikson R.L. 2003. J. Med. Chem., 46, 4625.
23. Schmidt, B., Baumann S., Narlawar R., Braun H.A., Larbig G. 2006, Neurodegen. Dis., 3, 290.
24. Lichtenthaler, S.F., Wang R., Grimm H., Uljon, S.N., Masters, C.L., Beyreuther, K. 1999, PNAS, 96, 3053.
25. Qi-Takahara, Y., Morishima-Kawashima M., Tanimura Y., Dolios, G., Hirotani, N., Horikoshi, Y., Kametani, F., Maeda, M., Saido, T.C., Wang, R., Ihara, Y. 2005, J. Neurosci., 25, 436.
26. Beher, D., Wrigley J.D.J., Owens A.P., Shearman M.S. 2002. J. Neurochem., 82, 563.
27. Esh, C., Patton L., Kalback W., Kokjohn, T.A., Lopez, J., Brune, D., Newell, A.J., Beach, T., Schenk, D., Games, D., Paul, S., Bales, K., Ghetti, B., Castano, E.M., Roher, A.E. 2005, Biochemistry, 44, 13807.
28. Weidemann, A., Eggert S., Reinhard Friedrich B.M., Vogel, M., Paliga, K., Baier, G., Masters, C.L., Beyreuther, K., Evin, G. 2002, Biochemistry, 41, 2825.
29. Wolfe, M.S. 2006, Biochemistry, 45, 7931.
30. De Strooper, B. 2003, Neuron, 38, 9.
31. Annaert, W.G., Levesque L., Craessaerts K., Dierinck, I., Snellings, G., Westaway, D., George-Hyslop, P.S., Cordell, B., Fraser, P., De Strooper, B. 1999, J. Cell Biol., 147, 277.

32. Lazarov, V.K., Fraering P.C., Ye W., Wolfe, M.S., Selkoe, D.J., Li, H. 2006, PNAS, 103, 6889.
33. Franberg, J., Welander H., Aoki M., Winblad, B., Tjernberg, L.O., Frykman, S. 2007, Biochemistry, 46, 7647.
34. Brunkan, A.L., Goate A.M. 2005, J. Neurochem., 93, 769.
35. Mastrangelo, P., Mathews P.M., Chisti M.A., Schmidt, S.D., Gu, Y., Yang, J., Mazzella, M.J., Coomaraswamy, J., Horne, P., Strome, B., Pelly, H., Levesque, G., Ebeling, C., Jiang, Y., Nixon, R.A., Rozmahel, R., Fraser, P.E., St George-Hyslop, P., Carlson, G.A., Westaway, D. 2005, PNAS, 102, 8972.
36. Yu, G., Chen F., Nishimura M., Steiner, H., Tandon, A., Kawarai, T., Arawaka, S., Supala, A., Song, Y.Q., Rogaeva, E., Holmes, E., Zhang, D.M., Milman, P., Fraser, P., Haass, C., St George-Hyslop, P. 2000, Acta Neurol. Scand. Suppl. , 176, 6.
37. Kimberly, W.T., Xia W., Rahmati T., Wolfe M.S., Selkoe D.J. 2000, J. Biol. Chem., 275, 3173.
38. Selkoe, D., Kopan R. 2003, Annual Review of Neuroscience, 26, 565.
39. Thinakaran, G., Borchelt D.R., Lee M.K., Slunt, H.H., Spitzer, L., Kim, G., Ratovitsky, T., Davenport, F., Nordstedt, C., Seeger, M., Hardy, J., Levey, A.I., Gandy, S.E., Jenkins, N.A., Copeland, N.G., Price, D.L., Sisodia, S.S. 1996, Neuron, 17, 181.
40. Yu, G., Nishimura M., Arawaka S., Levitan, D., Zhang, L., Tandon, A., Song, Y.Q., Rogaeva, E., Chen, F., Kawarai, T., Supala, A., Levesque, L., Yu, H., Yang, D.S., Holmes, E., Milman, P., Liang, Y., Zhang, D.M., Xu, D.H., Sato, C., Rogaev, E., Smith, M., Janus, C., Zhang, Y., Aebersold, R., Farrer, L.S., Sorbi, S., Bruni, A., Fraser, P., St George-Hyslop, P. 2000, Nature, 407, 48.
41. Esler, W.P., Das C., Campbell W.A., Kimberly, W.T., Kornilova, A.Y., Diehl, T.S., Ye, W., Ostaszewski, B.L., Xia, W., Selkoe, D.J., Wolfe, M.S. 2002, Nat. Cell Biol., 4, E110.
42. Zhou, S., Zhou H., Walian P.J., Jap B.K. 2007, Biochemistry, 46, 2553.
43. Esler, W.P., Kimberly W.T., Ostaszewski B.L., Diehl, T.S., Moore, C.L., Tsai, J.Y., Rahmati, T., Xia, W., Selkoe, D.J., Wolfe, M.S. 2000, Nat. Cell Biol., 2, 428.
44. Francis, R., McGrath G., Zhang J., Ruddy, D.A., Sym, M., Apfeld, J., Nicoll, M., Maxwell, M., Hai, B., Ellis, M.C., Parks, A.L., Xu, W., Li, J., Gurney, M., Myers, R.L., Himes, C.S., Hiebsch, R., Ruble, C., Nye, J.S., Curtis, D. 2002, Dev. Cell, 3, 85.
45. Goutte, C., Tsunozaki M., Hale V.A., Priess J.R. 2002, PNAS, 99, 775.
46. Steiner, H., Winkler E., Edbauer D., Prokop, S., Basset, G., Yamasaki, A., Kostka, M., Haass, C. 2002, J. Biol. Chem., 277, 39062.
47. Luo, W.-j., Wang H., Li H., Kim, B.S., Shah, S., Lee, H.J., Thinakaran, G., Kim, T.W., Yu, G., Xu, H. 2003, J.Biol. Chem., 278, 7850.
48. Bergman, A., Hansson E.M., Pursglove S.E., Farmery, M.R., Lannfelt, L., Lendahl, U., Lundkvist, J., Naslund, J. 2004, J.Biol. Chem., 279, 16744.
49. Capell, A., Grunberg J., Pesold B., Diehlmann, A., Citron, M., Nixon, R., Beyreuther, K., Selkoe, D.J., Haass, C. 1998, J.Biol. Chem., 273, 3205.
50. Brown, M.S., Ye J., Rawson R.B., Goldstein J.L. 2000, Cell (Cambridge, Massachusetts), 100, 391.
51. Zhou, S., Zhou H., Walian P.J., Jap B.K. 2005, PNAS, 102, 7499.
52. Kimberly, W.T., LaVoie M.J., Ostaszewski B.L., *et al* 2003, PNAS, 100, 6382.
53. Munter, L.-M., Voigt P., Harmeier A., Kaden, D., Gottschalk, K.E., Weise, C., Pipkorn, R., Schaefer, M., Langosch, D., Multhaup, G. 2007, EMBO Journal, 26, 1702.
54. Kopan, R., Ilagan M.X. 2004, Nat. Rev. Mol. Cell Biol., 5, 499.
55. Herreman, A., Serneels L., Annaert W., Collen, D., Schoonjans, L., De Strooper, B. 2000, Nat. Cell Biol., 2, 461
56. Barten, D.M., Guss V.L., Corsa J.A., Loo, A., Hansel, S.B., Zheng, M., Munoz, B., Srinivasan, K., Wang, B., Robertson, B.J., Polson, C.T., Wang, J., Roberts, S.B., Hendrick, J.P., Anderson, J.J., Loy, J.K., Denton, R., Verdoorn, T.A., Smith, D.W., Felsenstein, K.M. 2005, J. Pharmacol. Exp. Ther., 312, 635.

57. Wong, H.-K., Sakurai T., Oyama F., Kaneko, K., Wada, K., Miyazaki, H., Kurosawa, M., De Strooper, B., Saftig, P., Nukina, N. 2005, J. Biol. Chem., 280, 23009.
58. Beglopoulos, V., Sun X., Saura C.A., Lemere, C.A., Kim, R.D., Shen, J. 2004, J. Biol. Chem., 279, 46907.
59. Fraering, P.C., LaVoie M.J., Ye W., Strub, J.M., Dolios, G., LaVoie, M.J., Ostaszewski, B.L., van Dorsselaer, A., Wang, R., Selkoe, D.J., Wolfe, M.S. 2004, Biochemistry, 43, 323.
60. Pissarnitski, D. 2007, Curr. Opin. Drug Discov. Devel., 10, 392.
61. Schmidt, B., Baumann S., Braun H.A., Larbig G. 2006, Curr. Top. Med. Chem. , 6, 377.
62. Kornilova, A.Y., Das C., Wolfe M.S. 2003, J. Biol. Chem., 278, 16470.
63. Weihofen, A., Lemberg M.K., Friedmann E., Rueeger, H., Schmitz, A., Paganetti, P., Rovelli, G., Martoglio, B. 2003, J. Biol. Chem., 278, 16528.
64. Shearman, M.S., Beher D., Clarke E.E., Lewis, H.D., Harrison, T., Hunt, P., Nadin, A., Smith, A.L., Stevenson, G., Castro, J.L. 2000, Biochemistry, 39, 8698.
65. McLendon, C., Xin T., Ziani-Cherif C., Murphy, M.P., Findlay, K.A., Lewis, P.A., Pinnix, I., Sambamurti, K., Wang, R., Fauq, A., Golde, T.E. 2000, Faseb J, 14, 2383.
66. Castro Pineiro, J.L., Smith A.L., Stevenson G.I. (Merck Sharp & Dohme Limited, UK). WO2001066564, 2001, 34 pp.
67. Esler, W.P., Kimberly W.T., Ostaszewski B.L., et al 2002, PNAS, 99, 2720.
68. Audia, J.E., Mabry T.E., Nissen J.S., McDaniel S.L. (Elan Pharmaceuticals, Inc., USA; Eli Lilly and Company). WO9932453, 1999, 114 pp.
69. Dovey, H.F., John V., Anderson J.P., Chen, L.Z., de Saint Andrieu, P., Fang, L.Y., Freedman, S.B., Folmer, B., Goldbach, E., Holsztynska, E.J., Hu, K.L., Johnson-Wood, K.L., Kennedy, S.L., Kholodenko, D., Knops, J.E., Latimer, L.H., Lee, M., Liao, Z., Lieberburg, I.M., Motter, R.N., Mutter, L.C., Nietz, J., Quinn, K.P., Sacchi, K.L., Seubert, P.A., Shopp, G.M., Thorsett, E.D., Tung, J.S., Wu, J., Yang, S., Yin, C.T., Schenk, D.B., May, P.C., Altstiel, L.D., Bender, M.H., Boggs, L.N., Britton, T.C., Clemens, J.C., Czilli, D.L., Dieckman-McGinty, D.K., Droste, J.J., Fuson, K.S., Gitter, B.D., Hyslop, P.A., Johnstone, E.M., Li, W.Y., Little, S.P., Mabry, T.E., Miller, F.D., Audia, J.E. 2001, J. Neurochem., 76, 173.
70. Lanz, T.A., Himes C.S., Pallante G., Adams, L., Yamazaki, S., Amore, B., Merchant, K.M. 2003, J. Pharm. Exp. Ther., 305, 864.
71. Geling, A., Steiner H., Willem M., Bally-Cuif L., Haass C. 2002, EMBO reports, 3, 688.
72. Hadland, B.K., Manley N.R., Su D., Longmore, G.D., Moore, C.L., Wolfe, M.S., Schroeter, E.H., Kopan, R. 2001, PNAS, 98, 7487.
73. Lanz, T.A., Hosley J.D., Adams W.J., Merchant K.M. 2004, J. Pharm. Exp. Ther., 309, 49.
74. Wong, G.T., Manfra D., Poulet F.M., Zhang, Q., Josien, H., Bara, T., Engstrom, L., Pinzon-Ortiz, M., Fine, J.S., Lee, H.J., Zhang, L., Higgins, G.A., Parker, E.M. 2004, J. Biol. Chem., 279, 12876.
75. Siemers, E., Skinner M., Dean R.A., Gonzales, C., Satterwhite, J., Farlow, M., Ness, D., May, P.C. 2005, Clin. Neuropharmacol., 28, 126.
76. Siemers, E.R., Quinn J.F., Kaye J., Farlow, M.R., Porsteinsson, A., Tariot, P., Zoulnouni, P., Galvin, J.E., Holtzman, D.M., Knopman, D.S., Satterwhite, J., Gonzales, C., Dean, R.A., May, P.C. 2006, Neurology, 66, 602.
77. Seiffert, D., Bradley J.D., Rominger C.M., Rominger, D.H., Yang, F., Meredith, J.E. Jr, Wang, Q., Roach, A.H., Thompson, L.A., Spitz, S.M., Higaki, J.N., Prakash, S.R., Combs, A.P., Copeland, R.A., Arneric, S.P., Hartig, P.R., Robertson, D.W., Cordell, B., Stern, A.M., Olson, R.E., Zaczek, R. 2000, J. Biol. Chem., 275, 34086.
78. Zaczek, R., Olson R.E., Seiffert D.A., Thompson L.A. (Bristol-Myers Squibb Company, USA). US6737038, 2004, 45 pp.
79. Fuwa, H., Takahashi Y., Konno Y., Watanabe, N., Miyashita, H., Sasaki, M., Natsugari, H., Kan, T., Fukuyama, T., Tomita, T., Iwatsubo, T. 2007, ACS Chem. Biol., 2, 408.
80. Rishton, G.M., Retz D.M., Tempest P.A., Novotny, J., Kahn, S., Treanor, J.J., Lile, J.D., Citron, M. 2000, J. Med. Chem., 43, 2297.

81. Kreft, A.F., Cole D.C., Woller K.R., Stock, J.R., Diamanitis, G., Kurbrak, D.M., Kutterer, K.M., Moore, W.J., Casebier, D. (Wyeth, John, and Brother Ltd., USA; Arqule, Inc.). WO2002057252, 2002, 133 pp.
82. Josien, H.B., Clader J.W., Bara T.A., *et al.* (Schering Corporation, USA). WO2006004880, 2006, 147 pp.
83. Belanger, P.C., Collins I.J., Hannam J.C., *et al.* (Merck Sharp & Dohme Limited, UK; Merck Frosst Canada + Co.). WO0170677, 2001, 199 pp.
84. Churcher, I., Harrison T., Kerrad S., *et al.* (Merck Sharp & Dohme Limited, UK). WO2004031137, 2004, 78 pp.
85. Lewis, H.D., Harrison T., Shearman M.S. (Merck Sharp & Dohme Limited, UK). WO2006123184, 2006, 44 pp.
86. Brands, K.M.J., Brewer S.E., Davies A.J., *et al.* (Merck Sharp & Dohme Limited, UK). GB2427193, 2006, 23 pp.
87. Hendrix, M., Baumann K., Grosser R., *et al.* (Bayer Aktiengesellschaft, Germany). WO2003059335, 2003, 181 pp.
88. Flohr, A., Galley G., Jakob-Roetne R., *et al*. (Switz.). WO2005075327, 2005, 38 pp.
89. Neitzel, M. (Elan Pharmaceuticals, Inc., USA). WO2006078753, 2006, 111 pp.
90. Konradi, A.W., Mattson M.N., Semko C.M., Ye X.M. (Elan Pharmaceuticals, Inc., USA). WO2007024651, 2007, 102 pp.
91. Bowers, S., Garofalo A.W., Hom R.K., *et al.* (Elan Pharmaceuticals, Inc., USA). WO2007022502, 2007, 141 pp.
92. Galley, G., Kitas E.A., Jakob-Roetne R. (F. Hoffmann-La Roche AG, Switz.). WO2006005486, 2006, 107 pp.
93. Flohr, A., Galley G., Jakob-Roetne R., Kitas E.A., Wostl W. (Switz.). WO2007020190, 2007, 18 pp.
94. Flohr, A., Jakob-Roetne R., Wostl W. (Hoffmann-La Roche Inc., USA). WO2006061136, 2006, 58 pp.
95. Galley, G., Goodnow R.A., Peters J.-U. (Hoffmann-La Roche Inc., USA). WO2004235819, 2004, 27 pp.
96. Greenberg, B., Hill D.C., Jacobs R., Sisodia S.S. (AstraZeneca AB, Swed.; University of Chicago). WO2006065218, 2006, 60 pp.
97. Netzer, W.J., Dou, F., Cai, D., Veach. D., Jean, S., Li, Y., Bornmann, W.G., Clarkson, B., Xu, H., Greengard, P. 2003, PNAS, 100, 12444.
98. Fraering, P.C. 2005, J. Biol. Chem., 280, 41987.
99. Cheng, S., Comer D.D., Mao L., Balow G.P., Pleynet D. (Neurogenetics, Inc., USA). WO2004110350, 2004, 178 pp.
100. Fisher, A., Bar-Ner N., Karton Y. (Israel Institute for Biological Research, Israel). WO2003092580, 2003, 102 pp.
101. Caccamo, A., Oddo S., Billings L.M., Green, K.N., Martinez-Coria, H., Fisher, A., LaFerla, F.M. 2006, Neuron, 49, 671.
102. Laras, Y., Quelever G., Garino C., Pietrancosta, N., Sheha, M., Bihel, F., Wolfe, M.S., Kraus, J.L. 2005, Biol. Org. Chem., 3, 612.
103. Brodney, M.A., Coffman K.J., Kleinman E.F., O'Neill B.T., Chen Y.L. (Pfizer Inc, USA). WO2007034326, 2007, 137 pp.
104. Beher, D., Bettati M., Checksfield G.D., *et al.* (Merck Sharp & Dohme Limited, UK). WO2005013985, 2005, 74 pp.
105. Burkamp, F., Checksfield G.D., Fletcher S.R., *et al*. (Merck Sharp & Dohme Ltd., UK). WO2007054739, 2007, 42 pp.
106. Blurton, P., Burkamp F., Churcher I., Harrison T., Neduvelil J. (Merck Sharp & Dohme Limited, UK). WO2006008558, 2006, 58 pp.
107. Wilson, F., Reid A., Reader V., *et al.* (Cellzome A.-G., Germany). WO2006045554, 2006, 57 pp.
108. Ramsden, N., Wilson F. (Cellzome A.-G., Germany). WO2006048219, 2006, 35 pp.

109. Narlawar, R., Perez Revuelta B.I., Baumann K., Schubenel, R., Haass, C., Steiner, H., Schmidt, B. 2007, Bioorg. Med. Chem. Lett., 17, 176.
110. Pratico, D., Trojanowski J.Q. 2000, Neurobiol. Aging, 21, 441.
111. McGeer, P.L., McGeer E.G. 2001, Archives of Neurology, 58, 1790.
112. in 't Veld, B.A., Ruitenberg A., Hofman A., Launer, L.J., van Duijn, C.M., Stijnen, T., Breteler, M.M., Stricker, B.H. 2001, N. Engl. J. Med., 345, 1515.
113. Etminan, M., Gill S., Samii A. 2003, BMJ, 327, 128.
114. Avramovich, Y., Amit T., Youdim M.B.H. 2002, J. Biol. Chem., 277, 31466.
115. Weggen, S., Eriksen J.L., Das P., Sagi, S.A., Wang, R., Pietrzik, C.U., Findlay, K.A., Smith, T.E., Murphy, M.P., Bulter, T., Kang, D.E., Marquez-Sterling, N., Golde, T.E., Koo, E.H. 2001, Nature, 414, 212.
116. Eriksen, J.L., Sagi S.A., Smith T.E., Weggen, S., Das, P., McLendon, D.C., Ozols, V.V., Jessing, K.W., Zavitz, K.H., Koo, E.H., Golde, T.E. 2003, J. Clin. Investigation, 112, 440.
117. Kukar, T., Murphy M.P., Eriksen J.L., Sagi, S.A., Weggen, S., Smith, T.E., Ladd, T., Khan, M.A., Kache, R., Beard, J., Dodson, M., Merit, S., Ozols, V.V., Anastasiadis, P.Z., Das, P., Fauq, A., Koo, E.H., Golde, T.E. 2005, Nature Med., 11, 545.
118. Gasparini, L., Rusconi L., Xu H., del Soldato P., Ongini E. 2004, J. Neurochem., 88, 337.
119. Takahashi, Y., Hayashi I., Tominari Y., Rikimaru, K., Morohashi, Y., Kan, T., Natsugari, H., Fukuyama, T., Tomita, T., Iwatsubo, T. 2003, J. Biol. Chem., 278, 18664.
120. Beher, D., Clarke E.E., Wrigley J.D.J., Martin, A.C., Nadin, A., Churcher, I., Shearman, M.S. 2004, J. Biol. Chem., 279, 43419.
121. Morihara, T., Chu T., Ubeda O., Beech W., Cole G.M. 2002, J. Neurochem., 83, 1009.
122. Weggen, S., Eriksen J.L., Sagi S.A., Pietrzik, C.U., Ozols, V., Fauq, A., Golde, T.E., Koo, E.H. 2003, J. Biol. Chem., 278, 30748.
123. Zhou, Y., Su Y., Li, B., Liu, F., Ryder, J.W., Wu, X., Gonzalez, D.,Whitt, P.A., Gelfanova, V., Hale, J.E., May, P.C., Paul, S.M., Ni, B. 2003, Science, 302, 1215.
124. Narlawar, R., PerezRevuelta B.I., Haass C., Steiner, H., Schmidt, B., Baumann, K. 2006, J. Med. Chem., 49, 7588.
125. Peretto, I., Radaelli S., Parini C., Zandi, M., Raveglia, L.F., Dondio, G., Fontanella, L., Misiano, P., Bigogno, C., Rizzi, A., Riccardi, B., Biscaioli, M., Marchetti, S., Puccini, P., Catinella, S., Rondelli, I., Cenacchi, V., Bolzoni, P.T., Caruso, P., Villetti, G., Facchinetti, F., Del Giudice, E., Moretto, N., Imbimbo, B.P. 2005, J. Med. Chem., 48, 5705.
126. Stock, N., Munoz B., Wrigley J.D., Shearman, M.S., Beher, D., Peachey, J., Williamson, T.L., Bain, G., Chen, W., Jiang, X., St-Jacques, R., Prasit, P. 2006, Bioorg. Med. Chem. Lett., 16, 2219.
127. Lim, G.P., Yang F., Chu T., Chen, P., Beech, W., Teter, B., Tran, T., Ubeda, O., Ashe, K.H., Frautschy, S.A., Cole, G.M. 2000, J. Neurosci., 20, 5709.
128. Sung, S., Yang H., Uryu K., Lee, E.B., Zhao, L., Shineman, D., Trojanowski, J.Q., Lee, V.M., Pratico, D. 2004, Am. J. Path., 165, 2197.
129. Jantzen, P.T., Connor K.E., DiCarlo G., Wenk, G.L., Wallace, J.L., Rojiani, A.M., Coppola, D., Morgan, D., Gordon, M.N. 2002, J. Neurosci., 22, 2246.
130.Rogers, J., Kirby L.C., Hempelman S.R., Berry, D.L., McGeer, P.L., Kaszniak, A.W., Zalinski, J., Cofield, M., Mansukhani, L., Willson, P.1993, Neurology, 43, 1609.
131. Wechter, W.J. (Loma Linda University Medical Center, USA). WO2000013684, 2000, 10 pp.
132. Clarke, E.E., Churcher I., Ellis S., Wrigley, J.D., Lewis, H.D., Harrison, T., Shearman, M.S., Beher, D. 2006, J. Biol. Chem., 281, 31279.
133. D'Adamio, L., Matsuda S. (Albert Einstein College of Medicine of Yeshiva University, USA). WO2006138355, 2006, 39 pp.

Alzheimer-Demenz: Ein Pla(qu)e – mit Hoffnung auf Besserung?

Entwicklung von Wirkstoffen zur Ursachenforschung und eventueller Therapie der Krankheit

Keywords: Alzheimer, Aβ, Sekretasen

Dipl.-Biochem. Nicole Höttecke, Clemens Schöpf-Institut für Organische Chemie und Biochemie, TU Darmstadt

Stefanie Baumann, Clemens Schöpf-Institut für Organische Chemie und Biochemie, TU Darmstadt

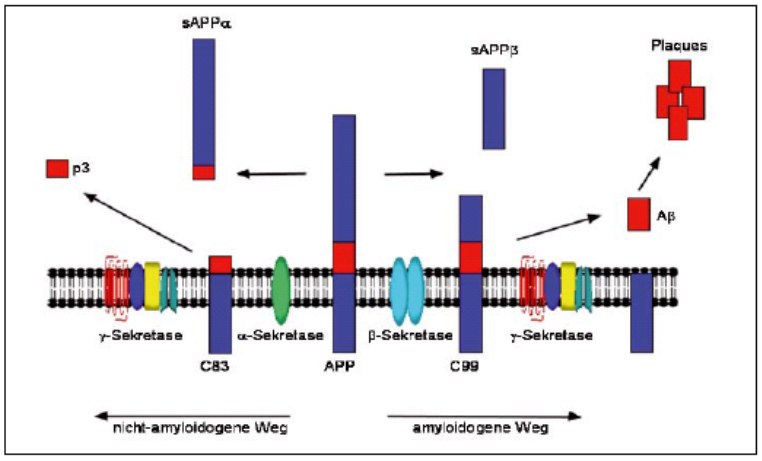

Abb. 1: APP Abbau durch β- und γ-Sekretase führt zu amyloiden Plaques.

Die Alzheimer-Demenz ist heute die häufigste Form der Demenz (demens lat.=verwirrt) und mit zunehmender Lebenserwartung der Menschheit werden auch die Patientenzahlen steigen. Es besteht also ein großes Interesse die Ursachen zu erforschen und geeignete Wirkstoffe für eine Therapie zu entwickeln.

Die Alzheimer-Demenz (AD) ist eine verheerende Krankheit, da sie den Betroffenen das Erinnerungsvermögen raubt und mit starken Persönlichkeitsveränderungen assoziiert ist. Die Alzheimerkrankheit wurde zum ersten Mal 1906 von Alois Alzheimer als eine „krankhafte Veränderung der Gehirnrinde" beschrieben. In diesen Veränderungen wurden zwei verschiedene Proteinablagerungen identifiziert: intrazelluläre, amyloide Plaques und extrazelluläre, neurofibrilläre Bündel. Die Plaques bestehen aus amyloidem-β-Peptid (Aβ), welches durch einen „falschen" Abbau des membranständigen, amyloiden Vorläuferproteins (*Amyloid Precursor Protein*, APP) gebildet wird. APP kann auf zwei verschiedenen Wegen

BIOforum 6/2008, S. 32–34, GIT VERLAG GmbH & Co. KG, Darmstadt www.gitverlag.com www.PRO-4-PRO.com

abgebaut werden, 1) über den „normalen“, nicht-amyloidogenen Weg und 2) über den amyloidogenen Weg, welcher für die Bildung des pathogenen Aβ verantwortlich ist. (Abb. 1)

Der nicht-amyloidogenen Weg

Bei dem nicht-amyloidogenen Weg, der bei gesunden Menschen einen Anteil von etwa 90% ausmacht, wird APP zunächst von der α-Sekretase, einer membrangebundenen Metalloprotease in der Aβ-Sequenz geschnitten, was zu dem löslichen sAPPα und dem membrangebundenen Fragment C83 führt. Bei anschließender Spaltung von C83 durch die γ-Sekretase, eine membrangebundene Aspartylprotease, wird das nicht zur Aggregation neigende Peptid p3 freigesetzt. Wird APP jedoch sequentiell von den beiden Aspartylproteasen β- und γ-Sekretase abgebaut, dann entsteht pathogenes Aβ. Die β Sekretase (β-*site APP cleavinge enzyme* oder BACE-1) generiert ein extra- zelluläres Fragment (sAPPβ) und ein intrazelluläres, membrangebundenes Fragment C99, aus dem nach Spaltung durch die γ-Sekretase Aβ-Peptide unterschiedlicher Länge entstehen. Die häufigsten Aβ-Peptide sind $Aβ_{38}$, $Aβ_{40}$ und $Aβ_{42}$, welche aus 38, 40 bzw. 42 Aminosäuren bestehen. Für die Aggregation gilt: je länger ein Aβ-Fragment ist, desto besser und schneller kann es sich zusammenlagern. Die Aggregation zu frühen Oligomeren wird als toxisches Prinzip erachtet. Daher ist die Bildung von $Aβ_{38}$ eher unbedenklich und $Aβ_{42}$ toxisch. Um die Entstehung von Aβ zu verhindern, könnte nun z.B. die α-Sekretase aktiviert oder die β- bzw. γ-Sekretase inhibiert werden. Da die α-Sekretase bei diversen Entzündungsmechanismen eine wichtige Rolle spielt, ist eine Aktivierung mit Risiken behaftet. BACE existiert in zwei Isoformen BACE-1 und 2, welche eine wichtige Rolle in der Myelinisierung von Nervenzellen übernehmen, die jedoch in AD Patienten weitgehend abgeschlossen ist. Bisher konnten nur wenige oral verfügbare Inhibitoren für klinische Studien erhalten werden. Auch eine vollständige Inhibition der γ-Sekretase würde, ähnlich wie bei BACE, unerwünschte Nebenwirkungen verursachen. Neben APP spaltet die γ-Sekretase nämlich weitere Substrate wie Notch, welches für die Zellproliferation und differenzierung notwendig ist. Diese unerwünschte Totalinhibition kann jedoch durch allosterische Regulation umgangen werden. So genannte γ-Sekretase-Modulatoren (GSMs) regulieren den APP-Metabolismus derart, dass vermehrt $Aβ_{38}$ und weniger pathologisches $Aβ_{42}$

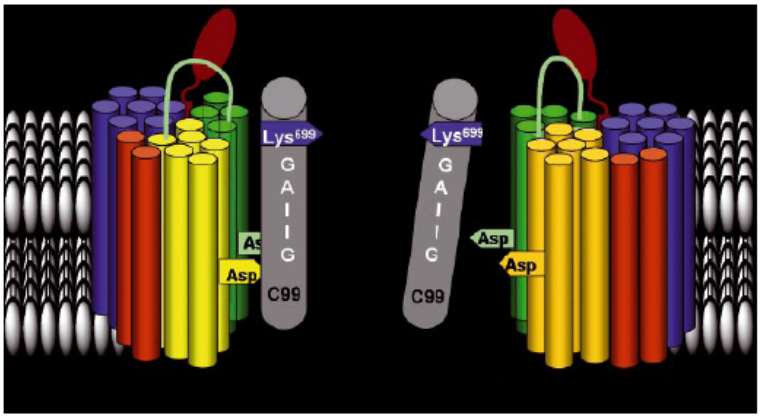

Abb.2: Schematischer Aufbau des γ-Sekretase-Komplexes mit gebundenem GSM an Lys699

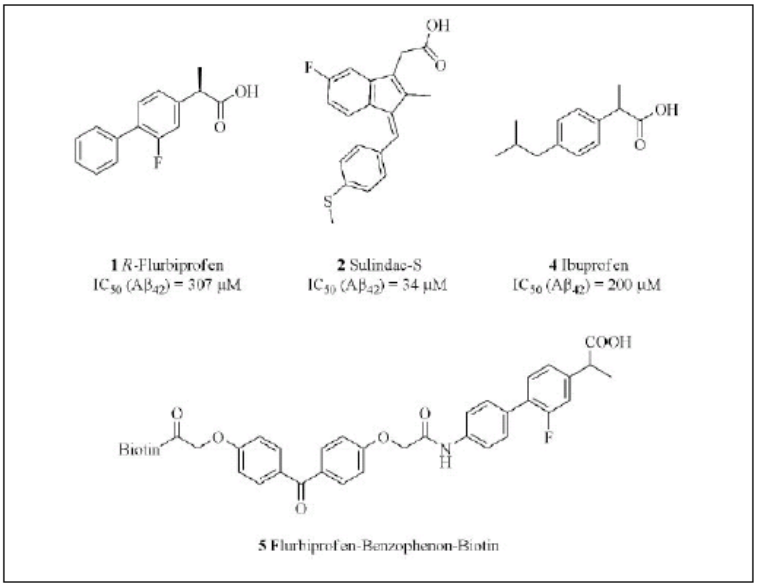

Abb.3: NSAIDs und GSM-Photoprobe, Flurbiprofen-Benzophenon-Biotin (5)

gebildet wird. Die γ-Sekretase ist ein membranlokalisierter Enzymkomplex, der aus vier Proteinen zusammengesetzt ist: Präsenilin (PS), Nicastrin (Nct), *anterior pharynx defective-1* (Aph-1) und presenilin enhancer-2 (Pen-2). Präsenilin 1 (PS1) ist eine Aspartylprotease mit 9 (oder 10) Transmem-brandomänen und zwei Aspartaten, welche als katalytisches Heterodimer agieren und sich auf den Transmembrandomänen 6 (Asp_{257}) und 7 (Asp_{385}) befinden. Die Substratspaltung, bei der das Substrat eventuell als Dimer vorliegt, findet in der Membran statt. Dies ist ein eher ungewöhnlicher Spaltungsmechanismus, da die Spaltung in der hydrophoben Membran Wasser benötigt. Die beiden Präseniline (PS1 und PS2) kontrollieren die Aktivität der γ Sekretase und Mutationen in den codierenden Genen auf Chromosom 14 bzw. 1 führen zu familiären Formen der AD (FAD). Obwohl PS für die Aktivität der γ-Sekretase verantwortlich ist, kann diese nur in der Gegenwart der drei Proteine aus dem Komplex aktiv sein, da es ohne Aktivierung nur als Holoprotein vorliegt. Nct ist ein Typ-1 Transmembranprotein, welches für die Substraterkennung sowie für den Substrateintritt in den Komplex notwendig ist, indem es mit dem *N*-Terminus des Substrats interagiert. (Abb.2)

Aph-1, ein 7-Transmembranprotein, bildet mit Nct einen Subkomplex, der für die Stabilisierung des PS-Holoproteins notwendig ist. Pen-2 ist ein zwei-Membrandomänenprotein und ist für

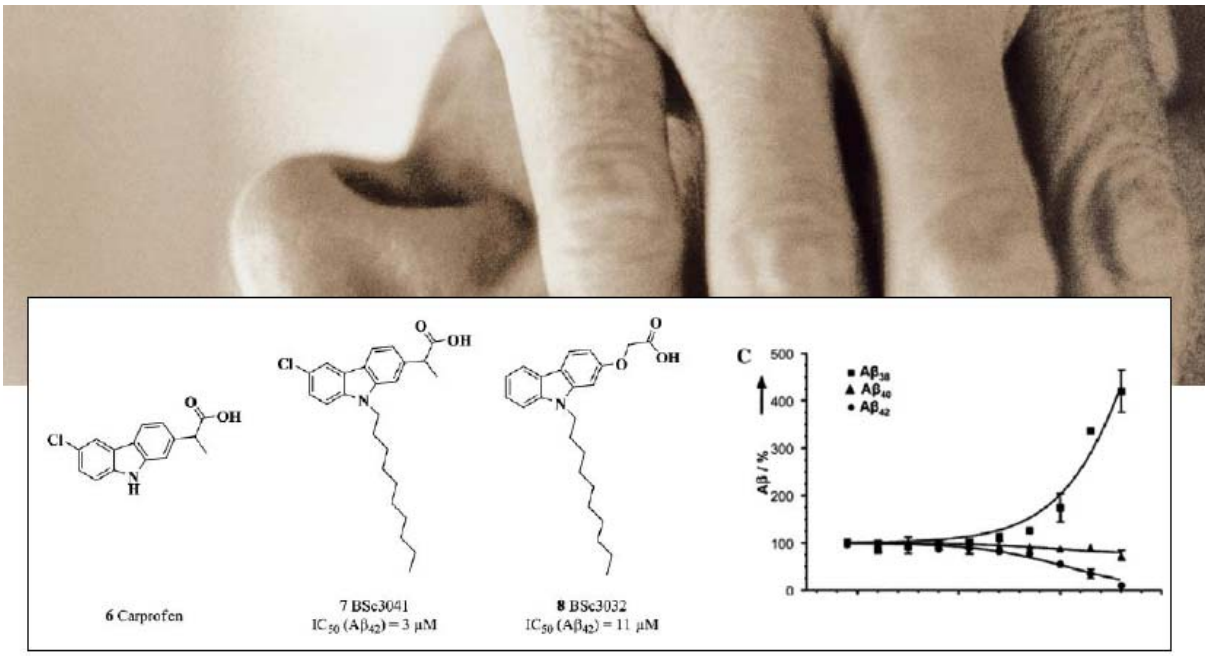

Abb.4: GSM-Leitstruktur des AK Schmidts mit Dosis-Wirkungs-Kurve von BSc3041 (7)

die Stabilität des PS-Nct Subkomplexes verantwortlich. Seine *C*-terminale Domäne induziert die Entstehung des katalytisch aktiven PS Heterodimers, die Endoproteolyse, und stabilisiert anschließend die beiden entstehenden Fragmente. Strukturanalyse des kristallisierten Enzyms würde die Inhibitorentwicklung vereinfachen, da ein strukturbasiertes Wirkungsdesign ermöglicht würde. Dieses gelang bislang aufgrund der Membranlokalisation des γ-Sekretase-Enzym-komplexes sowie der notwendigen Lipidstabilisierung nicht. Es konnte gezeigt werden, dass entzündungshemmende Wirkstoffe, die so genannten nichtsteroidalen Antirheumatika (non-steroidal antiinflammatory drugs, NSAIDs), wie *R*-Flurbiprofen (1), Sulindac-S (2) oder Ibuprofen (3) den Fortgang von AD hemmen können. Sulindac-S z.B. zeigt eine selektive $A\beta_{42}$-senkende Aktivität (IC_{50} = 34 µM) und wirkt damit als GSM. (Abb.3)

Photoaffinitätsstudien mit einer GSM-Photoprobe des NSAID-Derivats R-Flurbiprofen (5) zeigten, dass 5 nicht an den γ-Sekretase-Komplex bindet, sondern an das Substrat APP. Die Markierung wurde an den Aminosäuren 28-36 von Aβ lokalisiert, dies entspricht der Dimerisierungsregion.

Stand der Forschung:

An der TU Darmstadt wurden GSMs entwickelt, die als Grundgerüst das NSAID Carprofen (6) aufweisen. (Abb. 4) Für eine Modulation sind zwei Funktionalitäten essentiell: eine Carbonsäure, die mit dem Substrat interagiert und ein langer lipophiler Rest, welcher für die Orientierung des Modulators in der Membran verantwortlich zu sein scheint. Des Weiteren gelang der Aktivitäts-Transfer auf Carbazolderivate [8], die im Gegensatz zu Carprofen kein stereogenes Zentrum ($IC_{50}(A\beta_{42})$=11µm) aufweisen. Die Substanzen sind nahezu equipotent und momentane Untersuchungen fokussieren auf eine Aktivitätssteigerung. (Abb.4)

Es wird vermutet, dass die Carbonsäure an Lysin699 im APP bindet (Abb. 2), das direkt am Membrandurchtritt lokalisiert ist. Durch Mutationsstudien konnte gezeigt werden, dass diese basische Aminosäure für die Modulation wichtig ist, da nur die basische Arginin-Mutante weiterhin Modulation zeigt. Weiterführende Untersuchungen zu der Bindungsstelle am Substrat, zu der Orientierung des GSMs in der Membran und generell zu der Lokalisation des Komplexes in der Zelle werden an der TU Darmstadt durchgeführt.

Ausblick

2008 endete die klinische Phase III Studie des NSAIDs *R*-Flurbiprofen [5] ohne signifikante, kognitive Verbesserungen. Es wurde eine relativ hohe Dosierung von 2x 800 mg/Tag gewählt, da das Überwinden der Blut-Hirn-Schranke und somit die Verfügbarkeit im Gehirn weniger als 5% beträgt. Weitere, viel versprechende Kandidaten sind Mercks GSM-1 und E2012 von *Eisai und Torrey Pines Pharmaceuticals*. E2012 wurde 2008 in die Phase I Studie aufgenommen, deshalb sind erste Phase II-Daten frühestens ab 2010 zu erwarten.

Referenzen

[1] Baumann *et al.*: Medicinal Chemistry of Alzheimer Disease, ed. A. Martinez, Research Signpost, 193 (2008)

[2] Wolfe M. S.: Biochemistry, 45, 7931 (2006)

[3] Kukar, T. L. *et al.*: Nature, 453, 7197 (2008)

[4] Narlawar R. *et al.*: Bioorg. Med. Chem. Lett., 17, 176 (2007)

[5] Narlawar R.: J. Med. Chem., 49 (26), 7588 (2006)

[6] Munter L.-M. *et al.*: EMBOJournal, 26, 1702 (2007)

Kontakt:

Dipl.-Biochem. Nicole Höttecke

Stefanie Baumann

Clemens Schöpf-Institut für Organische Chemie und Biochemie, TU Darmstadt

Tel.: 06151/162047

nicole.hoettecke@gmx.de

3.3 Untersuchungen der Membrananker-Eigenschaften von NSAID-abgeleiteten γ-Sekretase Modulatoren

Der Inhalt dieses Kapitels wurde bereits veröffentlicht:
Stefanie Baumann, Nicole Höttecke, Robert Schubenel, Karlheinz Baumann, Boris Schmidt *Bioorg. Med. Chem. Lett.* **2009**, *19*, 6986-6990. "NSAID-derived γ-secretase modulators. Part III: Membrane anchoring."

Durch die Synthese von 7 Carbazol-Derivaten unter Variation des lipophilen Restes wurde untersucht, ob dieser Rest als Membrananker fungieren kann.

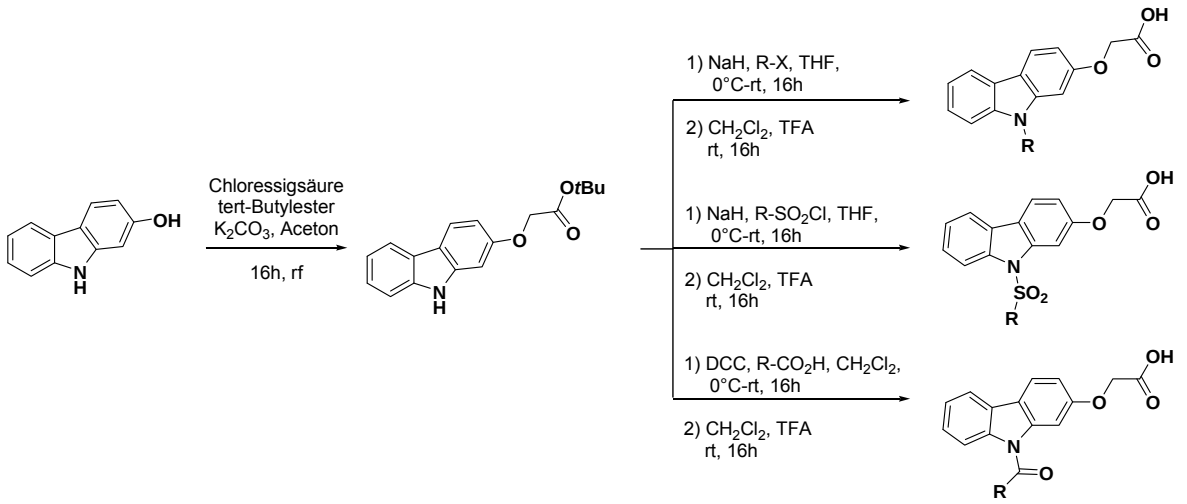

Abb. 21: Synthese der Carbazol-Derivate, um die Membrananker-Eigenschaft zu untersuchen.

Der lipophile Rest konnte unter Aufbau eines tertiären Amins, eines Carbonsäureamids oder Sulfonamids an das Carbazol-Gründgerüst substituiert werden. Durch das Einführen einer Doppelbindung in den lipophilen Alkylrest (Ölsäure- bzw. Elaidinsäure-Derivat) konnte eine um Faktor zwei gesteigerte Aktivität ($IC_{50}(A\beta_{42})$ = 13 μM) im Vergleich mit dem gesättigten Octadecan-Derivat ($IC_{50}(A\beta_{42})$ = 26 μM) beobachtet werden.
Eine mögliche Erklärung dieser Aktivitätssteigerung ist die Lokalisierung des Alkyl-Substituenten in der Membran, da eine Doppelbindung den Alkyl-Rest rigider werden lässt und die Inkorporation in die Membran vereinfacht. Es ist überraschenderweise irrelevant, ob die Doppelbindung *cis*- oder *trans*-konfiguriert vorliegt, denn Beide zeigen die gleiche modulatorische Aktivität auf die Aβ-Sekretion ($IC_{50}(A\beta_{42})$ = 13 μM). Die Vermutung, dass ein rigider lipophiler Rest das Einlagern in die Membran erleichtert und somit eine Steigerung der modulatorischen Eigenschaft zur Folge hat, konnte durch Derivatisierung des

Grundgerüstes mit einem *para*-substituierten Azofarbstoff ($IC_{50}(A\beta_{42}) = 9\ \mu M$) bestätigt werden. Im Gegensatz dazu zeigen in *m*-Position substituierte Aromaten als lipophiler Rest keine Aktivität auf die Aβ-Sekretion mehr.

Durch diese Untersuchungen wurde die Vermutung erhärtet, dass der lipophile Rest als Membrananker agiert. Ein rigider linearer lipophiler Rest erleichtert die Einlagerung in die Membran wo hingegen eine Verzweigung des lipophilen Substituenten diese Einlagerung erschwert, was zu einem vollständigen Verlust der modulatorischen Aktivität führt.

Liste der von Nicole Höttecke von 2006-2009 synthetisierten Verbindungen:

BSc3770
BSc3853
BSc3854
BSc3915
BSc3955
Bsc3956
BSc3984

NSAID-derived γ-secretase modulators. Part III. Membrane anchoring

Stefanie Baumann,[a] Nicole Höttecke,[a] **Robert Schubenel,**[b] Karlheinz Baumann,[b] Boris Schmidt[a]*

[a]*Clemens Schöpf-Institute of Chemistry and Biochemistry, Technische Universität Darmstadt, Petersenstr. 22, D-64287 Darmstadt, Germany, Fax: (+49) 6151-163278, E-mail: schmidt_boris@t-online.de*

[b]*F. Hoffmann-La Roche Ltd., Pharmaceuticals Division, Preclinical Research CNS, Bldg. 70/345, CH-4070 Basel, Switzerland*

This is where the receipt/accepted dates will go; Received Month XX, 2000; Accepted Month XX, 2000 (BMCL RECEIPT)

Abstract— Selective lowering of $A\beta_{42}$ levels with small-molecule substrate targeting γ-secretase modulators (sGSMs), such as some non-steroidal anti-inflammatory drugs, is a promising therapeutic approach for Alzheimer's disease. In the present article we have synthesized *N*-substituted carbazole- and *O*-substituted fenofibrate-derived sGSMs and present the activity data. Out of 19 screened compounds, 7 exhibited promising activity against $A\beta_{42}$ secretion at a low micromolar level. We presume, that the sGSMs interact with lys624 next to the membrane and that the lipophilic substituents anchor the compound orientation in the membrane.

γ-Secretase is one of two aspartyl proteases held responsible for the generation of the Alzheimer's disease causing pathology; amyloid β-peptide (Aβ) aggregation to amyloid plaques. The understanding of the precise mechanism of Aβ generation is crucial for the development of drugs targeting the disease. Small-molecule substrate targeting γ-secretase modulators (sGSMs) have shown promise in therapeutic treatment of Alzheimer's disease.[1] These sGSMs seem to interfere with substrate recognition/cleavage and shift the precision of γ-secretase cleavage from the beta-amyloid 42 to the beta-amyloid 38 site to generate more $A\beta_{38}$ and less $A\beta_{42}$. This activity is summarized as straight modulation of γ-secretase. The development of modulators will benefit from precise information on the binding site(s), but up to now this information is rather limited.

Selected NSAIDs, e.g. ibuprofen, sulindac sulfide, and flurbiprofen were found to modulate the secretion of Aβ *in vitro* and *in vivo*.[2,3,4] Some cyclooxygenase-2 (COX-2) specific inhibitors, e.g. celecoxib, and the peroxisome proliferator-activated receptor-γ (PPAR-γ) antagonist, fenofibrate (**3,** Figure 1) were found to increase $A\beta_{42}$ levels selectively, resulting in inverse modulation of γ-secretase activity.[5,6]

We recently described *N*-substituted carprofen derivatives and carbozolyloxyactetic acids as γ-secretase modulators (Figure 1).[7,8] The introduction of a lipophilic substituent, which may vary from arylsulfone to alkyl, turned 2-carbazolyloxyacetic acids into γ-secretase modulators (e.g., **4**: IC_{50} ($A\beta_{42}$) = 7.5 μM, **5**: IC_{50} ($A\beta_{42}$) = 2.9 μM). The most active compounds displayed activity in the low micromolar range and little or no effect on the γ-secretase cleavage at the ε-site. Furthermore, cell-based studies with $A\beta_{42}$-lowering compounds have revealed that sGSMs do not affect the cleavage of other γ-secretase substrates, such as Notch and others.[3,6,9-12]

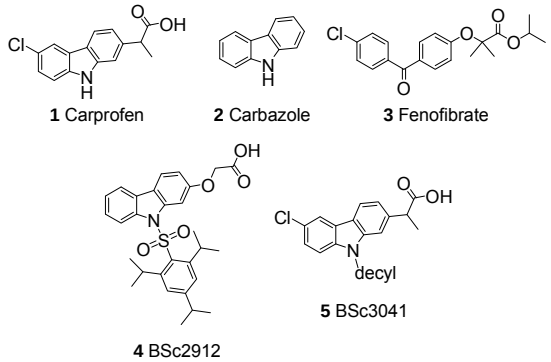

Figure 1. Carprofen (**1**), carbazole (**2**), fenofibrate (**3**) and the most active derivatives BSc2912 (**4**) and BSc3041 (**5**).

Biotinylated, photoactivatable probes were developed to identify the target of flurbiprofen- and fenofibrate-derived sGSMs.[11] Surprisingly, these photoprobes did not label the core proteins of the γ-secretase complex, but instead labelled the β-amyloid precursor protein (APP), APP carboxy-terminal fragments (CTFs) and Aβ peptide in human neuroglioma H4-cells. sGSM interaction was localized to the residues 29–36 of Aβ, a region critical for aggregation. This substrate targeting by sGSMs results in alteration of $A\beta_{42}$ production and inhibition of Aβ aggregation.[13] Substrate labeling has been competed by other sGSMs, and labeling of an APP γ-secretase substrate was more efficient than of a Notch substrate. The established binding site

of flurbiprofen-derived sGSMs resides close to the membrane surface, and implies high lipophilicity in combination with an acidic functional group is necessary for binding. This combination is unusual for a therapeutic drug, but common to amphiphilic surfactants, thus creating an obstacle for drug development.

Fenofibrate (**3**) is used as lipid-regulating agent in humans. In H4-cells, **3** raises $A\beta_{42}$ by over 300% and decreases $A\beta_{38}$ by up to 60% in a dose-dependent fashion, while $A\beta_{40}$ levels are not altered.[5,14] At these concentrations, fenofibrate did not show toxic effects in the lactose dehydrogenase (LDH) and 3-(4,5-dimethyl-thiazol-2-yl)-2,5-diphenyltetrazolium bromide (MTT) assays. Notably, the active metabolite of fenofibrate, the corresponding fenofibric acid, did not raise $A\beta_{42}$ at doses up to 250 μM.

The results with the *N*-substituted carprofen derivatives and carbazolyloxyacetic acids prompted us to investigate the detailed effects of the lipophilic substituents of *N*-substituted carbazolyloxyacetic acids. Therefore, lipophilic substituents like *trans*- and *cis*-oleic acid were introduced. *cis*-Configurated oleic acid is a component of biological lipid bilayers and should incorporate into the cellular membrane readily. Sterically more demanding substituents like aza-benzene, naphthalene, or biphenyl were linked to the carbazolic backbone testing space availability. These carbazolyloxyacetic acid derivatives have been synthesized according to Scheme 1 and are summarized in Table 1. One derivative (**8h**) features a compact photoreactive sububunit aiming to minimize the tether used in previous crosslinking experiments. Such probes can be useful to identify binding sites on proteins either by mass spectrometry or via additional labeling. The synthesis is outlined in Scheme 2 and described in the supplement.

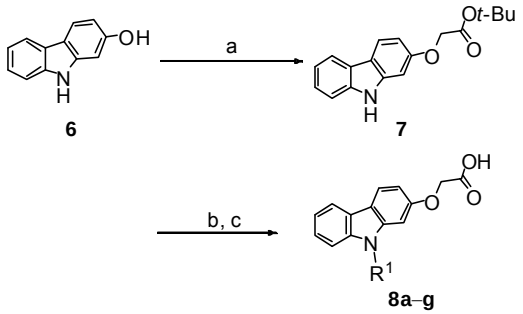

Scheme 1. Synthesis of carbazole-derived sGSMs. *Reagents and conditions*: a) *t*-butyl 2-bromoacetate, K_2CO_3, acetone, reflux; b) KO*t*-Bu, R^1X, THF, 0 °C to r.t.; c) 20% TFA, CH_2Cl_2.

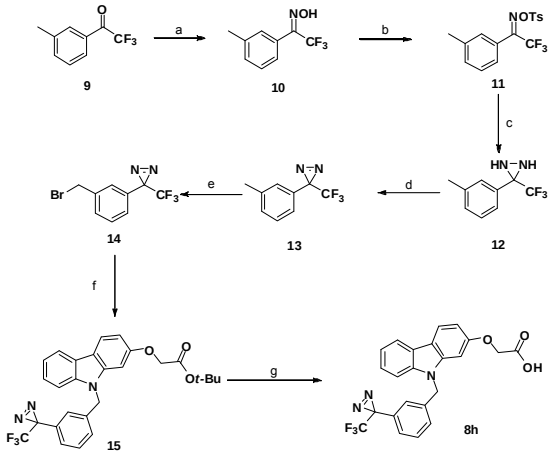

Scheme 2. Synthesis of a carbazole-derived sGSM **8h** equipped with a photoreactive unit. *Reagents and conditions*: a) NH_2OH*HCl, py, EtOH, reflux; b) TsCl, DIEA, DMAP, CH_2Cl_2, 0 °C to r.t.; c) NH_3, Et_2O -78°C to r.t.; d) I_2, MeOH, Et3N, pH > 7; e) NBS, AIBN, CCl_4, reflux; f)**7**, KO*t*-Bu, THF, 0 °C to r.t., 12 h, g) TFA, CH_2Cl_2, 0 °C to r.t., 2-8 h.

In addition, we tried to convert the inverse γ-secretase modulating effects of fenofibrate into straight
modulation. The corresponding *O*-alkylated oximes (Table 1) were readily accessible by straightforward synthesis (Scheme 3, 11a-g)

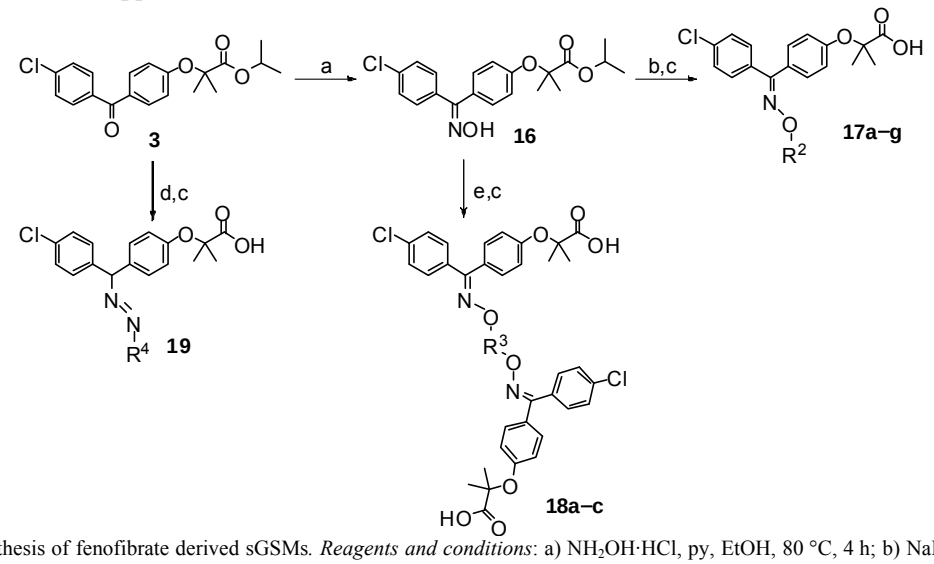

Scheme 3. Synthesis of fenofibrate derived sGSMs. *Reagents and conditions*: a) $NH_2OH{\cdot}HCl$, py, EtOH, 80 °C, 4 h; b) NaH, R^2X, DMF, 0 °C to r.t., 6–12 h; c) 2 N NaOH, MeOH, r.t., 4–12 h; d) 2,4-dinitrophenylhydrazine, H_2SO_4, MeOH, r.t, 2 h; e) NaH, $X–R^3–X$ (0.5 equiv), DMF, 0 °C to r.t., 6–12 h.

Table 1. Compounds **8–19**.

Entry	Compds	BSc number	R	Substituent
1	**8a**	3770	R^1	octadecyl
2	**8b**	3853	R^1	*trans*-oleic acid
3	**8c**	3854	R^1	decacarbonyl
4	**8d**	3915	R^1	*cis*-oleic acid
5	**8e**	3955	R^1	8-(*N*,*N*-dimethyl)-4-sulfonylnaphthalene
6	**8f**	3956	R^1	4´-(*N*,*N*-dimethyl)-1-sulfonylazabenzene
7	**8g**	3984	R^1	4'-methylbiphenyl-3-carbonitrile
8	**8h**	3958	R^1	3-(3-methylphenyl)-3-(trifluoromethyl)-3*H*-diazirine
9	**17a**	3934	R^2	Octyl
10	**17b**	3935	R^2	Nonyl
11	**17c**	3936	R^2	Decyl
12	**17d**	3937	R^2	Undecyl
13	**17e**	3938	R^2	Dodecyl
14	**17f**	3939	R^2	tetradecyl
15	**17g**	3940	R^2	hexadecyl
16	**18a**	3941	R^3	Octyl
17	**18b**	3942	R^3	Nonyl
18	**18c**	3943	R^3	Decyl
19	**19**	3989	R^4	2,4-dinitrophenylhydrazyl

The ongoing discussion on the existence of two (or even more) binding sites in the γ-secretase complex advocates for an investigation into the potential distance between these sites. Two modulating monomer units linked by a variable spacer may form a more active dimer interacting with the two potential binding sites. The length of these spacers would thus provide information about the distance between both binding sites. Fenofibrate dimers with variable alkyl tethers offer access to such distance mapping. The conversion of the fenofibrate with 2,4-dinitrophenylhydrazine provided the hydrazone **13** (Scheme 3). The UV-activity and intrinsic color of **13** may be exploited in cellular mechanistic studies of γ-secretase modulation.

To evaluate the compounds **8a–h**, **17a–g**, **18a–c**, **19** for their potency to modulate Aβ secretion, we used the Aβ liquid phase electrochemiluminescence (LPECL) assay to measure Aβ isoforms.[7] Cell viability was measured by a colorimetric cell proliferation assay (CellTiter 96TM AQ assay, Promega) utilizing the bioreduction of MTS (Owen's reagent) to formazan. The results are summarized in Table 2 and the dose-dependent curves of the most active compounds are shown in Figure 2.
Introduction of a double bond by substitution with *cis*- and *trans*-configurated oleic acid did not show any differences in potency. Both isomers, *E* (**8b**) and *Z* (**8d**) inhibited $A\beta_{42}$ secretion with an IC_{50} of 13 μM. Remarkably, there is a 2-fold increase in potency compared to the saturated analogue **8a** (BSc3770). The introduction of an E- or Z-double bond seems to stabilize the membrane orientation of the lipophilic anchor resulting in increased potency. In addition linear lipophilic alkyl chains, even amides (**8c**) and sulfonamides are tolerated. We suggest that linear, lipophilic substituents are useful anchors, given that *para*-substituted benzenes (**8f**) are modulators in contrast to *meta*-substituted benzenes (**8e,g,h**) showing no activity at all.
The activities of the fenofibrate derivatives have been determined at an initial concentration of 40 μM (see Supporting Information). As expected, fenofibrate (BSc3931) and the oxime **16** showed inverse modulation, the fenofibrate acid (BSc3932) displayed no activity at all (data not shown). The *O*-substituted compounds **17a** (BSc3934) and **17c** (BSc3936) displayed modulating effects. At a concentration of 40 μM the $A\beta_{42}$ level was reduced by 60%, while the $A\beta_{38}$ level was increased. The modulating effects of the dimers **18a**,**b** are not as strong, but still significantly stronger than those of flurbiprofen or indomethacin (see Supporting Information), which are benchmarks for GSM activity. The C12 dimer **18c** (BSc3943) does not show any effect on Aβ secretion.

Table 2. Modulation and cell toxicity results for compounds **8–19**.

Entry	Compds	BSc number	Cell toxicity (μM)	EC_{50} $A\beta_{38}$ (μM)	IC_{50} $A\beta_{40}$ (μM)	IC_{50} $A\beta_{42}$ (μM)
1	**8a**	3770	-	1.4	>80	26.0
2	**8b**	3853	n.t.[a]	9.3	>40	13.0
3	**8c**	3854	n.t.	12.6	>40	22.4
4	**8d**	3915	-	9.2	>40	13.1
5	**8e**	3955	80	>40	>40	>40
6	**8f**	3956	n.t.	7.6	>80	9.0
7	**8g**	3984	-	>80	>80	>80
8	**8h**	3958	-	>80	>80	>80
9	**17a**	3934	80	16.1	47.6	36.2
10	**17b**	3935	-	>40	>40	>40
11	**17c**	3936	-	>80	>80	36.1
12	**17d**	3937	-	>40	>40	>40
13	**17e**	3938	80	>40	>40	>40
14	**17f**	3939	-	>80	>80	>80
15	**17g**	3940	-	>80	>80	>80
16	**18a**	3941	-	47.6	37.3	23.7
17	**18b**	3942	80	>40	>40	>40
18	**18c**	3943	80	>40	>40	>32.6
19	**19**	3989	80	47.6	37.3	17.0

[a] n.t. = not tested.

Two out of eleven fenofibrate derivatives showed modulating effects at low concentrations with the most active being the *O*-alkylated C8 derivative **17a** (BSc3934). The modulating tendency is visible with all other alkylated derivatives **17b–g**, however, only at higher concentrations. Hydrazone **19** (BSc3989) inhibited total Aβ. The dimers **18a–c** showed modulatory effects at high concentrations. Some compounds showed cellular toxicity at a concentration of 80 μM in H4-cells. As fenofibrate is an approved drug, the *in silico* parameters are established and adequate. The introduction of the lipophilic substituent

caused a dramatic increase of the clogP value (fenofibrate: tPSA: 52.6, clogP: 5.2; fenofibrate-C8-oxime: tPSA: 57.1, clogP: 10.2). We presume, that the lipophilic anchor of the compounds is essential for orientation within the membrane. The maximum alkyl chain length should therefore not exceed the length of a natural phospholipid (see **8a–d**, Table 2). The results of the fenofibrate dimers indicate that the maximum chain length has been reached with C12. Furthermore, our results do not indicate an interaction with more than one binding site.

We compared the structures of highly active compounds (see supplement of ref. 13) to rationalize the binding mode of straight sGSMs. Apparently, a carboxylic acid moiety is essential for potency. We assume, that this functionality interacts with a lysine (maybe lys624) of the substrate APP, which is located next to the membrane interface. Thereby, the lipophilic substituents of the sGSMs serve as membrane anchors. Binding to the substrate may avoid substrate dimerization involving the GAIIG motif (see Supporting Information), thereby driving the cleavage shift away from $A\beta_{42}$.

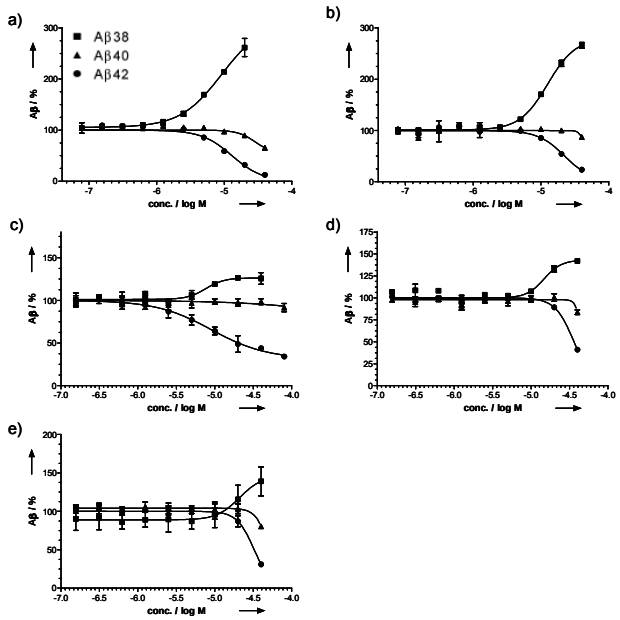

Figure 2. Dose–response curves for the most active *N*-substituted carbazolyloxyacetic acid and fenofibrate derivatives; Aβ (% of control). (A) Compound **8d**. (B) Compound **8c**. (C) Compound **8f**. (D) Compound **17a** (E) Compound **18c**.

In summary, the introduction of a lipophilic substituent turned fenofibrate- and carbazole-derived carboxylic acids into sGSMs, which display selective reduction of $A\beta_{42}$ and an increase of the less aggregatory $A\beta_{38}$ fragment. The most active compounds display activity on APP overexpressing cell lines in the low micromolar range. Some of these sGSMs do not target the γ-secretase complex directly, but rather bind to its substrate APP, thereby changing the cleavage pattern. The dimerization of APP may be influenced by this sGSM binding. The lipophilic substituents anchor the compound in the membrane.

Acknowlegements:

We thank the DFG (B.S. and S.B., SPP1085 (SCHM1012-3-1/2), the EU (B.S. and S.B., APOPIS contract LSHM-CT-2003-503330) BMBF (N.H., KNDD) for support of this work..

References and notes:

1. Schmidt, B.; Baumann, S.; Narlawar, R.; Braun, H. A.; Larbig, G. *Neurodegen. Dis*. **2006**, *3*, 290-297.
2.Avramovich, Y.; Amit, T.; Youdim, M. B. H. *J. Biol. Chem.* **2002**, *277*, 31466.
3. Weggen, S.; Eriksen, J. L.; Das, P.; Sagi, S. A.; Wang, R.; Pietrizik, C. U.; Findlay, K. A.; Smith, T. E.; Murphy, M. P.; Bulter, T.; Kang, D. E.; Marquez-Sterling, N.; Golde, T. E.; Koo, E. H. *Nature* **2001**, *414*, 212.
4. Eriksen, J. L.; Sagi, S. A.; Smith, T. E.; Weggen, S.; Das, P.; McLendon, D. C.; Ozols, V. V.; Jessing, K. W.; Zavitz, K. H.; Koo, E. H.; Golde, T. E. *J. Clin. Invest.* **2003**, *112*, 440.
5. Kukar, T.; Murphy Michael, P.; Eriksen Jason, L.; Sagi Sarah, A.; Weggen, S.; Smith Tawnya, E.; Ladd, T.; Khan Murad, A.; Kache, R.; Beard, J.; Dodson, M.; Merit, S.; Ozols Victor, V.; Anastasiadis Panos, Z.; Das, P.; Fauq, A.; Koo Edward, H.; Golde Todd, E. *Nature Med.* **2005**, *11*, 545.
6. Gasparini, L.; Rusconi, L.; Xu, H.; del Soldato,P.; Ongini, E. *J. Neurochem.* **2004**, *88*, 337.
7. Narlawar, R.; Perez Revuelta, B. I.; Baumann, K.; Schubenel, R.; Haass, C.; Steiner, H.; Schmidt, B. *Bioorg. Med. Chem. Lett.* **2007**, *17*, 176.
8. Narlawar, R.; PerezRevuelta, B. I.; Haass, C.; Steiner, H.; Schmidt, B.; Baumann, K. *J. Med. Chem.* **2006**, *49*, 7588.
9. Takahashi, Y.; Hayashi, I.; Tominari, Y.; Rikimaru, K.; Morohashi, Y.; Kan, T.; Natsugari, H.; Fukuyama, T.; Tomita, T.; Iwatsubo, T. *J. Biol. Chem.* **2003**, *278*, 18664.
10. Beher, D.; Clarke, E. E.; Wrigley, J. D. J.; Martin, A. C. L.; Nadin, A.; Churcher, I.; Shearman, M. S. *J. Biol. Chem.* **2004**, *279*, 43419.
11. Morihara, T.; Chu, T.; Ubeda, O.; Beech, W.; Cole, G. M. *J. Neurochem.* **2002**, *83*, 1009.

12. Weggen, S.; Eriksen, J. L.; Sagi, S. A.; Pietrzik, C. U.; Golde, T. E.; Koo, E. H. *J. Biol. Chem.* **2003**, *278*, 30748.
13. Kukar, T. L.; Ladd, T. B.; Bann, M. A.; Fraering, P. C.; Narlawar, R.; Maharvi, G. M.; Healy, B.; Chapman, R.; Welzel, A. T.; Price, R. W.; Moore, B.; Rangachari, V.; Cusack, B.; Eriksen, J.; Jansen-West, K.; Verbeeck, C.; Yager, D.; Eckman, C.; Ye, W.; Sagi, S.; Cottrell, B. A.; Torpey, J.; Rosenberry, T. L.; Fauq, A.; Wolfe, M. S.; Schmidt, B.; Walsh, D. M.; Koo, E. H.; Golde, T. E. *Nature* **2008**, *453*, 925.
14. Gebel, T.; Arand, M.; Oesch, F. *FEBS Letters* **1992**, *309*, 37.

Supporting Information

NSAID-derived γ-secretase modulators. Part III. Membrane anchoring

Stefanie Baumann,[a] Nicole Höttecke,[a] Karlheinz Baumann,[b] Robert Schubenel,[b] Boris Schmidt[a]*

[a]*Clemens Schöpf-Institute of Chemistry and Biochemistry, Technische Universität Darmstadt, Petersenstr. 22, D-64287 Darmstadt, Germany, Fax: (+49) 6151-163278, E-mail: schmidt_boris@t-online.de*

[b]*F. Hoffmann-La Roche Ltd., Pharmaceuticals Division, Preclinical Research CNS, Bldg. 70/345, CH-4070 Basel, Switzerland*

Table of Content:

1. General Comments

The ^{1}H NMR spectra were recorded on a Bruker AC 300 spectrometer at 300 Hzand Bruker AC 500 spectrometer at 500 Hz. The ^{13}C NMR spectra were recorded on a Bruker AC 300 spectrometer at 75 Hzand Bruker AC 500 spectrometer at 125 Hz. Chemical shifts are reported as ppm downfield from Me_4Si. Mass spectrometry was performed on a Bruker-Franzen Esquire LC mass spectrometer. Flash column chromatography was carried out using Merck silica gel 60 (40–63 and 15–40 μm) and 60G (5–40 μm). Thin-layer chromatography (TLC) was carried out using aluminum sheets precoated with silica gel 60 F254 (0.2 mm; E. Merck). Chromatographic spots were visualized by UV and/or spraying with an acidic, ethanolic solution of p-anisaldehyde or an ethanolic solution of ninhydrin followed by heating. For preparative TLC, plates precoated with silica gel 60 F254 (2.0 mm; E. Merck) were used.

2. Experimental methods and spectral data of *N*-substituted carbazole-derived sGSMs

***tert*-Butyl 2-(9*H*-carbazol-2-yloxy)acetate (7):**
Anhydrous K_2CO_3 (4.53 g, 32.75 mmol) was added to a stirred solution of 2-hydroxy carbazole (2.00 g, 10.92 mmol) in acetone (25 mL) and stirred at ambient temperature for 30 min. *tert*-Butyl chloroacetate (1.870 mL, 13.10 mmol) was added and the reaction mixture was heated at 60–70 °C for 12 h. The mixture was cooled to room temperature and filtered. The residue was washed with acetone (3×). Combined organic extract was evaporated *in vacuo* and purified by flash column chromatography (CH_2Cl_2) to yield the title compound as a yellow solid (2.63 g, 99%)
^{1}H NMR (300 MHz, $CDCl_3$): δ = 7.99 (s, 1H, H-9), 7.92-7.85 (m, 2H, H-4/5), 7.28-7.26 (m, 2H, H-7/8), 7.19-7.12 (m, 1H, H-6), 6.81-6.76 (m, 2H, H-1/3), 4.52 (s, 2H, H-14), 1.45 (s, 9H, H-16) ppm.

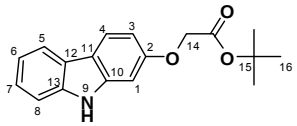

General procedure for *N*-alkylation of tert-butyl 2-(9*H*-carbazol-2-yloxy)acetate derivatives
KO*t*-Bu (1.2 equiv) was added to a stirred solution of THF (5 mL/mmol) *tert*-butyl 2-(9*H* carbazol-6-yloxy)acetate (**7**) (1.0 equiv) at 0 °C. After 30 minutes alkyl halide (1.5 equiv) dissolved in THF was added. The reaction mixture was stirred at ambient temperature for 6-24 h. The heterogeneous reaction mixture was quenched with NH_4Cl (sat. aq), diluted with CH_2Cl_2 and then washed sequentially with H_2O and brine. The organic extract was dried over anhydrous Na_2SO_4 and evaporated *in vacuo* to give crude compound. The crude compound was purified by flash column chromatography (CH_2Cl_2–hexane, 1:100).

***tert*-Butyl 2-(9-octadecyl-9*H*-carbazol-2-yloxy)acetate (BSc4022):**
Reactants: 0.241 g (1.00 mmol) **7**, 0.516 mL (1.50 mmol) 1-bromooctadecan, 0.135 g (1.20 mmol) KO*t*-Bu, 3 mL THF.
Yield: 0.076 mg (14%) as a colourless solid
Mp: 62°C
^{1}H NMR (300 MHz, $CDCl_3$): δ = 8.02-7.96 (m, 2H, H-4/5), 7.43-7.34 (m, 2H, H-6/7), 7.23-7.18 (m, 1H, H-3), 6.91 (d, ^{4}J = 2.1 Hz, 1H, H-1), 6.84 (dd, ^{3}J = 8.5 Hz, ^{4}J = 2.3 Hz, 1H, H-8), 4.65 (s, 2H), 4.22 (t, ^{3}J = 7.3 Hz, 2H), 1.85 (q, ^{4}J = 7.5 Hz, 2H), 1.53 (s, 9H), 1.28-1.26 (m, 30H), 0.90 (t, J = 6.8 Hz, 3H) ppm.

^{13}C NMR (75 MHz, $CDCl_3$): δ = 168.2 (C-15), 157.2 (C-2), 141.6 (C-13), 130.7 (C-12), 124.5 (C-4), 122.9 (C-10), 121.0 (C-7), 119.6 (C-5), 118.9 (C-6), 117.6 (C-11), 108.4 (C-8), 107.0 (C-3), 94.7 (C-1), 82.3 (C-16), 66.4 (C-14), 43.1 (C-18), 31.9 , 29.7, 29.6, 29.5, 29.4, 29.3, 27.3 (CH_2), 28.1 (C-17), 22.7 (C-34), 14.1 (C-35) ppm.
MS: (m/z, 70eV, EI) = 549 (M^+), 493, 254, 196, 180.

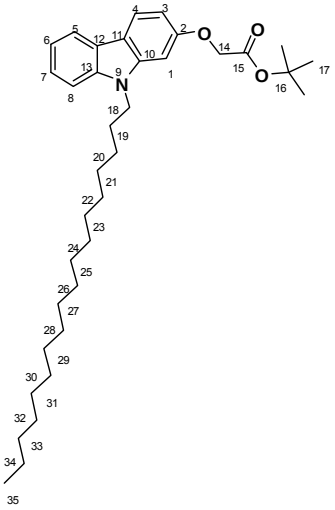

***tert*-Butyl 2-(9-((2'-cyanobiphenyl-4-yl)methyl)-9*H*-carbazol-2-yloxy)acetate (BSc4023)**
Reactants: 0.150 g (0.51 mmol) **7**, 0.206 mL (0.76 mmol) 4'-bromomethyl biphenyl-2-carbonitrile, 0.068 g (0.61 mmol) KO*t*-Bu, 3 mL THF.
Yield: 0.170mg (69%) as a colourless solid
^{1}H NMR (300 MHz, $CDCl_3$): δ = 7.98–8.05 (m, 2H H-24/25), 7.70–7.75 (m, 1H, H-27), 7.59 (m, 1H, H-26), 7.21–7.46 (m, 7H, H-4/5/6/7/8/21/20), 6.83–6.89 (m, 2H, H-1/3), 5.49 (s, 2H, H-14), 4.59 (s, 2H, H-18), 1.45 (s, 9H, H-17) ppm.
^{13}C NMR (75 MHz, $CDCl_3$): δ = 168.1 (C-18), 157.5 (C-2), 144.9 (C-22), 141.8 (C-13), 140.9 (C-23), 137.6 (C-12), 137.4 (C-19), 133.8 (C-25), 132.8 (C-28), 130.0 (C-27), 129.2 (C-20), 127.6 (C-24), 126.7 (C-26), 124.9 (C-21), 123.2 (C-22), 121.2 (C-4), 119.7 (C-7), 119.6 (C-5), 118.7 (C-29), 117.8 (C-10), 111.2 (C-11), 108.7 (C-6), 107.8 (C-3/8), 94.8 (C-1), 82.3 (C-16), 66.4 (C-14), 46.2 (C-18), 28.0 (C-17) ppm.
MS: (m/z, 70eV, EI): 489 $(M)^+$, 433, 192.

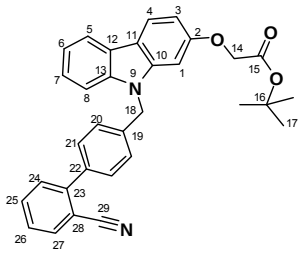

General procedure for amidation of *tert*-butyl 2-(9*H*-carbazol-2-yloxy)acetate derivatives
KO*t*-Bu (1.2 equiv) was added to a stirred solution of THF (5 mL/mmol) *tert*-butyl 2-(9*H*carbazol-6-yloxy)acetate (**7**) (1 equiv) at 0 °C. After 30 minutes acid chloride (1.5 equiv) was added. The reaction mixture was stirred at ambient temperature for 6–24 h. The heterogeneous reaction mixture was quenched with NH_4Cl (sat. aq), diluted with CH_2Cl_2 and then washed sequentially with H_2O and brine. The organic extract was dried over anhydrous $MgSO_4$ and evaporated *in vacuo* to give crude compound. The crude compound was purified by flash column chromatography (CH_2Cl_2–hexane, 1:50).

***tert*-Butyl 2-(9-decanoyl-9*H*-carbazol-2-yloxy)acetate (BSc4024):**
Reactants: 0.200 g (0.83 mmol) **7**, 0.258 mL (1.25 mmol) decanonyl chloride, 0.112 g (1.00 mmol) KO*t*-Bu, 6 mL THF.
Yield: 0.158 g, (42%) as a yellow solid
^{1}H NMR (300 MHz, $CDCl_3$): δ = 8.04 (d, ^3J = 7.7 Hz, 1H, H-4), 7.96 (d, ^4J = 2.2 Hz, 1H, H-1), 7.92-7.87 (m, 1H, H-5), 7.85 (d, ^3J = 8.5 Hz, 1H, H-8), 7.43-7.31 (m, 2H, H-6/7), 7.00 (dd, ^3J = 8.5 Hz, ^4J = 2.2 Hz, 1H, H-3), 4.64 (s, 2H, C-14), 3.10 (t, ^3J = 7.3 Hz, 2H, H-19), 1.96-1.84 (m, 2H, H-20), 1.52 (s, 9H, H-17), 1.47-1.19 (m, 12H, CH_2), 0.97-0.82 (m, ^3J = 6.8, 3H, H-27).
^{13}C NMR (75 MHz, $CDCl_3$): δ = 173.2 (C-18), 167.7 (C-15), 157.7 (C-2), 139.7 (C-13), 138.2 (C-12), 126.3 (C-10), 125.8 (C-7), 123.3 (C-4), 120.2 (C-11), 120.2 (C-5), 119.0 (C-6), 115.7 (C-8), 111.6 (C-3), 102.8 (C-1), 82.2 (C-16), 66.0 (C-14), 38.9 (C-19), 31.7, 29.3, 29.2, 29.1 (CH_2), 27.9 (C-17), 24.2, 22.4 (CH_2), 13.9 (C-26) ppm.

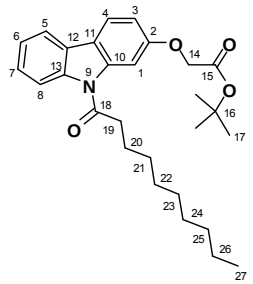

General procedure for the amidation of *tert*-butyl 2-(9*H*-carbazol-2-yloxy)acetate derivatives
DCC (1.5 equiv) was added to a stirred solution of THF (5 mL/mmol) *tert*-butyl 2-(9*H*carbazol- 6-yloxy)acetate (**7**) (1 equiv), carboxylic acid (1.5 equiv) and catalytic amount of DMAP at 0 °C. The reaction mixture was stirred at ambient temperature for 6–24 h. The heterogeneous reaction mixture was quenched with $NaHCO_3$ (sat. aq), diluted with CH_2Cl_2 and then washed sequentially with H_2O and brine. The organic extract was dried over anhydrous $MgSO_4$ and evaporated *in vacuo* to give crude compound. The crude compound was purified by flash column chromatography (CH_2Cl_2–hexane, 1:5).

(*E*)-*tert*-Butyl 2-(9-(octadec-9-enyl)-9*H*-carbazol-2-yloxy)acetate (BSc4018):
Reactants: 0.200 g (0.83 mmol) **7**, 0.469 mL (1.66 mmol) elaidic acid, 0.258 g (1.25 mmol) DCC, catalytic amount DMAP, 6 mL CH_2Cl_2.
Yield: 0.231 g, (50%) as a yellow solid.
^{1}H NMR (300 MHz, $CDCl_3$): δ = 8.04 (d, ^3J = 7.8 Hz, 1H, H-4), 7.97 (d, ^4J = 2.2 Hz, 1H, H-1), 7.91-7.89 (m, 1H, H-7), 7.86 (d, ^3J = 8.5 Hz, 1H, H-5), 7.43-7.32 (m, 2H, H-6/7), 7.01 (dd, ^3J = 8.5 Hz, ^4J =2.2 Hz, 1H, H-3), 5.42-5.34 (m, 2H, H26/27), 4.64 (s, 2H, H-14), 3.10 (t, J = 7.3 Hz, 2H, H19), 2.03-1.86 (m, 6H, H-20/25/28), 1.52 (s, 9H, H-17), 1.45-1.20 (m, 20H, CH_2), 0.87 (t, J = 6.7 Hz, 3H, H-35) ppm.
^{13}C NMR (75 MHz, $CDCl_3$): δ = 173.4 (C-16), 167.9 (C-15),157.9 (C-2), 139.9 (C-13), 138.4 (C-12), 130.5 (C-26), 130.2 (C-27), 126.5 (C-10), 126.0 (C-7), 123.5 (C-4),120.4 (C-11), 120.2 (C-5), 119.2 (C-6), 115.9 (C-8), 111.8 (C-3), 103.0 (C-1), 82.4 (C-16), 66.1 (C-14), 39.1, 32.6, 31.9, 29.7, 29.6, 29.5, 29.4, 29.3, 29.2, 29.1, 29.0 (CH_2), 28.0 (C-17), 24.6, 22.7 (CH_2), 14.1 (C-35) ppm.

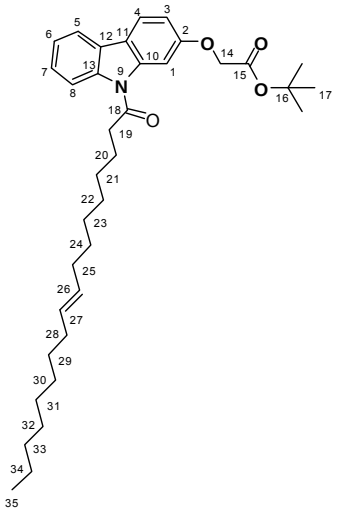

(*Z*)-*tert*-Butyl 2-(9-oleoyl-9*H*-carbazol-2-yloxy)acetate (BSc4025)
Reactants: 0.100 g (0.42 mmol) **7**, 0.234 mL (0.83 mmol) oleic acid, 0.130 mg (0.63 mmol) DCC, catalytic amount DMAP, 3 mL CH_2Cl_2.
Yield: 0.070 mg, (30%) as a colourless oil.
^{1}H NMR (300 MHz, $CDCl_3$): δ = 8.04 (d, ^3J = 8.4 Hz, 1H, H-5), 7.97 (d, ^4J = 2.2 Hz, 1H, H-1), 7.90 (dd, ^3J = 7.4 Hz, ^4J = 1.2 Hz, 1H, H-8), 7.86 (d, ^3J = 8.5 Hz, 1H, H-4), 7.44-7.31 (m, 2H, H-6/7), 7.01 (dd, ^3J = 8.5 Hz, ^4J =2.3 Hz, 1H, H-3), 5.41-5.30 (m, 2H, H-26/27), 4.64 (s, 2H, H-14), 3.11 (t, ^3J = 7.3 Hz, 2H, H-19), 2.11-1.85 (m, 6H, H-20/25/28), 1.58-1.48 (s, 9H, H-17), 1.37 (m, 20H, CH_2), 0.94-0.83 (m, 3H, H-35) ppm.
^{13}C NMR (75 MHz, $CDCl_3$): δ = 173.4 (C-18), 167.9 (C-15), 157.9 (C-2), 139.9 (C-13), 138.4 (C-12), 130.0 (C-26), 129.8 (C-27), 126.5 (C-10), 126.0 (C-7), 123.5 (C-4), 120.4 (C-11), 120.2 (C-5), 119.3 (C-6), 116.0 (C-8), 111.8 (C-3), 103.0 (C-1), 82.5 (C-16), 66.1 (C-14), 39.1, 31.9, 29.8, 29.7, 29.6, 29.5, 29.4, 29.2 (CH_2), 28.1 (C-17), 27.2, 24.7, 22.7 (CH_2), 14.1 (C-35) ppm.

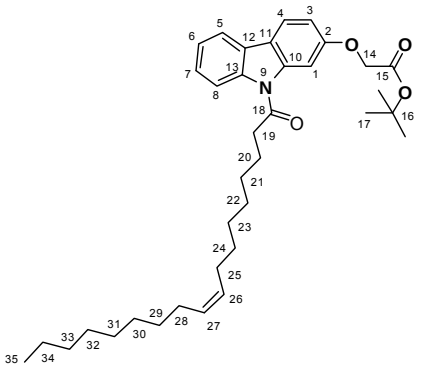

General procedure for *N*-sulfonylation of carbazole derivatives
NaH (60% dispersion, 1.2 equiv) was combined with THF (5 mL/mmol) and cooled to 0 °C. *tert*-butyl 2-(9*H*-carbazol-6-yloxy)acetate (**7**) (1 equiv) was added to the stirring slurry in portions. After 30 minutes *R*-sulfonyl chloride (1.2 equiv) dissolved in THF was added and the reaction was stirred at ambient temperature for 6–24 h. The heterogeneous reaction mixture was quenched with NH_4Cl (sat. aq.), diluted with CH_2Cl_2 and then washed sequentially with H_2O and brine (2×). The organic extract was dried over anhydrous Na_2SO_4 and evaporated *in vacuo* to give crude compound. The crude compound was purified by flash column chromatography using (CH_2Cl_2–hexane, 2:3) to afford the desired product.

***tert*-Butyl 2-(9-(5-(dimethylamino)naphthalen-1-ylsulfonyl)-9*H*-carbazol-2-yloxy)acetate (BSc4027):**

Reactants: 0.100 g (0.42 mmol) **7**, 0.134 mL (0.50 mmol) dansyl chloride, 0.020 g (0.50 mmol) NaH, 3 mL THF.

Yield: 0.060 g (99%) as a green solid

^{1}H NMR (300 MHz, $CDCl_3$): δ = 7.88 (d, ^3J = 8.5 Hz, 1H, H-4), 7.67 (d, ^3J = 8.7 Hz, 1H, CH), 7.54-7.52 (m, 1H, CH), 7.30-7.19 (m, 4H, CH), 6.85-6.68 (m, 4H, CH), 6.50-6.42 (m, 2H, CH), 4.02 (s, 2H, H-14), 2.21 (m, 6H, H-28), 0.90 (s, 9H, H-17) ppm.

^{13}C NMR (75 MHz, $CDCl_3$): δ = 167.7 (C-15), 157.9 (C-2), 151.7 (C-22), 139.8 (C-18), 138.6 (C-13), 134.6 (C-26), 131.2 (C-23), 129.9 (C-12) 128.6 (C-20), 128.5 (C-24), 127.5 (C-10) 126.1 (C-25), 125.5 (C-11), 123.6 (C-7), 122.8 (C-19), 120.8 (C-4), 119.6 (C-27), 119.4 (C-5), 118.7 (C-6), 115.5 (C-21), 114.7 (C-8), 112.7 (C-3), 100.2 (C-1), 82.5 (C-16), 66.1 (C-14), 45.2 (C-28), 28.0 (C-17) ppm.

MS: (m/z, 70eV, ESI) = 553 (M + Na).

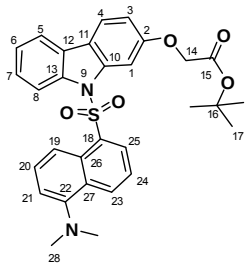

(*E*)-*tert*-Butyl 2-(9-(4-((4-(dimethylamino)phenyl)diazenyl)phenylsulfonyl)-9*H*-carbazol-2-yloxy)acetate (BSc4027)

Reactants: 0.050 g (0.19 mmol) NH01, 0.072 mL (0.22 mmol) dabsyl chloride, 0.015 g (0.38 mmol) NaH, 2 mL THF.

Yield: 0.064 g, (58%) as a red solid

^{1}H NMR (300 MHz, $CDCl_3$): δ = 8.29 (d, ^3J = 8.3 Hz, 1H, CH), 7.93 (d, ^4J = 2.3 Hz, 1H, CH), 7.87 (dt, ^3J = 8.8 Hz, ^4J = 2.0 Hz, 2H, CH), 7.81-7.73 (m, 4H, CH), 7.72-7.65 (m, 2H, CH), 7.41 (dt, ^3J = 8.2 Hz, ^4J = 1.3 Hz, 1H, CH), 7.31 (t, J = 7.4 Hz, 1H, CH), 7.01 (dd, ^3J = 8.6, Hz., ^4J = 2.3 Hz, 1H, CH) 6.67 (d, ^3J = 8.54 Hz, 2H, H-24), 4.68 (s, 2H, H-14), 3.04 (s, 6H, H-26), 1.56 (s, 9H, H-17) ppm.

^{13}C NMR (75 MHz, $CDCl_3$): δ = 167.8 (C-15), 158.0 (C-21), 157.3 (C-2), 143.5 (C-25), 139.5 (C-22), 138.4 (C-18), 136.6 (C-3), 127.5 (C-19), 126.5 (C-12), 125.5 (C-23), 124.8 (C-7), 124.2 (C-20), 122.5 (C-4), 120.7 (C-5), 119.7 (C-11), 119.3 (C-6), 115.2 (C-8), 113.0 (C-24), 111.4 (C-3), 100.8 (C-1), 82.6 (C-16), 66.2 (C-14), 40.2 (C-26), 28.1 (C-17) ppm.

MS: (m/z, 70eV, ESI) = 607 (M + Na).

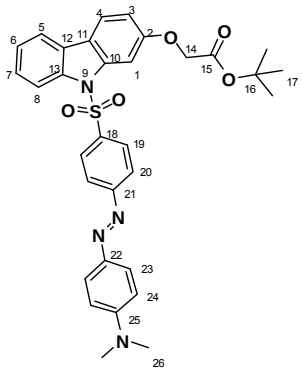

General procedure for *tert*-butyl ester cleavage of *N*-substituted *tert*-butyl 2-(9*H*-carbazol-2-yloxy)acetates

A solution of *t*-butyl ester in 20% trifluoroacetic acid in CH_2Cl_2 (5 mL/mmol) was stirred at ambient temperature for 4 to 12 h. After completion of reaction (TLC), solvent was evaporated *in vacuo* to get crude product. The crude acid was purified by crystallization (CH_2Cl_2–hexane) to afford the desired product.

2-(9-Octadecyl-9*H*-carbazol-2-yloxy)acetic acid (8a, **BSc3770)**

Reactants: 0.102 g (0.186 mmol) **BSc4022**, 0.500 mL TFA, 2 mL (CH_2Cl_2).

Yield: 0.040 g, (44%) as a colourless solid

Mp: 118.6°C

^{1}H NMR (300 MHz, Acetone): δ = 7.99 (d, ^3J = 7.8 Hz, 1H, H-4), 7.98 (d, ^3J = 8.5 Hz, 1H, H-5), 7.45 (d, ^3J = 8.2 Hz, 1H, H-7), 7.32 (d, ^3J = 8.2 Hz, 1H, H-6), 7.13 (d, ^3J = 7.8 Hz, 1H, H-3), 7.09 (d, ^4J = 2.2 Hz, 1H, H-1), 6.85 (dd, ^4J = 2.2 Hz, J = 8.5 Hz, 1H, H-8),4.80 (s, 2H, H-14), 4.34 (t, ^3J = 7.2 Hz, 2H, H-16), 1.85 (q, ^3J = 7.3 Hz, 2H, H-17), 1.20-1.41 (m, 3H, CH_2), 0.86 (t, ^3J = 6.6 Hz, 3H, H-33) ppm.

^{13}C NMR (75 MHz, Acetone): δ = 164.2 (C-15), 155.4 (C-2), 142.6 (C-13), 141.6 (C-12), 125.3 (C-4), 123.8 (C-10), 121.7 (C-7), 120.2 (C-5), 119.7 (C-6), 118.0 (C-11), 109.6 (C-8), 100.9 (C-3), 95.3 (C-1), 66.0 (C-14), 43.4 (C-16), 32.6, 27.8, 23.3 (CH_2), 14.3 (C-33) ppm.

MS: (m/z, 70eV, EI) = 493 (M^+), 436, 254, 196, 167.

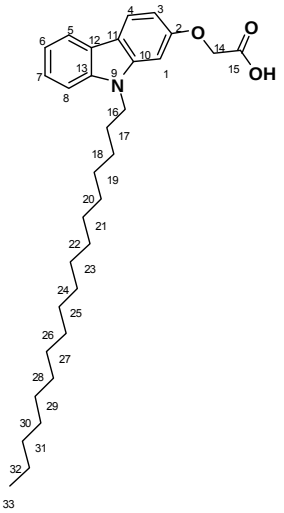

2-(9-((2'-cyanobiphenyl-4-yl)methyl)-9H-carbazol-2-yloxy)acetic acid (8g, BSc3984)

Reactants: 0.020 g (0.04 mmol) **BSc4023**, 0.500 mL TFA, 2 mL (CH_2Cl_2).

Yield: 0.010g, (57%) as a colourless solid

^{1}H NMR (500 MHz, $CDCl_3$) δ = 8.03 (m, 2H, CH), 7.71 (d, ^3J = 7.6 Hz, 1H, CH), 7.61 (t, ^3J = 7.9 Hz, 1H, CH), 7.47-7.37 (m, 6H,CH), 7.31-7.21 (m, 3H,CH), 6.91-6.87 (m, 1H, CH), 6.77 (^3J = 10.1 Hz, ^2J = 2.2 Hz, 1H, CH), 5.51 (s, 2H, H-14), 4.2 (s, 2H, H-16) ppm.

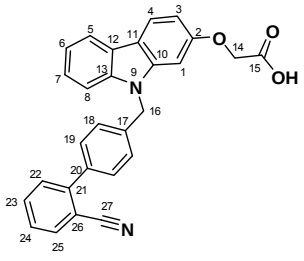

2-(9-Decanoyl-9*H*-carbazol-2-yloxy)acetic acid (8c, BSc3854)
Reactants: 0.050 g (0.11 mmol) **BSc4024**, 0.250 mL TFA, 1 mL (CH_2Cl_2).
Yield: 0.035 g (80%) as a yellow solid
^{1}H NMR (500 MHz, acetone-d_6): δ = 8.08 (d, ^3J = 8.0 Hz, 1H, H-4), 7.88-7.92 (m, 3H, H-3/6/7), 7.25-7.37 (m, 2H, H-1/5), 6.97 (dd, ^4J = 2.3 Hz, ^3J = 8.4 Hz, 1H, H-8), 4.72 (s, 2H, H-14), 3.61-3.48 (m, 2H, H-17), 3.12 (t, ^3J = 7.2 Hz, 2H, H-18), 2.27-1.93 (m, 2H, H-19), 1.86-1.76 (m, 2H, H-20), 1.80-1.90 (m, 2H, H-21), 1.41-1.51 (m, 2H, H-22),1.11-1.31 (m, 4H, H-23/24) 0.82 (^3J = 6.7 Hz, H, H-25) ppm.
^{13}C NMR (125 MHz, acetone-d_6): δ = 173.0 (C-16), 157.7 (C-15), 139.5 (C-13), 138.2 (C-12), 126.0 (C-10),125.8 (C-7), 123.2 (C-4), 120.1 (C-11), 119.9 (C-5), 118.9 (C-6), 115.8 (C-8), 111.2 (C-3), 103.0 (C-1), 72.2 (C-14), 65.1, 61.0, 38.6, 31.5,30.0, 28.8, 24.3 (CH_2), 14.0 (C-27) ppm.
MS: (m/z, 70eV, EI) = 395 (M^+), 241, 196, 182, 166, 154.

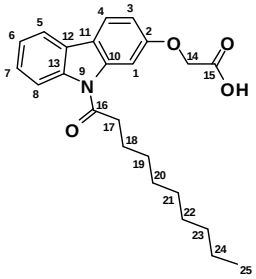

(*E*)-2-(9-(Octadec-9-enyl)-9*H*-carbazol-2-yloxy)acetic acid (8b, BSc3853)
Reactants: 0.050 g (0.09 mmol) **BSc4018**, 0.250 mL TFA, 1 mL (CH_2Cl_2).
Yield: 0.027 mg (60%) as a colourless solid
^{1}H NMR (300 MHz, acetone-d_6): δ = 7.66 (d, J = 8.0 Hz, 1H, H-4), 7.55-7.44 (m, 3H, H-3/6/7), 6.96-6.84 (m, 2H, H-1/5), 6.56 (dd, J = 8.5, J = 2.3 Hz, 2H, H-8), 4.92-4.89 (m, 2H, H-24/25), 4.30 (s, 2H, H-14), 3.23-3.10 (m, 2H, H-17), 2.70 (t, J = 7.28 Hz, 2H, H-18), 1.51-1.38 (m, 6H, H-23/36/32), 1.07-0.79 (m, 20H, CH_2), 0.41-0.37 (m, 3H, H-33) ppm.
^{13}C NMR (75 MHz, acetone-d_6): δ = 173.2 (C-16), 169.4 (C-15), 157.9 (C-2), 139.6 (C-13), 138.3 (C-12), 130.2 (C-24), 130.0 (C-25), 126.1 (C-10), 125.9 (C-7), 123.3 (C-4), 120.2 (C-11), 120.1 (C-5), 119.0 (C-6), 116.0 (C-8), 111.3 (C-3), 103.1 (C-1), 65.1 (C-14), 61.1, 38.8, 32.4, 31.7, 30.2, 30.0, 29.7, 29.4, 29.2, 29.1, 29.0, 28.8, 28.7, 24.4, 22.4 (CH_2), 13.7 (C-33) ppm.
MS: (m/z, 70eV, EI) = 506(M^+), 241, 196, 182, 154.

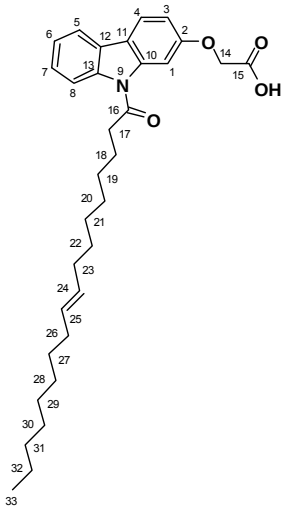

(*Z*)-2-(9-Oleoyl-9H-carbazol-2-yloxy)acetic acid (8d, BSc3915)
Reactants: 0.070 g (0.13 mmol) **BSc4025**, 0.250 mL TFA, 1 mL (CH_2Cl_2).
Yield: 0.034 g (54%) as colourless solid
Mp: 101.1 °C
^{1}H NMR (500 MHz, acetone-d_6): δ = 8.03 (d, J = 2.0 Hz, 1H, H-1), 7.97 (d, J = 8.3 Hz, 1H, H-4), 7.89 (d, J = 7.6 Hz, 1H, H-8), 7.85 (d, J = 8.5 Hz, 1H, H-5), 7.42-7.39 (m, 1H, H-7), 7.34 (t, J = 7.4 Hz, 1H, H-6), 7.01 (dd, J = 8.5, J = 2.1 Hz, 1H, H-3), 5.36-5.34 (m, 2H, H-24/25), 4.78 (s, 2H, H-14), 3.08 (t, J = 7.3 Hz, 2H, H-17), 2.05-1.99 (m, 2H, H-23), 1.90 (q, J = 7.4 Hz2H, H-26), 1.52-1.44 (m, 2H, H-32), 1.41-1.26 (m, 22H, CH_2), 0.89-0.85 (m, 3H, H-33) ppm.
^{13}C NMR (125 MHz, acetone-d_6): δ = 173.5 (C-16), 172.1 (C-15), 157.3 (C-2), 139.9 (C-13), 138.3 (C-12), 130.0 (C-24), 129.7 (C-25), 126.3 (C-7), 123.6 (C-4), 120.9 (C-10), 120.4 (C-5), 119.4 (C-6), 115.8 (C-8), 112.5 (C-11), 111.8 (C-3), 103.5 (C-1), 65.5 (C-14), 39.1, 31.9, 29.8, 29.7, 29.5, 29.4, 29.3, 29.2, 29.1, 29.0, 28.9, 27.2, 27.1, 26.6 (CH_2), 14.1 (C-33) ppm.
MS: (m/z, 70eV, EI) = 505 (M^+), 423, 269, 241, 182.

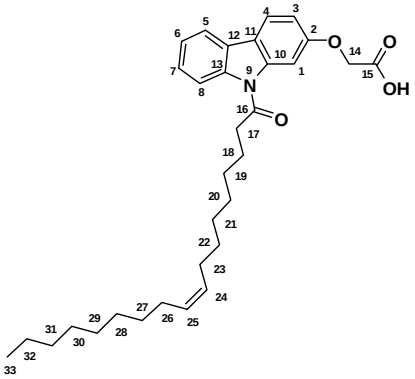

2-(9-(5-(Dimethylamino)naphthalen-1-ylsulfonyl)-9*H*-carbazol-2-yloxy)acetic acid (8e, BSc3955)
Reactants: 0.070 g (0.13 mmol) **BSc4027**, 0.500 mL TFA, 2 mL (CH_2Cl_2).
Yield: 0.055g (89%) as a green solid
^{1}H NMR (300 MHz, $CDCl_3$): δ = 9.34 (s, 1H, OH), 8.36 (d, ^3J = 8.5 Hz, 1H, CH), 8.14 (d, ^3J = 8.7 Hz, 1H, CH), 8.06 (d, ^3J = 8.2 Hz, 1H, CH), 7.86 (d, J = 7.3 Hz, 1H,CH), 7.76-7.57 (m, 3H, CH), 7.40-7.15 (m, 4H, CH), 7.06-6.76 (m, 1H, CH), 6.96 (d, ^3J = 7.6 Hz, 1H, CH), 6.85 (d, ^3J = 8.5 Hz, 1H, CH) 4.61 (s, 2H, C-14), 2.70 (s, 6H, H-26) ppm.
^{13}C NMR (75 MHz, $CDCl_3$): δ = 173.0 (C-15), 157.4 (C-2), 150.5 (C-20), 139.5 (C-16), 138.7 (C-13), 134.6 (C-24), 131.0 (C-21), 129.9 (C-12), 129.5 (C-10), 129.0 (C-18), 128.5 (C-22), 126.3 (C-23), 125.4 (C-25), 123.7 (C-7), 123.3 (C-17), 120.9 (C-4), 119.9 (C-11), 119.5 (C-5), 119.3 (C-6), 115.8 (C-19), 114.7 (C-8), 112.4 (C-3), 110.5 (C-1), 65.5 (C-14), 45.4 (C-26) ppm.
MS: (m/z, 70eV, EI) = 474 (M^+), 430, 366, 307, 240, 182, 170.

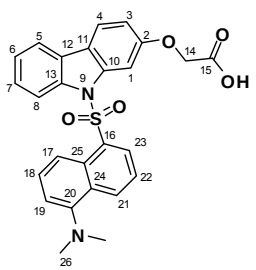

(*E*)-2-(9-(4-((4-(Dimethylamino)phenyl)diazenyl)phenylsulfonyl)-9*H*-carbazol-2-yloxy)-acetic acid (8f, BSc3956)

Reactants: 0.060 g (0.10 mmol) **BSc4027**, 0.500 mL TFA, 2 mL (CH_2Cl_2).

Yield: 0.045 g, (85%) as a red solid

^{1}H NMR (500 MHz, DMSO): δ = 8.11 (d, ^3J = 8.4 Hz, 1H, CH), 7.91 (d, ^3J = 8.5 Hz, 2H, CH), 7.83 (d, ^3J = 8.7 Hz, 2H, CH), 7.69-7.58 (m, 5H, CH), 7.39 (t, ^3J = 7.3, 1H, CH), 7.29 (t, ^3J = 7.5, 1H, CH), 6.95 (dd, ^3J = 8.6 Hz, ^4J = 2.2 Hz, 1H, CH), 6.69 (d, ^3J = 9.3 Hz, 2H, CH), 4.76 (s, 2H, H-14), 2.94 (s, 6H, H-25) ppm.

^{13}C NMR (125 MHz, DMSO): δ = 169.8 (C-15), 157.6 (C-2), 155.6 (C-23), 153.1 (C-19), 142.3 (C-20), 138.2 (C-16), 137.1 (C-13), 135.1 (C-12), 127.4 (C-17), 126.3 (C-21), 125.3 (C-7), 124.2 (C-18), 122.1 (C-4), 121.2 (C-5), 119.7 (C-6), 114.3 (C-8), 112.6 (C-23), 111.3 (C-3), 99.8 (C-1), 64.8 (C-14) ppm.

MS: (m/z, 70eV, EI) = 528 (M^+), 484, 396, 241, 224.

UV: 449 nM

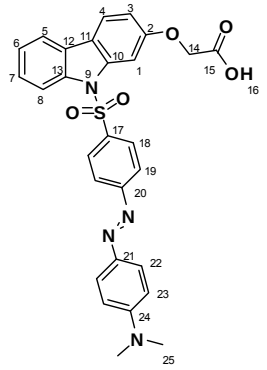

3. Experimental methods and spectral data of 8h:

2,2,2-Trifluoro-1-*m*-tolylethanone oxime (10)

A solution of trifluoracetophenone (2.00 g, 10.60 mmol) and hydroxylamine hydrochloride (745 mg, 10.60 mmol) in dry EtOH (10 mL) und pyridine (22 mL) was heated at 80 °C for 4 h. The solvent was evaporated and the residue was diluted with diethyl ether (70 mL) and then washed sequentially with H_2O (3x 30 mL). The combined organic extracts were dried over anhydrous Na_2SO and evaporated *in vacuo* to give crude compound. The crude compound was purified by flash column chromatography (hexane–EtOAc, 4:3).

Yield: 1.98 g (92%) as colourless solid

^{1}H NMR (500 MHz, $CDCl_3$): δ = 9.00 (s, OH), 7.30-7.27 (m, 2H, H-4/-6), 7.23-7.18 (m, 2H, H-2/-3), 2.31 (d, J = 7.9, 3H, H-9) ppm

^{13}C NMR (125 MHz, $CDCl_3$): δ = 172.2 (C-7), 138.8 (C-1), 131.8 (C-5), 129.4 (C-2) 128.8 (C-6), 126.4 (C-3), 122.1 (C-4), 119.9 (C-8), 117.7 (C-8), 21.8 (C-9) ppm.

MS (EI): m/z = 203 (M^+).

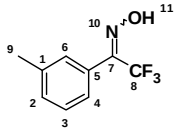

2,2,2-Trifluoro-1-*m*-tolylethanone-*O*-tosyloxime (11)

4-TsCl (937 mg, 4.93 mmol) was added portionwise to a solution of 2,2,2-trifluoro-1-*m*-tolylethanone oxime (1.0 g, 4.93 mmol), DIEA (943 µL, 5.52 mmol) and DMAP (46 mg, 0.37 mmol) in CH_2Cl_2 (8 mL) at 0 °C. After 40 min the cooling was removed and the solution was stirred for 2 h at r.t. Then the reaction mixture was washed with H_2O (3 x 30 mL). The organic phase was dried over anhydrous Na_2SO and evaporated *in vacuo* to give crude compound. The crude compound was purified by flash column chromatography (CH_2Cl_2–petroleum ether, 3:4).

Yield: 1.23 g (70%) as colourless solid

^{1}H NMR (500 MHz, $CDCl_3$): δ = 7.83-7.80 (m, 2H, H-11), 7.32-7.09 (m, 6H, H-2/-3/-4/-6/-12), 2.40 (d, *J* = 9.2 Hz, 3H, H-14), 2.31 (d, *J* = 8.6 Hz, 3H, H-9) ppm.

^{3}C NMR (125 MHz, $CDCl_3$): δ = 168.8 (C-7), 146.5 (C-10), 139.1 (C-13), 132.8 (C-1), 131.9 (C-5), 130.3 (C-2), 129.8 (C-12), 129.1 (C-6), 129.0 (C-3), 126.4 (C-11), 125.0 (C-4), 114.4 (C-8), 22.2 (C-14), 21.8 (C-9) ppm.

MS (EI): m/z = 357 $(M)^+$.

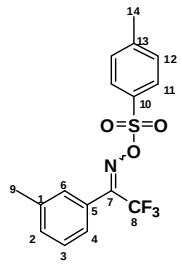

3-*m*-Tolyl-3-(trifluoromethyl)diaziridine (12)

To a solution of 2,2,2-trifluoro-1-*m*-tolylethanone-*O*-tosyloxime (1.0 g, 2.80 mmol) in diethyl ether (7 mL), liquid ammonia (6 mL, distilled over sodium) was added at –78 °C. The tube was capped and the solution was stirred for 2 h at -78 °C in the dark. Under warming to r.t. the ammonia was allowed to evaporate. The etheric solution was filtered and washed with H_2O (3x 20 mL). The organic phase was dried over anhydrous Na_2SO and evaporated *in vacuo* to give crude compound. The crude compound was purified by flash column chromatography (hexane–CH_2Cl_2, 20:1).

Yield: 504 mg (89%) as colourless oil

^{1}H NMR (500 MHz, $CDCl_3$): δ = 7.34-7.26 (m, 2H, H-3/-6), 7.25-7.17 (m, 2H, H-2/-4), 2.69 (d, *J* = 8.5 Hz, 1H), 2.31 (s, 3H, H-9), 2.14 (d, *J* = 9.0 Hz, 1H) ppm.

^{13}C NMR (125 MHz, $CDCl_3$): δ = 132.8 (C-5), 131.3 (C-1), 130.3 (C-8), 129.7 (C-6), 129.1 (C-3), 126.9 (C-2), 125.6 (C-4), 80.8 (C-7), 21.8 (C-9) ppm.

MS (EI): m/z = 203 $(M+H)^+$.

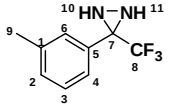

3-*m*-Tolyl-3-(trifluoromethyl)-3*H*-diazirine (13)

3-*m*-Tolyl-3-(trifluoromethyl)diaziridine (300 mg, 1.48 mmol) was solved in CH_2Cl_2 (8 mL) and Et_3N (0.6 mL, 4.33 mmol) was added. The solution was cooled to 0 °C and iodine (413 mg, 1.63 mmol) was added in small portions. The solution was stirred for 2 h at r.t. and then washed with 1M NaOH (2 x 25 mL), dest. H_2O (2 x 25 mL) and sat. NaCl (25 mL). The organic phase was dried over anhydrous $MgSO_4$ and evaporated *in vacuo* to give crude compound. The crude compound was purified by flash column chromatography (hexane–CH_2Cl_2, 20:1).

Yield: 198 mg (67%) as colourless oil

^{1}H NMR (500 MHz, $CDCl_3$): δ = 7.22-7.18 (m, 2H), 7.15 (d, *J* = 7.6 Hz, 1H), 6.95 (d, *J* = 7.7 Hz, 1H), 2.28 (s, 3H, H-9) ppm.
^{13}C NMR (125 MHz, $CDCl_3$): δ = 139.2 (C-5), 130.8 (C-1), 129.5 (C-8), 129.1 (C-6), 127.4 (C-3), 124.0 (C-2), 123.7 (C-4), 84.0 (C-7), 32.0 (C-8, CF), 23.0 (C-8, CF), 21.8 (C-9), 14.5 (C-8, CF) ppm.
MS (EI): m/z = 200 $(M)^+$.

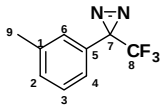

3-(3-(Bromomethyl)phenyl)-3-(trifluoromethyl)-3*H*-diazirine (14)
A solution of 3-*m*-Tolyl-3-(trifluoromethyl)-3*H*-diazirine (100 mg, 0.50 mmol) in CCl_4 (4 mL) was heated to 70 °C and NBS (80 mg, 0.45 mmol) was added. After 10 min AIBN (8 mg, 0.05 mmol) was added and the reaction mixture was stirred for 2 h under reflux. The formed precipitate was filtered and the solvent was evaporated carefully. The crude compound was purified by flash column chromatography (hexane–CH_2Cl_2, 20:1).
Yield: 73 mg (52%) as colourless oil
^{1}H NMR (300 MHz, $CDCl_3$): δ = 7.40-7.31 (m, 2H, H-3/-6), 7.19-7.08 (m, 2H, H-2/-4), 4.38 (s, 2H, H-9) ppm.
^{13}C NMR (75 MHz, $CDCl_3$): δ = 138.8 (C-5), 130.3 (C-1), 129.8 (C-8), 129.4 (C-6), 128.9 (C-3), 126.9 (C-2), 123.8 (C-4), 79.8 (C-7), 32.1 (C-9), 31.6 (C-8, CF), 22.6 (C-8, CF), 14.1 (C-8, CF) ppm.

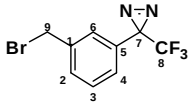

***tert*-Butyl-2-(9-(3-(3-(trifluoromethyl)-3*H*-diazirine-3-yl)benzyl)-9*H*-carbazol-2-yloxy)-acetate (15)**
7 (25 mg, 0.084 mmol) was solved at 0 °C in THF (5 mL) and KO*t*-Bu (12 mg, 0.101 mmol) was added. After 30 min 3-(3-(bromomethyl)phenyl)-3-(trifluoromethyl)-3*H*-diazirine (35 mg, 0.126 mmol) was added in the dark. The reaction mixture was stirred for 12 h at r.t. The heterogeneous reaction mixture was diluted with EtOAc (20 mL) and then washed sequentially with H_2O (3x 15 mL) and brine. The organic extract was dried over anhydrous $MgSO_4$ and evaporated *in vacuo* to give crude compound. The crude compound was purified by flash column chromatography (hexane–CH_2Cl_2, 5:4).
Yield: 18 mg (43%) as colourless solid
^{1}H NMR (300 MHz, $CDCl_3$): δ = 8.05-7.99 (m, 2H, H-4/-5), 7.37-7.35 (m, 1H, H-8), 7.27-7.24 (m, 3H, H-6/-7/-21), 7.09 (d, *J* = 4.02 Hz, 1H, H-24), 6.89 (m, 2H, H-20/22), 6.86 (d, *J* = 6.1 Hz, 1H, H-3), 6.79 (d, *J* = 6.5 Hz, 1H, H-1), 5.44 (s, 2H, H-18), 4.58 (s, 2H, H-14), 1.45 (s, 9H, H-17) ppm.
^{13}C NMR (75 MHz, $CDCl_3$): δ = 174.6 (C-15), 157.5 (C-2), 142.6 (C-13), 138.7 (C-23), 129.8 (C-12), 129.5 (C-19), 127.5 (C-25), 125.7 (C-4/24), 125.0 (C-21), 124.4 (C-22/-20), 123.2 (C-7/-10), 121.3 (C-5), 119.8 (C-6), 117.6 (C-11), 108.5 (C-8), 107.8 (C-3), 94.7 (C-1), 84.2 (C-26), 82.4 (C-16), 66.3, (C-14), 46.2 (C-18), 28.0 (C-17) ppm.
MS (ESI): m/z = 495$(M)^+$.

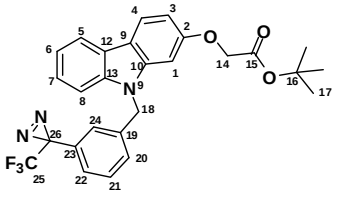

2-(9-(3-(3-(Trifluoromethyl)-3*H*-diazirine-3-yl)benzyl)-9*H*-carbazol-2-yloxy)acetic acid (8h, BSc3958)

tert-Butyl-2-(9-(3-(3-(trifluoromethyl)-3*H*-diazirine-3-yl)benzyl)-9*H*-carbazol-2-yloxy)-acetate (12 mg, 0.024 mmol) was solved in CH_2Cl_2 (2 mL) and TFA (0.4 mL) was added. The solution was stirred for 6 h at r.t., filtered, and the solvent was evaporated. The crude compound was purified by flash column chromatography (hexane–CH_2Cl_2, 5:4).

Yield: 8 mg (76%) as colourless solid

^{1}H NMR (300 MHz, $CDCl_3$): δ = 8.05-7.98 (m, 2H, H-4/-5), 7.45-7.33 (m, 1H, H-8), 7.27-7.24 (m, 3H, H-6/-7/-21), 7.197.17 (m, 1H, H-24), 6.97-6.94 (m, 2H, H-20/22), 6.88 (d, *J* = 6.1 Hz, 1H, H-4), 6.76 (d, *J* = 6.5 Hz, 1H, H-1), 5.36 (s, 2H, H-18), 4.65 (s, 2H, H-14) ppm.

^{13}C NMR (75 MHz, $CDCl_3$): δ = 169.4 (C-15), 154.5 (C-2), 139.8 (C-13), 138.7 (C-21), 129.8 (C-12), 129.5 (C-17), 126.2 (C-24), 125.7 (C-4/-22), 125.0 (C-19), 123.7 (C-18/-20), 122.5 (C-7/-10), 121.3 (C-5), 119.8 (C-6), 117.0 (C-11), 108.3 (C-8), 107.4 (C-3), 94.3 (C-1), 84.2 (C-23), 66.3, (C-14), 46.2 (C-16) ppm.

MS (ESI): m/z = 440 $(M+H)^+$.

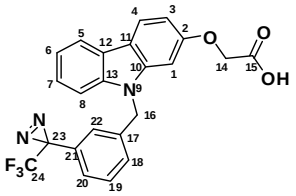

4. Experimental methods and spectral data of *O*-substituted fenofibrate-derived sGSMs

Isopropyl 2-(4-((4-chlorophenyl)(hydroxyimino)methyl)phenoxy)-2-methylpropanoate (16, BSc3933)

Fenofibrate (2.000 g, 5.54 mmol), hydroxylamine hydrochloride (0.962 g, 13.86 mmol), and pyridine (22 mL) were dissolved in ethanol (10 mL) and the reaction mixture was stirred overnight at 80 °C. Solvent was evaporated, and the residue was diluted with CH_2Cl_2 and then washed with H_2O (3x 30 mL) and brine (1x 30 mL). The organic extract was dried over anhydrous Na_2SO_4 and evaporated *in vacuo*. The crude compound was purified by flash column chromatography using (CH_2Cl_2–MeOH, 15:1) to yield the title compound as colourless solid (1.46 g, 70.2%)

^{1}H NMR (300 MHz, $CDCl_3$): δ = 8.6 (s, OH), 7.27-7.44 (m, 4H), 7.26 (dd, *J* = 8.9 Hz, *J* = 2.2 Hz, 2H), 6.75 (dd, *J* = 9.0, 2.2 Hz, 2H), 5.09 (m, 1H), 1.6 (d, *J* = 12.8 Hz, 6H), 1.15 (dd, *J* = 11.9, 5.6 Hz, 6H) ppm.

^{13}C NMR (75 MHz, $CDCl_3$): δ = 173.5 (C-12), 156.4 (C-9), 135.3 (C-5), 134.9 (C-1), 131.2 (C-4), 130.7 (C-3), 129.4 (C-7), 129.3 (C-2), 125.1 (C-6), 117.9 (C-8), 79.2 (C-10), 69.1 (C-13), 25.4 (C-11), 21.5 (C-14) ppm.

MS (ESI): *m/z* = 376$^{\cdot}$$(M^+)$.

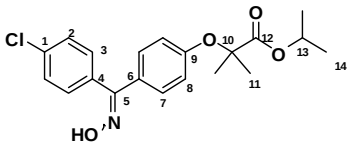

General procedure for *O*-alkylation of Isopropyl 2-(4-((4-clorophenyl)-hydroxy-imino)ethyl) henoxy) -2-methylpropanoate

Isopropyl 2-(4-((4-clorophenyl)hydroxyimino)ethyl)phenoxy)-2-methylpropanoate (**10**, 1 equiv) was added to a stirred suspension of NaH (1.2 equiv) in DMF (5 mL/mmol) at 0 °C. After 30 minutes alkyl halide (1.2 equiv) dissolved in DMF was added. The reaction mixture was stirred at ambient temperature for 6–24 h. The heterogeneous reaction mixture was quenched with NH_4Cl (sat. aq), diluted with EtOAc and the solution was washed with water. The aqueous solution was extracted with EtOAc (3x 50 mL). The combined organic extract was washed with H_2O, brine and dried over anhydrous Na_2SO_4 and rotary evaporated. The crude compound was purified by flash column chromatography using ethyl acetate and cyclohexane mixtures.

Isopropyl 2-(4-((4-chlorphenyl)octyloxyimino)methyl)phenoxy)-2-methylpropanoat (BSc3974)

Reactants: 0.300 g (0.80 mmol) **10**, 0.038 g NaH (0.96 mmol), 0.230 g 1-iodooctane (0.96 mmol), 4 mL DMF.
Yield: 0.190 g, 52%, colourless oil.
^{1}H NMR (300 MHz, $CDCl_3$): δ = 7.32-7.18 (m, 4H), 6.78 (dd, *J* = 8.8, 2.0 Hz, 2H), 6.71 (dd, *J* = 8.8 Hz, *J* = 2.2 Hz, 2H), 4.98 (m, 1H), 4.06 (t, *J* = 10 Hz, 2H, H-15), 1.59-1.52 (m, 8H), 1.18-1.12 (m, 16H), 0.79 (t, *J* = 6.6 Hz, 3H; H-22) ppm.
^{13}C NMR (75 MHz, $CDCl_3$): δ = 173.5 (C-12). 156.7 (C-9), 154.8 (C-5), 134.5 (C-1), 132.0 (C-4), 130.8 (C-3), 129.8 (C-6), 129.4 (C-7), 128.7 (C-2), 118.3 (C-8), 79.2 (C-10), 74.8 (C-15), 69.0 (C-13), 31.9 (C-20), 29.6 (C-19), 29.5 (C-18), 29.4 (C-17), 25.9 (C-16), 25.5 (C-11), 22.7 (C-21), 21.5 (C-14), 14.1 (C-22) ppm.
ESI-MS: m/z (%) = 510 (M+Na).

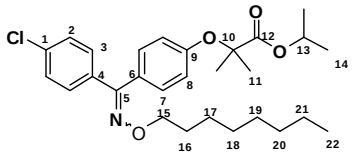

Isopropyl 2-(4-((4-chlorophenyl)(nonyloxyimino)methyl)phenoxy)-2-methylpropanoate (BSc3975)

Reactants: 0.300 g (0.80 mmol) **10**, 0.038 g NaH (0.96 mmol), 0.200 g 1-bromononane (0.96 mmol), 4 mL DMF.
Yield: 0.190 g, 50%, colourless oil.
^{1}H NMR (300 MHz, $CDCl_3$): δ = 7.33-7.17 (m, 4H), 6.78 (d, *J* = 8.8 Hz, 2H), 6.71 (d, *J* = 8.9 Hz, 2H), 5.00 (m, 1H), 4.08 (m, 2H, H-15), 1.58-1.51 (m, 8H), 1.18-1.12 (m, 18H), 0.80 (t, *J* = 6.5 Hz, 3H; H-23) ppm.
^{13}C NMR (75 MHz, $CDCl_3$): δ = 172.5 (C-12). 155.7 (C-9), 153.8 (C-5), 134.7 (C-1), 130.9 (C-4), 129.9 (C-3), 128.8 (C-6), 128.4 (C-7), 127.7 (C-2), 117.3 (C-8), 78.1 (C-10), 73.8 (C-15), 68.1 (C-13), 30.9 (C-21), 28.7 (C-20), 28.5 (C-19), 28.4 (C-18), 28.2 (C-17), 24.9 (C-16), 24.4 (C-11), 21.7 (C-22), 20.5 (C-14), 13.1 (C-23) ppm.
ESI-MS: m/z (%) = 524 (M+Na).

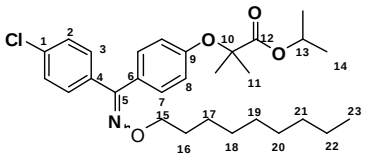

Isopropyl 2-(4-((4-chlorophenyl)(decyloxyimino)methyl)phenoxy)-2-methylpropanoate (BSc3976)

Reactants: 0.200 g (0.53 mmol) **10**, 0.024 g NaH (0.64 mmol), 0.141 g 1-bromodecane (0.64 mmol), 3 mL DMF.

Yield: 0.170 g, 68%, colourless oil.

^{1}H NMR (300 MHz, $CDCl_3$): δ = 7.43-7.24 (m, 4H), 6.94 (d, *J* = 8.9 Hz, 2H), 6.85 (d, *J* = 8.9 Hz, 2H), 5.10 (m, 1H), 4.16 (m, 2H, H-15), 1.86 (m, 2H), 1.68-1.60 (m, 8H), 1.27-1.21 (m, 18H), 0.80 (t, *J* = 6.8 Hz, 3H; H-24) ppm.

^{13}C NMR (75 MHz, $CDCl_3$): δ = 173.5 (C-12). 156.7 (C-9), 154.8 (C-5), 135.7 (C-1), 131.9 (C-4), 129.8 (C-3), 128.4 (C-6), 128.7 (C-7), 128.3 (C-2), 118.3 (C-8), 79.2 (C-10), 74.8 (C-15), 69.0 (C-13), 34.0 (C-22), 32.9 (C-21), 31.9 (C20), 29.6 (C-19), 29.5 (C-18), 29.4 (C-17), 25.9 (C-16), 25.7 (C-11), 21.5 (C-23), 21.5 (C-14), 14.1 (C-24) ppm.

ESI-MS: m/z (%) = 538 (M+Na).

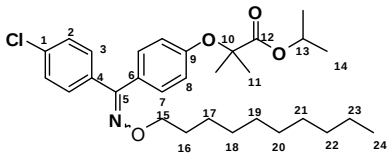

Isopropyl 2-(4-((4-chlorophenyl)(undecyloxyimino)methyl)phenoxy)-2-methylpropanoate (BSc3977)

Reactants: 0.050 g (0.13 mmol) **10**, 0.024 g NaH (0.16 mmol), 0.038 g 1-bromoundecane (0.16 mmol), 1 mL DMF.

Yield: 0.048 g, 70%, colourless oil.

^{1}H NMR (300 MHz, $CDCl_3$): δ = 7.41-7.32 (m, 4H), 6.86 (d, *J* = 9 Hz, 2H), 6.79 (d, *J* = 9 Hz, 2H), 5.08 (m, 1H), 4.14 (m, 2H, H-15), 3.41 (m, 2H), 1.91-1.84 (m, 2H), 1.67-1.60 (m, 8H), 1.27-1.20 (m, 18H), 0.80 (t, *J* = 6 Hz, 3H; H-25) ppm.

^{13}C NMR (75 MHz, $CDCl_3$): δ = 173.5 (C-12). 155.7 (C-9), 154.8 (C-5), 135.0 (C-1), 131.9 (C-4), 130.8 (C-3), 129.4 (C-6), 128.7 (C-7), 128.3 (C-2), 118.3 (C-8), 79.2 (C-10), 74.8 (C-15), 69.0 (C-13), 34.0 (C-23), 32.9 (C-21), 31.9 (C20), 29.6 (C-19), 29.5 (C-18), 29.4 (C-17), 29.3 (C-22), 25.9 (C-16), 25.5 (C-11), 22.7 (C-24), 21.5 (C-14), 14.1 (C-24) ppm.

ESI-MS: m/z (%) = 552 (M+Na).

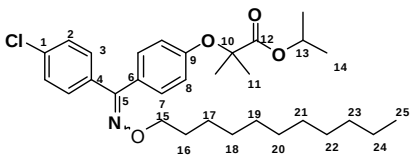

Isopropyl 2-(4-((4-chlorophenyl)(dodecyloxyimino)methyl)phenoxy)-2-methyl-propanoate (BSc3978)

Reactants: 0.050 g (0.13 mmol) **10**, 0.024 g NaH (0.16 mmol), 0.040 g 1-bromododecane (0.16 mmol), 1 mL DMF.
Yield: 0.056 g, 79%, colourless oil.
^{1}H NMR (500 MHz, $CDCl_3$): δ = 7.32-7.19 (m, 4H), 6.78 (d, *J* = 8.8 Hz, 2H), 6.71 (d, *J* =8.6 Hz, 2H), 5.01 (m, 1H), 4.08 (m, 2H, H-15), 3.33 (m, 2H), 1.79-1.76 (m, 2H), 1.56-1.53 (m, 4H), 1.36-1.33 (m, 6H), 1.24-1.13 (m, 18H), 0.81 (t, *J* = 6.7 Hz, 3H; H-26) ppm.
^{13}C NMR (125 MHz, $CDCl_3$): δ = 176.0 (C-12). 156.7 (C-9), 155.8 (C-5), 134.2 (C-1), 134.9 (C-4), 133.2 (C-3), 131.7 (C-6), 131.1 (C-7), 130.6 (C-2), 120.6 (C-8), 81.5 (C-10), 77.1 (C-15), 71.5 (C-13), 36.3 (C-24), 35.13 (C-23), 34.2 (C22), 31.9 (C-21), 31.9 (C-20), 31.8 (C-19), 31.7 (C-18), 31.6 (C-17), 28.2 (C-11), 27.6 (C-25), 25.0 (C-16), 23.8 (C-14), 16.4 (C-24) ppm.
ESI-MS: m/z (%) = 567 (M+Na).

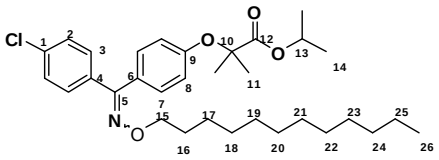

Isopropyl 2-(4-((4-chlorophenyl)(tetradecyloxyimino)methyl)phenoxy)-2-methylpropanoate (BSc3979)

Reactants: 0.050 g (0.13 mmol) **10**, 0.024 g NaH (0.16 mmol), 0.044 g 1-bromotetradecane (0.16 mmol), 1 mL DMF.
Yield: 0.042 g, 56%, colourless oil.
^{1}H NMR (500 MHz, $CDCl_3$): δ = 7.33-7.18 (m, 4H), 6.78 (d, *J* = 8.8 Hz, 2H), 6.71 (d, *J* =8.7 Hz, 2H), 5.01 (m, 1H), 4.08 (m, 2H, H-15), 3.34 (m, 2H), 1.79-1.77 (m, 4H), 1.59-1.52 (m, 8H), 1.34-1.26 (m, 22H), 0.81 (t, *J* = 6.7 Hz, 3H; H-28) ppm.
^{13}C NMR (125 MHz, $CDCl_3$): δ = 174.4 (C-12). 157.0 (C-9), 156.3 (C-5), 136.0 (C-1), 134.8 (C-4), 132.2 (C-3), 131.2 (C-6), 131.1 (C-7), 129.7 (C-2), 118.6 (C-8), 79.5 (C-10), 75.1 (C-15), 69.3 (C-13), 34.3 (C-26), 33.2 (C-25), 33.2 (C-24), 30.0 (C-23), 29.9 (C-22), 29.9 (C21), 29.8 (C-20), 29.7 (C-19), 29.4 (C-18), 29.1 (C-17), 28.4 (C-11), 28.3 (C-16), 23.0 (C-27), 21.8 (C-14), 14.4 (C-28) ppm.
ESI-MS: m/z (%) = 594 (M+Na).

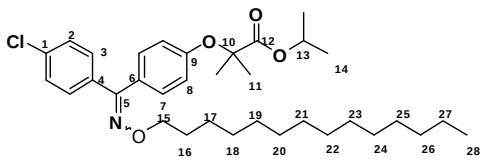

Isopropyl 2-(4-((4-chlorophenyl)(hexadecyloxyimino)methyl)phenoxy)-2-methylpropanoate
(BSc3980)

Reactants: 0.050 g (0.13 mmol) **10**, 0.024 g NaH (0.16 mmol), 0.049 g 1-bromohexadecane (0.16 mmol), 1 mL DMF.
Yield: 0.057 g, 73%, colourless oil.
^{1}H NMR (300 MHz, $CDCl_3$): δ = 7.40-7.28 (m, 4H), 6.79 (d, *J* = 8.8 Hz, 2H), 6.76 (d, *J* =8.7 Hz, 2H), 5.06 (m, 1H), 4.16 (m, 2H, H-15), 3.41 (m, 2H), 1.88-1.84 (m, 4H), 1.64-1.60 (m, 8H), 1.44-1.42 (m, 4H), 1.27-1.20 (m, 22H), 0.81 (t, *J* = 6.7 Hz, 3H; H-30) ppm.
^{13}C NMR (75 MHz, $CDCl_3$): δ = 173.5 (C-12). 157.0 (C-9), 156.3 (C-5), 136.0 (C-1), 134.8 (C-4), 130.8 (C-3), 129.4 (C-6), 128.7 (C-7), 128.3 (C-2), 118.3 (C-8), 78.4 (C-10), 74.2 (C-15), 69.1 (C-13), 34.0 (C-28), 32.9 (C-27), 31.9 (C-26), 29.7 (C-25), 29.5 (C-24), 29.4 (C23), 29.3 (C-22), 29.1 (C-21), 28.8 (C-20), 28.6 (C-19), 28.5 (C-18), 28.2 (C-17), 28.3 (C-16), 25.5 (C-11), 22.7 (C29), 21.5 (C-14), 14.1 (C-30) ppm.
ESI-MS: m/z (%) = 623 (M+Na).

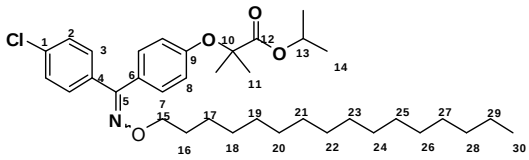

General procedure for isopropyl ester cleavage of *O*-substituted isopropyl 2-(4-((4-chlorophenyl)(hydroxyimino)methyl)phenoxy)-2-methylpropanoates

A solution of isopropyl ester in 2N NaOH in methanol (5 mL/mmol) was stirred at 70 °C overnight. After completion of reaction (TLC), solvent was evaporated *in vacuo* to get crude product. The heterogeneous reaction mixture diluted with EtOAc, acified with 2N HCl (pH ~ 4) and the solution was washed with water. The aqueous solution was extracted with EtOAc (3x 50 mL). The combined organic extract was washed with H_2O, brine and dried over anhydrous Na_2SO_4 and rotary evaporated. If necessary, the crude compound was purified by flash column chromatography using ethyl acetate and hexane mixtures.

2-(4-((4-Chlorophenyl)(octyloxyimino)methyl)phenoxy)-2-methylpropanoic acid
(17a, BSc3934)

Reactants: 0.190 g (0.43 mmol) BSc3974, 0.36 mL 2N NaOH (4.3mmol), 5 mL MeOH.
Yield: 0.170 g, 98%, colourless oil.
^{1}H NMR (300 MHz, $CDCl_3$): δ = 7.44-7.21 (m, 4H), 6.94 (d, *J* = 9 Hz, 2H), 6.85 (d, *J* = 9 Hz, 2H), 4.11 (m, 2H, H-13), 3.31 (m, 2H), 1.64-1.58 (m, 6H), 1.33-1.21 (m, 10H), 0.89 (t, *J* = 6 Hz, 3H, H-20) ppm.
^{13}C NMR (75 MHz, $CDCl_3$): δ = 178.6 (C-12), 158.3 (C-9), 158.4 (C-5), 137.0 (C-1), 135.6 (C-4), 133.6 (C-3), 131.7 (C-6), 129.7 (C-7), 129.3 (C-2), 119.7 (C-8), 75.6 (C-10), 75.5 (C-13), 32.9 (C-18), 30.4 (C-17), 30.2 (C-16), 30.1 (C-14), 27.1 (C-15), 25.8 (C-11), 23.7 (C-19), 14.5 (C-20) ppm.
ESI-MS: m/z (%) = 446 (M^+).

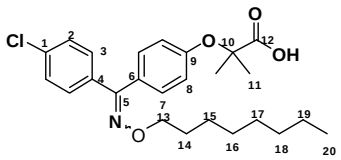

2-(4-((4-Chlorophenyl)(nonyloxyimino)methyl)phenoxy)-2-methylpropanoic acid (17b, BSc3935)

Reactants: 0.270 g (0.60 mmol) BSc3975, 1.5 mL 2N NaOH (6.00 mmol), 7 mL MeOH.
Yield: 0.240 g, 97%, colourless oil.
^{1}H NMR (300 MHz, $CDCl_3$): δ = 7.43-7.21 (m, 4H), 6.94 (d, *J* = 9 Hz, 2H), 6.85 (d, *J* = 9 Hz, 2H), 4.11 (m, 2H, H-13), 3.31 (m, 2H), 1.65-1.58 (m, 6H), 1.27-1.21 (m, 12H), 0.89 (t, *J* = 6 Hz, 3H, H-20) ppm.
^{13}C NMR (75 MHz, $CDCl_3$): δ = 178.6 (C-12). 158.4 (C-9), 158.4 (C-5), 135.6 (C-1), 135.6 (C-4), 131.9 (C-3), 131.7 (C-6), 130.5 (C-7), 129.7 (C-2), 119.6 (C-8), 75.6 (C-10), 75.5 (C-13), 33.1 (C-19), 30.7 (C-18), 30.4 (C-17), 30.3 (C-16), 30.1 (C-14), 27.1 (C-15), 25.9 (C-11), 23.7 (C-20), 14.5 (C-21) ppm.
ESI-MS: m/z (%) = 460 (M^+).

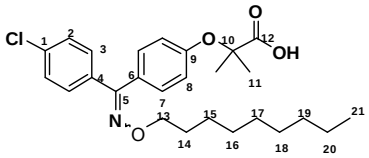

2-(4-((4-Chlorophenyl)(decyloxyimino)methyl)phenoxy)-2-methylpropanoic acid (17c, BSc3936)

Reactants: 0.115 g (0.23 mmol) BSc3976, 0.36 mL 2N NaOH (2.30 mmol), 4.8 mL MeOH.
Yield: 0.085 g, 78%, colourless oil.
^{1}H NMR (300 MHz, $CDCl_3$): δ = 7.43-7.21 (m, 4H), 6.91 (d, *J* = 9 Hz, 2H), 6.85 (d, *J* = 9 Hz, 2H), 4.11 (m, 2H, H-13), 3.31 (m, 2H), 1.65-1.58 (m, 6H), 1.27-1.21 (m, 14H), 0.89 (t, *J* = 6 Hz, 3H, H-20) ppm.
^{13}C NMR (75 MHz, $CDCl_3$): δ = 177.6 (C-12). 158.2 (C-9), 156.4 (C-5), 135.6 (C-1), 133.6 (C-4), 132.0 (C-3), 131.7 (C-6), 131.1 (C-7), 129.4 (C-2), 119.7 (C-8), 80.3 (C-10), 75.5 (C-13), 33.1 (C-20), 30.7 (C-19), 30.6 (C-18), 30.5 (C-17), 30.4 (C-16), 30.2 (C-14), 27.1 (C-15), 25.8 (C-11), 23.8 (C-21), 14.5 (C-22) ppm.
ESI-MS: m/z (%) = 474 (M^+).

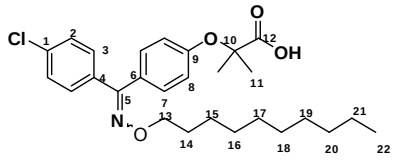

2-(4-((4-Chlorophenyl)(undecyloxyimino)methyl)phenoxy)-2-methylpropanoic acid (17d, BSc3937)

Reactants: 0.030 g (0.06 mmol) BSc3977, 0.09 mL 2N NaOH (0.60 mmol), 1 mL MeOH.
Yield: 0.022 g, 75%, colourless oil.
^{1}H NMR (500 MHz, $CDCl_3$): δ = 7.37-7.12 (m, 4H), 6.93 (d, *J* = 9 Hz, 2H), 6.82 (d, *J* = 9 Hz, 2H), 4.04 (m, 2H, H-13), 3.25 (dd, *J* = 3.24, 1.63 Hz, 2H), 1.74-1.40 (m, 6H), 1.37-1.02 (m, 16H), 0.84 (t, *J* = 6.6 Hz, 3H, H-20) ppm.
^{13}C NMR (75 MHz, $CDCl_3$): δ = 177.1 (C-12). 158.3 (C-9), 156.4 (C-5), 137.4 (C-1), 133.8 (C-4), 132.5 (C-3), 131.2 (C-6), 131.0 (C-7), 129.9 (C-2), 119.7 (C-8), 81.7 (C-10), 76.3 (C-13), 33.6 (C-21), 31.3 (C-20), 31.2 (C-19), 31.0 (C-18), 30.7 (C-17), 30.7 (C-16), 27.6 (C-14), 27.0 (C-15), 27.0 (C-11), 24.3 (C-22), 15.4(C-23) ppm.
ESI-MS: m/z (%) = 488 (M^+).

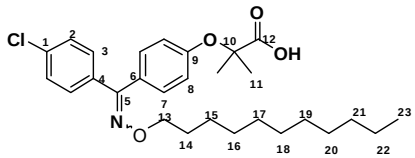

2-(4-((4-Chlorophenyl)(dodecyloxyimino)methyl)phenoxy)-2-methylpropanoic acid (17e, BSc3938)

Reactants: 0.033 g (0.06 mmol) BSc3978, 0.09 mL 2N NaOH (0.60 mmol), 1 mL MeOH.
Yield: 0.020 g, 66%, colourless oil.
^{1}H NMR (500 MHz, $CDCl_3$): δ = 7.41-7.13 (m, 4H), 6.89 (d, *J* = 8.8 Hz, 2H), 6.77 (d, *J* = 8.5 Hz, 2H), 4.10-3.96 (m, 2H), 3.23 (m, 2H), 1.64-1.38 (m, 6H), 1.36-1.13 (m, 18H), 0.79 (t, *J* = 6.63 Hz, 3H) ppm.
^{13}C NMR (125 MHz, $CDCl_3$): δ =178.9 (C-12), 159.1 (C-9), 157.3 (C-5), 138.2 (C-1), 137.4 (C-4), 132.4 (C-3), 130.1 (C-6), 130.1 (C-7), 129.7 (C-2), 119.0 (C-8), 88.2 (C-10), 65.4 (C-13), 33.5 (C-22), 31.2, 31.2, 30.9, 27.6, 27.5, 27.1, 27.0, 24.2, 24.1, 20.5 (C-23), 15.2 (C-24) ppm.
ESI-MS: m/z (%) = 502 (M^+).

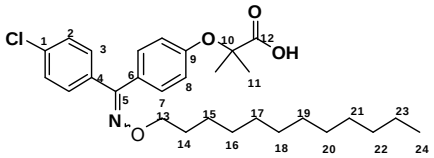

2-(4-((4-Chlorophenyl)(tetradecyloxyimino)methyl)phenoxy)-2-methylpropanoic acid (17f, BSc3939)

Reactants: 0.034 g (0.06 mmol) BSc3979, 0.09 mL 2N NaOH (0.60 mmol), 1 mL MeOH.
Yield: 0.024 g, 75%, colourless oil.
^{1}H NMR (500 MHz, $CDCl_3$): δ = 7.43-7.12 (m, 4H), 6.87 (d, *J* = 8.3 Hz, 2H), 6.77 (d, *J* = 8.1 Hz, 2H), 4.10-4.05 (m, 2H), 3.32-3.30 (m, 2H), 1.77-1.47 (m, 6H), 1.21-1.35 (m, 20H), 0.80 (t, *J* = 6.5 Hz, 3H) ppm.
^{13}C NMR (125 MHz, $CDCl_3$): δ = 177.6 (C-12), 158.4 (C-9), 156.9 (C-5), 140.4 (C-1), 137.3 (C-4), 132.9 (C-3), 132.5 (C-6), 131.1 (C-7), 130.4 (C-2), 119.5 (C-8), 81.0 (C-10), 74.7 (C-13), 35.3 (C-24), 34.5, 33.6, 31.3, 31.1, 31.1, 31.0, 30.4, 29.8, 26.9, 26.7, 24.3 (C-11), 22.9 (C-25), 15.4 (C-26) ppm.
ESI-MS: m/z (%) = 530 (M^+).

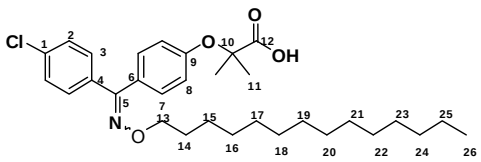

Isopropyl 2-(4-((4-chlorophenyl)(hexadecyloxyimino)methyl)phenoxy)-2-methylpropanoate
(17g, BSc3940)

Reactants: 0.036 g (0.06 mmol) BSc3979, 0.09 mL 2N NaOH (0.60 mmol), 1 mL MeOH.
Yield: 0.026 g, 78%, colourless oil.
^{1}H NMR (500 MHz, $CDCl_3$): δ = 7.73-7.15 (m, 4H), 6.80 (d, *J* = 8.5 Hz, 2H), 6.73 (d, *J* = 8.3 Hz, 2H), 4.06-3.99 (m, 2H), 3.34-3.32 (m, 2H), 1.76-1.73 (m, 2H), 1.57-1.48 (m, 2H), 1.34-1.31 (m, 6H), 1.19-1.12 (m, 22H), 0.78 (t, *J* = 6.5 Hz, 3H) ppm.
^{13}C NMR (125 MHz, $CDCl_3$): δ 178.2 (C-12), 158.9 (C-9), 158.9 (C-5), 139.2 (C-1), 138.7(C-4), 135.2 (C-3), 135.1 (C-6), 133.0 (C-7), 132.6 (C-2), 122.8 (C-8), 83.5 (C-10), 78.9 (C-13), 37.2 (C-26), 37.0, 36.2, 34.0, 33.8, 33.5, 33.4, 33.2, 32.8, 32.5, 31.2, 30.3, 29.7, 27.0 (C-11), 25.8 (C-27), 18.5 (C-28) ppm.
ESI-MS: m/z (%) = 558 (M^+).

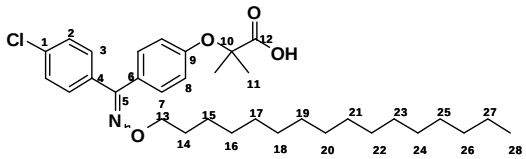

General procedure for *N*-alkylation and dimerization of Isopropyl 2-(4-((4-clorophenyl)hydroxyimino)ethyl) henoxy) -2-methylpropanoate
Isopropyl 2-(4-((4-clorophenyl)hydroxyimino)ethyl)phenoxy)-2-methylpropanoate (2.2 equiv) was added to a stirred suspension of NaH (2.2 equiv) in DMF (5 mL/mmol) at 0 °C. After 30 minutes alkyl halide (1 equiv) dissolved in DMF was added. The reaction mixture was stirred at ambient temperature for 6–24 h. The heterogeneous reaction mixture was quenched with NH_4Cl (sat. aq), diluted with EtOAc and the solution was washed with water. The aqueous solution was extracted with EtOAc (3x 50 mL). The combined organic extract was washed with H_2O, brine and dried over anhydrous Na_2SO_4 and rotary evaporated. The crude compound was purified by flash column chromatography using ethyl acetate and cyclohexane mixtures.

Isopropyl 2,2'-(4,4'-(1,14-bis(4-chlorophenyl)-3,12-dioxa-2,13-diazatetradeca-1,13-diene-1,14-diyl)bis(4,1-phenylene))bis(oxy)bis(2-methylpropanoate) (BSc3981)

Reactants: 0.100 g (0.26 mmol) **10**, 0.011 g NaH (0.26 mmol), 0.033 g 1,8-dibromooctane (0.12 mmol), 1 mL DMF.
Yield: 0.064 g, 62%, colourless oil.
^{1}H NMR (300 MHz, $CDCl_3$): δ = 7.31-7.18 (m, 8H), 6.77-6.71 (m, 8H), 5.08-4.97 (m, 2H), 4.07 (m, 4H, H-15, H-22), 1.59-1.52 (m, 16H), 1.24-1.12 (m, 20H) ppm.
^{13}C NMR (75 MHz, $CDCl_3$): δ = 172.5 (C-12), 155.7 (C-9), 153.8 (C-5), 134.0 (C-1), 132.0 (C-4), 130.8 (C-3), 129.8 (C-6), 129.4 (C-7), 128.7 (C-2), 117.3, 116.6, 116.3 (C-8), 78.2, 78.1, (C-10), 73.8, 73.7 (C-15, C-22), 68.1, 68.3 (C-13), 28.7, 28.3, 28.1, 24.9, 24.5, 24.1, 20.5 (C-14) ppm.
ESI-MS: m/z (%) = 862 (M^+).

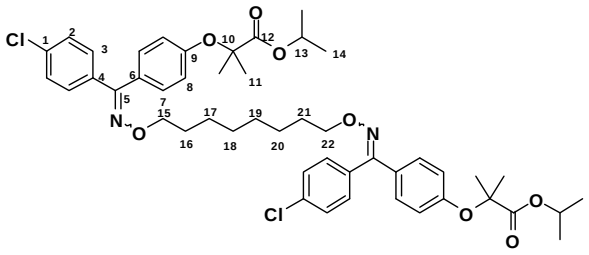

Isopropyl 2,2'-(4,4'-(1,16-bis(4-chlorophenyl)-3,14-dioxa-2,15-diazahexadeca-1,15-diene-1,16-diyl)bis(4,1-phenylene))bis(oxy)bis(2-methylpropanoate) (BSc3982)

Reactants: 0.100 g (0.26 mmol) **10**, 0.011 g NaH (0.26 mmol), 0.036 g 1,10-dibromodecane (0.12 mmol), 1 mL DMF.
Yield: 0.056 g, 52%, colourless oil.
^{1}H NMR (300 MHz, $CDCl_3$): δ = 7.39-7.27 (m, 8H), 6.89-6.68 (m, 8H), 5.03-4.98 (m, 2H), 4.16-4.14 (m, 4H, H-15, H-24), 1.70-1.56 (m, 16H), 1.26-1.21 (m, 24H) ppm.
^{13}C NMR (75 MHz, $CDCl_3$): δ = 173.4 (C-12), 157.8 (C-9), 154.9 (C-5), 134.0 (C-1), 132.0 (C-4), 131.6 (C-3), 129.8 (C-6), 129.6 (C-7), 128.7 (C-2), 118.4, 116.6 (C-8), 78.4 (C-10), 73.8, 73.7 (C-15, C-24), 68.3 (C-13), 29.7, 29.1, 28.8, 26.4, 25.9, 25.5, 24.5, 24.1, 20.4 (C-14) ppm.
ESI-MS: m/z (%) = 912 (M+Na).

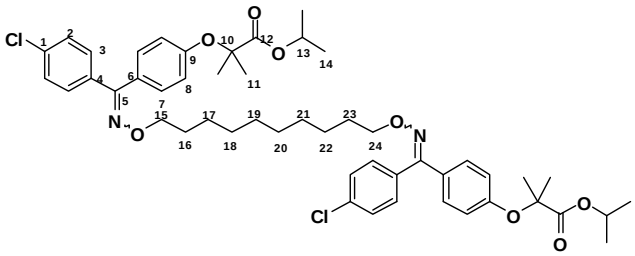

Isopropyl 2,2'-(4,4'-(1,18-bis(4-chlorophenyl)-3,16-dioxa-2,17-diazaoctadeca-1,17-diene-1,18-diyl)bis(4,1-phenylene))bis(oxy)bis(2-methylpropanoate) (BSc3983)

Reactants: 0.100 g (0.26 mmol) **10**, 0.011 g NaH (0.26 mmol), 0.040 g 1,12-dibromododecane (0.12 mmol), 1 mL DMF.
Yield: 0.0 g, %, colourless oil.
^{1}H NMR (300 MHz, $CDCl_3$): δ = 7.46-7.24 (m, 8H), 6.82-6.79 (m, 8H), 5.20-5.01 (m, 2H), 4.11-4.04 (m, 4H, H-15, H-26), 1.62-1.52 (m, 16H), 1.19-1.12 (m, 28H) ppm.
^{13}C NMR (75 MHz, $CDCl_3$): δ = 174.5 (C-12), 156.6 (C-9), 153.9 (C-5), 132.8 (C-1), 132.0 (C-4), 131.2 (C-3), 130.8 (C-6), 128.9, (C-7), 128.7 (C-2), 118.4, 119.6, 118.3 (C-8), 77.6 (C-10), 74.8, 74.8 (C-15, C-26), 69.1 (C-13), 29.6, 29.4, 29.1, 28.8, 26.4, 25.9, 25.5, 25.3, 24.5, 24.1, 21.5 (C-14) ppm.
ESI-MS: m/z (%) = 940 (M+Na).

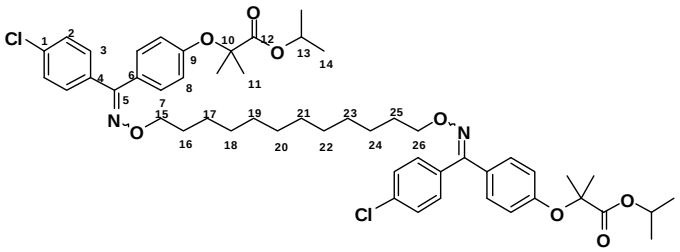

General procedure for isopropyl ester cleavage of dimeric *O*-substituted isopropyl 2-(4-((4 chlorophenyl)(hydroxyimino)methyl)phenoxy)-2-methylpropanoates

A solution of isopropyl ester (1 equiv) in 2N NaOH (20 equiv) in methanol (5 mL/mmol) was stirred at 70 °C overnight. After completion of reaction (TLC), solvent was evaporated *in vacuo* to get crude product. The heterogeneous reaction mixture diluted with EtOAc, acified with 2N HCl (pH ~ 4) and the solution was washed with water. The aqueous solution was extracted with EtOAc (3x 50 mL). The combined organic extract was washed with H_2O, brine and dried over anhydrous Na_2SO_4 and rotary evaporated. If necessary, the crude compound was purified by flash column chromatography using ethyl acetate and hexane mixtures.

2,2'-(4,4'-(1,18-Bis(4-chlorophenyl)-3,16-dioxa-2,17-diazaoctadeca-1,17-diene-1,18-diyl)bis(4,1-phenylene))bis(oxy)bis(2-methylpropanoic acid) (18a, BSc3941)

Reactants: 0.050 g (0.06 mmol) BSc3981, 0.09 mL 2N NaOH (1.2 mmol), 1 mL MeOH.
Yield: 0.043 g, 92%, colourless oil.
^{1}H NMR (500 MHz, $CDCl_3$): δ = 7.29-7.16 (m, 8H), 6.82-6.73 (m, 8H), 4.68-4.01 (m, 4H, H-13, H-20), 1.57-1.50 (m, 16H), 1.24-1.67 (m, 8H) ppm.
^{13}C NMR (125 MHz, $CDCl_3$): δ = 178.2 (C-12), 158.8 (C-9), 158.4 (C-5), 137.3, 136.3 (C-1), 133.7, 133.7 (C-4), 132.9, 132.5 (C-3), 131.6, 131.1 (C-6), 130.5, 130.3 (C-7), 130.0, 129.9 (C-2), 119.9, 119.3 (C-8), 80.8 (C-10), 76.3, 76.2 (C-13, C-20), 31.3, 30.9, 30.7, 30.7, 27.5, 26.8, 26.7 (C-11) ppm.
ESI-MS: m/z (%) = 777 (M^+).

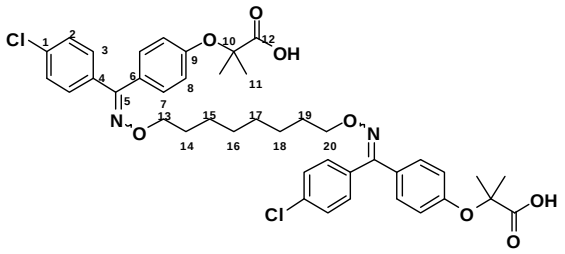

2,2'-(4,4'-(1,16-Bis(4-chlorophenyl)-3,14-dioxa-2,15-diazahexadeca-1,15-diene-1,16-diyl)bis(4,1-phenylene))bis(oxy)bis(2-methylpropanoic acid) (18b, BSc3942)
Reactants: 0.053 g (0.06 mmol) BSc3982, 0.09 mL 2N NaOH (1.2 mmol), 1 mL MeOH.
Yield: 0.047 g, 88%, colourless oil.
^{1}H NMR (500 MHz, $CDCl_3$): δ = 7.31-7.18 (m, 8H), 6.87-6.74 (m, 8H), 4.07-4.03 (m, 4H, H-13, H-22), 1.60-1.51 (m, 16H), 1.27-1.20 (m, 12H) ppm.
^{13}C NMR (125 MHz, $CDCl_3$): δ = 178.2 (C-12), 158.4 (C-9), 157.7, 157.0 (C-5), 137.3, 136.8 (C-1), 133.8, 133.7 (C-4), 132.9, 132.5 (C-3), 131.6, 131.1 (C-6), 130.4, 130.3 (C-7), 130.0, 129.9 (C-2), 119.9, 119.4 (C-8), 80.8, 80.8 (C-10), 76.4, 76.3 (C-13, C-22), 31.3, 31.1, 31.0, 30.9, 30.7, 30.7, 27.6, 26.8, 26.7 (C-11) ppm.

ESI-MS: m/z (%) = 806 (M^+).

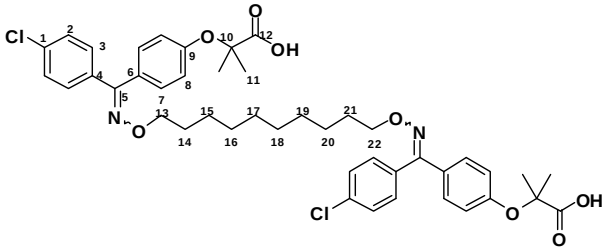

2,2'-(4,4'-(1,18-Bis(4-chlorophenyl)-3,16-dioxa-2,17-diazaoctadeca-1,17-diene-1,18-diyl)bis(4,1-phenylene))bis(oxy)bis(2-methylpropanoic acid) (18c, BSc3943)

Reactants: 0.055 g (0.06 mmol) BSc3983, 0.09 mL 2N NaOH (1.2 mmol), 1 mL MeOH.
Yield: 0.045 g, 88%, colourless oil.
^{1}H NMR (500 MHz, $CDCl_3$): δ = 7.39-7.18 (m, 8H), 6.80-6.69 (m, 8H), 4.08-4.04 (m, 4H, H-13, H-24), 1.58-1.46 (m, 16H), 1.20-1.14 (m, 16H) ppm.
^{13}C NMR (125 MHz, $CDCl_3$): δ = 178.4 (C-12). 155.7, 155.2 (C-9), 154.2, 154.2 (C-5), 134.6, 133.7 (C-1), 131.2, 131.0 (C-4), 129.9, 129.9 (C-3), 129.0, 128.5 (C-6), 127.9, 127.7 (C-7), 127.5, 127.4 (C-2), 116.9, 116.5 (C-8), 78.4 (C-10), 73.9, 73.8 (C-13, C-24), 32.4, 32.1, 28.8, 28.7, 28.2, 27.7, 27.1, 25.0, 24.4, 24.3, 20.5 (C-11) ppm.
ESI-MS: m/z (%) = 850 (M^+).

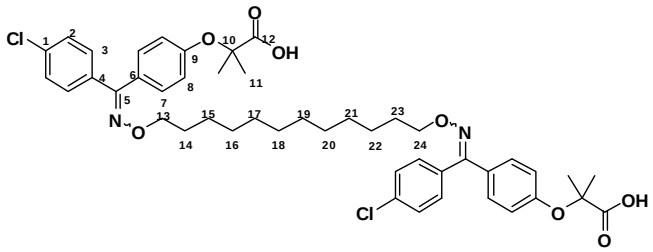

Isopropyl 2-(4-((4-chlorophenyl)(2-(2,4-dinitrophenyl)hydrazono)methyl)phenoxy)-2-methylpropanoate (BSc3899)
To a solution of 2,4-Dinitrophenyl)hydrazine (0.160 g, 0.82 mmol) and conc. H_2SO_4 (0.1 mmol) in methanol (8 mL) a solution of fenofibrat**e** (0.200 g, 0.55 mmol) in methanol (5 mL) was added dropewise. The reaction mixture was stirred at 50 °C for 2 h. The precipitate was filtered, washed with cold methanol, H_2O and $KHCO_3$ (3%) and dried *in vacuo* to yield the title compound.
Yield: 0.205 g, 70% as a red solid
^{1}H NMR (300 MHz, $CDCl_3$): δ = 9.07 (d, *J* = 2.6 Hz, 1H, H-19), 8.16 (d, *J* = 9.6 Hz, 1H, H-17), 8.36 (d, *J* = 9.6, 1H, H-16), 7.66-7.51 (m, 2H, H-3), 7.40-7.20 (m, 2H, H-7), 7.11 (d, *J* = 8.8 Hz, 2H, H-2), 6.855 (d, *J* = 9.0 Hz, 2H, H-8), 5.14-5.05 (m, 1H, H-13), 1.73-1.53 (m, 6H, H-11), 1.31-1.18 (m, 6H, H-13) ppm.
^{13}C NMR (75 MHz, $CDCl_3$): δ = 173.3 (C-12), 157.4 (C-9), 155.6 (C-5), 145.2 (C-15), 138.8 (C-18), 136.6 (C-1), 131.0 (C-17), 130.8 (C-4), 130.6 (C-3), 129.8 (C-7), 128.9 (C-2), 129.0 (C-20), 124.5 (C-6), 123.4 (C-19), 116.6 (C-16), 114.5 (C-8), 79.4 (C-10), 69.4 (C-13), 25.4 (C-11), 21.5 (C-14) ppm.
MS (ESI): m/z = 539 (M^+).

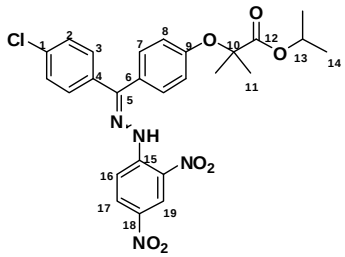

2-(4-((4-chlorophenyl)(2-(2,4-dinitrophenyl)hydrazono)methyl)phenoxy)-2-methylpropanoic acid (19, BSc3898)

A solution of BSc3899 (0.141 g, 0.26 mmol) in 2 N NaOH (2.6 mmol) in methanol (5 mL) was stirred at 70 °C overnight. After completion of reaction (TLC), solvent was evaporated *in vacuo* to get crude product. The heterogeneous reaction mixture diluted with EtOAc, acified with 2N HCl (pH ~ 4) and the solution was washed with water. The aqueous solution was extracted with EtOAc (3x 50 mL). The combined organic extract was washed with H_2O, brine and dried over anhydrous Na_2SO_4 and rotary evaporated *vacuo.* The crude compound was purified by flash column chromatography (CH_2Cl_2–MeOH, 10:1) to yield the title compound.

Yield: 0.036 g, 28% as a red solid

^{1}H-NMR (500 MHz, DMSO): δ = 8.88 (d, *J* = 3.2 Hz, 1H, H-17), 8.16 (d, *J* = 9.6 Hz, 1H, H-15), 8.36 (d, *J* = 9.6 Hz, 1H, H-14), 7.66-7.51 (m, 2H, H-3), 7.40-7.20 (m, 2H, H-7), 7.11 (d, *J* = 8.8 Hz, 2H, H-2), 6.855 (d, *J* = 9.0 Hz, 2H, H-8), 1.53 (s, 6H, H-11) ppm.

^{13}C-NMR (75 MHz, $CDCl_3$): δ = 175.2 (C-12), 157.4 (C-9), 155.6 (C-5), 144.8 (C-13), 138.8 (C-16), 136.4 (C-1), 131.0 (C-4), 130.3 (C-3), 130.0 (C-15), 129.6 (C-2), 129.0 (C-18), 124.4 (C-6), 123.4 (C-17), 116.6 (C-14), 114.8 (C-8), 79.3 (C-10), 69.4 (C-13), 25.7 (C-11) ppm. **MS (ESI):** m/z = 497 (M^+).

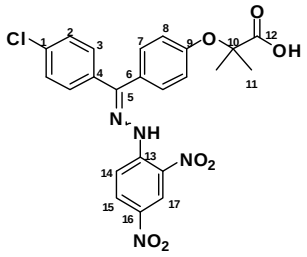

5. Figure_SI: Binding mode of sGSMs.

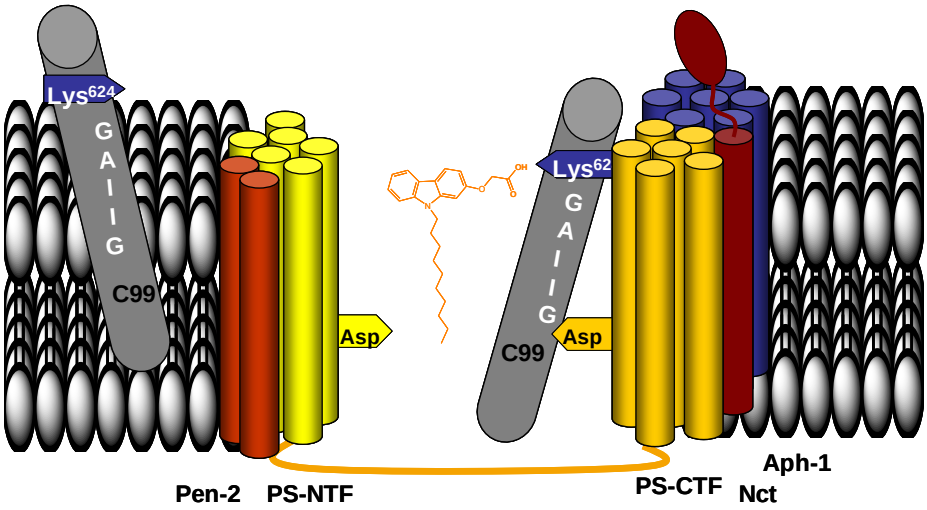

Figure_SI: Binding mode of sGSMs.

We compared the structures of highly active compounds to rationalize the binding mode of sGSMs. Apparently, a carboxylic acid moiety is essential for potency. We assume, that this functionality interacts with a lysine (maybe lys624) of the substrate APP which is located next to the membrane interface. Thereby, the lipophilic substituents of the sGSMs serve as membrane anchors.

.

3.4 Untersuchung der Bindungstasche von NSAID-abgeleiteten γ-Sekretase-Modulatoren durch Derivatisierung der Seitenkette und Austausch der Carbonsäurefunktion durch Säureisostere.

Der Inhalt dieses Kapitels wird im Januar 2010 bei *J.Med.Chem* zur Veröffentlichung eingereicht: Es handelt sich hier um ein vorläufiges Manuskript, aufgrund der fehlenden experimentellen Daten der Koautoren.
Nicole Höttecke, Andrea Zall, Daniel Kieser, Eva Fuchs, Katrin Schneider, Dirk Steinbacher, Robert Schubenel, Karlheinz Baumann, Boris Schmidt "NSAID-derived γ-secretase modulators: PartIV: The isosteric replacement of a carboxylic acid on a carbazole scaffold."

Durch eine Struktur-Aktivitäts-Analyse von 16 synthetisierten Carbazol-Derivaten wurde die Bedeutung der Carbonsäurefunktion für die γ-Sekretase-Modulation untersucht.

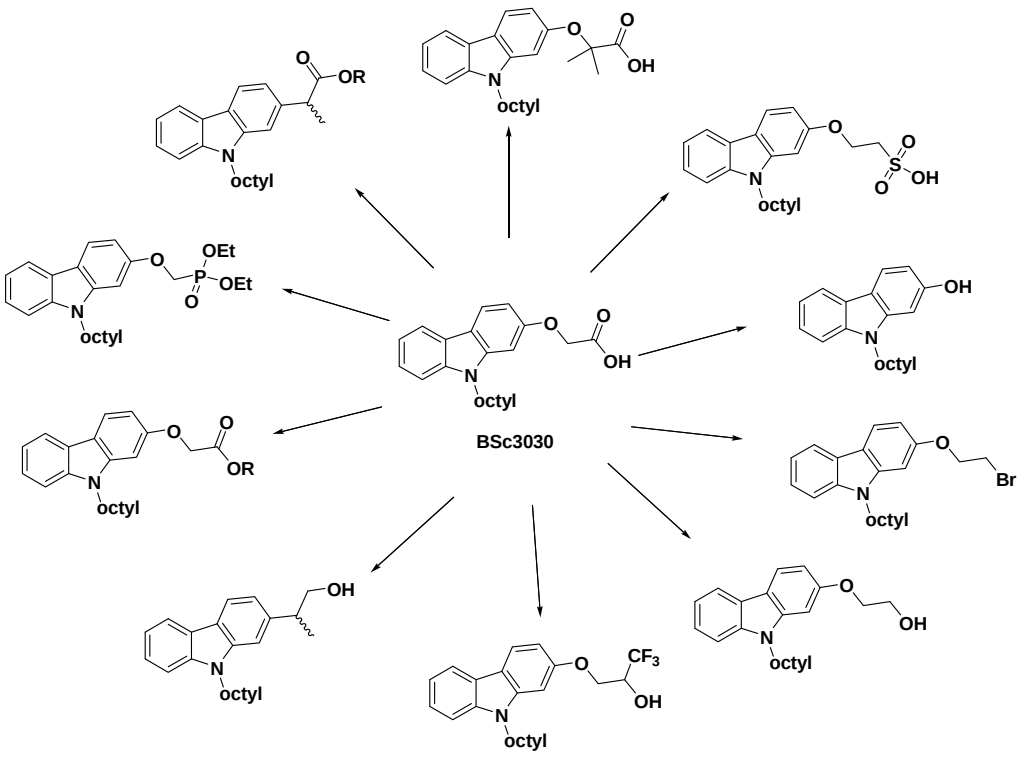

Abb. 22: Übersicht der Carbazol-Derivate zur Untersuchung der Seitenkette.

Eine Dimethylierung der Methylengruppe der Seitenkette zeigte keine signifikante Änderung auf die Aβ-Sekretion. Bei Kettenverlängerung und Austausch der Carbonsäurefunktion durch eine Sulfonsäure, konnte eine modulatorische Aktivität beobachtet werden. Diese

Aktivität führte bei einer Konzentration von 80 μM jedoch nur zu einer Erniedrigung der $A\beta_{42}$-Sekretion auf 70% und somit konnte kein IC_{50}-Wert ermittelt werden. Die noch vorhandene, aber reduzierte modulatorische Aktivität deutet darauf hin, dass nur ein Linker von 2-3 Atomen zwischen dem arylischen Grundgerüst und dem anscheinend notwendigen aziden H-Atom der Säure zu einer signifikanten modulatorischen Aktivität führt. Ein kürzerer Linker wie im *N*-Octyl-2-hydroxycarbazol zeigte keine modulatorische Aktivität. Der Ersatz der Carbonsäurefunktion durch Derivate mit einem Bromid oder einer Alkoholfunktion führte zu keiner modulatorische Aktivität auf die γ-Sekretase, was darauf hindeutet, dass das azide H-Atom essentiell für die modulatorische Aktivität ist. Durch Substitution der die Alkoholfunktion-tragenden Seitenkette mit einer Methyl- oder Trifluormethylgruppe wurden überraschenderweise inverse GSMs erhalten. Interessanterweise zeigten sowohl ein Methyl- ($IC_{50}(A\beta_{42}) = 27$ μM) als auch ein Ethylester ($IC_{50}(A\beta_{42}) = 31$ μM) modulatorische Aktivität auf die Aβ-Sekretion, bei nur geringer Potenzminderung verglichen mit der freien Carbonsäurefunktion ($IC_{50}(A\beta_{42}) = 19$ μM). Dieses lässt ein celluläres Prodrug-System vermuten, wobei die aktive Carbonsäurefunktion im Gehirn freigesetzt werden könnte. Wir vermuten, dass der Transporter mit einer Esterase assoziiert ist, die kurzkettige, unverzweigte Ester hydrolysieren kann, denn die modulatorische Aktivität nimmt mit der Länge und dem Grad der Verzweigung des Esters ab. Ebenso zeigen kurzkettige Ester, die an einer α-verzweigten Seitenkette lokalisiert sind, keine modulatorische Aktivität.

Liste der von Nicole Höttecke von 2006-2009 synthetisierten Verbindungen:

BSc3985
BSc3986
BSc4004
BSc4006
BSc4021
BSc4029
BSc4030
BSc4051
BSc4052
BSc4053
BSc4056
BSc4057
BSc4058
BSc4062
BSc4079

NSAID-derived γ-secretase modulators: Part IV: The isosteric replacement of a carboxylic acid on a carbazole scaffold

*Nicole Höttecke[a], Andrea Zall[a], Daniel Kieser[a], Eva C. Fuchs[a], Katrin Schneider[a], Dirk T. Steinbacher[a], Robert Schubenel[b], Karlheinz Baumann[b], Boris Schmidt.[a]**

[a]Clemens Schöpf-Institute of Chemistry and Biochemistry, Technische Universität Darmstadt, Petersenstr. 22, D-64287 Darmstadt, Germany.

[b]F. Hoffmann-La Roche Ltd., Pharmaceuticals Division, Preclinical Research CNS, Bldg. 70/345, CH-4070 Basel, Switzerland.

E-mail: schmidt_boris@t-online.de

[*] Prof. Dr. Boris Schmidt

Tel: (+49) 6151-163075

Fax: (+49) 6151-163278

E-Mail: schmidt_boris@t-online.de

ABSTRACT: Modulation of γ-secretase activity holds potential for the treatment of Alzheimer's disease. Most NSAID-derived γ-secretase modulators feature a carboxylic acid, which may impair blood brain barrier permeation. Therefore the structure activity relationship of 33 carbazoles featuring diverse carboxylic acid isosteres or metabolic precursors therefore was established in a cellular amyloid secretion assay. The activity was linked to either the acidity of the carboxylic acid isostere or the ability to undergo metabolic activation.

KEYWORDS: Alzheimer's disease, γ-secretase modulation, carboxylic acid isosteres, Carprofen.

Alzheimer's disease (AD) is the most common neurodegenerative disease, it is a devastating illness effecting more than 20 million patients globally. The brain atrophy associated with AD is accompanied by the hallmark amyloid plaques and fibrillary tangles. The plaques consist of aggregated oligomeric amyloid-β-peptides (Aβ) of various lengths wherein $A\beta_{42}$ is more prone to aggregate than $A\beta_{40}$ or $A\beta_{38}$.[1] These Aβ-peptides are generated by sequential processing of the amyloid precursor protein (APP) by β- and γ-secretase. The γ-secretase catalyses the critical step in the liberation of these Aβ isoforms, and is thus a promising target in the prevention of AD. The membrane located γ-secretase-complex consists of four proteins: Nicastrin (Nct), Aph-1, Pen-2 and presenilin (PS1 or PS2).[2] PS1 is a 9 transmembrane domain (TMD) protein which bears two catalytic aspartates Asp^{257} and Asp^{385} in the transmembrane domains 6 and 7.[3-5] These catalytic domains cleave APP within the membrane, implicating an unusual regulated intramembrane proteolysis (RIP) in the lipophilic membrane.[6-8]

Several inhibitors for this process have been reported recently.[7] However, most of these inhibit the cleavage of other γ-secretase substrates such as Notch, which is responsible for

cell proliferation. Some NSAIDs (non-steroidal anti inflammatory drugs) show a partial inhibition, the so called modulation of the γ-secretase cleavage, which is characterised by increased $A\beta_{38}$ secretion and decreased $A\beta_{42}$ secretion.[9] Photoaffinity labelling experiments with a *R*-flurbiprofen derivative indicate a binding site for NSAID-derived γ-secretase modulators directly on the substrate APP close to the GxxxG region,[10-11] which is responsible for substrate dimerization and may control the processing by γ-secretase. We suggested an interaction of the NSAID's carboxylic acid with a basic amino acid, perhaps lysine[624], on APP, which is located in vicinity of the GxxxG motif, at the membrane interface.[12]

We recently reported on *N*-alkylated carprofen-derivatives with lipophilic side chains and *N*-sulfonylated or *N*-alkylated carbazolyloxyacetic acids to be substrate targeting γ-secretase modulators (sGSMs).[13-14] The *N*-alkyl chain strongly enhances the modulator activity; this may be partially due to modulator orientation via a membrane anchoring effect. (Scheme 1)

Scheme 1. Carprofen (**1**) is the sGSM-lead structure of **2** and **3**.

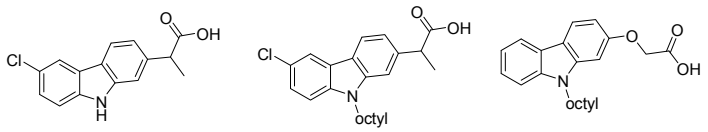

1 Carprofen **2 BSc3039** **3 BSc3030**

Herein we report the replacement of the carboxylic acid of sGSMs **2** (IC_{50} ($A\beta_{38}$) = not determined, IC_{50} ($A\beta_{40}$) > 40 μM, IC_{50} ($A\beta_{42}$) = 6.9 μM) and **3** (EC_{50} ($A\beta_{38}$) = 24 μM, IC_{50} ($A\beta_{40}$) > 40 μM, IC_{50} ($A\beta_{42}$) = 19 μM) by several carboxylic acid isosteres. This replacement aimed to reduce the topological polar surface area and the amphiphilicity of the lipophilic acids. This was expected to improve potential blood brain barrier (BBB) permeation.[13-14] Carboxylic acid isosteres require related chemical environments as the carboxylic acid for target binding and thus some of them were expected to display γ-secretase modulatory effects. We chose several well established carboxylic acid isosteres

such as tetrazole, sulfonic acid, sulfone amides and tetronates, alcohols or amino functionalities to obtain either straight or inverse γ-secretase modulators. In addition, we explored the available space at the modulator binding site by the introduction of sterically demanding groups. The synthesis was carried out according to scheme 2. (explicit synthesis: see supporting information)

Scheme 2.[a] General synthesis of carboxylic isosteres on a carbazole backbone.

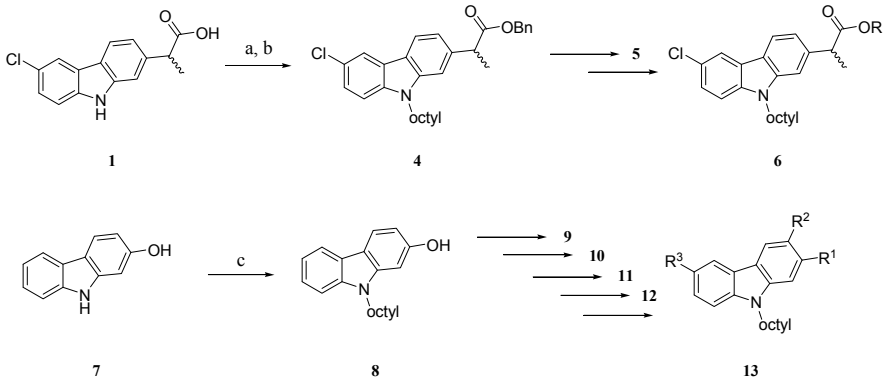

[a]Reagents: (a) benzylbromide, K_2CO_3, acetone, rf; (b) octylbromide, NaH, THF, 0°C-rt; (c) octylbromide, NaH, THF, 0°C-rt.

We kept the length of the supposed lipid anchor at 8 carbon atoms, making a compromise between lipophilicity and activity although this anchor is not the most active sGSM. The side chain of **3** (BSc3030) bears a methylene group which is an important structural feature as an additional methylene group diminished activity. This effect was observed for the carboxylic acid **10a** and to a lesser extent for the sulfonic acid **10b**. Surprisingly, the dimethylation (**11a**) of the unsubstituted methylene diminished activity although moderately potent γ-secretase activity modulating fenofibrate-derivatives have been described.[12] However, the replacement by a salicylic acid (**10c**) displayed a modulatory effect with an IC_{50} ($A\beta_{42}$) = 38 μM. The salicylic acid locks the extended carbon chain in a *Z*-configuration resulting in sufficiently close positioning of the carboxylic acid.

Equipotent modulatory activity as **10c** was achieved by a tetronic- (**10d**) and tetramic acid (**10e**), which are rarely employed as carboxylic acid isosteres. Only a sterically more demanding tetronate (**10f**) turned into a full inhibitor. (Scheme 3)

Scheme 3. [a] Synthesis of the higher substituted tetronate **10f**.

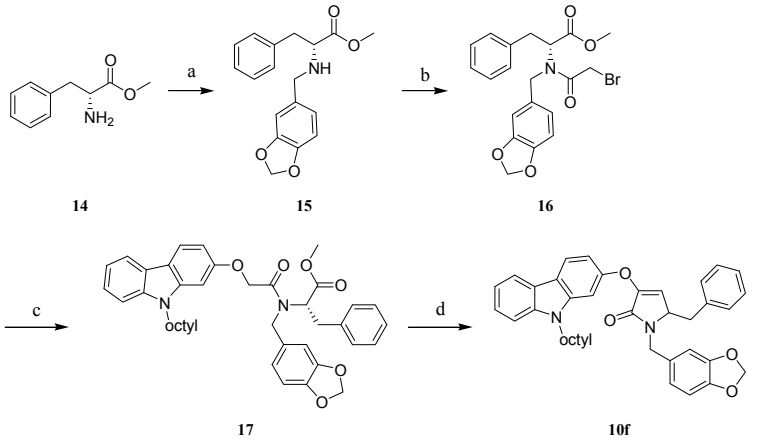

[a]Reagents: (a) piperonal, $Na(AcO)_3BH$, DCE, rt, 5h; (b) bromoacetyl bromide, TEA, DCM, rt, 2,5h; (c) **8**, K_2CO_3, acetone, rf; (d) KO*t*Bu, THF, rt.

On the contrary, established isosteres like the tetrazoles (**10h**) or the 2,2,2-trifluoroethanol (**9a**) did not exert γ-secretase modulatory activity until a concentration of 20 μM or turned out to be inverse GSM. The linear alcohol **10g** and bromide **9b** were inactive. However, the α-branched alcohol **6a** acted as an inverse GSM.

The amines **10i, 11b-d** did not show modulatory activity. Whereas the nitrile **9c** displayed inverse modulation and the acidic sulfonimide **6b** showed straight inhibition. These results indicate the necessity of an acidic proton for modulatory activity on this scaffold. This confirmed our hypothesis that modulators interact with a basic amine on the substrate, because all sGSMs of this series exhibit a pKa value in the range 2-5.

Scheme 4. Synthesis of C3-substituted carbazole **13a**.

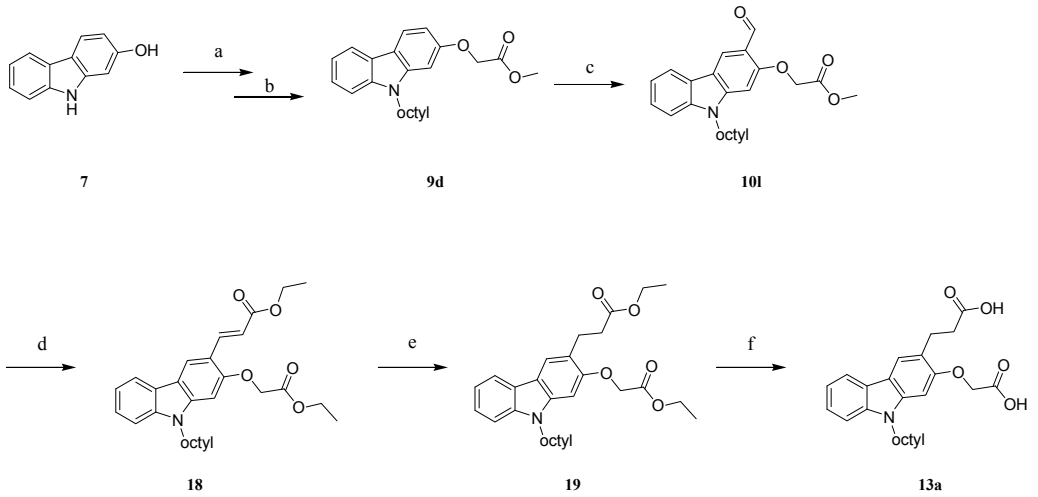

[a]Reagents: (a) octyliodide, NaH, THF, DMF, -70°C-rt, 12h; (b) bromoacetic acid methylester, K_2CO_3, acetone, rf. 12h; (c) *N*,*N*.diisopropylformamide, $POCl_3$, H_2O, DCE, 80°C, 2-5d; (d) phosphonium salt, NaOEt, EtOH, 80°C, 20h; (e) Pd/C, H_2, EtOH, HCl, rt, 24h; (f) KOH, MeOH, rt/64°C, 2d.

Additional substituents in the C-3 position of **3** revealed a tolerance for small functional groups like an aldehyde (**11e**), but an additional acetic acid side chain (**13a**) diminished activity. (Scheme 4) These findings suggest a defined binding pocket for the modulators.

Table 1. Activity report of *N*-octylcarprofen and *N*-octylcarbazole carboxylic acid isosteres.

Entry	Compd.	Compd. Code	R^1	R^2	R^3	[%]		
						$A\beta_{38}$	$A\beta_{40}$	$A\beta_{42}$
1	5a	BSc4053		H	Cl	[redacted]	[redacted]	50[a]
2	6a	BSc4021		H	Cl	[redacted]	[redacted]	21[a]
3	6b	BSc4056	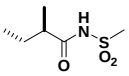	H	Cl	[redacted]	[redacted]	32
4	8	BSc4029	-OH	H	H	[redacted]	[redacted]	>80
5	9a	BSc4062	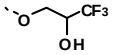	H	H	[redacted]	[redacted]	12[a]
6	9b	BSc4004	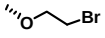	H	H	>40	>40	>40
7	9c	BSc3891	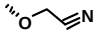	H	H	74[b]	105[b]	252[b]
8	10a	BSc4005	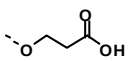	H	H	>80	>80	>80
9	10b	BSc4079	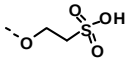	H	H	[redacted]	[redacted]	>80

10	10c	BSc4003	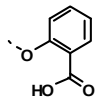	H	H	23[a]	>80	38
11	10d	BSc3972	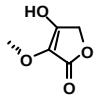	H	H	21[a]	>80	37
12	10e	BSc3990	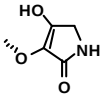	H	H	8[a]	72	28
13	10f	BSc3966	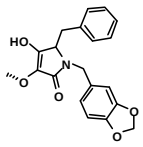	H	H	31	32	24
14	10g	BSc4030	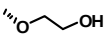	H	H			>40
15	10h	BSc3892	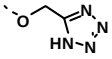	H	H	165[b]	102[b]	113[b]
16	10i	BSc4019	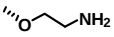	H	H	>80	>80	>80
17	11a	BSc3985	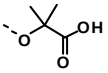	H	H	>40	>40	>40
18	11b	BSc4122	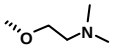	H	H			>10
19	11c	BSc4124	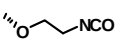	H	H			>80
20	11d	BSc4123	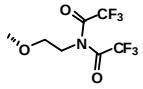	H	H			>80
21	11e	BSc4041	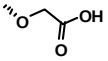		H			32
22	13a	BSc4050	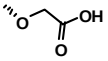	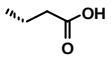	H			>80
23	13b	BSc4048	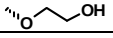		H			80

[a] EC_{50} values are displayed.

[b] Tested at 20 µM.

The methyl ester **9d** displayed unexpected modulatory activity with an IC_{50} ($A\beta_{42}$) = 27 µM, a marginal loss in activity compared to the carboxylic acid **3** with an IC_{50} for $A\beta_{42}$ of 19 µM. Further investigation confirmed the tolerance of short linear esters. However, the activity decreased with increasing length of the ester. The ethyl ester (**11f**) showed modulatory activity (IC_{50} ($A\beta_{42}$) = 31 µM), but *iso*-propyl (**11g**) or *iso*-butyl ester (**10j**) did not show modulatory activity. On the contrary, the tertiary butyl ester **9e** acted as an inverse GSM and increased $A\beta_{42}$ levels at EC_{50} = 19 µM. Equally the phosphoric diethyl ester showed inverse modulatory effects with an EC_{50} ($A\beta_{42}$) = 13 µM. These findings

suggest metabolic activation, e.g. an esterase releasing the active carboxylic acid. This esterase seems to tolerate short linear esters as substrates. This presumption was confirmed by investigation of the α-branched side chain of Carprofen-esters (**4, 5b, c**) which did not show modulatory activity. Consequently, short α, α´-linear esters fulfil criteria for a prodrug system in this cellular assay. This potential prodrug system is still under investigation. Finally, an additional aldehyde in the C-3 position (**10l**) of the methyl ester is not tolerated and resulted in straight γ-secretase inhibition.

Table 2. Activity report of *N*-octylcarbazole and *N*-octylcarpofen esters.

Entry	Compd.	Compd. Code	R^1	R^2	R^3	[%]		
						$A\beta_{38}$	$A\beta_{40}$	$A\beta_{42}$
1	4	BSc3018	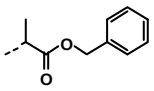	H	Cl	■	■	>80
2	5b	BSc4051		H	Cl	■	■	15[a]
3	5c	BSc4052	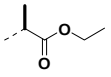	H	Cl	■	■	21[a]
4	9d	BSc4028	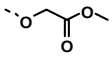	H	H	■	■	27
5	9e	BSc3029	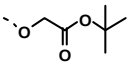	H	H	■	■	19[a]
6	10j	BSc3986	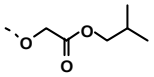	H	H	■	■	>80
7	10k	BSc4006	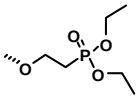	H	H	■	■	13[a]
8	10l	BSc4038	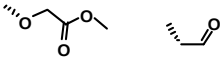		H	■	■	89
9	11f	BSc4057	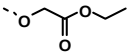	H	H	■	■	31
10	11g	BSc4058	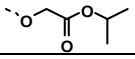	H	H	■	■	49[a]

[a] EC_{50} values are displayed.

As none of the acid isosteres displayed improved potency of the lead acid **3**, a closely related compound (**20**, BSc3040) was selected for further investigations. Serendipitously, the C-9-derivative **20** showed a remarkable BBB permeation in APP_{swe} Tg mice at a single 10 mg/kg oral dosage suspended in NaCl and gelatine. The plasma and brain concentration

of the modulator were monitored over a period of 5 hours. The brain concentration was found to continuously increase to a plasma/brain ration of approximately 2:1. (Figure 1) However, no significant $A\beta_{42}$ changes were observed at this timepoint. These unchanged Aβ levels were recently linked to the double transgenic mice exhibiting NSAID-resistant PS1 mutations.[15-16] The remarkable brain permeation reduces the need for a potential prodrug system. However, the significant brain levels of the acid **20** do not imply localisation of the compound at the site required for modulatory activity.

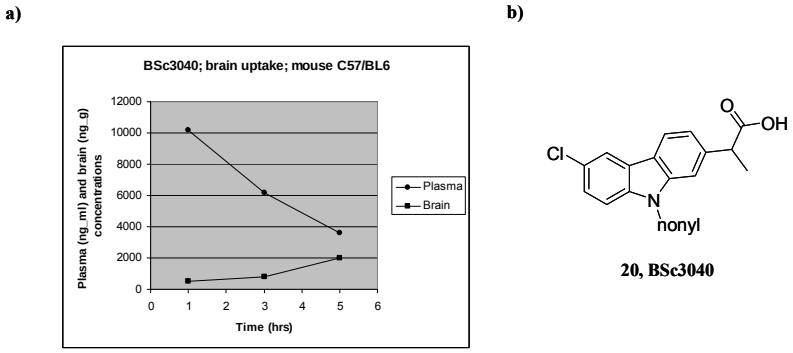

Figure 1. BSc3040 (**20**) penetrates the BBB in C57/BLg mice at an oral dosage of 10 mg/kg.

We were able to replace the carboxylic acid by isosteres preserving modulatory activity. These finding confirm the necessity of an acidic proton on this class of γ-secretase modulators. Most sGSMs are found in a pKa-range of 2-5. This small pKa-range supports our hypothetical interaction with lysine[624]. The location of this lysine, directly at the membrane interface close to the GxxxG dimerization motif, suggests a modulation mechanism as an APP dimerization inhibitor, shifting the cleavage site to the less toxic $A\beta_{38}$. The optimum spacer length between the arylic backbone and carboxylic acid was determined to be 2-3 carbon or oxygen atoms. However, introduction of a rigid aryl spacer allowed an elongation of up to 4 atoms. We identified a potential prodrug system based on short linear esters, which complements the remarkable BBB penetrations of the free acid **20**.

ACKNOWLEDGMENT: We thank the BMBF (B.S., N.H., A.Z. KNDD) for support of this work.

SUPPORTING INFORMATION: Synthetic procedure and spectral data of the tested compounds and method of the *in vivo* mouse experiment.

REFERENCES

1. Beher, D.; Wrigley, J. D.; Owens, A. P.; Shearman, M. S., Generation of *C*-terminally truncated Aβ peptides is dependent on γ-secretase activity. *J. Neurochem.* **2002,** *82* (3), 563-575.
2. Wolfe, M. S., The γ-secretase complex: membrane-embedded proteolytic ensemble. *Biochemistry* **2006,** *45* (26), 7931-7939.
3. Kaether, C.; Haass, C.; Steiner, H., Assembly, trafficking and function of γ-secretase. *Neurodegener. Dis.* **2006,** *3* (4-5), 275-283.
4. Brunkan, A. L.; Goate, A. M., Presenilin function and γ-secretase activity. *J. Neurochem.* **2005,** *93* (4), 769-792.
5. Kimberly, W. T.; Xia, W.; Rahmati, T.; Wolfe, M. S.; Selkoe, D. J., The Transmembrane Aspartates in Presenilin 1 and 2 Are Obligatory for γ-Secretase Activity and Amyloid β-Protein Generation. *J. Biol. Chem.* **2000,** *275* (5), 3173-3178.
6. Steiner, H.; Fluhrer, R.; Haass, C., Intramembrane proteolysis by γ-secretase. *J. Biol. Chem.* **2008,** *283* (44), 29627-29631.
7. Baumann, S.; Hoettecke, N.; Narlawar, R.; Schmidt, B., γ -Secretase as a target for AD. *Med. Chem. Alzheimer's Dis.* **2008**, 193-224.
8. Brown, M. S.; Ye, J.; Rawson, R. B.; Goldstein, J. L., Regulated intramembrane proteolysis: a control mechanism conserved from bacteria to humans. *Cell* **2000,** *100* (4), 391-398.
9. Weggen, S.; Eriksen, J. L.; Das, P.; Sagi, S. A.; Wang, R.; Pietrzik, C. U.; Findlay, K. A.; Smith, T. E.; Murphy, M. P.; Bulter, T.; Kang, D. E.; Marquez-Sterling, N.; Golde, T. E.; Koo, E. H., A subset of NSAIDs lower amyloidogenic $A\beta_{42}$ independently of cyclooxygenase activity. *Nature* **2001,** *414* (6860), 212-216.
10. Kukar, T. L.; Ladd, T. B.; Bann, M. A.; Fraering, P. C.; Narlawar, R.; Maharvi, G. M.; Healy, B.; Chapman, R.; Welzel, A. T.; Price, R. W.; Moore, B.; Rangachari, V.; Cusack, B.; Eriksen, J.; Jansen-West, K.; Verbeeck, C.; Yager, D.; Eckman, C.; Ye, W.; Sagi, S.; Cottrell, B. A.; Torpey, J.; Rosenberry, T. L.; Fauq, A.; Wolfe, M. S.; Schmidt, B.; Walsh, D. M.; Koo, E. H.; Golde, T. E., Substrate-targeting γ-secretase modulators. *Nature* **2008,** *453* (7197), 925-929.
11. Munter, L. M.; Voigt, P.; Harmeier, A.; Kaden, D.; Gottschalk, K. E.; Weise, C.; Pipkorn, R.; Schaefer, M.; Langosch, D.; Multhaup, G., GxxxG motifs within the amyloid precursor protein transmembrane sequence are critical for the etiology of $A\beta_{42}$. *Embo J.* **2007,** *26* (6), 1702-1712.
12. Baumann, S.; Hoettecke, N.; Schubenel, R.; Baumann, K.; Schmidt, B., NSAID-derived γ-secretase modulators. Part III: Membrane anchoring. *Bioorg. Med. Chem. Lett.* **2009,** *19* (24), 6986-6990.

13. Narlawar, R.; Perez Revuelta, B. I.; Baumann, K.; Schubenel, R.; Haass, C.; Steiner, H.; Schmidt, B., *N*-Substituted carbazolyloxyacetic acids modulate Alzheimer associated γ–secretase. *Bioorg. Med. Chem. Lett.* **2007,** *17* (1), 176-182.
14. Narlawar, R.; Perez Revuelta, B. I.; Haass, C.; Steiner, H.; Schmidt, B.; Baumann, K., Scaffold of the cyclooxygenase-2 (COX-2) inhibitor carprofen provides Alzheimer γ-secretase modulators. *J. Med. Chem.* **2006,** *49* (26), 7588-7591.
15. Czirr, E.; Leuchtenberger, S.; Dorner-Ciossek, C.; Schneider, A.; Jucker, M.; Koo, E. H.; Pietrzik, C. U.; Baumann, K.; Weggen, S., Insensitivity to $A\beta_{42}$-lowering nonsteroidal anti-inflammatory drugs and γ-secretase inhibitors is common among aggressive presenilin-1 mutations. *J. Biol. Chem.* **2007,** *282* (34), 24504-24513.
16. Page, R. M.; Baumann, K.; Tomioka, M.; Perez-Revuelta, B. I.; Fukumori, A.; Jacobsen, H.; Flohr, A.; Luebbers, T.; Ozmen, L.; Steiner, H.; Haass, C., Generation of $A\beta_{38}$ and $A\beta_{42}$ is independently and differentially affected by familial Alzheimer disease-associated presenilin mutations and γ-secretase modulation. *J. Biol. Chem.* **2008,** *283* (2), 677-683.

Supporting Information

NSAID-derived γ-secretase modulators: Part IV: The isosteric replacement of a carboxylic acid on a carbazole scaffold

Nicole Höttecke[a], Andrea Zall[a], Daniel Kieser[a], Eva C. Fuchs[a], Katrin Schneider[a], Dirk T. Steinbacher[a], Karlheinz Baumann[b], Robert Schubenel[b], Boris Schmidt.[a]*

[a]*Clemens Schöpf-Institute of Chemistry and Biochemistry, Technische Universität Darmstadt, Petersenstr. 22, D-64287 Darmstadt, Germany, Fax: (+49) 6151-163278, E-mail: schmidt_boris@t-online.de*

[b]*F. Hoffmann-La Roche Ltd., Pharmaceuticals Division, Preclinical Research CNS, Bldg. 70/345, CH-4070 Basel, Switzerland*

Table of Content:

1. General comments:

Thin-layer chromatography (TLC) was carried out using aluminium sheets precoated with silica gel 60 F254 (0.2 mm; E. Merck). Chromatographic spots were visualized by UV and/or spraying with a methanolic solution of vanillin/H_2SO_4 or aq. $KMNO_4$ solution followed by heating. Silica gel chromatography was carried out using Merck silica gel 60 (0.063-0.2 mm). Melting Points were determined on a Mettler FP 51 melting point apparatus and are uncorrected. The ^{1}H and ^{13}C spectra were recorded on a Bruker AC 300 (300 MHz) and AC 500 spectrometer (500 MHz). Chemical shifts are reported as % values (ppm) and adjusted at the central line of the deuterated solvent (MeOD, $CDCl_3$). Mass spectrometry was performed on a Bruker-Franzen Esquire LC mass spectrometer (ESI) and a double focused MAT 95 (EI).

HPLC analysis was carried out using: an Agilent 1100 with a reversed phase column (Zorbax Eclipse XDB-C8; 4.6*150 mm) and a 254 nm detector. The eluent is composed of H_2O (1% TFA) (A) and acetonitrile (B) with a gradient: 30 to 100% B within 15 min (Nicole.M). The purity is given in area [%]. All reagents and solvents (THF, DMF, CH_2Cl_2, ethyl acetate, MeOH) were purchased at ABCR, Acros and Alfa Aesar, TCI, Sigma Aldrich and VWR. Methanol abs. was additionally dried over magnesium.

2. Experimental methods and spectral data of carboxylic acid isosteres on a carbazolic scaffold:

2.1 General procedure for ether/ester formation:

To a suspension of anhydrous K_2CO_3 (3.0 eq.) in acetone or DMF was added 2-hydroxy-*N*-octyl-carbazole (BSc4029) or a corresponding carboxylic acid (BSc3030/BSc3039) (1 eq.) and the alkylhalogenide (1.5 eq.). The reaction mixture was heated under reflux until the reaction was completed. (TLC control) The mixture was cooled to room temperature and filtered. The residue was washed with acetone (3×). The combined organic extract was evaporated *in vacuo* and purified by silica gel chromatography to yield the title compound.

2.2 General procedure for reduction with $LiAlH_4$:

To a solution of the corresponding ester (1 eq.) in THF at -78°C was added $LiAlH_4$ (2.5 eq.). The reaction mixture was stirred at -78°C until the reaction was completed (TLC control) and quenched by sequential addition of H_2O (1 mL by usage of 1 g $LiAlH_4$), 1M NaOH (2 mL by usage of 1 g $LiAlH_4$), H_2O (3 mL by usage of 1 g $LiAlH_4$). After stirring for 30 min the mixture was filtered through Celite, concentrated *in vacuo* and purified by silica gel chromatography to yield the title compound.

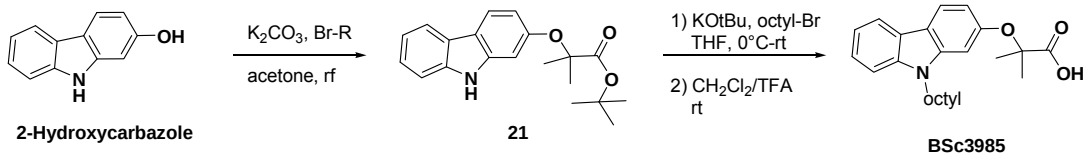

Scheme SI1: Detailed synthesis of Bsc3985

tert-Butyl 2-(9*H*-carbazol-2-yloxy)-2-methylpropanoate (21)

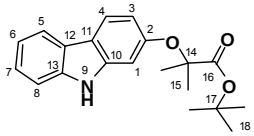

According to general procedure 2.1: 2-Hydroxycarbazole (1.500 g, 8.19 mmol), K_2CO_3 (3.395 g, 24.56 mmol), *tert*.-butyl-2-bromo-2-methylpropanoate (1.834 mL, 9.83 mmol), acetone (20 mL).
Yield: 0.395 g (18%), colourless solid.
HPLC: 8.6 min (95%);
^{1}H NMR (300 MHz, $CDCl_3$): δ = 8.01 (s, 1H, H-9), 7.97 (d, ^3J = 7.7 Hz, 1H), 7.90 (d, ^3J = 8.5 Hz, 1H), 7.40-7.30 (m, 2H), 7.24-7.16 (m, 1H), 6.94 (d, ^4J = 1.8 Hz, 1H), 6.83 (dd, ^3J = 8.5, ^4J = 2.2 Hz, 1H), 1.62 (s, 6H, H-15), 1.46 (s, 9H, C-18).
^{13}C NMR (75 MHz, $CDCl_3$): δ = 173.6 (C-16), 154.8 (C-2),140.3 (C-13), 139.7 (C-12), 124.8 (C-7) 123.3 (C-10), 220.5 (C-4), 119.6 (C-5), 119.5 (C-6), 118.2 (C-11), 112.4 (C-8), 110.3 (C-3), 100.9 (C-1), 81.5 (C-14), 80.0 (C-17), 27.8 (C-18), 25.5 (C-15).

tert.-Butyl 2-methyl-2-(9-octyl-9*H*-carbazol-2-yloxy)propanoate (22)

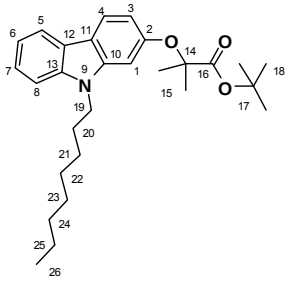

KO*t*Bu (0.043 g, 0.38 mmol) was added to a stirred solution of THF (1 mL) **21**(0.050 g, 0.19 mmol) at 0 °C. After 30 min octyliodide (0.067 g, 0.28 mmol) was added and the reaction mixture was allowed to stir at rt for 16 h. The heterogeneous reaction mixture was quenched by addition of NH_4Cl (sat. aq), extracted with CH_2Cl_2 (3x 10 mL). The combined organic layers were sequentially washed with H_2O and brine, dried over $MgSO_4$, concentrated *in vacuo* and purified by silica gel chromatography (CH_2Cl_2–hexane, 1:3) to give 0.027 g (27%) of **22** as yellow oil.
HPLC:11.1 min (98%)
^{1}H NMR (300 MHz, $CDCl_3$) ppm δ: = 8.02-7.97 (m, 1H, H-5), 7.92 (d, ^3J = 8.5 Hz, 1H, H-4), 7.43-7.32 (m, 2H, H-6/7), 7.19 (m, 1H, H-8), 6.93 (d,^{4} J = 2.0 Hz, 1H, H-1), 6.81 (dd,^3J = 8.5 Hz, ^{4} J = 2.2 Hz, 1H, H-3), 4.20 (t, ^3J = 7.3 Hz, 1H, H-19), 1.84 (pen, ^3J = 7.2 Hz, 2H, H-20), 1.64 (s, 6H, H-15), 1.48 (s, 9H, H-17), 1.43-1.21 (m, 10H, 21-25), 0.87 (t, J = 6.7 Hz, 3H, H-26).
^{13}C NMR (75 MHz, $CDCl_3$) ppm δ: = 173.6 (C-16), 154.7 (C-2), 141.4 (C-13), 140.7 (C-12), 124.6 (C-7), 122.8 (C-10), 120.4 (C-5), 119.6 (C-4), 118.8 (C-6), 117.8 (C-11), 111.6 (C-8), 108.4 (C-3), 99.4 (C-1), 81.5 (C-14), 80.0 (C-17), 43.1 (C-19), 31.8 (C-20), 29.4, 29.2 (CH_2), 28.9 (C-18), 27.9, 27.4 (CH_2), 25.5 (C-15), 22.6 (C-25), 14.0 (C-26).
MS (m/z, 70 eV) = 437 (M^+), 336, 295, 196.

2-Methyl-2-(9-octyl-9*H*-carbazol-2-yloxy)propanoic acid (BSc3985)

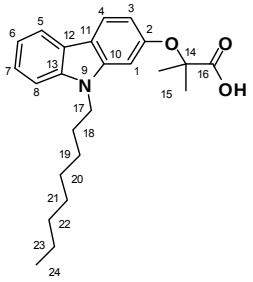

A solution of **22** (0.027 g, 0.06 mmol) in a mixture of 20% trifluoroacetic acid in CH_2Cl_2 (2 mL) was stirred at ambient temperature for 12h. After completion of reaction (TLC) the solvent was evaporated *in vacuo*. The obtained crude acid was purified by crystallization (CH_2Cl_2–hexane) to give 0.010 g (44%) of **BSc3985** as a colourless solid.

HPLC: 9.4 min (91%)

^{1}H NMR (500 MHz, $CDCl_3$) ppm δ: = 8.02 (d, ^3J = 7.6 Hz, 1H, H-5), 7.95 (d, ^3J = 8.4 Hz, 1H, H-4), 7.45-7.40 (m, 1H, H-7), 7.35 (d, ^3J = 8.2 Hz 1H, H-8), 7.25-7.20 (m, 1H, H-6), 7.01 (d, ^4J = 1.9 Hz, 1H, H-1), 6.87 (dd, ^3J = 8.4 Hz, ^4J = 2.0 Hz, 1H, H-3), 4.19 (t, ^3J = 7.2 Hz, 2H, H-17), 1.86-1.79 (m, 2H, H-18), 1.68 (s, 6H, H-15), 1.39-1.20 (m, 10H, H-19/20/21/22/23), 0.87 (t, ^3J = 7.0 Hz, 3H, H-24).

^{13}C NMR (125 MHz, $CDCl_3$) ppm δ: = 178.4 (C-16), 153.0 (C-2), 141.2 (C-13), 140.8 (C-12), 125.1 (C-7), 122.6 (C-10), 120.6 (C-4), 119.9 (C-5), 119.0 (C-11), 118.9 (C-6) 112.8 (C-8), 108.6 (C-2), 101.5 (C-1), 80.3 (C-11), 43.1 (C-17), 31.7 (C-18), 29.3, 29.1, 28.8, 27.3 (CH_2), 25.1 (C-17), 22.5 (C-23) 14.3 (C-24).

MS (m/z, 70 eV) = 381 (M^+), 295, 196.

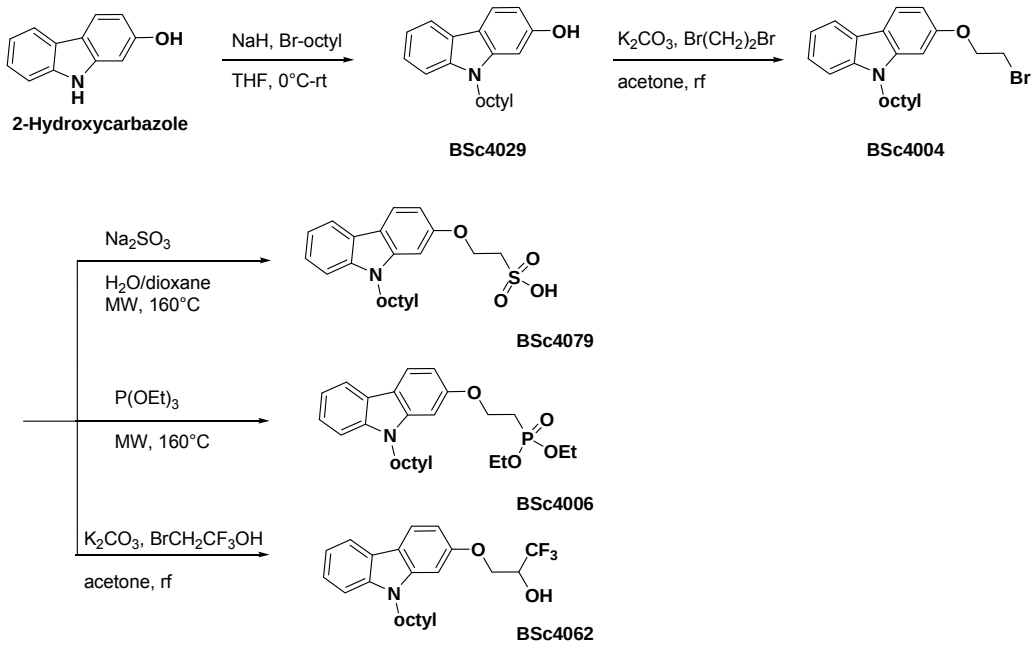

Scheme SI2: Detailed synthesis of BSc4004, BSc4006, BSc4029, BSc4062 and BSc4079.

2-Hydroxy-*N*-octylcarbazole (BSc4029)

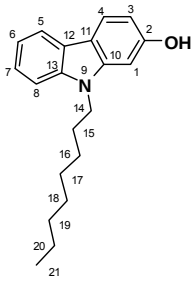

To a suspension of NaH (0.820 g, 20.48 mmol) in THF (20 mL) under argon atmosphere was added 2-hydroxycarbazole (1.50 g, 8.19 mmol) at a temperature of 0°C. After 30 min stirring octylbromide (1.500 g, 7.78 mmol) was added and the reaction mixture was allowed to warm to rt. After 12h the reaction mixture was quenched by drop wise addition of H_2O until gas formation ceased. The obtained mixture was extracted three times with CH_2Cl_2 (30 mL). The combined organic layers were washed with brine, dried over $MgSO_4$, concentrated *in vacuo* and purified by silica gel column chromatography (gradient starting with cyclohexane to cyclohexane: CH_2Cl_2 1:2) to give 1.580 g (74%) of **BSc4029** as a colourless solid.
HPLC:9.2 min (96%)
^{1}H NMR (500 MHz, $CDCl_3$) ppm δ: = 7.96 (d, ^3J = 8.3 Hz, 1H, H-5), 7.90 (d,^3J = 8.3 Hz, 1H, H-4), 7.36 (m, 1H, H-8), 7.34 (m, 1H, H-7), 7.19 (td, ^3J = 7.0 Hz, ^4J = 1.2 Hz, 1H, H-6), 6.82 (d, ^4J = 2.2 Hz, 1H, H-1), 6.72 (dd, ^3J = 8.3 Hz, ^4J = 2.2 Hz, 1H, H-3), 4.81–5.43 (b.s., 1H, OH), 4.18 (t, ^3J = 7.5 Hz, 2H, H-14), 1.82 (q, ^3J = 7.5 Hz, 2H, H-15), 1.20–1.41 (m, 10H, H-16-H-20), 0.86 (t, ^3J = 6.8 Hz, 3H, H-21).
^{13}C NMR (125 MHz, $CDCl_3$) ppm δ: = 154.7 (C-2), 141.9 (C-12) 140.6 (C-13), 124.4 (C-8), 123.0 (C-10), 121.2 (C-5), 119.4 (C-6), 118.9 (C-7), 116.9 (C-11), 108.4 (C-4), 108.0 (C-3), 95.0 (C-1), 43.1 (C-14), 31.8 (C-15), 29.4, 29.2, 28.8, 27.31, 22.6 (CH_2), 14.1 (C-21).
MS (m/z, 70 eV, ESI) = 318.4 [M+Na]

2-(2-Bromoethoxy)-9-octyl-9*H*-carbazole (BSc4004)

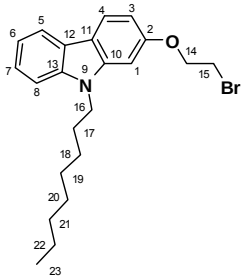

According to general procedure 2.1: BSc4029 (0.100 mg, 0.34 mmol), 1,2-dibromoethane (3.180 mg, 16.93 mmol), K_2CO_3 (0.141 g, 1.02 mmol), acetone (30 mL).
Yield: 80 mg (51%), colourless solid
HPLC: 10.8 min (98%)
^{1}H NMR (300 MHz, $CDCl_3$): δ = 8.01 (d, ^3J = 7.7 Hz, 1H, H-5), 7.97 (d, ^3J = 8.5 Hz, 1H, H-4), 7.44-7.35 (m, 2H, H-6/7), 7.24-7.19 (m, 1H, H-8), 6.90 (d, ^4J = 2.2 Hz, 1H, H-1), 6.85 (dd, ^3J = 8.5 Hz, ^4J = 2.2 Hz,1H, H-3), 4.43 (t, ^3J = 6.3 Hz, 2H, H-14), 4.23 (t, ^3J = 7.3 Hz, 2H, H-16), 3.74-3.69 (m, 2H, H-15), 1.90-1.82 (m, 2H, H-17), 1.44-1.23 (m, 10H, CH_2), 0.89 (t, ^3J = 7.0 Hz, 3H, H-23).
^{13}C NMR (75 MHz, $CDCl_3$): δ = 157.3 (C-2), 141.6 (C-13), 140.7 (C-12), 124.6 (C-7), 122.9 (C-11), 121.1 (C-5), 119.6 (C-4), 118.9 (C-6), 117.5 (C-12), 109.5 (C-8), 107.3 (C-3), 94.8 (C-1), 68.6 (C-22), 43.1 (C-14), 31.8, 29.4, 29.3, 29.2, 28.8, 27.3, 22.6 (CH_2), 14.0 (C-23).

2-(9-Octyl-9H-carbazol-2-yloxy)ethanesulfonic acid (BSc4079)

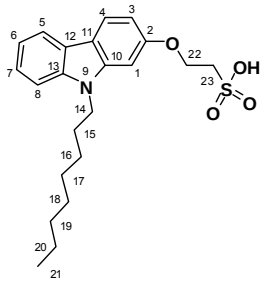

To a solution of BSc4004 (0.020 g, 0.05 mmol) in a mixture of H_2O (0.050 mL) and dioxane (0.050 mL) was added Na_2SO_3 (0.032 g, 0.25 mmol) and the resulting mixture was heated at 160°C under microwave irradiation until the reaction was completed. (TLC control) The reaction mixture was concentrated *in vacuo*, the resulting solid dissolved in $EtOH_{abs.}$ and concentrated *in vacuo* to give 0.007 g (35%)of BSc 4079 as a colourless solid.

HPLC:7.0 min (93%)

^{1}H NMR (500 MHz, MeOD) ppm δ: = 7.97-7.94 (m, 1H, H-5), 7.93 (d, ^3J = 8.5 Hz, 1H, H-4), 7.41 (d, ^3J = 8.2 Hz, 1H, H-6), 7.37-7.30 (m, 1H, H-7), 7.18-7.10 (m, 1H, H-8), 6.84 (dd, ^3J = 8.5 Hz, ^4J = 2.2 Hz, 1H, H-3), 7.04 (d, ^4J = 2.1 Hz, 1H, H-1), 4.32 (t, ^3J = 7.1 Hz, 2H, H-14), 4.53-4.47 (m, 2H, H-22), 3.38-3.33 (m, 2H, H-23), 1.89-1.81 (m, 2H, H-15), 0.86 (m, 10H), 1.32-1.24 (t, ^3J = 7.0 Hz, 3H, H-21).

^{13}C NMR (125 MHz, MeOD) ppm δ: = 143.1 (C-2), 142.0 (C-13), 125.3 (C-7), 124.3 (C-12), 121.8 (C-5), 120.2 (C-4), 119.8 (C-6) 118.2 (C-10), 109.7 (C-8), 109.1 (C-3), 100.5 (C-11), 95.2 (C-1), 65.3 (C-22), 51.9 (C-23), 43.7 (C-14), 32.9, 30.7, 30.3, 29.9, 28.2, 23.6 (CH_2), 14.4 (C-21).

MS (m/z, 70 eV, ESI) = 402 (M^-).

Diethyl 2-(9-octyl-9*H*-carbazol-2-yloxy)ethylphosphonate (BSc4006)

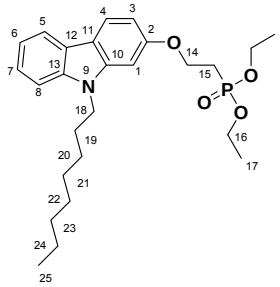

BSc4004 (0.020 g, 0.05 mmol) was dissolved in triethylphosphite (0.012 g, 0.08 mmol) and heated at 160°C under microwave irradiation until the reaction was completed. (TLC control) The reaction mixture was concentrated *in vacuo* to give 0.025 mg (99%) of BSc4006 as colourless oil.

HPLC: 9.8 min (97%)

^{1}H NMR (300 MHz, $CDCl_3$): δ = 7.99 (d, ^3J = 7.7 Hz, 1H, H-5), 7.95 (d, ^3J = 8.5 Hz, 1H, H-4), 7.42-7.33 (m, 2H, H-6/7), 7.20 (dt, ^3J = 7.9 Hz, ^4J = 1.7 Hz, 1H, H-8), 6.87 (d, ^4J = 2.1 Hz, 1H, H-1), 6.83 (d, ^3J = 8.5 Hz, ^4J = 2.1 Hz, 1H, H-3), 4.42-4.33 (m, 2H, H-18), 4.27-4.12 (m, 6H, H-14/16), 2.39 (td, ^2J = 18.7 Hz, ^3J = 7.5 Hz, 2H, H-15), 1.85 (quin., ^3J = 7.2 Hz, 2H, H-19), 1.39 (t, ^3J = 7.1 Hz, 6H, H-17), 1.31-1.24 (m, 10H, CH_2), 0.87 (t, ^3J = 6.7 Hz, 3H, H-25).

^{13}C NMR (75 MHz, $CDCl_3$): δ = 157.5 (C-2), 141.7 (C-13), 140.6 (C-12), 124.4 (C-7), 122.9 (C-10), 121.1 (C-4), 119.5 (C-)5, 118.9 (C-6), 117.2 (C-11), 108.5 (C-7), 107.5 (C-3) 94.2 (C-1), 62.6, 61.9, 43.1, 31.8, 29.4, 29.2, 28.8, 27.7, 27.3, 25.9, 22.6 (CH_2), 16.4 (C-25), 14.0 (C-17), **MS** (m/z, 70 eV, EI) = 460 (M^+), 361, 196, 165, 137.

1,1,1-Trifluoro-3-(9-octyl-9*H*-carbazol-2-yloxy)propan-2-ol (BSc4062)

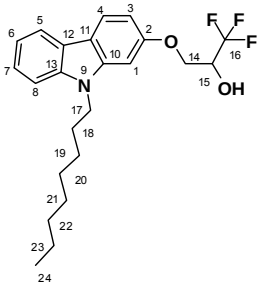

According to general procedure 2.1: BSc4029 (0.030 g, 0.10 mmol), 3-bromo-1,1,1-trifluro-2-propanol (0.032 mL, 0.30 mmol), K_2CO_3 (0.084 mg, 0.060 mmol), acetone (2 mL).
Yield: 0.028 g (69%), colourless solid
HPLC: 9.8 min (97%)
^{1}H NMR (500 MHz, $CDCl_3$) ppm δ: = 8.02 (d, ^3J = 7.7 Hz, 1H, H-5), 7.98 (d, ^3J = 8.5 Hz, 1H, H-4), 7.44-7.40 (m, 1H, H-6), 7.37 (d, ^3J = 8.1 Hz, 1H, H-8), 7.24-7.21 (m, 1H, H-7), 6.90 (d, ^4J = 2.0 Hz, 1H, H-1), 6.86 (dd, ^3J = 8.5 Hz, ^4J = 2.2 Hz, 1H, H-3), 4.45 (deca, ^4J = 3.4 Hz, 1H, H-15), 4.39 (dd, ^3J = 9.9 Hz, ^4J =3.0 Hz, 1H, H-14), 4.30 (dd, ^3J = 9.9 Hz, ^4J = 6.4 Hz, 1H, H-14), 4.23 (t, ^3J = 7.3 Hz, 2H, H-16), 3.15-2.77 (m, 1H, OH), 1.90-1.82 (m, 2H, H-17), 1.45-1.20 (m, 10H, H-18-H-22), 0.88 (t, ^3J = 6.8 Hz, 3H, H-23).
^{13}C NMR (125 MHz, $CDCl_3$) ppm δ: = 157.0 (C-2), 141.5 (C-13), 140.7 (C-12), 124.8 (C-7), 122.8 (C-10), 121.2 (C-4), 119.7 (C-5), 119.0 (C-6), 117.9 (C-11), 108.6 (C-8), 107.1 (C-3), 94.6 (C-1), 69.4 (C-15), 66.6 (C-14), 43.1 (C-16), 31.8, 29.4, 29.2, 28.8, 27.3, 22.6 (CH_2), 14.0 (C-23).
MS (m/z, 70 eV, EI) = 407 [M^+], 308, 294, 196, 167.

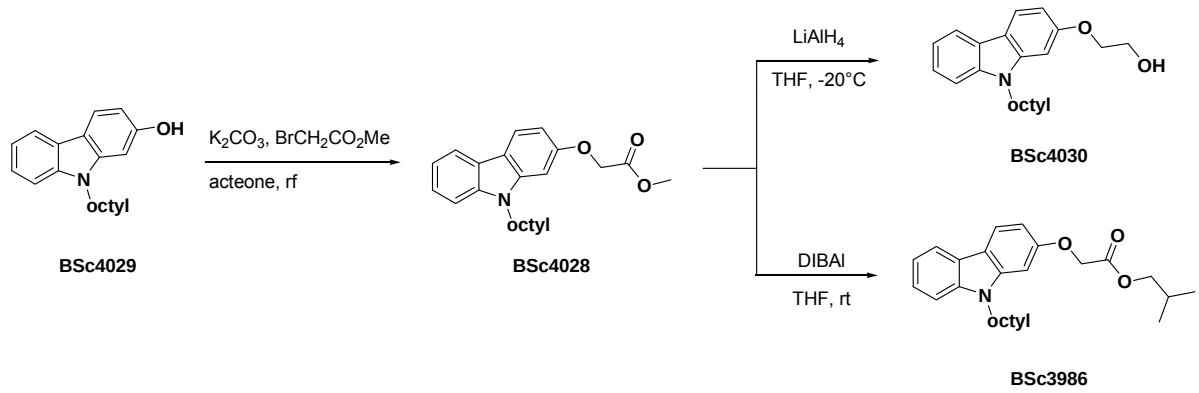

Scheme SI3: Detailed synthesis of BSc3986, BSc4028, BSc4030.

2-(9-Octyl-9*H*-carbazol-2-yloxy)ethanol (BSc4030)

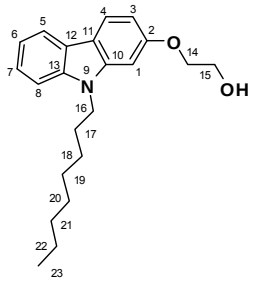

According to general procedure 2.1: BSc4028 (0.020 mg, 0.05 mmol), $LiAlH_4$ (0.012 mg (0.25 mmol), THF (2 mL).
Yield: 9 mg (53%), colourless oil
HPLC: 9.2 min (96%)
^{1}H NMR (500 MHz, $CDCl_3$) ppm δ: = 8.00 (d, ^3J = 7.7 Hz, 1H, H-5), 7.96 (d, ^3J = 8.5 Hz, 1H, H-4), 7.41-7.37 (m, 1H, H-7), 7.36 (d, ^3J = 7.7 Hz, 1H, H-6), 7.22-7.18 (m, 1H, H-8), 6.90 (d, ^4J = 2.1 Hz, 1H, H-1), 6.86 (dd, ^3J = 8.5 Hz, ^4J = 2.1 Hz, 1H, H-3), 4.25-4.20 (m, 4H, H-14/16), 4.05-4.02 (m, 2H, H-15), 1.88-1.82 (m, 2H, H-17), 0.89-0.83 (m, 10H, CH_2), 1.28 (t, ^3J = 7.0 Hz, 3H, H-23).
^{13}C NMR (125 MHz, $CDCl_3$) ppm δ: = 157. 9 (C-2), 141.7 (C-13), 140.6 (C-12), 124.5 (C-7), 122.9 (C-10), 121.1 (C-4), 119.5 (C-5), 118.9 (C-6), 117.2 (C-11), 108.4 (C-8), 107.3 (C-3), 94.2 (C-1), 69.7 (C-14), 61.7 (C-15), 43.1 (C-16), 31.9, 29.7, 29.2, 28.8, 27.3, 22.6 (CH_2), 14.1 (C-23).
MS = (m/z, 70 eV, EI): 339 (M^+), 295, 240, 196, 167.

2-(9-Octyl-9*H*-carbazol-2-yloxy)ethyl isobutyrate (BSc3986)

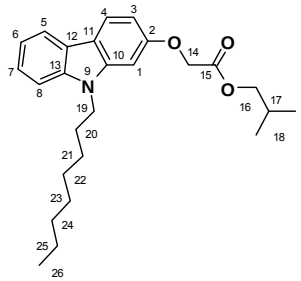

To a solution of BSc4028 (0.060 g, 0.17 mmol) in toluene (1.5 mL) was added DIBAl (0.407 mL, 0.50 mmol) After stirring for 12h 2M HCl was added to the reaction mixture until the salts had dissolved. The obtained solution was extracted with ethyl acetate (3x 10 mL). The combined organic layers were washed with brine (20 mL), dried over $MgSO_4$ and concentrated *in vacuo* to give 0.058 g (96%) of **BSc3986** as a yellow solid.
HPLC: 10.7 min (96%)
^{1}H NMR (500 MHz, $CDCl_3$) ppm δ: = 8.00 (d, ^3J = 7.6 Hz, 1H, H-5), 7.97 (d, ^3J = 8.5 Hz, 1H, H-4), 7.44-7.33 (m, 2H, H-6/7), 7.20 (dt, ^3J = 7.9 Hz, ^3J = 1.1 Hz, 1H, H-8), 6.92 (d, ^4J = 2.2 Hz, 1H, H-1), 6.85 (dd, ^3J = 8.5 Hz, ^4J = 2.2 Hz, 1H, H-3), 4.77 (s, 2H, H-14), 4.22 (t, ^3J = 7.3, Hz, 1H, H-19), 4.03 (d, ^3J = 6.7 Hz, 1H, H-16), 2.02-1.94 (m, 1H,H-17), 1.89-1.80 (m, 2H, H-20), 1.42-1.22 (m, 10H, CH_2), 0.90-0.84 (m, 6H, H-18), 0.95-0.90 (m, 3H, H-26).
^{13}C NMR (125 MHz, $CDCl_3$) ppm δ: = 169.5 (C-15), 157.2 (C-2), 141.6 (C-13), 140.7 (C-12), 124.6 (C-4), 122.8 (C-10), 121.1 (C-7), 119.6 (C-5), 118.9 (C-6), 117.8 (C-11), 108.5 (C-8), 106.9 (C-3), 94.9 (C-1), 71.3, 66.1, 43.1, 31.8, 29.4, 29.2, 28.8 (CH_2), 27.7 (C-17), 27.3 (C-16), 22.6 (C-18), 14.03 (C-26).
MS (m/z, 70 eV) = 409 (M^+), 310, 294, 254. 196, 180.

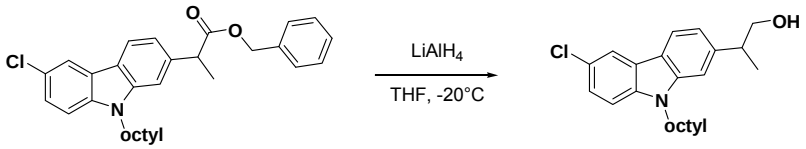

BSc3018 **BSc4021**

Scheme SI4: Detailed synthesis of BSc4021.

2-(3-Chloro-9-octyl-9H-carbazol-7-yl)propan-1-ol (BSc4021)

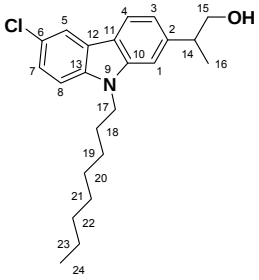

According to general procedure 2.2: BSc3018 (0.050 g, 0.10 mmol), $LiAlH_4$ (0.009 g, 0.22 mmol), THF (3 mL).
Yield: 0.038 g = 97% colourless solid
HPLC: 9.9 min (97%)
^{1}H NMR (500 MHz, $CDCl_3$) ppm δ: = 8.01-8.00 (m, 1H, H-5), 7.99 (d, ^3J = 8.0 Hz, 1H, H-4), 7.38-7.37 (m, 2H, H-7/8), 7.25 (t, ^4J = 1.9 Hz, 1H, H-1), 7.12 (dd, ^3J = 8.1 Hz, ^4J = 1.4 Hz, 1H, H-3), 4.70 (s, 1H, OH), 4.26 (t, ^3J = 7.3 Hz, 2H, H-17), 3.81 (d, ^3J = 6.8 Hz, 1H, H-15), 3.16 (sex, ^3J = 6.9 Hz, 1H, H-14), 1.88-1.81 (pen, ^3J = 7.3Hz, 1H, H-17), 1.39 (d, J = 7.0 Hz, 3H, H-16), 1.29-1.21 (m, 10H, H-19-23), 0.88 (t, ^3J = 6.7 Hz, 3H, H-24).
^{13}C NMR (125 MHz, $CDCl_3$) ppm δ: = 142.3 (C-2), 141.3 (C-10),138.9 (C-11), 125.4 (C-5), 124.4 (C-6), 123.8 (C-13), 120.8 (C-7), 120.7 (C-12), 110.8 (C-4), 118.5 (C-3), 109.6 (C-8), 107.9 (C-1), 68.9 (C-23), 43.1 (C-14), 31.7 (C-15), 19.3, 20.1, 28.9, 27.3, 22.6 (CH_2), 18.0 (C-24), 14.0 (C-21).
MS (m/z, 70 eV) = 371 (M^+), 340, 272, 240, 209.

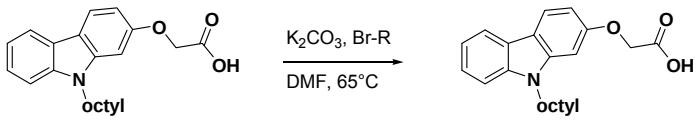

BSc3030

BSc4057: R = Et
BSc4058: R = *iPr*

Scheme SI5: Detailed synthesis of BSc4057, BSc4058.

Ethyl 2-(9-octyl-9*H*-carbazol-2-yloxy)acetate (BSc4057)

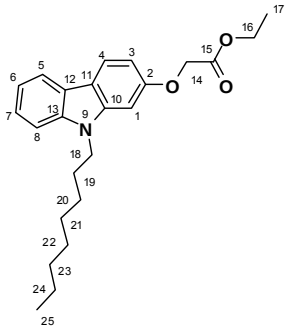

According to general procedure 2.1: BSc3030 (0.020 g, 0.06 mmol), ethylbromide (0.010 g, 0.09 mmol), K_2CO_3 (0.025 g, 0.18 mmol), DMF (2 mL).
Yield: 0.010 g (44%), colourless solid
HPLC: 10.2 min (99%)
^{1}H NMR (500 MHz, $CDCl_3$) ppm δ: = 8.00 (d, ^3J = 7.7 Hz, 1H, H-8), 7.97 (d, ^3J = 8.5 Hz, 1H, H-4), 7.42-7.37 (m, 1H, H-6), 7.35 (d, ^3J = 8.0 Hz, 1H, H-5), 7.22-7.17 (m, 1H, H-7), 6.92 (d, ^4J = 2.1 Hz, 1H, H-1), 6.84 (dd, ^3J = 8.5 Hz, ^4J =2.2 Hz, 1H, H-3), 4.75 (s, 2H, H-14), 4.31 (q, ^3J = 7.1 Hz, 2H, H-18), 4.22 (t, ^3J = 7.3 Hz, 2H, H-16), 1.88-1.80 (m, 2H, H-19), 1.32 (m, 13H, H-17/H-20-24), 0.87 (t, ^3J = 6.9 Hz, 3H, H-25).
^{13}C NMR (125 MHz, $CDCl_3$) ppm δ: = 169.1 (C-15), 157.1 (C-2), 141.6 (C-13), 140.8 (C-12) 124.6 (C-4), 122.8 (C-10), 121.1 (C-7), 119.6 (C-5), 118.9 (C-6), 117.8 (C-11), 108.5 (C-8), 106.9 (C-3), 95.0 (C-1), 66.3 (C-14), 61.4 (C-16), 43.2 (C-18), 31.8, 29.4, 29.2, 28.8, 27.3, 22.6 (CH_2), 14.2 (C-17), 14.1 (C-25).
MS (m/z, 70 eV, EI) = 381 (M^+), 352, 282, 254, 196.

***Iso*propyl 2-(9-octyl-9*H*-carbazol-2-yloxy)acetate (BSc4058)**

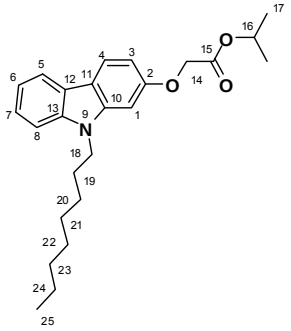

According to general procedure 2.1: BSc3030 (0.028 g, 0.08 mmol), *iso*propylbromide (0.015 g, 0.12 mmol), K_2CO_3 (0.033 g, 0.24 mmol), DMF (2 mL).
Yield: 0.024 g (76%), colourless solid
HPLC: 10.4 min (100%)
^{1}H NMR (500 MHz, $CDCl_3$) ppm δ: = 8.00 (d, ^3J = 7.7 Hz, 1H, H-8), 7.97 (d, ^3J = 8.5 Hz, 1H, H-4), 7.44-7.32 (m, 1H, H-7), 7.36 (d, ^3J = 8.0 Hz, 1H, H-6), 7.19-7.21 (m, 1H, H-5), 6.92 (d, ^4J = 2.1 Hz, 1H, H-1), 6.84 (dd, ^3J = 8.5 Hz, ^4J = 2.2 Hz, 1H, H-3), 5.18 (hept, ^3J = 6.2 Hz, 1H, H-16), 4.72 (s, 2H, H-14) 4.22 (t, ^3J = 7.3 Hz, 2H, H-18), 1.90-1.79 (m, 2H, H-19), 1.45-1.19 (m, 16H, H-17/H-20-24), 0.87 (t, ^3J = 6. 9 Hz, 3H, H-25).
^{13}C NMR (125 MHz, $CDCl_3$) ppm δ: = 168.7 (C-15), 157.2 (C-2) 141.6 (C-13), 140.7 (C-12) 124.6 (C-4), 122.8 (C-10), 121.0 (C-7), 119.6 (C-5), 118.9 (C-6), 117.7 (C-11) 108.46 (C-8), 107.0 (C-3), 94.9 (C-1), 69.1 (C-16), 66.4 (C-14), 43.1 (C-18), 31.8, 29.4, 29.2, 28.8, 27.3, 22.6 (CH_2), 21.8 (C-17), 14.0 (C-25).
MS (m/z, 70 eV, EI) = 395 (M^+), 381,296, 282, 254.

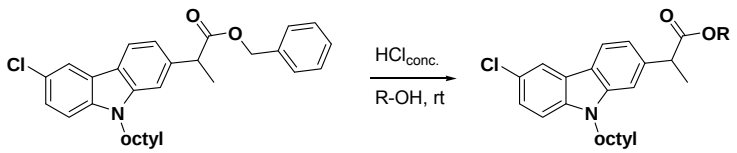

BSc3018

BSc4051: R = Me
BSc4052: R = Et

Scheme SI6: Detailed synthesis of BSc4051, BSc4052.

Methyl-2-(6-chloro-9-octyl-carbazol-2-yl)propanoate (BSc4051)

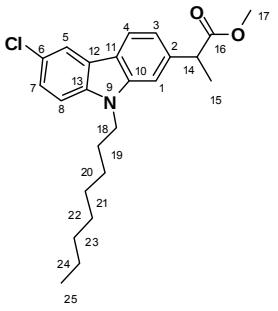

To a solution of BSc3018 (0.025 g, 0.057 mmol) in methanol (2 mL) was added catalytic amount of $HCl_{conc.}$. After stirring for 12h at rt the reaction was neutralized with 1M NaOH and extracted with CH_2Cl_2 (3x 10 mL). The combined organic layers were dried over $MgSO_4$, concentrated *in vacuo* to give 0.015 g (72%) of **BSc4051** as a colourless solid.
HPLC: 10.8 min (92%)
^{1}H NMR (500MHz, $CDCl_3$) ppm δ: = 7.93 (d, ^4J = 1.8 Hz, 1H, H-5), 7.89 (d, ^3J = 7.9 Hz, 1H, H-4), 7.31 (dd, ^4J = 2.0 Hz, ^3J = 6.6 Hz, 1H, H-7), 7.23-7.10 (m, 2H H-3/8), 7.09 (d, ^4J = 1.4 Hz, 1H, H-1), 4.18 (t, ^3J = 7.3 Hz, 2H, H-18), 3.84 (q, ^3J = 7.2 Hz, 1H, H-14), 3.60 (s, 3H, H-17), 1.75 (m, 2H, H-19), 1.53 (d, ^3J = 7.2 Hz, 3H, H-15), 1.29-1.16 (m, 10H, CH_2), 0.79 (t, ^3J = 6.8 Hz, 3H, H-25).
^{13}C NMR (500MHz, $CDCl_3$) ppm δ: = 175.6 (C-16), 145.4 (C-13), 141.5 (C-12), 139.5 (C-10), 126.0 (C-7), 124.7 (C-6), 124.1 (C-10), 121.5 (C-11), 121.1 (C-5), 120.3 (C-4), 119.3 (C-3), 110.0 (C-8), 108.1 (C-1), 52.5 (C-17), 46.4 (C-14), 43.6 (C-18), 32.1, 29.7, 29.5, 29.3, 27.7, 23.0 (CH_2), 19.5 (C-15), 14.4 (C-25).
MS (EI): m/z (%) = 401 (M^+), 340, 300, 240.
IR (cm^{-1}): ν = 2928 (m), 2857 (s), 1723 (w), 1460 (w), 1266 (s), 895 (s), 746 (m).

Ethyl-2-(6-chloro-9-octyl-carbazol-2-yl)propanoate (BSc4052)

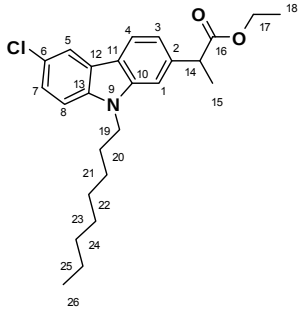

To a solution of BSc3018 (0.025 g, 0.057 mmol) in ethanol (2 mL) was added a catalytic amount of $HCl_{conc.}$. After stirring for 12h at rt the reaction was neutralized with 1M NaOH and extracted with CH_2Cl_2 (3x 10 mL). The combined organic layers were dried over $MgSO_4$ and concentrated *in vacuo* to give 0.011 g (51%) of **BSc4052** as a colourless solid.
HPLC: 11.0 min (91%)

^{1}H NMR (500MHz, $CDCl_3$) ppm δ: = 8.01 (d, ^4J = 2.0 Hz, 1H, H-5), 7.97 (d, ^3J = 8.0 Hz, 1H, H-4), 7.38 (dd, ^3J = 6.8 Hz, ^4J = 1.8 Hz, 1H, H-7), 7.33-7.40 (m, 1H, H-1), 7.29 (d, ^3J = 8.7 Hz, 1H, H-8), 7.18 (dd, J = ^{3}8.1 Hz, ^4J = 1.4 Hz, 1H, H-3), 4.26 (t, ^3J = 7.3 Hz, 2H, H-17), 4.21-4.08 (m, 2H, H-19), 3.90 (q, ^3J = 7.1 Hz, 1H, H-14), 1.88-1.80 (m, 2H, H-20), 1.62 (d, ^3J = 7.2 Hz, 3H, H-15), 1.38-1.24 (m, 10H, CH_2), 1.21 (t, ^3J = 7.0 Hz, 3H, H-18) 0.79 (t, ^3J = 7.0 Hz, 3H, H-26).
^{13}C NMR (500MHz, $CDCl_3$) ppm δ: = 175.1 (C-16), 141.5 (C-13), 140.0 (C-12), 139.5 (C-2), 125.9 (C-7), 124.7 (C-6), 124.2 (C-10), 121.4 (C-11), 121.0 (C-5), 120.3 (C-4), 119.3 (C-3), 110.0 (C-8), 108.1 (C-1), 61.2 (C-17), 46.6 (C-14), 43.6 (C-19), 32.2, 30.1, 29.8, 29.5, 29.3, 23.0 (CH_2), 19.5 (C-15), 14.5 (C-18), 14.4 (C-26).
MS (EI): m/z (%) = 413 (M^+), 340, 314, 240, 177.
IR (cm^{-1}): ν = 2928 (s), 1723 (m), 1462 (m), 1274 (s), 895 (s), 750 (s).

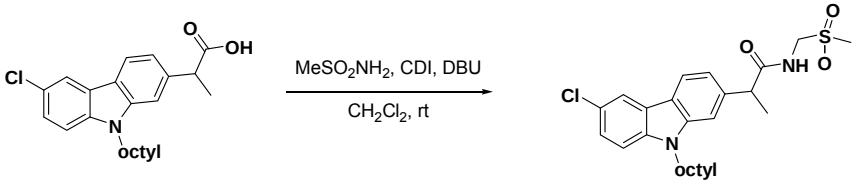

BSc3030 **BSc4056**

Scheme SI7: Detailed synthesis of Bsc4056.

2-(6-Chloro-9-octyl-9H-carbazol-2-yl)-*N*-(methylsulfonyl)propanamide (BSc4056)

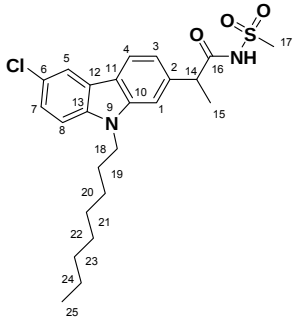

To a solution of BSc3030 (0.035 g, 0.09 mmol) in CH_2Cl_2 (2 mL) was added CDI (0.015 g, 0.09 mmol). After 20 min stirring at rt was added DBU (0.017 g, 0.11 mmol) and methylsulfonamide. After additional 2h stirring at rt was added Amberlyst$_{acidic}$, stirred for 10 min and the mixture was filtered. The filtrate was diluted with water, extracted with CH_2Cl_2, dried over $MgSO_4$, concentrated *in vacuo* and purified by silica gel chromatography (CH_2Cl_2: acetone; 5: 1) to give 0.038 g (83%) of **BSc4056** as a colourless solid.
HPLC: 9.450 min (94%)
^{1}H NMR (500 MHz, Acetone) ppmδ: = 8.11–7.98 (m, 2H, H-1, 8), 7.56-7.40 (m, 2H, H-4, 5), 7.33 (dd, 1H, H-3), 7.12 (dd, 1H, H-7), 4.33 (t, 2H, ^3J = 7.2 Hz, H-18), 3.99 (d, 1H, ^3J = 7.0 Hz, H-14), 3.14 (s, 3H, H-17), 1.46 (d, 3H, ,^3J = 7.0 Hz, H-15), 1.88-1.66 (m, 3H, H-19), 1.35-1.02 (m, 10H, CH_2), 0.83-0.65 (m, 3H, H-25).
^{13}C NMR (125 MHz, Acetone) ppmδ: = 171.8 (C-16), 140.3 (C-10), 138.3 (C-13), 125.2 (C-1), 123.8 (C-11), 122.4 (C-12), 121.0 (C-6), 120.8 (C-8), 119.2 (C-3), 117.4 (C-2), 108.9 (C-4), 106.9 (C-5), 47.3 (C-17), 46.4 (C-14), 42.3 (C-18), 30.7 (C-15), 28.3, 28.1, 27.9), 26.3, 21.6, 17.3 (CH_2), 13.1 (C-25).
MS (m/z, 70 eV, EI) = 462 [M^+].
IR (KBr, cm^{-1}): ν = 3460 (NH), 1687 (C=O), 1468 (S=O).

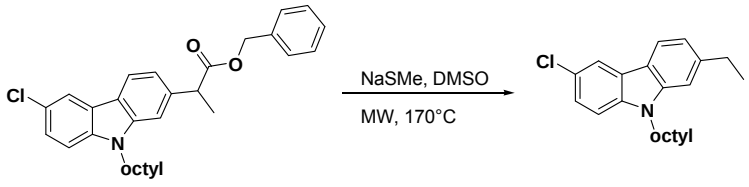

BSc3018 **BSc4053**

Scheme SI8: Detailed synthesis of BSc4053.

6-Chloro-2-ethyl-9-octyl-9*H*-carbazole (BSc4053)

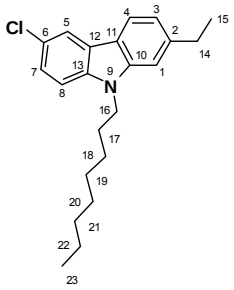

To a solution of BSc3018 (0.005 mg, 0.01 mmol) in DMSO (0.200 mL) was added MeSNa (0.001 g, 0.02 mmol) and the mixture was heated at 170°C for 60 min under microwave irradiation. The reaction mixture was quenched with H_2O (5 mL), extracted with CH_2Cl_2 (3x 5 mL). The combined organic layers were washed with brine, dried over $MgSO_4$, concentrated *in vacuo* and purified by silica gel chromatography (gradient cyclohexane to CH_2Cl_2) to give 0.003 g (89%) of **BSc4053** as a colourless solid.

HPLC: 11.3 min (99%)

^{1}H NMR (500 MHz, $CDCl_3$) ppm δ: = 7.92-7.86 (m, 2H, H-1/8), 7.30-7.00 (m, 4H, H-3/4/5/7), 4.16 (t, 2H, H-16), 2.77 (q, 2H, H-14), 1.77-1.74 (m, 2H, H-17), 1.55-1.53 (m, 3H, H-15), 1.29-1.17 (m, 10H, H-18/19/20/21/22), 0.80 (t, 3H, H-23).

^{13}C NMR (125 MHz, $CDCl_3$) ppm δ: = 124.0 (C-7), 119.3 (C-8), 118.7 (C-3), 118.6 (C-1), 108.4 (C-4), 106.8 (C-5), 42.1 (C-16), 30.8 (C-14), 28.7 (C-15), 28.3 (C-17), 28.1 (C-18), 27.9 (C-19), 26.3 (C-20), 21.6 (C-21), 15.2 (C-22), 13.0 (C-23).

MS (m/z, 70 eV, EI) = 341 $[M]^+$.

IR (cm^{-1}): ϒ = 1464 (C=O).

3.5 Untersuchungen zur Identifizierung der Bindungsstelle von NSAID-abgeleiteten γ-Sekretase Modulatoren

Der Inhalt dieses Kapitels wurde zur Veröffentlichung eingereicht:
Nicole Höttecke, Matthias Gralle, Maria Angela C. Dani, Karlheinz Baumann, Fred Wouters, Christian Czech, Boris Schmidt *Nature Chem. Biol.*, eingereicht. "The Modulation of Aβ production involves dimerization of APP."

Weitere Untersuchungen bezüglich der Bindungsstelle unserer γ-Sekretase Modulatoren wurden vorgenommen. Hierbei wurde BSc3040, unser potentester γ-Sekretase Modulator**,** verwendet ($IC_{50}(A\beta_{42})$ = 3.0 μM. Die beschriebene dreistufige Synthese (Route 1) konnte durch eine Einstufige (Route 2) ersetzt werden. Hierfür wurde das Carprofen mit einem Überschuss der Base NaH in ein Dianion überführt. Die höhere Nukleophilie des Stickstoff-Anions im Vergleich zu dem Sauerstoff-Anion erlaubt es selektiv nur den Stickstoff zu substituieren. Diese Synthese konnte mit 80%iger Ausbeute und >99%iger Reinheit durchgeführt werden, weitere Aufreinigungsschritte waren nicht nötig.

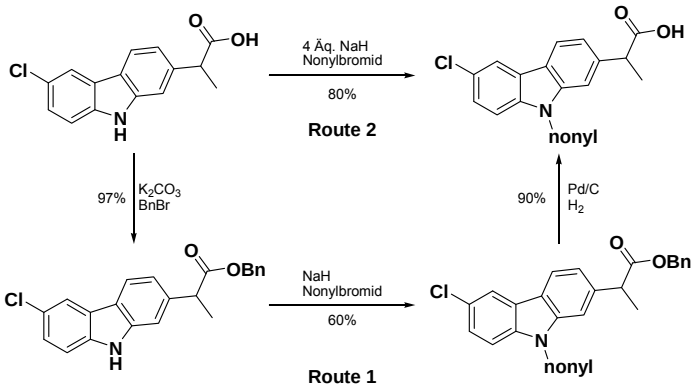

Abb. 23: Entwicklung einer Eintopf Synthese für BSc3040.

Da APPwt kein stabiles Dimer bildet, das sich über Western Blot-Analyse nachweisen lässt, wurde eine K624C-APP Mutante von unseren Kooperationspartnern bei Hoffmann-LaRoche generiert. Diese Mutante kann über das eingeführte Cystein eine kovalente Disulfidbrücke ausbilden und dadurch quantitativ dimerisieren und durch Western Blot detektiert werden. Um sicher zu stellen, dass die Dimerisierung über die Disulfidbrücke stattfindet, wurde als Kontrolle reduktives DTT (Dithiothreitol) zugeben, welches die entstandene Disulfidbrücke wieder zu den zwei Thiolen des Cysteins reduzierte. Durch Zugabe von BSc3040 oder einem γ-Sekretase-Modulator von Merck (GSM-1) konnte jedoch keine Reduktion des

Dimerisierungsgrades der K624C-Mutante festgestellt werden. Weitere Untersuchungen wurden in Kooperation mit der Gruppe von Fred Wouters in Göttingen durchgeführt. In dem etablierten Dimerisationsassay wurde der Dimerisierungsgrad des APP-Dimers untersucht. Es konnte nach Zugabe von 10 μM BSc3040 (der 3-fachen IC_{50}-Konzentration für $A\beta_{42}$) eine Verringerung des APPwt Dimerisierungsgrades um 40% detektiert werden. Bei der K624C-Mutante wurde keine Verringerung des Dimerisierungsgrades festgestellt. Dieses Resultat stimmt auch mit der zuvor durchgeführten Western Blot-Analyse überein**.** Wir spekulieren, dass die kovalente Disulfidbrücke zu stark ist, als dass BSc3040 diese brechen könnte. BSc3040 scheint als ein Dimerisierungsinhibitor durch Interaktion mit dem Monomer zu agieren, wobei der lipophile Anker und die Carbonsäurefunktion notwendig für die modulatorische Aktivität sind.

The Modulation of Aβ production involves dimerization of APP

Nicole Höttecke[a], Matthias Gralle[b], Maria Angela C. Dani[c], Karlheinz Baumann[d], Fred Wouters[c], Christian, Czech[d], Boris Schmidt.[a]*

[a]Clemens Schöpf-Institute of Chemistry and Biochemistry, Technische Universität Darmstadt, Petersenstr. 22, D-64287 Darmstadt, Germany.

[b]Dept. Evolutionary Genetics, Max Planck Institute for Evolutionary Anthropology, Deutscher Platz 6, D-04103 Leipzig, Germany.

[c]Laboratory for Molecular and Cellular Systems, Dept. of Neuro- and Sensory Physiology Centre II, Physiology and Pathophysiology, University of Göttingen, Humboldtallee 23, D-37073 Göttingen, Germany.

[d]F. Hoffmann-La Roche Ltd., Pharmaceuticals Division, Preclinical Research CNS, Bldg. 70/345, CH-4070 Basel, Switzerland.

[*] Prof. Dr. Boris Schmidt,
Clemens Schöpf-Institute of Chemistry and Biochemistry,
Technische Universität Darmstadt,
Petersenstr. 22, D-64287 Darmstadt, Germany.
Tel: (+49) 6151-163075
Fax: (+49) 6151-163278
E-mail: schmidt_boris@t-online.de

Introduction:

γ-Secretase is a promising target for the treatment of Alzheimer's disease (AD) because this intramembrane aspartylprotease catalyzes the crucial step in the generation of amyloid-β-peptide (Aβ) of various lengths (38, 40 or 42 amino acids). Aβ aggregates, so called plaques, are one of the pathological characteristics of AD. These extracellular plaques contain $A\beta_{40}$ and $A\beta_{42}$, which are the most pathogenic Aβ agents due to their aggregation properties. The shorter $A\beta_{38}$ species is not associated with AD pathology. Several γ-secretase inhibitors (GSI) were reported, but the majority of them inhibits the cleavage of other γ-secretase substrates like Notch, which is crucial for cellular differentiation. A subset of NSAIDs (non-steroidal anti-inflammatory drugs) was reported to alter the cleavage preferences of the γ-secretase to favour the non-toxic species $A\beta_{38}$ and reduce $A\beta_{42}$ levels.[1] Compounds with such properties are called γ-secretase modulators (GSM) and are subjects of clinical investigation. Narlawar *et al.* reported the potent γ-secretase modulator BSc3040, a derivative of the NSAID Carprofen, which decreases $A\beta_{42}$ with an IC_{50} = 3.0 μM in H4-cells while increasing $A\beta_{38}$ and leaving $A\beta_{40}$ levels unchanged, without significant effects on cyclooxygenase-1 and -2.[2] (Figure 1)

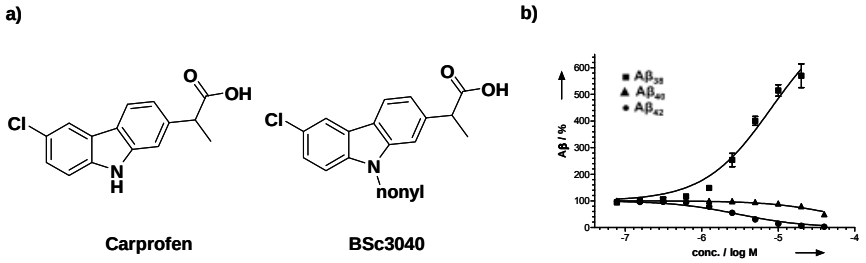

Figure 1: a) potent GSM based on the NSAID Carprofen, b) dose-response-curve of BSc3040 in APP overexpressing H4-cells.

Recent investigations by Kukar *et al* on the binding site of NSAID-derived GSMs utilized a reconstituted γ-secretase assay.[3] A crosslink experiment with biotinylated photoprobes of *R*-flurbiprofen labelled amyloid precursor protein (APP), APP-C-terminal fragment and Aβ at the Aβ region 29-36 (= 625-632 APP695) indicating a binding site on APP. This region contains a GxxxG motif and was identified as a hinge region responsible for APP dimerization, which may influence the orientation of APP and ultimately the Aβ secretion.[4-5] This GxxxG motif is located within the membrane at the amino acids 625-629. $Lysine^{624}$ is located directly next to this motif and may be targeted by GSMs equipped with a carboxylic

acid. This carboxylic acid may interact with the lysine^{624} by a either hydrogen bond or salt formation. The equally essential lipophilic chain of BSc3040 is supposed to act as a membrane anchor, which may be necessary to increase the effective concentration of the inhibitor at the membrane and thus reduce the fraction of the dimerized form of APP.[2,6] (Figure 2)

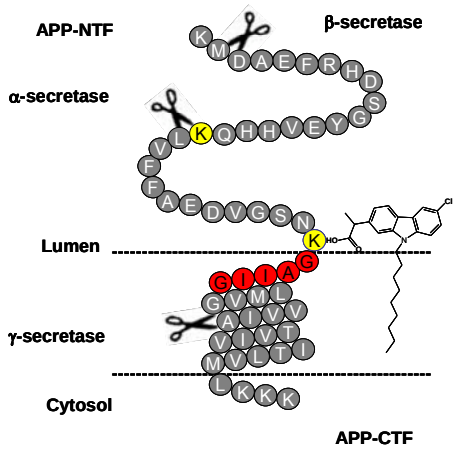

Figure 2: schematic: suggested mode of action of BSc3040. The carboxylic acid interacts with lysine^{624} while the lipophilic anchor localizes the inhibitor at the correct position to inhibit APP dimerization within the lipid bilayer.

The precise mechanism of substrate recognition and cleavage by γ-secretase is still subject to debate, the 1:1:1:1 stoichiometry of the active γ-secretase complex was recently established and there are several lines of evidence for a dimeric APP as one substrate among others.[7] Munter *et al.* reported that the γ-secretase cleavage of APP is intimately linked to the dimerization strength of the transmembrane substrate.[4]

However, this APP dimer hypothesis stands in contrast to the other substrates of γ-secretase, which are cleaved as monomers and thus stipulate high flexibility in this recognition/cleavage process. This issue is complicated further by the identification of different γ-secretase complexes varying in their subcomponent assembly.[8] The structural organisation of this complex responds to GSM treatment, which can take place through allosteric binding to γ-secretase or binding to the substrate/γ-secretase complex. Berezoska *et al.* used GFP/RFP labelled PS1 mutants to monitor this GSM induced structural reorganisation of the γ-secretase complex. The analyzes of fluorescence lifetime imaging (FLIM) and fluorescence resonance energy transfer (FRET) studies support a two state model of γ-secretase involving an open and a closed state of PS1.[9]

Results:

Investigation of APP dimerization by Western blot analysis

Dimerization of wild-type APP is very difficult to detect by SDS-PAGE and Western-blotting. In order to stabilize the APP dimers and to detect them by SDS-PAGE, we generated a mutated APP, replacing lysine at position 624 by cysteine. This APP K624C mutant forms stable dimers which can be detected by SDS-PAGE and subsequent Western-blotting. APP dimers appear as an additional band running at approximately double size of the APP monomer in the lysate of transfected cells. (Fig 3) To confirm the formation of the K624C-dimer, the mutant was treated with the reductive agent DTT, reducing the disulfide bridge formed by the two cysteines.[10] This dimer formation does not seem to be cell type specific. It can be detected readily in the lysate of cells of neuronal origin (SY5Y, N2a) or HEK293 cells (Figure 3). Interestingly, the analysis of APP processing shows that the extracellular portion of both wild-type and K624C mutant APP is secreted into the conditioned medium (Figure 3c), while Aβ secretion is strongly reduced in the mutant (Figure 3d). This reduction of Aβ was confirmed using ELISA measurements of the transfected cells (data not shown).

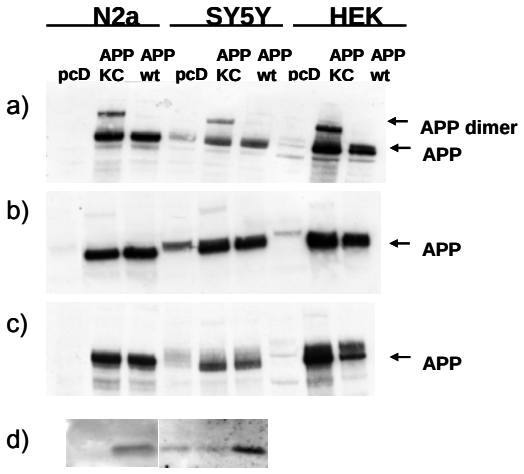

Figure 3: Western Blot analysis of the dimerization for APP-K624C mutant and APPwt:
a) cell lysate **b)** cell lysate with DDT **c)** conditioned medium with DDT **d)** Aβ secretion. APP-KC-mutant forms a stable dimer based on the disulfide bridges in N2a, SY5Y and HEK cells. Aβ secretion was strongly reduced.

APP dimerization state measurements by GFP-labelled APP

Further investigations were required to confirm the direct effect of the inhibitor on the substrate APP, preferentially a cellular assay. Therefore BSc3040 was tested in the dimerization assay established by Gralle *et al.* based on a GFP-labelled APP construct.[11]

We investigated the oligomerization state of APP in living B103 neuroblastoma cells by measuring Förster resonance energy transfer using fluorescence lifetime imaging microscopy.[11] The association of a donor fluorophore in APP-mGFP with an acceptor fluorophore in APP-mCherry is reflected in the characteristic reduction in the excited state lifetime of mGFP. In the presence of BSc3040, we observed that energy transfer from APP-mGFP to APP-mCherry was significantly reduced by 40% (Figure 4). These data show that a compound with clear γ-secretase modulatory activity influences APP dimerization at the concentrations required for all GSM like activity.

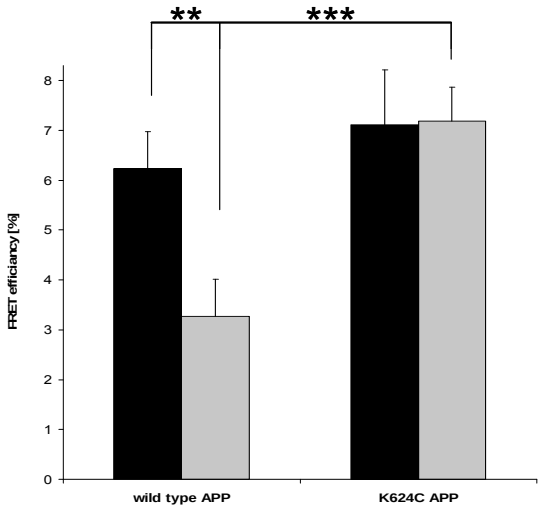

Figure 4: Action of BSc3040 APP dimers. 10 μM BSc3040 for 1h at 37°C decreases FRET efficiency in APPwt dimers by 40%. BSc3040 has no effect on FRET efficiency in covalently linked dimers of K624C mutant APP. (black control; grey: BSc3040) **: $p < 0.01$, ***: $p < 0.001$. n=14-25 cells per condition, 4 wells in transfections done on two different days.

Discussion:

A 40% reduction of cellular APPwt dimerization was observed for BSc3040 at a concentration of 10 μM, the 3-fold IC_{50} for $A\beta_{42}$ secretion. This reduction indicates either the complete dissociation of a subpopulation of APP dimers, or a conformational change increasing the distance between the *C*-termini of the APP molecules within the dimer. The specificity of this effect was tested using the K624C mutant of APP, which has been shown to form disulfide-bridged dimers and to dimerize quantitatively.[10-11] Under the same conditions as for wild-type APP, BSc3040 had no effect on the energy transfer within K624C-APP dimers. This finding strongly suggests a disruption of non-covalent APP dimers by BSc3040. A potential binding site for NSAID derived γ-secretase modulators was identified by Kukar et al. in the transmembrane domains of the APP monomer involving a

GxxxG sequence.[3] The K624C mutant seems not to be a suitable dimerization model, as it does not lead to a measurable secretion of Aβ, however contradictory observations were described recently.[5,10] The inactivity of BSc3040 on this mutant can be explained by two non-exclusive hypotheses: either the covalent cystine bridge in the mutant is so strong that it cannot be disrupted by BSc3040, or the modulator requires a salt bridge like interaction with lysine^{624} and therefore cannot bind to cysteine nor cystine. In either case, the clear difference in the effects of BSc3040 on wild-type and K624C mutant APP supports the interaction of the modulator with the substrate, which stands in line with the observations by Munter, Kukar and Eggert et al.[3-4,12] The cystine-linked dimer of the K624C mutant is suspected to interfere with APP metabolism independent of APP dimerization, this impairs the control value of this mutant. However, a regulatable dimerization of APP was established by Eggert *et al*. utilizing APP fused to a FKBP domain.[12] The dimerization of this chimera was induced by a FKBP binding membrane permeating drug. The controlled dimerization reduced Aβ secretion in N2a cells. In accordance with our findings, the induced dimers resist modulation of γ-secretase activity and some APP cleavage occurs independent of APP dimerization.

Thus the observed γ-secretase modulatory effects of BSc3040 may be explained by the inhibition of cellular APP dimerization in cells.

Supporting information:

Methods:

Aβ liquid phase electrochemiluminescence (LPECL) assay

We used the LPECL assay to measure Aβ isoforms to evaluate the compounds for their potency in modulating γ-secretase activity. APP-overexpressing cell lines were generated by stably transfecting human neuroglioma H4-cells obtained from ATCC (accession no. CRL-1573 or HTB-148) with human APP695 in vector pcDNA3.1.[2]

Transfection of cells

Cells were plated in 3x6 well plates and transfected with SatisFection according to manufacturer's instructions. After 48h, conditioned medium was collected and cells were lysed for 20 min at 0°C in lysis buffer of eukaryotic cells (10 mM Tris, pH 7.5, 1 mM EDTA, 20 mM glycerolphosphate, 50 mM NaF, 1 mM Na_3VO_4, 1 µM ocadaic acid, 0.5% NP-40, 0.5% TritonX-100) and supplemented with protease inhibitor. After centrifugation for 10min at 13000rpm, supernatants were collected and divided in reduced (DTT added) and not reduced samples.

SDS electrophoresis and immunoblotting

Equal protein quantities (15 µg) were separated on a 4-12% Criteriom XT Bis Tris Gel "BioRad no: 345-0125" for each samples reduced and not reduced and then transferred to a Hybond-C Extra nitrocellulose membrane. To detect APP and Aβ, membranes were incubated with the anti Aβ monoclonal antibody WO-2, (The Genetic Company, Zürich, Switzerland) at 4°C over night. Binding of the primary antibody was detected using subsequent incubation with anti mouse IgG, Horseradish peroxidase and ECL detection system (Amersham) and exposure on film for 5 min.

Dimerization assay

B103 neuroblastoma cells (a kind gift from David Schubert, Salk Institute, La Jolla, CA) were plated at 10^5 cells/well in DMEM+10% fetal calf serum on poly-L-ornithine-coated glass coverslips in 24-well plates (Corning Life Sciences, Lowell, MA) and were transfected with 0.3 µg wtAPP-mGFP and 0.3 µg wtAPP-mCherry or with 0.3 µg K624C-mGFP and 0.3 µg K624C-APP-mCherry and 0.6 µl magnetic nanoparticle MaTra beads per well on a 24-magnet plate (beads and magnet from IBA GmbH, Göttingen, Germany).[11] The medium was changed 1 h after transfection, and expression was allowed to proceed for a further

18-24 h. 1 h before measurements, 10 μM of BSc3040 was added to the medium. Coverslips were washed by a short immersion in PBS and mounted on a drop of imaging buffer (135 mM NaCl, 10 mM KCl, 0.4 mM $MgCl_2$, 2 mM $CaCl_2$, 10 mM HEPES, 0.1 % BSA) using a homemade silicone rubber gasket on a glass slide. Fluorescence lifetime imaging measurements were performed on a frequency domain setup using an Ar laser (Innova 304C, Coherent, Dieburg, Germany) at 488 nm.[13] The presence of APP-mCherry was confirmed using HBO lamp excitation. The filter cube from AHF (Tübingen, Germany) contained a dichroic LP495 and emission filter BP 515/30. The optimal threshold was set automatically (opthr module for MatLab by F. T. Marti, www.oersted.dtu.dk/personal/jw/jwpublic-/matlab/contrib/opthr.m). All further operations were performed with custom-written routines (Alessandro Esposito and Matthias Gralle) in MatLab (MathWorks, Natick, MT). The lifetime and total intensity values of each pixel in the threshold mask were stored, and the lifetimes for all pixels in the appropriate masks of all cells were joined for each experimental condition and imported into IgorPro (WaveMetrics, Lake Oswego, Oregon) for display.

Experimental data:

General remarks

Thin-layer chromatography (TLC) was carried out using aluminium sheets precoated with silica gel 60 F254 (0.2 mm; E. Merck). Chromatographic spots were visualized by UV and/or spraying with a methanolic solution of vanillin/H_2SO_4 or aq. $KMnO_4$ solution followed by heating. Flash column chromatography was carried out using Merck silica gel 60 (0.063-0.2 mm). Melting Points were determined on a Mettler FP 51 melting point apparatus and are uncorrected. The ^1H and ^{13}C spectra were recorded on a Bruker AC 300 (300 MHz) and AC 500 spectrometer (500 MHz). Chemical shifts are reported as % values (ppm) and adjusted at the central line of the deuterated solvent (MeOD, $CDCl_3$). Mass spectrometry was performed on a Bruker-Franzen Esquire LC mass spectrometer (ESI) and a double focused MAT 95 (EI).

IR-spectroscopy was detected by an FT-IR spectrometer (Perkin Elmer Paragon 1000 PC) using KBr carrier material. Elementary analysis was determined using a Perkin Elmer CHN 240B. HPLC analysis was carried out using: an Agilent 1100 with a reversed phase column (Zorbax Eclipse XDB-C8; 4.6*150 mm) and a 254 nm detector. The eluent is composed of H_2O (1% TFA) (A) and acetonitrile (B) with a gradient: 30 to 90% B within 12 min. All reagents and solvents (THF, DMF, CH_2Cl_2, ethyl acetate, MeOH) were purchased at ABCR,

Acros and Alfa Aesar, TCI, Sigma Aldrich and VWR. Methanol abs. was additionally dried over magnesium.

Experimental data

2-(6-chloro-9-nonyl-9*H*-carbazol-2-yl)propanoic acid (BSc3040)

Carprofen was isolated from Pfizer's Rimadyl® (100 mg per tablet). 15 tablets were powdered and suspended with 2N HCl (75 mL), extracted three times with ethyl acetate (50 mL). The combined organic layers were dried over $MgSO_4$ and concentrated *in vacuo* to give 1.43 g (95%) of Carprofen as a white solid.

To a suspension of NaH (0.37 g, 9.13 mmol) in THF (15 mL) was added Carprofen (0.50 g, 1.83 mmol) at a temperature of 0°C. After 30 min stirring nonylbromide (1.89 g, 9.13 mmol) was added. The reaction mixture was allowed to warm up to rt. After 12h the reaction mixture was quenched drop wise with H_2O until gas formation stops and was extracted once with CH_2Cl_2. The precipitate was filtered of, dissolved in water and acidified to pH 5 with 2M HCl. The aqueous solution was extracted twice with CH_2Cl_2, dried over $MgSO_4$ and concentrated *in vacuo* to give 0.58 g (80%) of **BSc3040** as a colourless solid. Mp: 103.4°C

HPLC: 9.977 min (98%)

^{1}H NMR (500 MHz, $CDCl_3$) ppm δ: = 7.99 (d, ^4J = 2.1, Hz, 1H, H-1), 7.96 (d, ^3J = 8.1, Hz, 1H, H-5), 7.38 (dd, ^3J = 8.6 Hz, ^4J = 2.1 Hz, 1H, H-7), 7.32 (d, ^4J = 2.1 Hz, 1H, H-8), 7.27 (d, ^3J = 8.6 Hz, 1H, H-4), 7.19 (dd, ^3J = 8.1 Hz, ^4J = 1.3 Hz, 1H, H-7), 4.22 (t, ^3J = 7.3, Hz, 2H, H-17), 3.93 (q, ^3J = 7.1 Hz, 1H, H-2), 1.82 (quin., ^3J = 7.3 Hz, 2H, H-18), 1.63 (d, ^3J = 7.2 Hz, 3H, H-16), 1.38-1.19 (m, 12H, H-19/20/21/22/23/24), 0.87 (t, ^3J = 7.1 Hz, 3H;H-25). **^{13}C NMR** (125 MHz, $CDCl_3$) ppm δ: = 180.4 (C-15), 141.0 (C-13), 139.0 (C-12), 138.1 (C-2), 125.5 (C-7), 124.2 (C-6), 123.6 (C-10), 121.2 (C-11), 120.6 (C-5), 119.9 (C-4), 118.7 (C-3), 109.5 (C-8), 107.8 (C-1), 45.8 (C-14), 43.1 (C-17), 31.7 (C-18), 29.3, 29.1, 29.1, 28.8, 27.1, 22.5 (CH_2), 18.5 (C-16), 14.0 (C-25). **MS** (m/z, 70 eV, EI) = 399 (M^+), 401, 286, 388, 400, 287. **IR** (KBr, cm^{-1}): $\tilde{\nu}$ = 1699.85 (COOH). **EA:** calculated for $C_{24}H_{30}ClNO_2$ (399.95): C: 72.07, N: 3.50, H: 7.56, found: C: 72.13, N: 3.39, H: 7.69.

References:

1 Weggen, S. *et al.* A subset of NSAIDs lower amyloidogenic $A\beta_{42}$ independently of cyclooxygenase activity. *Nature* **414**, 212-216 (2001).

2 Narlawar, R. *et al.* Scaffold of the cyclooxygenase-2 (COX-2) inhibitor carprofen provides Alzheimer γ-secretase modulators. *J. Med. Chem.* **49**, 7588-7591 (2006).

3 Kukar, T. L. *et al.* Substrate-targeting γ-secretase modulators. *Nature* **453**, 925-929 (2008).

4 Munter, L. M. *et al.* GxxxG motifs within the amyloid precursor protein transmembrane sequence are critical for the etiology of $A\beta_{42}$. *Embo J.* **26**, 1702-1712 (2007).

5 Kienlen-Campard, P. *et al.* Amyloidogenic processing but not amyloid precursor protein (APP) intracellular *C*-terminal domain production requires a precisely oriented APP dimer assembled by transmembrane GXXXG motifs. *J. Biol. Chem.* **283**, 7733-7744 (2008).

6 Narlawar, R. *et al. N*-Substituted carbazolyloxyacetic acids modulate Alzheimer associated γ–secretase. *Bioorg. Med. Chem. Lett.* **17**, 176-182 (2007).

7 Sato, T. *et al.* Active γ-secretase complexes contain only one of each component. *J. Biol. Chem.* **282**, 33985-33993 (2007).

8 Serneels, L. *et al.* γ-Secretase heterogeneity in the Aph1 subunit: relevance for Alzheimer's disease. *Science (New York, N.Y.)* **324**, 639-642 (2009).

9 Uemura, K. *et al.* Allosteric modulation of PS1/γ-secretase conformation correlates with Amyloid β(42/40) ratio. *PLoS One* **4**, e7893, doi:10.1371/journal.pone.0007893 (2009).

10 Scheuermann, S. *et al.* Homodimerization of amyloid precursor protein and its implication in the amyloidogenic pathway of Alzheimer's disease. *J. Biol. Chem.* **276**, 33923-33929 (2001).

11 Gralle, M., Botelho, M. G. & Wouters, F. S. Neuroprotective secreted amyloid precursor protein acts by disrupting amyloid precursor protein dimers. *J. Biol. Chem.* **284**, 15016-15025 (2009).

12 Eggert, S., Midthune, B., Cottrell, B. & Koo, E. H. Induced dimerization of the amyloid precursor protein (APP) leads to decreased amyloid-β protein (Aβ) production. *J. Biol. Chem.* **284**, 28943-28952 (2009).

13 Esposito, A., Gerritsen, H. C. & Wouters, F. S. Fluorescence lifetime heterogeneity resolution in the frequency domain by lifetime moments analysis. *Biophys. J.* **89**, 4286-4299 (2005).

3.6 Untersuchungen zum Einfluss der Casein Kinase 1 auf die γ-Sekretase

Der Inhalt dieses Kapitels wurde zur Veröffentlichung eingereicht:
Nicole Höttecke, Miriam Liebeck, Karlheinz Baumann, Robert Schubenel, Edith Winkler, Harald Steiner, Boris Schmidt *ChemMedChem*, eingereicht: 02.12.09. "Inhibition of γ-secretase by the CK1 inhibitor IC261 does not depend on CK1."

Der selektive Casein Kinase 1 Inhibitor IC261 reduziert auch die Aβ-Sekretion, weshalb ein Einfluss von CK1 auf die γ-Sekretase vermutet wird. Im Rahmen einer Struktur-Aktivitäts-Analyse wurden 15 Derivate von IC261 synthetisiert um den Einfluss der Casein Kinase 1 auf die γ-Sekretase zu untersuchen.

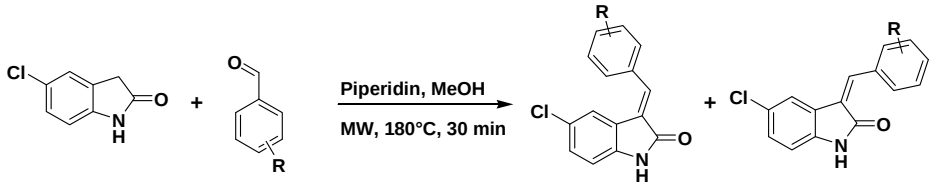

Abb. 24: Synthese der IC261 Derivate.

Die Wasserstoffbrücken-Akzeptoren (Methoxy) des Aryl-Substituenten von IC261 wurden durch alternative Wasserstoffbrücken-Akzeptoren, wie Fluor oder Sulfonsäure ausgetauscht. Hierbei erwiesen sich die Methoxy-Substituenten als essentiell, da alle alternativ getesteten Wasserstoffbrücken-Akzeptoren keine inhibitorische Aktivität auf die γ-Sekretase zeigten. Die Positionen der Methoxy-Gruppen wurden systematisch variiert, wobei alle Derivate die γ-Sekretase inhibierten. Ausschließlich IC261 zeigte inhibitorische Aktivität auf die CK1δ. Durch Methylierung des Indolidon-Stickstoffes in IC261 wurde eine Abnahme der Potenz im Vergleich zu IC261 erwartet, da die Ausbildung von zwei Wasserstoffbrücken-Bindungen verhindert wird. Im Gegensatz dazu wurde aber eine höhere inhibitorische Aktivität auf die γ-Sekretase ermittelt. Dieses Ergebnis schließt einen direkten Einfluss der CK1 auf die γ-Sekretase aus. Auch eine direkte Inhibition von IC261 auf die γ-Sekretase konnte durch den Kooperationspartner an der LMU München in einem aufgereinigten γ-Sekretase Assay ausgeschlossen werden. Es bleibt unklar durch welchen Mechanismus die γ-Sekretase durch IC261 und deren Derivate inhibiert wird. Wir vermuten, dass Abbauprodukte von IC261 eine inhibitorische Aktivität ausüben können, aber auch der Einfluss einer noch nicht identifizierten Kinase ist vereinbar mit den experimentellen Ergebnissen.

Alle Verbindungen wurden von Nicole Höttecke von 2006-2009 synthetisiert außer dem kommerziell erhältlichen Sunitinib.

DOI: 10.1002/cmdc.200((will be filled in by the editorial staff))

Inhibition of γ-secretase by the CK1 inhibitor IC261 does not depend on CK1

Nicole Höttecke[a], Miriam Liebeck[a], Karlheinz Baumann[b], Robert Schubenel[b], Edith Winkler[c], Harald Steiner[c], Boris Schmidt.[a]*

[a]Clemens Schöpf-Institute of Chemistry and Biochemistry, Technische Universität Darmstadt, Petersenstr. 22, D-64287 Darmstadt, Germany.

[b]F. Hoffmann-La Roche Ltd., Pharmaceuticals Division, Preclinical Research CNS, Bldg. 70/345, CH-4070 Basel, Switzerland.

[c]German Center for Neurodegenerative Diseases (DZNE) and Adolf-Butenandt-Institute, Biochemistry, Ludwig-Maximilians-University, Schillerstr. 44, 80336 Munich, Germany

[*] Prof. Dr. Boris Schmidt,
Clemens Schöpf-Institute of Chemistry and Biochemistry,
Technische Universität Darmstadt,
Petersenstr. 22, D-64287 Darmstadt, Germany.
Tel: (+49) 6151-163075
Fax: (+49) 6151-163278
E-mail: schmidt_boris@t-online.de

Abstract: *CK1 and γ-secretase are interesting targets for therapeutic intervention in the treatment of cancer and Alzheimer's disease. The CK1 inhibitor IC261 was reported to inhibit γ-secretase activity. The question is: Does CK1 inhibition directly influence γ-secretase activity? Therefore we analyzed the SAR of 15 analogues and their impact on γ-secretase activity. The most active compounds were investigated on CK1δ activity. These findings exclude a direct influence of CK1 on γ-secretase, because any change in the substitution pattern of IC261 diminished CK1 inhibition, whereas γ-secretase inhibition is still exerted by several analogues.*

Introduction

Alzheimer's disease is a devastating illness, which robs patients off the ability to manage their lives on their own. This illness is accompanied by protein aggregates in the brain composed of the amyloid-β-peptide (Aβ), which are called amyloid plaques.[1] The amyloid-β-peptide is generated by the subsequent degradation of the amyloid precursor protein (APP), a type I transmembrane protein, by two aspartyl proteases, the β-secretase and the γ-secretase. The γ-secretase is a promising target for therapeutic intervention as it liberates various Aβ-peptides with a length of 38, 40, or 42 amino acids.[2] The toxicity depends on the length: $A\beta_{42}$ is the most toxic species while $A\beta_{38}$ is regarded to be non-toxic as increased production of $A\beta_{38}$ does not diminish cellular viability. Several γ-secretase inhibitors (GSI), which decrease total Aβ levels, and several γ-secretase modulators (GSM), which shift the cleavage-site to the non toxic $A\beta_{38}$, have been identified so far.[3-5]

Flajolet *et al*.[6] reported IC261 (**1**) (scheme 1), a presumably selective casein kinase 1δ (CK1δ) inhibitor (IC_{50} = 2.57 µM in cells), to exert potent GSI like activity.[6-9] **IC261** causes a significant reduction of $A\beta_{40}$ (68%) and $A\beta_{42}$ (61%) levels in N2a cells within 5-50 µM concentration at 3h after incubation. A toxic effect was excluded, as toxicity was observed at a concentration of 50 µM only and 24h incubation time. The potential influence of CK1δ on γ-secretase activity and the similarity of IC261 with known, potent GSMs (Sulindac-S (**2**), Sulindac (**3**) and Sulindac-sulfon (**4**)) stimulated us to investigate the oxoindole-backbone of IC261, which is a common scaffold to kinase inhibition (scheme 1).

Results and Discussion

Synthesis of SAR:

A dual structure-activity-relationship analysis (SAR) towards γ-secretase and CK1 activity was carried out by systematical variation of the oxoindole substitution utilizing the CK1/IC261 co-crystallized structure (PDB: 1EH4). (Table 1) This structure guided the variation of the compounds aiming either at enhanced interaction with CK1 or to exclude interaction with CK1 (R^3 = Me, 15). All compounds were tested in the cellular Aβ generation assay.[10] The four most potent GSIs were subsequently investigated on their CK1δ activity to confirm the reported influence of CK1δ on the γ-secretase.[6] A further aim of this investigation was the identification of selective GSIs or even GSMs, void off cross-activity on CK1δ or related kinases.

The Knoevenagel condensation of these IC261-derivatives utilizes an oxoindole-derivative, a respective aldehyde and piperidine as a base. The reaction is carried out under microwave irradiation at 100°C for 30 min to provide the products in moderate to good yields.[11] The *Z*-isomer was enriched in the subsequent re-crystallisation. The proportion of the *E*/*Z* isomers was analyzed by HPLC-MS signal integration and the HPLC signals were definitely assigned to the molecular mass. (Scheme 2) The assignment of the two isomers to the two HPLC signals was established by ^{1}H NMR-spectroscopy.

The isomerization of the pure *Z*-isomer to the equilibrium of *E*- and *Z*-isomers was monitored by HPLC-MS for **9** (Scheme 2) and ^{1}H NMR-spectroscopy for **14**[12] (Scheme 3) to be complete within 2 days in methanol solution, which compares to the assay conditions: buffered H_2O, 24 h. Thus the cellular data are obtained for *E*/*Z* mixtures regardless of the purity of the initial isomer.

Aβ determination: H4-cells

IC261 (**1**) is a competitive ATP-binding-site inhibitor. The interaction with this binding-site was reported by Mashhoon *et al.* based on the co-crystallisation (PDB: 1EH4) of CK1 with IC261.[13]

1 features both a hydrogen-bond-donor in form of the indole-amin and three methoxy-substituents as hydrogen-bond-acceptors, which can be divided in two *o*- and one *p*-substitution. The structure analysis suggests two hydrogen-bonds of the indole-amine with Asp^{86} and Leu^{88}.[13] Notable interactions were assigned to the *o*-methoxy-group and Lys^{41} and an intermolecular interaction with a benzene hydrogen and interactions of the *p*-methoxy-group with Ser^{22} and Asp^{154}. (Figure 1)

The symmetric substitution pattern with two *o*-methoxy-groups enables interactions of both

rotamers. Both the E-isomer purity and the atrop-isomerism found in the co-crystal were captured from the equilibrium conformations in solution. The influence of the *o*-substitution was determined by a derivative bearing just one *o*-methoxy-group (**5**) and several derivatives where the methoxy-groups were replaced by fluorine (**6**), nitro (**7**) or sulfonic acid (**8**)**.**

Just one out of these derivatives (**5** $A\beta_{38}$ = 62%, $A\beta_{40}$ = 76%, $A\beta_{42}$ = 65%) displayed a significant decrease in Aβ-levels comparable to the activity of IC261 ($A\beta_{38}$ = 55%, $A\beta_{40}$ = 77%, $A\beta_{42}$ = 77%). The single *o*-substituent and the absence of a *p*-substituent may cause these minor changes in potency of **5**. A complete loss of activity was observed for those derivatives which lacked *o*-methoxy-groups. This observation demonstrates the essential role of the *o*-methoxy-group which fits exactly into the ATP-binding-site. This assumption was confirmed by introduction of an benzo[δ][1,3]dioxole (**9**) which did not display any significant activity on Aβ-levels. This group bears oxygen in the *m*-position, but has an additional methylene bridge to another oxygen in the *p*-position. The activity loss can be explained by sterical hindrance of the dioxole group, which may displace Asp^{154} thus disrupting essential hydrogen-bonds. Secondary, *m*-substitution is detrimental to activity, this was additionally tested by two fluorines (**10**) in the *m*-positions, which displayed surprisingly increased $A\beta_{42}$ generation of up to 112% at a concentration of 5 µM. This may be due to inverse modulation; such a switch from straight to inverse γ-secretase modulation on a common scaffold was observed previously.[6, 14]

Two additional hydrogen-bonds are formed by the *p*-substituted methoxy-group with Ser^{22} and Asp^{154}. Ser^{22} exerts the role of a gate keeper in CK1: Entry of the ATP in the binding site causes a conformational change into the closed form by Ser^{22}, which locks the binding site and prevents ATP-diffusion out of the binding site. This in turn stabilizes CK1 in the active conformation. The ability of **1** to form a hydrogen-bond with Ser^{22} locks the ATP-binding-site permanently. The position of Ser^{22} is fixed in the closed form of the pocket and thereby prevents the replacement of IC261 by ATP.

The interaction of a *p*-substituent with Ser^{22} was investigated by the introduction of both sterically demanding and functional groups (**11, 12**). These groups should prevent the conformational change into the closed form of the ATP-binding-site. The FDA-approved kinase inhibitor Sunitinib (**16**) was included into the investigation for the same rational. **11** did not show any effect on Aβ levels, but an unexpected inverse modulation of the γ-secretase was observed for **12**, which decreased the $A\beta_{38}$ levels and increased $A\beta_{42}$ levels. (Figure 2) The inverse modulation by **12** as well as **10** indicates the mechanism to be different from total inhibition of Aβ generation. The moderate inhibition of Aβ secretion ($A\beta_{38}$ = 26%, $A\beta_{40}$ = 53%, $A\beta_{42}$ = 26%) by **16** was not observed in the reconstituted assay. This indicates an indirect, potentially upstream mode of action.

As the IC261 substitution pattern (2,4,6-trimethoxybenzene) was found to be important for the activity, it was systematically varied into 2,3,4- and 3,4,5-trimethoxybenzene (**13, 14**). These two derivatives also exert a significant reduction in total Aβ. Although the *o*-positions of **14** ($A\beta_{38}$ = 54%, $A\beta_{40}$ = 72%, $A\beta_{42}$ = 65%) are substituted with hydrogens, it is equipotent to **1** ($A\beta_{38}$ = 55%, $A\beta_{40}$ = 77%, $A\beta_{42}$ = 77%). A distinct rise in activity was observed for **13** ($A\beta_{38}$ = 27%, $A\beta_{40}$ = 66%, $A\beta_{42}$ = 47%) with a methoxy-group in *o*-, *m*- and *p*-position.

The most important interaction was anticipated to be the indole-nitrogen forming two hydrogen-bonds with Asp^{86} and Leu^{88}.[13] This crucial interaction was challenged by a methyl-substitution of the nitrogen, expecting a 90% loss of activity. Surprisingly, a rise in activity of **15** compared to IC261 was observed. The three Aβ-species were significantly decreased to 35% for $A\beta_{38}$ and to 65% for $A\beta_{40}$ and $A\beta_{42}$ each. Particularly this observation was the first major evidence against the involvement of CK1 in our biological assay.

Activity determination on kinases

IC261 and the three most potent derivatives **13**, **15** and **12** were tested for inhibitory activity on CK1δ and 42 other kinases to evaluate the influence of CK1 on γ-secretase (Figure 3). Surprisingly only IC261 shows a significant inhibition of CK1δ (81% inhibitory activity, Table 1, Figure 3). As soon as the

substitution pattern differs from 2,4,6-trimethoxybenzene, no significant CK1 inhibition (> 80%) was observed. This is shown e.g. in the case of **13**, which bears a methoxy-group in the *m*- instead of the *o*-position. It exerts an inhibition of a mere 1% under the same conditions (Figure 3). In addition, no significant inhibitory activity on CK1δ was found for **15** and **12.**

12 and **13** are inactive on CK1δ yet display significant inhibition (98% and 89%) of the tyrosine kinase Flt3, which plays an important role in leukemia. However, Flt3 is not known to exert effects on APP metabolism.

Only the N-methylated indolinone **15** lacked significant inhibition (inhibitory activity < 20%) for all kinases tested, which confirms the relevance of N-methylation of indolinones in kinase inhibition. This N-H bond is essential for the inhibition of most kinases by indolinones.

Aβ determination: purified γ-secretase

These data agree with three possible explanations: 1) IC261 does not directly affect γ-secretase activity but a degradation product is responsible for γ–secretase inhibition, 2) IC261 is coincidently a weak γ-secretase inhibitor, which independently targets CK1 activity. 3) Another, yet unidentified kinase is responsible for the cellular activity. To investigate a direct effect on γ-secretase activity, IC261 was tested in a cell-free assay using lipid-reconstituted purified γ-secretase and purified APP C100-His_6 as substrate for Aβ generation,[15] i.e. under conditions, where no additional metabolism is present (Figure 4). No effect on the Aβ production by γ-secretase was observed at 50 µM, the highest effective concentration used in cultured cells by the study of Flajolet *et al*.[6] IC261 did also not exert a modulatory effect on the production of $Aβ_{38}$, $Aβ_{40}$ and $Aβ_{42}$ species in the cell-free assay at this concentration. γ-Secretase activity was also not affected at 150 µM IC261, however, γ-secretase inhibition was observed at a five-fold higher dose. This may be due to the resemblance of IC261 to known γ-secretase inhibitors derived from NSAIDs, which are characterized by IC_{50}ies around 100-300 µM e.g. **2**.[16-18] Consistent with previous results,[15, 19] presence of the highly potent GSI L-685,458 [20] at 0.5 µM completely blocked γ-secretase activity in this assay.

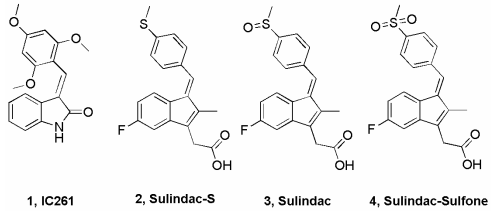

Scheme 1. Structural similarity of IC261 and the GSM of the Sulindac-series (**2-4**).

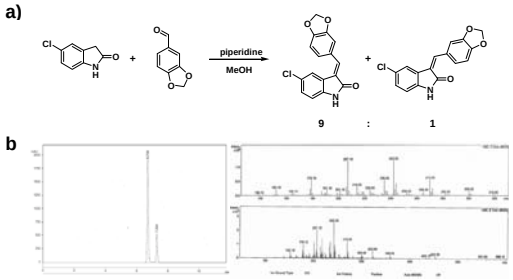

Scheme 2. E/Z isomerization of **9** analyzed by HPLC-MS.

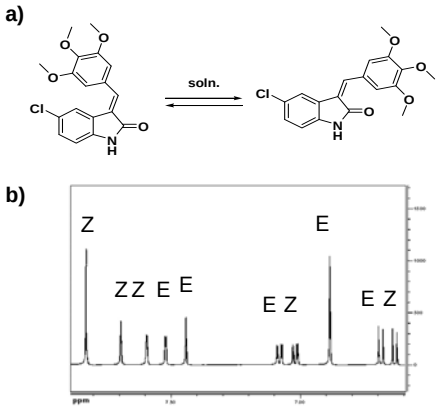

Scheme3. *E*/*Z* isomerization of **14** analyzed by ^{1}H-NMR-spectroscopy.

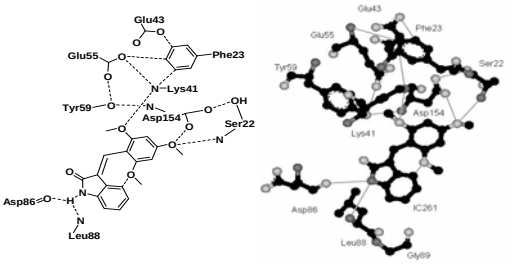

Figure 1. ATP-binding site interaction of **1** according to Mashhoon et al. (PDB: 1EH4).[13]

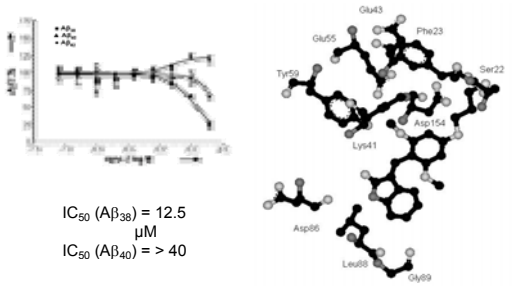

IC_{50} ($A\beta_{38}$) = 12.5 µM
IC_{50} ($A\beta_{40}$) = > 40

Figure 2. Modelled ATP-binding site interaction of **12** (based on PDB: 1EH4) and its dose-response curve

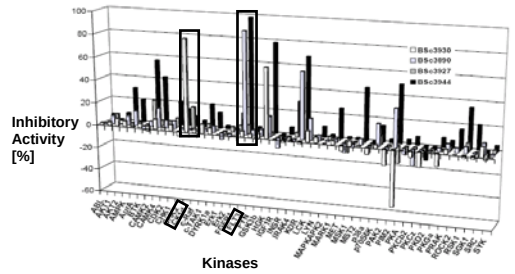

Figure 3. Kinase screening of 43 kinases from compounds 1 (BSc3930), 12 (BSc3944), 13 (BSc3890), 15 (BSc3927). Kinase inhibition is indicated by positive values. Negative values indicate kinase activation.

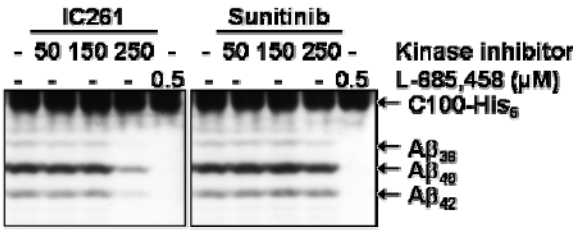

Figure 4: Cell-free γ-secretase assay in the presence of IC261, Sunitinib, or L-685,458[20] GSI as control.

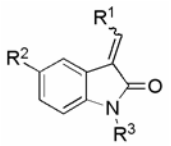

Table 1. Activity of Aβ generation of oxindoles at a concentration of 10 µM in H4-cells.

Cpd	*Code*	*R¹*	*R²*	*R³*	*CK1δ*[b] [%]	[%] Aβ38	Aβ40	Aβ42
1	BSc3930 IC261	2,4,6-trimethoxy-benzene	H	H	81	55	77	77
5	BSc3926	2-methoxybenzene	Cl	H	n.t.[c]	62	76	65
6	BSc3921	2-fluorobenzene	Cl	H	n.t.[c]	87	88	91
7	BSc3923	2-nitrobenzene	Cl	H	n.t.[c]	94	88	83
8	BSc3922	2-benzene sulfonic acid	Cl	H	n.t.[c]	101	96	88
9	BSc3928	benzo[δ][1,3]dioxole	Cl	H	n.t.[c]	86	93	90
10	BSc3914	3,5-difluorobenzene	Cl	H	n.t.[c]	81[a]	106[a]	112[a]
11	BSc3929	4-benzeneacetamide	Cl	H	n.t.[c]	99	97	97
12	BSc3944	4-chloropropoxy-benzene	Cl	H	9	66	93	123
13	BSc3890	2,3,4-trimethoxy-benzene	Cl	H	1	27	46	47
14	BSc3925	3,4,5-trimethoxy-benzene	Cl	H	n.t.[c]	54	72	65
15	BSc3927	2,4,6-trimethoxy-benzene	H	Me	13	35	65	65
16	Sunitinib	*N*-(2-(diethylamino)-ethyl)-2,4-dimethyl-1*H*-pyrrole-3-carboxamide	F	H	n.t.[c]	26	53	26

[a] Activity at a concentration of 5 µM

[b] Inhibitory activity at 10 µM

[c] n.t. = not tested

Conclusion

The cellular activity of IC261 and its activity in cell-free assays is inconsistent with an exclusively CK1δ mediated effect on Aβ secretion via γ-secretase inhibition. As the cell-free assay is not subject to CK1δ dependent regulation, a pleiotropic effect is suggested for the interference of Aβ secretion by IC261: a.) cellular γ-secretase inhibition may occur at high concentration of IC261 or through a metabolic activation of IC261. It is not clear, however, whether the interference of IC261 with γ-secretase activity at high concentration (in the cell-free assay at 250 µM, i.e. five times above the concentration used by Flajolet *et al.*[6] in the cellular assay) does reflect enzyme inhibition. The observed reduction in γ-secretase activity could also be due to

a damage of the lipid environment by this particular compound in the in vitro assays; b.) upstream modulation of Aβ metabolism by an unidentified mode of action, which does not necessarily involve CK1δ at low concentrations. Sunitinib, a promiscuous kinase inhibitor, was selected for structural similarity to IC261 and submitted to the assay panel. It reduces Aβ secretion in the cellular assay. However, Sunitinib did not display an effect on Aβ generation in the cell-free assay suggesting that an unidentified kinase may be involved in Aβ secretion in the cellular assay.

Even a subtle variation of the IC261 substitution pattern resulted in complete loss of CK1 inhibition but still exerts Aβ lowering capability (e.g. **13).**

In conclusion, our IC261 SAR data are inconsistent with CK1-dependent inhibition of γ-secretase. The most potent compounds are not suitable as lead structure for γ-secretase modulation in vivo, as long as they display significant inhibition of Flt3. Such off-target activity will impair further development.

Experimental Section

Assays:

Aβ liquid phase electrochemiluminescence (LPECL) assay:

We used the LPECL assay to measure Aβ isoforms to evaluate the compounds for their potency in modulating γ-secretase activity as previously described.[10]

Cell-free γ-secretase assay:

γ-Secretase activity was assessed *in vitro* using purified components as described previously using the final Q-Sepharose eluate fraction of γ-secretase as enzyme source.[15] For these assays, IC261 obtained from Sigma and Sunitinib from LC Laboratories, were used.

ProfilerPro Kinase Selectivity Assay System:[22]

ProfilerPro Kits 1 and 2 were used to investigate kinase activity. Each of these kits contains all necessary reagents to carry out in-house compound profiling against a panel of 48 kinases for twelve compounds and were utilized as described.[21] The ProfilerPro plates were read using of Caliper off-chip mobility shift assay technology. Results are displayed as % inhibition value.

General remarks:

Thin-layer chromatography (TLC) was carried out using aluminium sheets precoated with silica gel 60 F254 (0.2 mm; E. Merck). Chromatographic spots were visualized by UV and/or spraying with a methanolic solution of vanillin/H_2SO_4 or aq. $KMNO_4$ solution followed by heating. Flash column chromatography was carried out using Merck silica gel 60 (0.063-0.2 mm).

Melting Points were determined on a Mettler FP 51 melting point apparatus and are uncorrected. The ^{1}H NMR and ^{13}C NMR spectra were recorded on a Bruker AC 300 (300 MHz) and AC 500 spectrometer (500 MHz). Chemical shifts are reported as % values (ppm) and adjusted at the central line of the deuterated solvent (MeOD, $CDCl_3$). Mass spectrometry was performed on a Bruker-Franzen Esquire LC mass spectrometer (ESI) and a double focused MAT 95 (EI). The reaction was performed using a microwave from Biotage (Initiator 300 W). HPLC analysis was carried out using an Agilent 1100 with a reversed phase column (Zorbax Eclipse XDB-C8; 4.6*150 mm) and a 254 nM detector. The eluent is composed of H_2O (1% TFA) (A) and acetonitrile (B) with a gradient: 30 to 90% B within 12 min. All reagents and solvents (THF, DMF, CH_2Cl_2, ethyl acetate, MeOH) were purchased at ABCR, Acros and Alfa Aesar, TCI, Sigma Aldrich and VWR. Methanol abs. was additionally dried over magnesium.

Experimental data:

3-(2,4,6-Trimethoxybenzylidene)indolin-2-one (1) [BSc3930]

A mixture of 39 mg oxoindole (0.3 mmol), 58 mg 2,4,6-trimethoxybenzaldehyde (0.3 mmol), 30 µL piperidine in 1 mL methanol was heated at 100°C under microwave irradiation for 30 min. The precipitate was re-crystallized from methanol to give 80 mg (77%) as a yellow solid, mp 188°C.

^{1}H NMR (300 MHz, $CDCl_3$) ppmδ: = 9.96 (s, 1H, NH), 7.50 (s, 1H, H-10), 7.03 (t, ^3J = 7.6 Hz, 1H H-4), 6.83-6.70 (m, 3H, H-5/6/7), 6.15 (s, 2H, H-14/16), 3.82 (s, 3H, CH_3-16), 3.70 (s, 6H, CH_3-15), **MS** (m/z, 70 eV) = 311 (M^+), 280, 265, 158.

5-Chloro-3-(2-methoxybenzylidene)indolin-2-one (5) [BSc3926]

A mixture of 50 mg chlorooxoindole (0.3 mmol), 41 mg *o*-anisaldehyde (0.3 mmol), 30 µL piperidine in 1 mL methanol was heated at 100°C under microwave irradiation for 30 min. The precipitate was re-crystallized from methanol to give 21 mg (25%) as a yellow solid, mp 241°C.

^{1}H NMR (300 MHz, DMSO) ppm. δ: = 10.50 (s, 1H, NH), 7.71 (s, 1H, CH-10), 7.76 (dd, ^4J = 1.3 Hz, ^3J = 7.6 Hz, 1H, H-7), 7.43 (t, ^3J = 7.2 Hz, 1H, H-15), 7.30 (d, ^4J = 1.3 Hz, 1H, H-4), 7.13-7.00 (m, 3H, H-13/14/16), 6.79 (d, ^3J = 8.1 Hz, 1H, H-6), **MS** (m/z, 70 eV, EI) = 285 (M^+), 287, 254, 256.

5-Chloro-3-(2-fluorobenzylidene)indolin-2-one (6) [BSc3921]

A mixture of 50 mg chlorooxoindole (0.3 mmol), 37 mg 2-fluorobenzaldehyde, 30 µL piperidine in 1 mL methanol was heated at 100°C under microwave irradiation for 30 min. The precipitate was re-crystallized from methanol to give 30 mg (37%) as a yellow solid, mp 279°C.

^{1}H NMR (300 MHz, DMSO) ppm δ: = 10.80 (s, 1H, NH), 7.75 (t, ^3J = 8.2 Hz, 1H, H-15), 7.62 (d, *4J* = 2.1 Hz, 1H, CH-10), 7.58 (t, ^3J = 8.2 Hz, 1H, H-14), 7.43 (d, ^3J = 8.2 Hz, 1H, H-16), 7.37 (d, ^3J = 8.2 Hz, 1H, H-13), 7.30 (dd, ^4J = 2.1 Hz, ^3J = 8.3 Hz, 1H, H-6), 6.89 (d, ^3J = 8.3 Hz, 1H, H-7), **MS** (m/z, 70 eV) = 273 (M^+), 275, 254, 245, 178.

5-Chloro-3-(2-nitrobenzylidene)indolin-2-one (7) [BSc3923]

A mixture of 50 mg chlorooxoindole (0.3 mmol), 45 mg *o*-nitrobenzaldehyde (0.3 mmol), 30 µL piperidine in 1 mL methanol was heated at 100°C under microwave irradiation for 30 min. The precipitate was re-crystallized from methanol to give 52 mg (58%) as a yellow solid, mp 221°C.

^{1}H NMR (300 MHz, $CDCl_3$) ppm δ: = 10.16 (s, 1H, NH), 8.23 (d, ^3J = 7.7 Hz, 1H, H-6), 7.91 (s, 1H, CH-10), 7.72-7.62 (m, 3H, H-14/15/16), 7.05 (d, ^3J = 7.7 Hz, 1H, H-7), 6.75 (s, 1H, H-4), 6.70 (d, ^3J = 9.5 Hz, 1H, H-13), **MS** (m/z, 70 eV) = 300 (M^+), 270, 254, 256, 219, 190.

2-((5-Chloro-2-oxoindolin-3-ylidene)methyl)benzoic acid (8) [BSc3922]

A mixture of 50 mg chlorooxoindole (0.3 mmol), 62 mg 2-formylbenzenesulfonic acid (0.3 mmol), 30 µL piperidine in 1 mL methanol was heated at 100°C under microwave irradiation for 30 min. The precipitate was re-crystallized from methanol to give 42 mg (43%) as a yellow solid, mp >245°C.

^{1}H NMR (300 MHz, $CDCl_3$) ppm δ: = 10.16 (s, 1 H, NH), 8.39 (s, 1 H, CH-10), 8.06 (d, ^3J = 9.1 Hz, 1H, H-7), 7.40 (d, ^3J = 5.1 Hz, 1H, H-13), 7.38-7.20 (m, 2H, H-14/15), 7.05 (d, ^4J = 2.1 Hz, 1H, H-4), 6.98 (dd, ^3J = 9.1 Hz, ^4J = 2.1, 1H, H-6), 6.70 (d, ^3J = 9.3 Hz, 1H, H-13), MS (m/z, 70 eV) = 335 (M^+), 255, 253, 190, 167.

3-(Benzo[1,3]dioxol-5-ylmethylene)-5-chloroindolin-2-one (9) [BSc3928]

A mixture of 50 mg chlorooxoindole (0.3 mmol), 45 mg benz[1,3]dioxole-5-carbaldehyde (0.3 mmol), 30 µL piperidine in 1 mL methanol was heated at 100°C under microwave irradiation for 30 min. The precipitate was re-crystallized from methanol to give 35 mg (40%) as a yellow solid, mp 229°C.

^{1}H NMR (500 MHz, Acetone) ppm δ: = 8.63 (s, 1H, NH), 7.74 (s, 1H, CH-10), 7.66 (s, 1H, H-15), 7.64 (d, ^4J = 2.4 Hz, 1H, H-4), 7.28 (dd, ^4J = 1.7 Hz, ^3J = 8.0, 1H, H-12), 7.22 (dd, ^4J = 1.7 Hz, ^3J = 8.0 Hz, 1H, H-13) 7.01 (d, ^3J = 8.0 Hz, 1H, H-7), 6.92 (dd, ^3J = 8.0 Hz, ^4J = 2.4 Hz, 1H, H-6), 6.09 (s, 2H, CH_2-14), **MS** (m/z, 70 eV, ESI) = 300 ($M+H^+$).

3-(3,5-Difluorobenzylidene)indolin-2-one (10) [BSc3914]

A mixture of 30 mg chlorooxoindole (0.18 mmol), 45 mg 3,5-difluorobenzaldehyde (0.18 mmol), 18 µL piperidine in 1 mL methanol was heated at 100°C under microwave irradiation for 30 min. The precipitate was re-crystallized from methanol to give 12 mg (23%) as a yellow solid.

^{1}H NMR (300 MHz, DMSO) ppm δ: = 10.86 (br.s, 1H, NH), 8.17-8.12 (m, 1H, H-12_Z), 7.93 (s, 1H, H-10_Z), 7.82 (d, ^4J = 2.0 Hz, 1H, H-4_Z), 7.64 (s, 1H, H-10_E), 7.45 (d, ^3J = 6.6 Hz, 1H, H-12_E), 7.43-7.36 (m, 1H, H-$6_{E/Z}$), 7.35-7.26 (m, 2H, H-4_E/H-$7_{E/Z}$), 6.90 (d, ^3J = 8.3 Hz, 1H, H-14_E), 6.85 (d, ^3J = 8.3 Hz, 1H, H-14_Z), **MS** (m/z, 70 eV) = 291 (M^+), 263, 178.

2-(4-Formylphenoxy)acetamide

85 mg 4-hydroxybenzaldehyde (0.7 mmol) and 130 mg 4-chloroacetamide were added to a suspension of 20 mL acetone, 290 mg potassium carbonate and catalytic amounts of potassium iodide. The mixture was refluxed for 48h, the precipitate was filtrated afterwards and the solvent was removed *in vacuo* to give 143 mg (99%) as a light yellow solid.

2-(4-((5-Chloro-2-oxoindolin-3-ylidene)methyl)phenoxy)acet-amide (11) [BSc3929]

A mixture of 50 mg chlorooxoindole (0.3 mmol), 53 mg 2-(4-formyl-phenoxy)acetamide (0.3 mmol), 30 µL piperidine in 1 mL methanol was heated at 100°C under microwave irradiation for 30 min. The precipitate was re-crystallized from methanol to give 42 mg (43%) as a yellow solid, mp 132°C.

^{1}H NMR (300 MHz, DMSO) ppm δ: = 10.53 (s, 1H, NH), 8.40 (d, ^3J = 8.9 Hz, 1H, H-7), 8.11 (s, 1H, CH-10), 7.71 (s, 1H, H-4), 7.50-7.32 (m, 2H, NH_2), 7.14-7.04 (m, 2H H-12), 6.96 (dd, ^3J = 8.9 Hz, 1H, H-6), 6.73 (d, ^3J = 8.2 Hz, 2H, H-13), 4.46 (s, 2H, CH_2-15), **MS** (m/z, 70 eV) = 328 (M^+), 271, 243, 178.

4-(3-Chloropropoxy)benzaldehyde

A mixture of 616 mg 4-hydroxybenzaldehyde (5.0 mmol), 1 mL 1-bromo-2-chloropropane (10.0 mmol), 2000 mg potassium carbonate in 14 mL

acetone were refluxed for 48h, the precipitate was filtered off. The filtrate was concentrated *in vacuo* to give 980 mg (99%) as a brown solid.[22-24]

5-Chloro-3-(4-(3-chloropropoxy)benzylidene)indolin-2-one (12) [BSc3944]

A mixture of 50 mg chlorooxoindole (0.3 mmol), 59 mg 4-(3-chloropropoxy)benzaldehyde (0.3 mmol), 30 µL piperidine in 1 mL methanol was heated at 100°C under microwave irradiation for 30 min. The precipitate was re-crystallized from methanol to give 25 mg (25%) as a yellow solid, mp 124°C.

^{1}H NMR (300 MHz, DMSO) ppm δ: = 10.03 (s, 1H, NH), 8.32 (d, ^3J = 8.9 Hz, 2H, H-12$_E$), 7.65 (s, 1H, CH-10$_Z$), 7.58 (d, ^4J = 2.0 Hz, 1H, H-4$_Z$), 7.55 (d, ^3J = 8.9 *Hz,* 2H, H-12$_Z$), 7.40 (s, 1H, CH-10$_E$), 7.40 (d, ^4J = 2.0 Hz, 1H, H-4$_E$), 7.07 (dd, ^4J = 2.0 Hz, ^3J = 8.5 Hz, 1H, H-6$_Z$), 7.06 (dd, ^4J = 2.0 Hz, ^3J = 8.5 Hz, 1H, H-6$_E$), 6.96 (d, ^3J = 8.9 Hz, 2H, H-13$_Z$), 6.89 (d, ^3J = 8.9 Hz, 2H, H-13$_E$), 6.76 (d, ^3J = 8.5 Hz, 1H, H-7$_Z$), 6.75 (d, ^3J = 8.5 Hz, 1H, H-7$_E$). 4.15 (t, ^3J = 5.9 Hz, 2H, H-15$_Z$), 4.14 (t, ^3J = 5.9 Hz, 2H, H-15$_E$), 3.72 (t, ^3J = 6.3 Hz, 2H, H-17$_Z$), 3.69 (t, ^3J = 6.3 Hz, 2H, H-17$_E$), 2.25-2.18 (m, 2H, H-16$_{E/Z}$), **MS** (m/z, 70 eV) = 347 (M^+), 350, 271, 243, 178.

5-Chloro-3-(2,3,4-trimethoxybenzylidene)indolin-2-one (13) [BSc3890]

A mixture of 50 mg chlorooxoindole (0.3 mmol), 59 mg 2,3,4-trimethoxybenzaldehyde (0.3 mmol), 30 µL piperidine in 1 mL methanol was heated at 100°C under microwave irradiation for 30 min. The precipitate was re-crystallized from methanol to give 62 mg (60%) as a yellow solid, mp 198°C.

^{1}H NMR (300 MHz, DMSO) ppm δ: = 10.72 (br.s, 1H, NH), 8.61 (d, ^3J = 9.0 Hz, 1H, H-12$_E$), 7.88 (s, 1H, H-10$_E$), 7.73 (d, ^4J = 2.1 Hz, 1H, H-4$_E$), 7.65 (s, 1H, H-10$_Z$), 7.44 (d, ^3J = 9.4 Hz, 1H, H-12$_Z$), 7.46 (s, 1H, H-4$_Z$), 7.26 (dd, ^3J = 8.3 Hz, ^4J = 2.1 Hz, 1H, H-6$_Z$), 7.21 (dd, ^3J = 8.3 Hz, ^4J = 2.1 Hz, 1H, H-6$_E$), 7.00 (d, ^3J = 8.8 Hz, 1H, H-13$_Z$), 6.90 (d, ^3J = 9.1 Hz, 1H, H-13$_E$) 6.88 (dd, ^3J = 8.3 Hz, 1H, H-7$_Z$), 6.81 (d, ^3J = 8.3 Hz, 1H, H-7$_E$), 3.91 (s, 3H, H-15$_E$), 3.90 (s, 3H, H-15$_Z$), 3.88 (s, 3H, H-16$_E$), 3.83 (s, 3H, H-16$_Z$), 3.81 (s, 3H, H-17$_Z$), 3.78 (s, 3H, H-17$_E$), **MS** (m/z, 70 eV) = 345 (M^+), 314, 299, 217.

5-Chloro-3-(3,4,5-trimethoxybenzyliden)indolin-2-one (14) [BSc3925]

A mixture of 50 mg chlorooxoindole (0.3 mmol), 58 mg 3,4,5-trimethoxybenzaldehyde (0.3 mmol), 30 µL piperidine in 1 mL methanol was heated at 100°C under microwave irradiation for 30 min. The precipitate was re-crystallized from methanol to give 35 mg (34%) as a yellow solid, mp 228°C.

^{1}H NMR (300 MHz, DMSO) ppm δ: = 10.70 (s, 1H, NH), 8.04 (s, 2H, H-12), 7.89 (s, 1H, CH-10), 7.80 (d, ^3J = 2.1 Hz, 1H, H-4), 7.20 (dd, ^3J = 8.3 Hz, ^4J = 2.1 Hz, 1H, H-6), 6.63 (d, ^3J= 8.3 Hz, 1H, H-7), 3.84 (s, 6H, H-16), 3.75 (s, 3H, H-17), **MS** (m/z, 70 eV) = 368 (M+Na).

1-Methyl-3-(2,4,6-trimethoxybenzyliden)indolin-2-one (15) [BSc3927]

A mixture of 44 mg *N*-methyloxoindole (0.3 mmol), 58 mg 2,4,6-trimethoxybenzaldehyde (0.3 mmol), 30 µL piperidine in 1 mL methanol was heated at 100°C under microwave irradiation for 30 min. The precipitate was re-crystallized from methanol to give 82 mg (84%) as a yellow solid, mp 206°C.

^{1}H NMR (300 MHz, $CDCl_3$) ppm δ: = 7.69 (s, 1H, CH-10$_Z$), 7.18 (s, 1H, CH-10$_E$), 7.14-7.08 (m, 1H, H-6), 6.91-6.88 (m, 1H, H-4), 6.81-6.76 (m, 1H, H-5), 6.71-6.68 (m, 1H, H-7), 6.11 (s, 2H, H-13), 3.81 (s, 3H, CH_3-16), 3.68 (s, 6H, CH_3-15), 3.19 (s, 3H, N-CH_3), **MS** (m/z, 70 eV) = 325 (M^+), 194, 279, 172.

Acknowledgements

Funding: This work was supported by the Competence Network for Neurodegenerative Diseases (KNDD) “Degenerative Dementias: Target identification, Validation and Translation into Treatment Strategies” of the Bundesministerium für Bildung und Forschung (BMBF) (H.S., N.H.).

Keywords: ((IC261 · CK1 · γ-secretase inhibition · cancer · Alzheimer’s disease))

References

[1] R. Jakob-Roetne, H. Jacobsen, *Angew. Chem. Int. Ed.* **2009**, *48*, 3030-3059.

[2] D. Beher, J. D. Wrigley, A. P. Owens, M. S. Shearman, *J. Neurochem.* **2002**, *82*, 563-575.

[3] S. Weggen, J. L. Eriksen, P. Das, S. A. Sagi, R. Wang, C. U. Pietrzik, K. A. Findlay, T. E. Smith, M. P. Murphy, T. Bulter, D. E. Kang, N. Marquez-Sterling, T. E. Golde, E. H. Koo, *Nature* **2001**, *414*, 212-216.

[4] L. Gasparini, E. Ongini, G. Wenk, *J. Neurochem.* **2004**, *91*, 521-536.

[5] S. Weggen, J. L. Eriksen, S. A. Sagi, C. U. Pietrzik, V. Ozols, A. Fauq, T. E. Golde, E. H. Koo, *J. Biol. Chem.* **2003**, *278*, 31831-31837.

[6] M. Flajolet, G. He, M. Heiman, A. Lin, A. C. Nairn, P. Greengard, *Proc. Natl. Acad. Sci. U S A* **2007**, *104*, 4159-4164.

[7] G. Cozza, A. Gianoncelli, M. Montopoli, L. Caparrotta, A. Venerando, F. Meggio, L. A. Pinna, G. Zagotto, S. Moro, *Bioorg. Med. Chem. Lett.* **2008**, *18*, 5672-5675.

[8] R. Narlawar, B. I. Perez Revuelta, K. Baumann, R. Schubenel, C. Haass, H. Steiner, B. Schmidt, *Bioorg. Med. Chem. Lett.* **2007**, *17*, 176-182.

[9] S. Baumann, N. Hoettecke, R. Schubenel, K. Baumann, B. Schmidt, *Bioorg. Med. Chem. Lett.* **2009**, *19*, 6986-6990.

[10] R. Narlawar, B. I. Perez Revuelta, C. Haass, H. Steiner, B. Schmidt, K. Baumann, *J. Med. Chem.* **2006**, *49*, 7588-7591.

[11] W. Zhang, M. L. Go, *Bioorg. Med. Chem.* **2009**, *17*, 2077-2090.

[12] R. Cincinelli, G. Cassinelli, S. Dallavalle, C. Lanzi, L. Merlini, M. Botta, T. Tuccinardi, A. Martinelli, S. Penco, F. Zunino, *J. Med. Chem.* **2008**, *51*, 7777-7787.

[13] N. Mashhoon, A. J. DeMaggio, V. Tereshko, S. C. Bergmeier, M. Egli, M. F. Hoekstra, J. Kuret, *J. Biol. Chem.* **2000**, *275*, 20052-20060.

[14] R. Narlawar, M. Pickhardt, S. Leuchtenberger, K. Baumann, S. Krause, T. Dyrks, S. Weggen, E. Mandelkow, B. Schmidt, *ChemMedChem* **2008**, *3*, 165-172.

[15] E. Winkler, S. Hobson, A. Fukumori, B. Dumpelfeld, T. Luebbers, K. Baumann, C. Haass, C. Hopf, H. Steiner, *Biochemistry* **2009**, *48*, 1183-1197.

[16] D. Beher, E. E. Clarke, J. D. J. Wrigley, A. C. L. Martin, A. Nadin, I. Churcher, M. S. Shearman, *J. Biol. Chem.* **2004**, *279*, 43419-43426.

[17] Y. Takahashi, I. Hayashi, Y. Tominari, K. Rikimaru, Y. Morohashi, T. Kan, H. Natsugari, T. Fukuyama, T. Tomita, T. Iwatsubo, *J. Biol. Chem.* **2003**, *278*, 18664-18670.

[18] P. C. Fraering, W. Ye, J.-M. Strub, G. Dolios, M. J. LaVoie, B. L. Ostaszewski, A. van Dorsselaer, R. Wang, D. J. Selkoe, M. S. Wolfe, *Biochemistry* **2004**, *43*, 9774-9789.

[19] Y. M. Li, M. T. Lai, M. Xu, Q. Huang, J. DiMuzio-Mower, M. K. Sardana, X. P. Shi, K. C. Yin, J. A. Shafer, S. J. Gardell, *PNAS* **2000**, *97*, 6138-6143.

[20] M. S. Shearman, D. Beher, E. E. Clarke, H. D. Lewis, T. Harrison, P. Hunt, A. Nadin, A. L. Smith, G. Stevenson, J. L. Castro, *Biochemistry* **2000**, *39*, 8698-8704.

[21] G. Manning, D. B. Whyte, R. Martinez, T. Hunter, S. Sudarsanam, *Science* **2002**, *298*, 1912-1934.

[22] R. Apodaca, C. A. Dvorak, W. Xiao, A. J. Barbier, J. D. Boggs, S. J. Wilson, T. W. Lovenberg, N. I. Carruthers, *J. Med. Chem.* **2003**, *46*, 3938-3944.

[23] C. Ekambome Bassene, F. Suzenet, N. Hennuyer, B. Staels, D.-H. Caignard, C. Dacquet, P. Renard, G. Guillaumet, *Bioorg. Med. Chem. Lett.* **2006**, *16*, 4528-4532.

[24] N. Mahindroo, C.-C. Wang, C.-C. Liao, C.-F. Huang, I. L. Lu, T.-W. Lien, Y.-H. Peng, W.-J. Huang, Y.-T. Lin, M.-C. Hsu, C.-H. Lin, C.-H. Tsai, J. T. A. Hsu, X. Chen, P.-C. Lyu, Y.-S. Chao, S.-Y. Wu, H.-P. Hsieh, *J. Med. Chem.* **2006**, *49*, 1212-1216.

Received: ((will be filled in by the editorial staff))

Published online: ((will be filled in by the editorial staff))

3.7 Synthese des selektiven ADAM10 Inhibitors GI254023X für Untersuchungen von Entzündungsprozessen

Der Inhalt dieses Kapitels wurde zur Veröffentlichung bereits veröffentlicht:
Nicole Höttecke, Andreas Ludwig, Sabine Foro, Boris Schmidt *Neurodegener. Dis.*, Zur Publikation angenommen: 09.1209. "Improved synthesis of the ADAM10 inhibitor GI254023X."

Jessica Pruessmeyer, Christian Martin, Franz M. Hess, Nicole Schwarz, Sven Schmidt, Tanja Kogel, Nicole Hoettecke, Boris Schmidt, Antonio Sechi, Stefan Uhlig, Andreas Ludwig *J. Biol. Chem.* Zur Publikation angenommen: doi: 10.1074/jbc.M109.059394. "The disintegrin and metalloproteinase 17 (ADAM17) mediates inflammation-induced shedding of syndecan-1 and -4 by lung epithelial cells."

Um ADAM10 mediierte Entzündungsprozesse untersuchen zu können wurde (angelehnt an die Synthese von GlaxoSmith&Kline) der Inhibitor GI254023X synthetisiert.

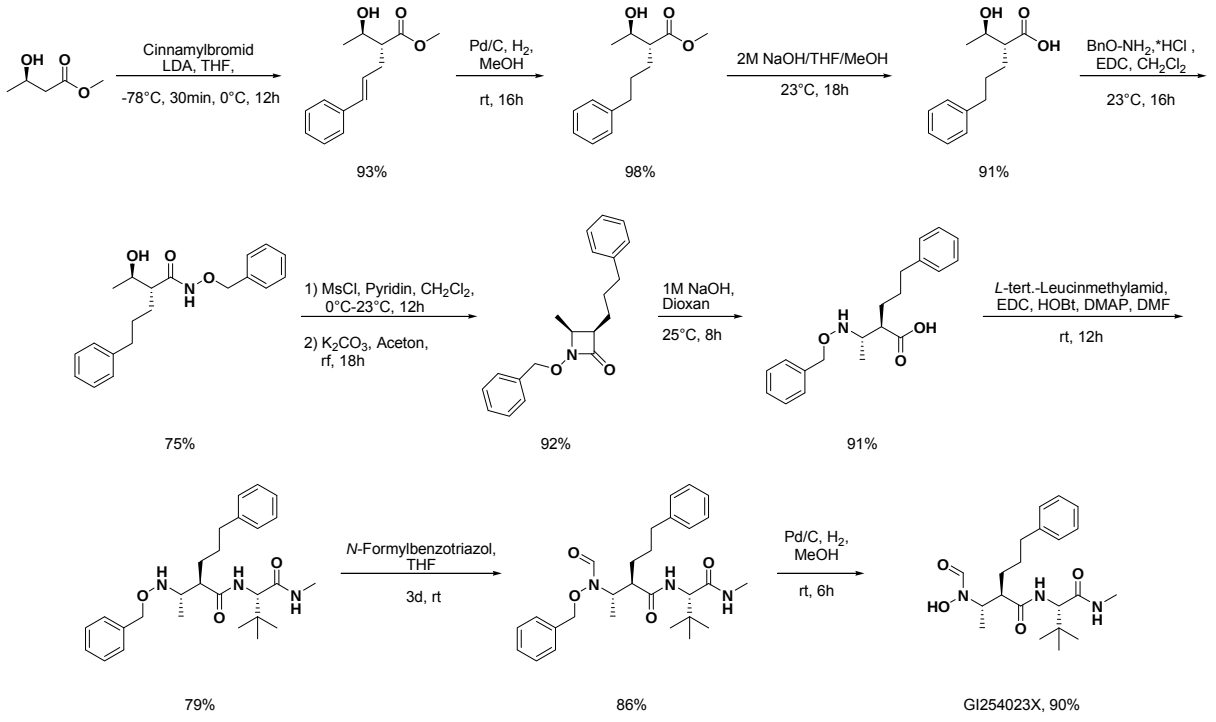

Abb. 25: Verbesserte Synthese des ADAM10 Inhibitors GI254023X. Die Synthese erfolgte durch Nicole Höttecke von 2008-2009.

Es konnte eine Verbesserung der Synthese bezüglich Detektionsmöglichkeit und Säurestabilität der Intermediate erzielt werden. Dieses gelang durch den Austausch

Tetrahydropyranyl-Schutzgruppe, welche bei 220 nM absorbiert, durch eine Benzyl-Schutzgruppe, was eine Detektion bei 254 nM erlaubt. Ebenso verhindert der Wechsel der Schutzgruppe das Auftreten von diastereomeren Intermediaten währende der Synthese. Ein weiterer Vorteil der Benzyl-Schutzgruppe ist die kommerzielle Verfügbarkeit, welche die Synthesekosten drastisch reduzierte.

Durch die Kombination von den Peptidkupplungsreagenzien EDC, HOBt und DMAP konnte das Einführen des *L-tert.*-Leucinmethylamides von der in der Literatur beschriebenen Ausbeute von 33% auf 79% erhöht werden. Mit diesem verbesserten Syntheseschritt erhöhte sich die Gesamtausbeute meiner Synthese auf 38% im Vergleich zu den 22% der beschriebenen GSK Syntheseroute.

Improved synthesis of the ADAM10 inhibitor GI254023X

Nicole Hoettecke[a], Andreas Ludwig[b], Sabine, Foro[a], Boris Schmidt.[a]*

[a]Clemens Schöpf-Institute of Chemistry and Biochemistry, Technische Universität Darmstadt, Petersenstr. 22, D-64287 Darmstadt, Germany.
[b]Institute of Pharmacology and Toxicology, RWTH Aachen University, Pauwelsstr. 30, D-52074 Aachen.

Running head: Improved GI254023X synthesis.

Keywords: Metalloproteinase, ADAM10/17, neurodegenerative disease, inflammation, cancer

[*] Prof. Dr. Boris Schmidt,
Clemens Schöpf-Institute of Chemistry and Biochemistry,
Technische Universität Darmstadt,
Petersenstr. 22, D-64287 Darmstadt, Germany.
Tel: (+49) 6151-163075
Fax: (+49) 6151-163278
E-mail: schmidt_boris@t-online.de

Abstract:

The metalloproteinase ADAM10 and ADAM17 are involved in various diseases: neurodegeneration, cancer and inflammation. Inhibition of these proteases is a promising target in the treatment of inflammation and cancer. Herein we present an improved synthesis of the ADAM10 reference inhibitor GI254023X in higher overall yield, enhanced detection ability and increased acid stability, providing easier handling. This upscaled synthesis, free of diastereomeric intermediates ensures single batch identity, thus warranting reproducibility in further biological investigation.

Introduction:

The disintegrin and metalloproteinase proteases ADAM10 and ADAM17 are involved in neurodegenerative diseases, cancer and inflammation.[1] The surface expressed proteases ADAM10 and ADAM17 cleave the amyloid precursor peptide APP and thereby prevent the generation of the Aβ fragment which is implicated in the generation of amyloid plaques and the development of Alzheimer's disease. ADAM10 and ADAM17 also shed several members of the EGF-receptor ligand family leading to the generation of functionally active ligands that signal cell proliferation in various types of cancer and hyperproliferative diseases. Finally, both proteases shed inflammatory mediators including IL-6 receptor, TNFα, TNFα-receptors, transmembrane chemokines, L-selectin and endothelial adhesion molecules (VCAM-1, JAM-A, VE-cadherin) and thereby affect activation and recruitment of leukocytes.

The inhibition of shedding by ADAM10 and ADAM17 is considered a promising strategy to target cell proliferation and migration in cancer and inflammation. Several inhibitors for ADAM10 and ADAM17 have been described, many of these belong to the peptidomimetic hydroxamic acid inhibitors for metalloproteinase such as batimastat (**1**) and marimastat (**2**).[2-4] These inhibitors affect numerous metalloproteinases, this lack of selectivity may have contributed to their failure in clinical trials. Recent research has demonstrated that ADAM10 and ADAM17 differentially mediate various shedding events depending on the substrate, cell type and stimulatory conditions. Therefore, it is advantageous to increase the specificity of the inhibitors for selected ADAMs. We have recently characterized the reference inhibitor GI254023X (**3**) for ADAM10 (IC_{50} = 5.3 μM) with only minimal effect on ADAM17 (IC_{50} = 541 μM), while no additional ADAM is affected (Scheme 1).[5, 6] Inhibition of the metalloproteinases 9 and 13 were observed at low micromolar level, but they do not interfere with the investigated shedding events,[6] however, a sAPPα reduction to 30% were detected in neuroblastoma cells at a concentration of 10 μM.[7] This inhibitor served in a number of

collaborative studies as an important tool to study cell proliferation and migration in models of cancer and inflammation.[1] Unfortunately, this reference inhibitor is no longer available by commercial suppliers.

Glaxo Smith&Kline disclosed a synthesis of GI254023X (**3**) in a patent application.[8] (Scheme 2). The original synthesis started with $LiNEt_2$ mediated alkylation of the enantiomerically pure (*R*)-(-)-hyxdroxybutyrate (**4**) with cinnamylbromide followed by a subsequent hydrogenation over palladium on carbon to obtain (*R*)-methyl-2-((*R*)-1-hydroxyethyl)-5-phenylpentanoate (**6**). The following saponification to **7** was performed with 1M NaOH in a mixture of THF/MeOH. The hydroxylamine moiety was introduced using 2-tetrahydropyranyl-oxyamine in combination with EDC. Activation of the hydroxyl group with methanesulfonyl chloride and subsequent cyclization resulted in the β-lactam ring (**9**). Basic cleavage of the β-lactam ring and formylation of the amine with a mixed anhydride provided the key building block of GI254023X in 81% yield. Introduction of *L-tert.*-leucinemethylamide (**21**), which was prepared in two steps from Boc-*L-tert.*-leucine with BOP reagent, HOBt and nMM, led to **12** in a moderate yield of 36%. The final deprotection of **12** with acetic acid in water provided GI254023X in an overall yield of 20%.[8]

An upscaled synthesis of **3** in an overall yield of a mere 20% yield implies high costs for reagents and starting materials. Furthermore, the THP protected intermediates (**8-12**) do not absorb at 254 nM wavelengths, which impairs their handling by standard TLC and HPLC equipment. The undefined stereogenic centre of the tetrahydropyrane (THP) results in diastereomeric intermediates, complicating analysis and purification even further. An upscalable synthesis is thus required for this reference inhibitor, as single batch identity is essential for reproducibility and comparability of animal trials. Therefore our aim was to improve the synthesis of **1** with respect to costs, yields and detectability.

Material and Methods

Synthesis:

The first three steps of the improved synthesis follow the Glaxo synthesis.[8] However, the THP-hydroxylamine was replaced by benzyl-hydroxylamine, which was introduced using EDC in a DMF/water mixture in good yield (75%) (Scheme 4).[9] This exchange provides several advantages in respect of costs and substance handling. The latter is due to the detection at 254 nM compared to 215 nM of the THP-protected analogue. Additionally, the intermediates **13-17** are less acid labile and diastereomers were avoided at all reaction steps.

The alcohol **13** was activated with methanesulfonyl chloride and cyclized to the β-lactam intermediate **14** in very good yield (92%).[8] Single crystal X-ray diffraction analysis of **14** confirmed the relative configuration, (Figure1) of the intermediate lactam.

The high yielding (91%) β-lactam-cleavage is followed by the amide generation with *L-tert*.-leucinemethylamide (**21**). This sterically hindered amide formation typically proceeds in yields around 35%. Careful optimisation delivered EDC hydrochloride, HOBt and additional activation with DMAP, as superior reagents. This allowed the isolation of **16** in good yield (76%).

We replaced Glaxo's *L-tert.*-leucinemethylamide (**21**) synthesis starting with Boc-*L-tert.*-leucine by Malons´ *et al.* method (Scheme 4).[10, 11] This method requires a 2 step protocol from commercial building blocks replacing the previous formal 3 step synthesis. However *L-tert.*-leucine (**18**) is far more suitable for upscaled synthesis due to the ease of handling and atom economy.

Preparation of the formamide **17** was carried out in two variants: 1) by usage of the reported mixed anhydride (64%), or 2) by usage of *N*-formylbenzotriazole as formylation reagent (83%).[14, 15] The decision to introduce the formamide at the end of this route is reasoned by the ability of formamides to form *E*/*Z* isomers, which complicate spectroscopic analysis.[16, 17] Hydrogenation of **17** delivered GI254023X in very good yield (90%).[9] Noteworthy, **3** is not detectable at 254 nM, but rather at a range from 210-220 nM and is thus the single compound in this synthesis requiring more than standard detection equipment. (Figure 2)

Cellular CX3CL1-cleavage assay:

CX3CL1-expressing ECV304 cells were grown on 6-well plates in DMEM medium containing 10%FCS. Confluent cell layers were washed and incubated in DMEM medium containing the indicated concentrations of metalloproteinase inhibitor GI254023X (n=3 for each concentration) for 16 h. Subsequently, supernatants were harvested, cleared by 10 min centrifugation at 10000g and analyzed for the presence of soluble and transmembrane CX3CL1, respectively. Quantification was carried out by use of a specific ELISA for CX3CL1 as described previously.[5] Means were calculated from triplicate determinations, results were plotted as dose-response curve and EC_{50} values were determined using GraphPadPrism 5.01 software (San Diego, CA).

Results:

In conclusion we have developed an improved synthesis for GI254023X (**3**) with respect to costs, yields and detectability. This allowed us to produce multigram quantities for ongoing biological studies. The batch obtained by the new route displays significantly enhanced biological activity in comparison to an original batch obtained from Glaxo Smith&Kline in 2007. We credit this activity difference to a decomposition of the reference sample over the storage period of two years at 4°C. This decomposition was revealed by HPLC analysis in comparison to a fresh batch of BSc4075. (Figure 2) Thus we recommend storage at -20°C for prolonged periods.

Discussion:

The exchange of the THP protective group by the inexpensive benzyl group results in improved detectability with standard laboratory equipment at 254 nM. Additional advantages are: improved stability of the less acid labile benzyl group and the avoidance of formation of diastereomeric intermediates with the undefined stereogenic centre as an accompaniment of the usage of the THP protective group. *L-tert*.-leucinemethylamide (**21**) was generated in a two step synthesis starting with *L-tert.*-leucine (**18**) to replace Boc-*L-tert*.-leucine (**19**) from the Glaxo synthesis. Furthermore, the amide formation of the two building blocks **15** and **21** was improved from 36% to 79%, which improved overall yield of the divergent synthesis to 38% from the reported 20%.

References:

[1] Pruessmeyer J, Ludwig A: The good, the bad and the ugly substrates for ADAM10 and ADAM17 in brain pathology, inflammation and cancer. Semin. Cell Dev. Biol. 2009;20:164-74.

[2] Marimastat: BB 2516, TA 2516. Drugs R. D, 2003;4:198-203.

[3] Groves MD, Puduvalli VK, Conrad CA, Gilbert MR, Yung WK, Jaeckle K, Liu V, Hess KR, Aldape KD, Levin VA: Phase II trial of temozolomide plus marimastat for recurrent anaplastic gliomas: a relationship among efficacy, joint toxicity and anticonvulsant status. J. Neurooncol. 2006;80:83-90.

[4] Parsons SL, Watson SA, Steele RJ: Phase I/II trial of batimastat, a matrix metalloproteinase inhibitor, in patients with malignant ascites. Eur. J. Surg. Oncol. 1997;23:526-31.

[5] Hundhausen C, Misztela D, Berkhout TA, Broadway N, Saftig P, Reiss K, Hartmann D, Fahrenholz F, Postina R, Matthews V, Kallen K-J, Rose-John S, Ludwig A: The disintegrin-like metalloproteinase ADAM10 is involved in constitutive cleavage of CX3CL1 (fractalkine) and regulates CX3CL1-mediated cell-cell adhesion. Blood 2003;102:1186-95.

[6] Ludwig A, Hundhausen C, Lambert MH, Broadway N, Andrews RC, Bickett DM, Leesnitzer MA, Becherer JD: Metalloproteinase inhibitors for the disintegrin-like metalloproteinases ADAM10 and ADAM17 that differentially block constitutive and phorbol ester-inducible shedding of cell surface molecules. Comb. Chem. High Throughput Screen 2005;8:161-71.

[7] Endres K, Postina R, Schroeder A, Mueller U, Fahrenholz F.: Shedding of the amyloid precursor protein-like protein APLP2 by disintegrin-metalloproteinases. Febs J. 2005; 272:5808-20.

[8] Andrews RC, Andersen MW, Cowan DJ, Deaton DN, Dickerson SH, Drewry DH, Gaul MD, Luzzio MJ, Marron BE, Rabinowitz MH. Preparation of peptidyl formamide compounds as therapeutic agents. (Glaxo Group Limited, UK; et al.). 2000. 127 pp.

[9] Walz AJ, Miller MJ: Synthesis and biological activity of hydroxamic acid-derived vasopeptidase inhibitor analogues. Org. Lett. 2002;4:2047-50.

[10] Malon P, Pancoska P, Budesinsky M, Hlavacek J, Pospisek J, Blaha K: Amino acids and peptides. CLXXXII. Chiroptical properties and conformation of *N*-acetyl-L-amino

acids *N*'-methylamides with aliphatic side chains. Collect. Czech. Chem. Commun. 1983;48:2844-61.

[11] Randolph JT, Chen H-J, Degoey DA, Flentge CA, Flosi WJ, Grampovnik DJ, Huang PP, Hutchinson DK, Kempf DJ, Klein LL, Yeung MC. Preparation of amino acid hydrazide derivatives as HIV protease inhibitors. (Abbott Laboratories, USA). 2005. 281 pp.

[12] Thorstensson F, Wangsell F, Kvarnstroem I, Vrang L, Hamelink E, Jansson K, Hallberg A, Rosenquist A, Samuelsson B: Synthesis of novel potent hepatitis C virus NS3 protease inhibitors: Discovery of 4-hydroxy-cyclopent-2-ene-1,2-dicarboxylic acid as a *N*-acyl-*L*-hydroxyproline bioisostere. Bioorg. Med. Chem. 2007;15:827-38.

[13] Rosenquist A, Thorstensson F, Johansson P-O, Kvarnstroem I, Ayesa S, Classon B, Rakos L, Samuelsson B. Preparation of peptidomimetic compounds as HCV NS3 serine protease inhibitors. (Medivir AB, Swed.). 2005. 179 pp.

[14] Ten Haken P, Naisby TW, Gary ACG. Fungicides of certain *N*-acyl amino acid derivatives and their use. (Shell Internationale Research Maatschappij B. V., Neth.). 1982. pp. 29 pp.

[15] Katritzky AR, Chang HX, Yang B: *N*-Formylbenzotriazole: a stable and convenient *N*- and *O*-formylating agent. Synthesis 1995:503-5.

[16] Liu M-H, Chen C, Liu C-W: Theoretical Study of Formamide Tautomers-A Discussion of Enol-Keto Isomerizations and Their Corresponding Energies. Struct. Chem. 2004;15:309-16.

[17] Siddall TH, III: Direct measurement of the rate of internal rotation in a formamide. Inorg. Nucl. Chem. Lett. 1965;1:155-9.

Acknowledgements:

We would like to thank Prof. Harald Kolmar and his group (Technische Universität Darmstadt, Clemens Schöpf-Institute of Chemistry and Biochemistry, Petersenstrasse 22, D-64287 Darmstadt) for the use of their HPLC. We also thank Prof. Dr. Hartmut Fuess, Technische Universität Darmstadt, FG Strukturforschung, FB Material- und Geowissenschaften, Petersenstrasse 23, D-64287 Darmstadt, for diffractometer time. This work was supported in part by the SFB 542; project A12 of the German Research Foundation.

Figures:

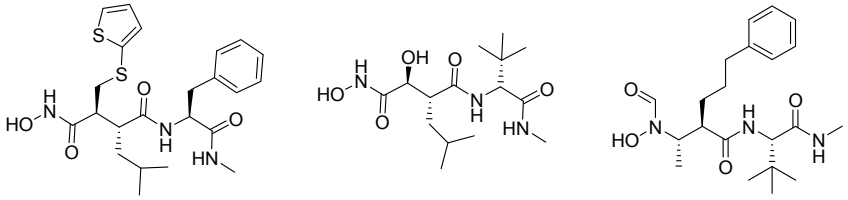

1 Batimastat **2 Marimastat** **3 GI254023X**

Scheme 1: ADAM10 inhibitors.

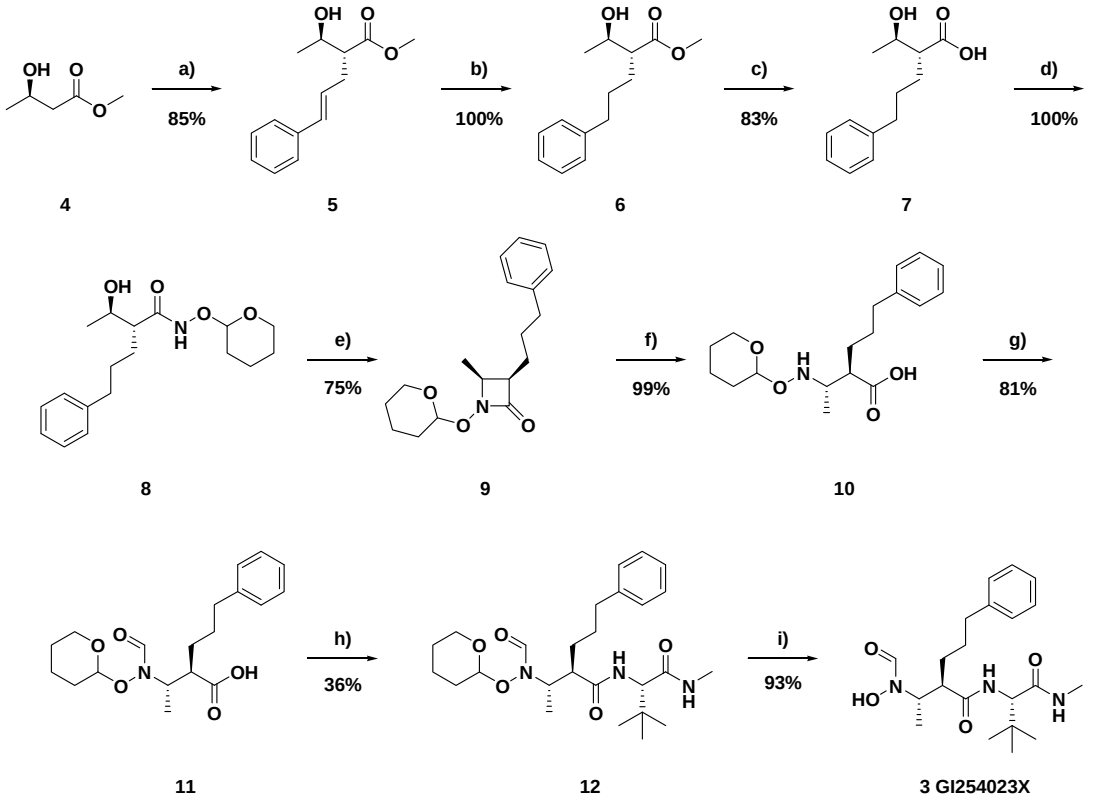

Scheme 2: *Reagents and conditions:* **a)** Cinnamylbromide, LDA, THF, -78°C, 30min, 0°C, 16h; **b)** Pd/C, H_2, MeOH, rt, 16h; **c)** 2M NaOH/THF/MeOH = 1/3/1, 23°C, 20h; **d)** 2-tetrahydropyranyl-oxyamine, EDC, CH_2Cl_2, 23°C, rt, 16h; **e) 1)** MsCl, pyridine, CH_2Cl_2, 0°C-23°C, 14h; **2)** K_2CO_3, acetone, rf, 28h; **f)** 1M NaOH, dioxane, 23°C, 23h; **g)** pyridine, formic acetic anhydride 0°C→25°C; **h)** *L-tert*.-leucinemethylamide, BOP reagent, HOBt, nMM, DMF, 25°C, 20h; **i)** acetic acid/water, 4/1, 50°C, 16h. Overall yield of the divergent synthesis strategy: 20%.

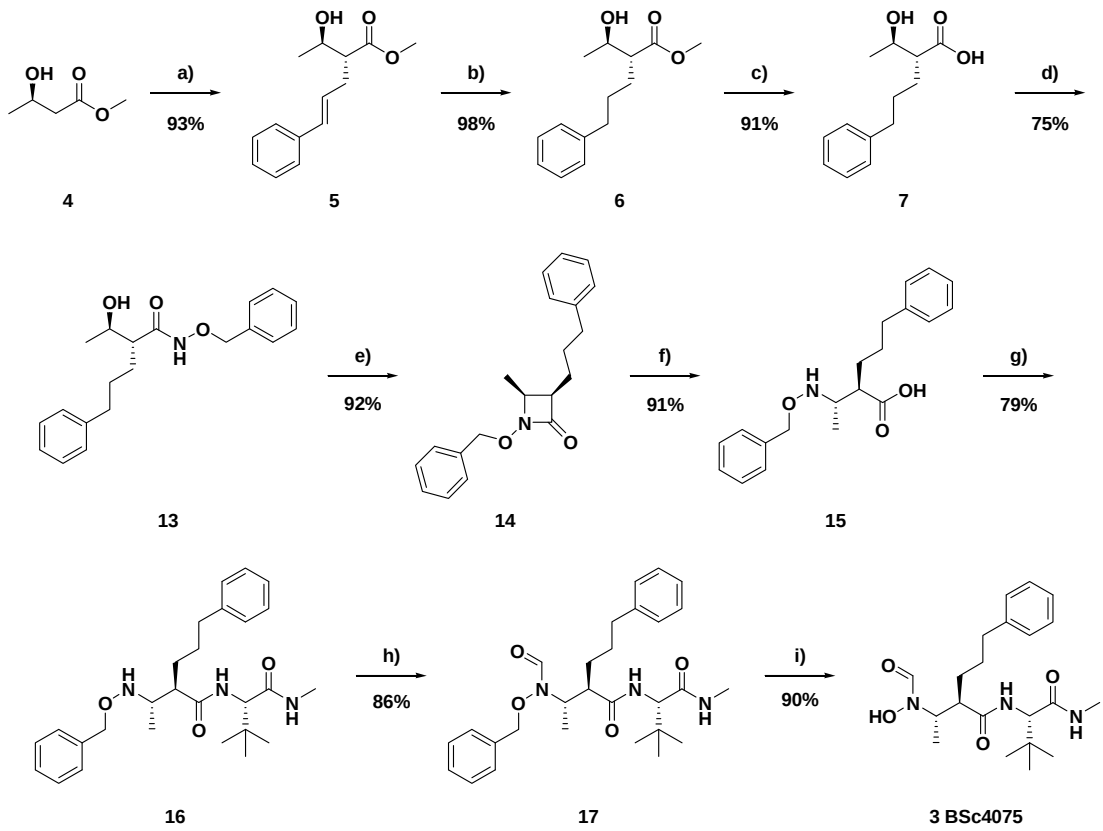

Scheme 3: *Reagents and conditions:* **a)** Cinnamylbromide, LDA, THF, -78°C, 30min, 0°C, 12h; **b)** Pd/C, H_2, MeOH, rt, 18h; **c)** 2M NaOH/THF/MeOH = 1/3/1, rt, 18h; **d)** *O*-benzylhydroxylamine*HCl, EDC*HCl, DMF/H_2O = 1/6, pH 4.5, rt, 8h; **e)** 1) MsCl, pyridine, CH_2Cl_2, 0°C-rt, 12h; 2) K_2CO_3, acetone, rf, 18h; **f)** 1M NaOH, dioxane, 8h, 25°C; **g)** *L-tert.*-leucinemethylamide, EDC, HOBt, DMAP, DMF, rt, 12h; **h)** *N*-formylbenzotriazole, THF, 3d, rt; **i)** Pd/C, H_2, MeOH, rt, 6h. Overall yield of the divergent synthesis strategy: 38%

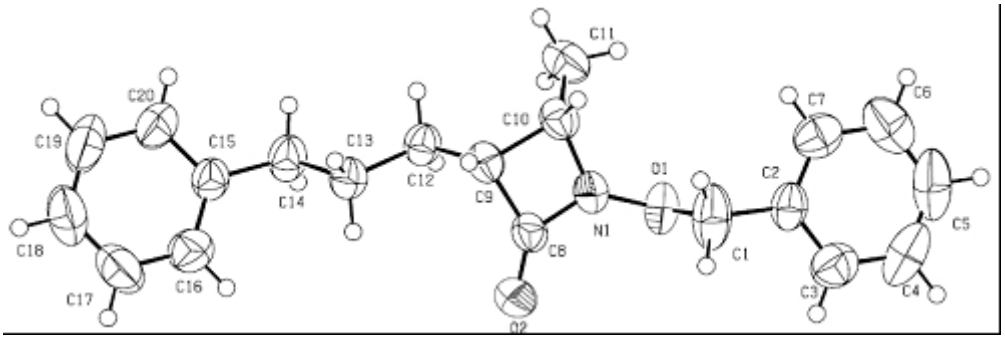

Figure 1: X-Ray analysis of **14**.

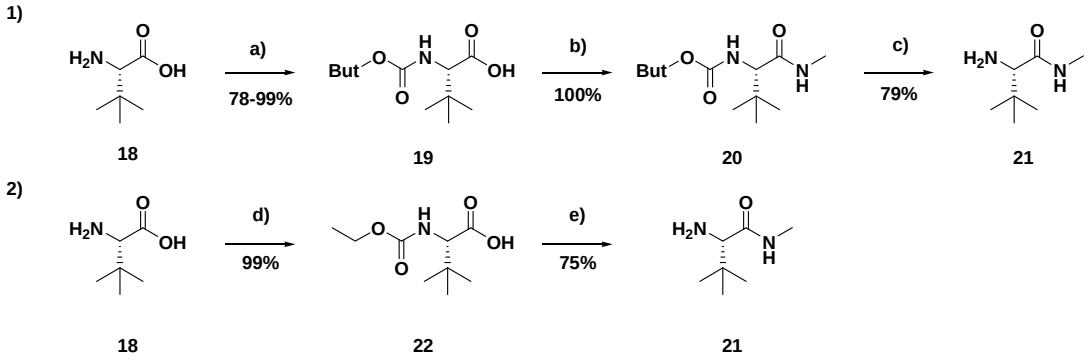

Scheme 4: *Reagents and conditions:* **1)** patent synthesis: **a)** Boc_2O, triethylamine, dioxane[9, 10] **b)** CDI, methylamine*HCl, triethylamine, CH_2Cl_2, 25°C, 19h; **c)** TFA, CH_2Cl_2, 0°C→25°C, 18h. **2)** Alternative route: **d)** ethyl chloroformate, 2M NaOH, 60°C, 12h; **e)** acetyl chloride, rf, 6h, methylamine (etheral solution), 0°C, 12h.

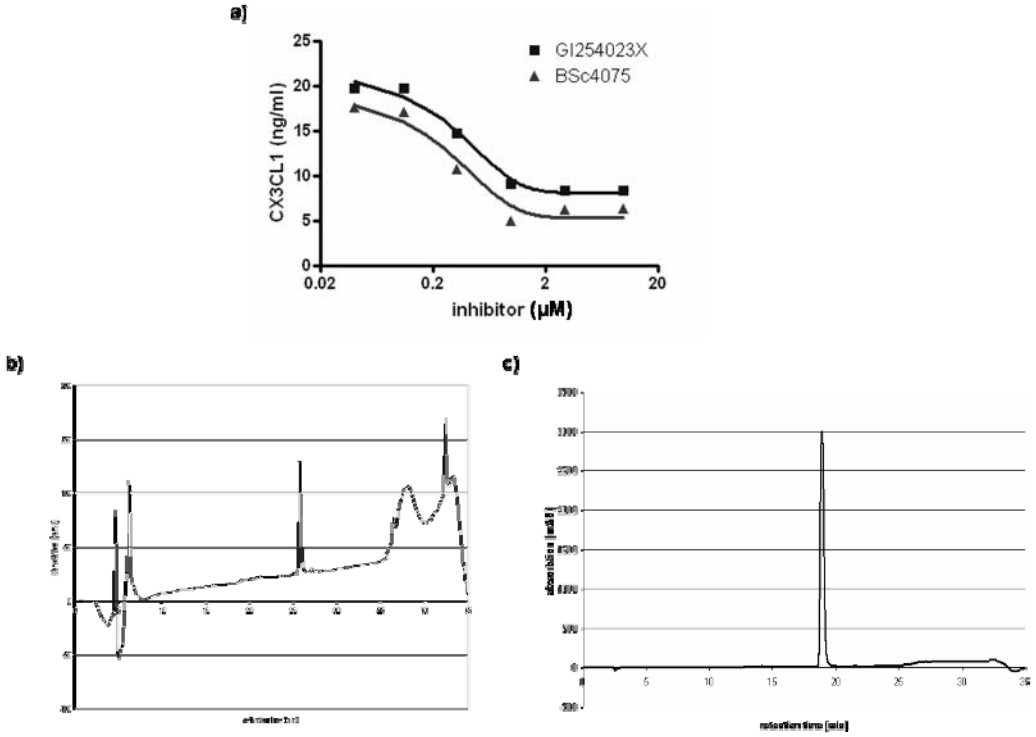

Figure 2: a) GI254023X and BSc4075 were assayed for inhibition of ADAM10-mediated cleavage of the transmembrane chemokine CX3CL1 expressed on ECV304 cells. Soluble CX3CL1 released by the cells in the presence of increasing concentrations of the inhibitors over a time period of 16h was determined by ELISA. **b)** HPLC analysis of GI254023X at 220 nM, **b)** HPLC analysis of BSc4075 at 220 nM.

Supporting information:

General remarks:

Thin-layer chromatography (TLC) was carried out using aluminium sheets precoated with silica gel 60 F254 (0.2 mm; E. Merck). Chromatographic spots were visualized by UV and/or spraying with a methanolic solution of vanillin/H_2SO_4 or aq. $KMNO_4$ solution followed by heating. Flash column chromatography was carried out using Merck silica gel 60 (0.063-0.2 mm). Melting Points were determined on a Mettler FP 51 melting point apparatus and are uncorrected. The ^{1}H and ^{13}C spectra were recorded on a Bruker AC 300 (300 MHz) and AC 500 spectrometer (500 MHz). Chemical shifts are reported as % values (ppm) and adjusted at the central line of the deuterated solvent (MeOD, $CDCl_3$). Mass spectrometry was performed on a Bruker-Franzen Esquire LC mass spectrometer (ESI) and a double focused MAT 95 (EI).

HPLC analysis was carried out using: 1) an Agilent 1100 with a reversed phase column (Zorbax Eclipse XDB-C8; 4.6*150 mm) and a 254 nM detector. The eluent is composed of H_2O (1% TFA) (A) and acetonitrile (B) with a gradient: 30 to 90% B within 12 min. 2) a varian prepstar with a reversed phase column (phenomenex synergi hydro RP 80A; 4.6*250 mm) and a variable detector (Varian pro star) using wavelengths of 220 nM and 280 nM. The eluent is composed of H_2O (0.1% TFA) (A) and acetonitrile (B) with a gradient: 10 to 60% B (30 min rather 3) 40 min) and 5 min 90 acetonitrile for re-equilibration. All reagents and solvents (THF, DMF, CH_2Cl_2, ethyl acetate, MeOH) were purchased at ABCR, Acros and Alfa Aesar, TCI, Sigma Aldrich and VWR. Methanol abs. was additionally dried over magnesium. X-Ray analysis was carried out with CAD-4/PC Software (Nonius, 1996); cell refinement: CAD-4/PC Software; data reduction: REDU4 (Stoe & Cie, 1987); program(s) used to solve structure: SHELXS97 (Sheldrick, 1997); program(s) used to refine structure: SHELXL97 (Sheldrick, 1997); molecular graphics: PLATON (Spek, 2003); software used to prepare material for publication: SHELXL97.

Experimental data:

(*R*,*E*)-Methyl 2-((*R*)-1-hydroxyethyl)-5-phenylpent-4-enoate (5)

To a solution of diisopropylamine (18.85 g, 186.23 mmol) in THF (200 mL) was added *n*-BuLi (2.5 M, 74.49 mL, 186.23 mmol) at a temperature of -78°C. After 30 min stirring **4** (10.00 g, 84.65 mmol) was added slowly within 20 min. After additional 30 min stirring cinnamylbromide (18.35 g, 93.12 mmol) and DMPU (32 mL, 10%v/v) were added. The reaction mixture was allowed to warm up to 0-1°C (fridge). After 16h the reaction mixture was quenched with saturated NH_4Cl (30 mL), poured into 1M HCl (200 mL) and was extracted three times with ethyl acetate (200 mL) The combined organic layers were dried over $MgSO_4$, filtered and concentrated *in vacuo* and purified by silica gel chromatography (with a gradient from cyclohexane to 3:1 cyclohexane : ethyl acetate) to give 16.15 g (81%) of **5** as a yellow solid. **^{1}H NMR** (500 MHz, $CDCl_3$) ppm δ: = 7.29 (m, 5H, H-10/H-11/H-12), 6.46 (m, 1H, H-7), 6.22-6.06 (m, 1H, H-8), 4.00 (br.s, 1H, H-4), 3.71 (s, 3H, H-1), 2.70 (m, 1H, H-3), 2.61-2.55 (m, 2H, H-6), 1.31-1.22 (d, ^3J = 6.4 Hz, 3H, H-5). **HPLC:** 5.758 min (method: 1).

(*R*)-Methyl-2-((*R*)-1-hydroxyethyl)-5-phenyl-pentanoate (6)

To a solution of **5** (16.15 g, 68.93 mmol) in MeOH (150 mL) was added 10% Pd on activated carbon (0.162 g, 10 w/w). The resulting suspension was flushed over a period of 5 min with hydrogen and then stirred for 1h at rt and normal pressure. The catalyst was removed by filtration through Celite and the filtrate was concentrated *in vacuo* to give 16.00 g (98%) of **6** as a yellow solid. **^{1}H NMR** (500 MHz, $CDCl_3$) ppm δ: = 7.22-7.17(m, 2H, H-11), 7.14-7.04 (m, 3H, H-10/12), 3.89-3.75 (m, 1H, H-4), 3.62 (s, 3H, H-1), 2.62-2.48 (q, ^3J = 6.3 Hz, 2H, H-8), 2.43-2.26 (m, 1H, H-3), 1.17-1.07 (m, 4H, H-6/7), 1.58 (d, ^3J = 6.4 Hz, 3H, H-5). **HPLC:** 5.758 min (method: 1).

(*R*)-2-((*R*)-1-Hydroxyethyl)-5-phenylpentanoic acid (7)

To a solution of **6** (16.00 g, 67.71 mmol) in MeOH (50 mL) and THF (150 mL) was added 2M NaOH (50 mL). The reaction mixture was stirred at rt for 24h, concentrated *in vacuo* and extracted once with cyclohexane (100 mL). The aqueous layer was acidified to pH=2 with aq. H_2SO_4 and extracted three times with ethyl acetate (100 mL). The combined organic layers combined ethyl acetate layers were dried over $MgSO_4$, filtered and concentrated *in vacuo* to give 13.68 g (91%) of **7** as a yellow solid. **^{1}H NMR** (300 MHz, $CDCl_3$) ppm δ: = 7.35-7.25 (m, 2H, H-10), 7.20 (m, 3H, H-10/H-11), 6.93 (br.s, 2H, OH), 3.96 (q, ^3J = 6.4 Hz, 1H, H-3),

2.75-2.57 (m, 2H, H-7), 2.47-2.41 (m, 1H, H-2), 1.80-1.60 (m, 4H, H-5/H-6), 1.28-1.23 (m, 3H, H-4). **HPLC:** 4.417 min (method: 1).

(*R*)-*N*-(Benzyloxy)-2-((*R*)-1-hydroxyethyl)-5-phenylpentanamide (13)

To a solution of **7** (0.20 g, 0.90 mmol) in H_2O (6 mL) and DMF (6 mL) was added *O*-benzyl-hydroxylamine-hydrochloride (0.22 g, 1.35 mmol) at rt and the pH was adjusted to 4.5 with aq. $NaHCO_3$. To the reaction mixture was added EDC (0.17 g, 0.9 mmol) and the pH of the solution was kept at pH=4 with 1M HCl. After stirring at rt for 1h the reaction mixture was extracted twice with ethyl acetate (30 mL). The combined organic layers were washed sequentially with 1M citric acid (100 mL), $NaHCO_3$ aq. (100 mL) and brine (100 mL). The organic layer was dried over $MgSO_4$, filtered and concentrated *in vacuo* to give 0.22 g (75%) of **13** as a colourless solid. **^{1}H NMR** (500 MHz, $CDCl_3$) ppm δ: = 7.37-7.08 (m, 10H, H-9-11/H-14-16), 4.83 (s, 2H, H-12), 3.93-3.73 (m, 1H, H-2), 2.55 (t, ^3J = 7.3 Hz, 2H, H-8), 1.87 (d, ^3J = 3.4 Hz, 1H, H-3), 1.76-1.35 (m, 4H, H-5/H-6), 1.24-1.01 (m, 3H, H-1). **HPLC:** 6.019 min (method: 1).

(3*R*,4*S*)-1-(Benzyloxy)-4-methyl-3-(3-phenylpropyl)azetidin-2-one (14)

To a solution of **13** (1.27 g, 3.89 mmol) in CH_2Cl_2 (10 mL) was added pyridine (1.66 g, 20.93 mmol) and mesyl chloride (0.54 g, 4.67 mmol) at 0°C. The reaction mixture was allowed to warm to rt and stirred for 16h. The reaction was quenched with 2M HCl (10 mL) and extracted three times with CH_2Cl_2 (20 mL). The combined organic layers were washed with brine (50 mL), dried over $MgSO_4$ and concentrated *in vacuo*, to give 1.51 g (96%) of the intermediate as a yellow solid. A suspension of the intermediate (1.513 g, 3.73 mmol) and K_2CO_3 (1.548 g, 11.20 mmol) in acetone (10 mL) was heated under reflux for 24h. The suspension was filtered, the filtrate concentrated *in vacuo* and purified by silica gel chromatography (with a gradient cyclohexane to CH_2Cl_2) to give 1.11 g (96%) of **14** as an oil. **^{1}H NMR** (500 MHz, $CDCl_3$) ppm δ: = 7.42-7.34 (m, 5H, H-9/H-15/H-16), 7.30-7.25 (m, 2H, H-14), 7.20-7.15 (m, 3H, H-8/H-10), 4.96 (d, ^2J = 11.3 Hz, 1H, H-12), 4.91 (d, ^2J = 11.3 Hz, 1H, H-12), 7.35 (dt, ^3J = 5.5 Hz, ^3J = 6.3 Hz, 1H, H-3), 2.82 (dt, ^3J = 7.5 Hz, ^3J = 7.6 Hz, 1H, H-2), 2.71-2.55 (m, 2H, H-6), 1.88-1.40 (m, 4H, H-4/H-5), 1.01 (d, ^3J = 6.4 Hz, 3H, H-10). **MS** (m/z, 70 eV, EI) = 310 (M^+), 194, 277, 250, 236. **HPLC:** 8.382 min (method: 1).

(*R*)-2-((*S*)-1-(Benzyloxyamino)ethyl)-5-phenylpentanoic acid (15)

To a solution of **14** (0.47 g, 1.51 mmol) in dioxane (4.9 mL, 3.250 mL/mmol) was added 1M NaOH (2.27 mL, 1.5 mL/mmol) and the reaction mixture was stirred at 25°C for 6h. The reaction mixture was extracted with cyclohexane and the aqueous layer was acidified to pH=3 with 1M HCl and extracted three times with ethyl acetate (20 mL). The combined ethyl acetate layers were washed with brine (50 mL), dried over $MgSO_4$, filtered and concentrated *in vacuo* to give 0.45 g (91%) of **15** as a colourless solid. **^{1}H NMR** (300 MHz, $CDCl_3$) ppm δ: = 7.44-7.31 (m, 5H, H-7/H-8, H-14), 7.32-7.24 (m, 2H, H-6), 7.23-7.14 (m, 3H, H-13/H-15), 4.79 (q, ^3J = 11.6, Hz, 2H, H-4), 3.31 (dq, ^3J = 6.8 Hz, ^4J = 4.2 Hz, 1H, H-3), 2.84-2.76 (m, 1H, H-2), 2.71-2.58 (m, 2H, H-12), 1.97-1.57 (m, 3H, H-11/12), 1.47-1.32 (m, 1H, H-11/12), 1.06 (d, ^3J = 6.8 Hz, 3H, H-9). **α-D** (DCM. 2 mg/2 mL): + 9.0 **HPLC:** 6.410 min (method: 1).

(*R*)-2-((*S*)-1-(Benzyloxyamino)ethyl)-*N*-((*S*)-3,3-dimethyl-1-(methylamino)-1-oxobutan-2-yl)-5-phenylpentanamide (16)

To a solution of **15** (0.30 g, 0.92 mmol) in DMF abs. (6 mL) under argon atmosphere was added EDC (0.21 g, 1.10 mmol) and HOBt (0.12 g, 0.87 mmol). After stirring at rt for 15 min DMAP (0.11 g, 0.87 mmol) and **20** (0.16 g, 1.10 mmol) were added. The reaction mixture was quenched after 12h with 1M citric acid (20 mL) and extracted twice with ethyl acetate (30 mL). The combined organic layers were washed sequentially with aq. $NaHCO_3$ and brine, dried over Na_2SO_4, filtered and concentrated *in vacuo* to give 0.33 g (79%) of **16** as a colourless solid. **^{1}H NMR** (500 MHz, $CDCl_3$) ppm δ: = 7.29-7.21 (m, 5H, H-10/H-11/H-18), 7.18-7.14 (m, 2H, H-9), 7.08 (dd, ^3J = 7.5 Hz, ^3J = 7.5 Hz, 2H, H-17/H-19), 6.61 (br.s, 1H, NH), 4.75 (d, ^2J = 11.5 Hz, 1H, H-7), 4.71 (d, ^2J = 11.5 Hz, 1H, H-7), 4.28 (d, ^3J = 9.3 Hz, 1H, H-4), 3.17-3.15 (m, 1H, H-1), 2.62 (t, ^3J = 8.1 Hz, 3H, H-6), 2.56-2.46 (m, 3H, H-2/H-15), 1.71-1.64 (m, 1H, H-15), 1.56-1.46 (m, 2H, H-13/H-15), 1.40-1.31 (m, 1H, H-13), 0.99 (d, ^3J = 6.5 Hz, 3H, H-12), 0.91 (s, 9H, H-21). **^{13}C NMR** (125 MHz, $CDCl_3$) ppm δ: = 173.2 (C-3), 171.2 (C-5), 142.0 (C-16), 128.5, 128.4, 128.3, 128.2, 128.1 (CH), 125.7 (C-19), 76.5 (C-7), 60.5 (C-4), 57.6 (C-1), 47.7 (C-2), 35.8 (C-15), 34.4 (C-20), 29.4 (C-14), 28.3 (C-13), 26.8 (C-21), 25.9 (C-6), 14.2 (C-12). **MS** (m/z, 70 eV, EI) = 455 (M^+), 394, 304, 273, 91, 86. **HPLC:** 6.444 min (method: 1).

(*R*)-2-((*S*)-1-(*N*-(Benzyloxy)formamido)ethyl)-*N*-((*S*)-3,3-dimethyl-1-(methylamino)-1-oxobutan-2-yl)-5-phenylpentanamide (17)

To a solution of **16** (1.14 g, 2.51 mmol), in THF (22 mL) under argon atmosphere was added *N*-formylbenzotriazole (0.66 g, 4.46 mmol). The reaction mixture was stirred at rt for 3d and then concentrated *in vacuo*. The residue was dissolved in ethyl acetate (20 mL) and extracted three times with 1M NaOH (20 mL). The organic layer was dried over Na_2SO_4, filtered and concentrated *in vacuo*. The compound was purified by silica gel chromatography (50:1, CH_2Cl_2 : MeOH) to give 1.04 g (86%) of **17** as a colourless solid. Mp: 137°C. **^{1}H NMR** (500 MHz, D6-DMSO) ppm δ: = 8.45-8.34 (br.s, 1H, H-7), 8.17-8.08 (br.s, 1H, H-7), 8.02 (d, ^3J = 9.5 Hz, 1H, NH), 7.81 (d, ^3J = 4.5 Hz, 1H, NH), 7.48 (d, ^3J = 6.7 Hz, 2H, H-11), 7.43-7.37 (m, 3H, H-10/H-12), 7.22-7.19 (m, 3H, H-18), 7.13-7.10 (m, 3H, H-17/H-19), 5.56-5.47 (d, ^3J = 7.8 Hz, 1H, NH´), 5.08-4.83 (m, 2H, H-8), 4.32 (br.s, 1H, H-6´), 4.28-4.26 (m, 1H, H-3), 3.87 (br.s, 1H, H-6) 2.96 (br.s, 1H, H-5), 2.59-2.55 (m, 1H, H-15), 2.53 (d, ^3J = 4.2 Hz, 3H, H-1), 2.46-2.38 (m, 3H, H-15), 1.77-1.69 (m, 1H, H-15´), 1.67-1.57 (m, 1H, H-14), 1.53-1.49 (m, 1H, H-14´) 1.46-1.35 (m, 2H, H-13), 1.30-1.25 (m, 1H, H-14) 1.25 (s, 3H, H-22´), 1.24-1.20 (d, ^3J = 6.6 Hz,, 3H, H-22), 1.18-1.13 (m, 1H, H-14´), 1.07-1.05 (m, 1H, H-15´) 0.94 (s, 9H, H-21), 0.90 (s, 3H, H-21´). **^{13}C NMR** (125 MHz, D6-DMSO) ppm δ: = 173.0 (C-4), 170.9 (C-2),142.5 (C-16), 129.6, 129.4, 128.7, 128.5, 128.4, 125.8 (CH), 60.3 (C-3), 48.7 (C-5), 47.9 (C-5´), 35.3 (CH_2), 34.3 (C-10), 33.7,30.0, 28.5 (CH_2), 27.2 (C-21), 25.7 (CH_2), 25.5 (CH_3), 25.3 (CH_3), 24.8 (CH_2). **MS** (m/z, 70 eV, ESI) = 504 (M+Na). **HPLC:** 7.173 min (method: 1)**.**

(*R*)-*N*-((*S*)-3,3-Dimethyl-1-(methylamino)-1-oxobutan-2-yl)-2-((*S*)-1-(*N*-hydroxyform-amido)ethyl)-5-phenylpentanamide (3)

To a solution of **17** (3.03 g, 6.29 mmol) in MeOH (236 mL) was added 10% Pd on activated carbon (0.300 g, 10% w/w). The resulting suspension was flushed over a period of 5 min with hydrogen and then stirred at rt and normal pressure for 6h. The catalyst was removed by filtration through a 0.30 µm filter, the filtrate was concentrated *in vacuo* and recrystallized from CH_2Cl_2 with Et_2O to give 2.22 g (90%) of **3** as a colourless solid. **^{1}H NMR** (500 MHz, D4-MeOH) ppm δ: = 8.29 (s, 1H, H-7´), 8.00 (s, 1H, H-7), 7.21 (t, ^3J = 7.6 Hz, 2H, H-14), 7.16-7.07 (m, 3H, H-13/H-15), 4.55-4.48 (m, 1H, H-6´), 4.27 (s, 1H, H-3), 3.87-3.81 (m, 1H, H-6), 2.89-2.85 (m, 1H, H-5), 2.81-2.77 (m, 1H, H-5´), 2.63 (s, 3H, H-1), 2.61-2.56 (m, 1H, H-11), 2.52-2.46 (m, 1H, H-11), 1.89-1.81 (m, 2H, H-11´), 1.75-1.66 (m, 2H, H-10´), 1.57-1.42 (m, 4H, H-9/H-10), 1.28 (d, ^3J =6.5 Hz, 3H, H-8), 1.19 (d, ^3J = 6.7 Hz, 3H, H-8´),

1.00 (s, 9H, H-17). **^{13}C NMR** (125 MHz, D4-MeOH) ppm δ: = 175.9 (C-4), 173.1 (C-2), 164.1 (C-7), 159.6 (C-7), 143.7 (C-12), 129.4, 126.7 (C-13/C-14/C-15), 62.2 (C-3), 58.7 (C-6), 53.7 (C-5´), 50.2 (C-5), 36.8 (C-12), 35.2 (C-16), 34.8 (C-12´), 31.3 (C-11), 31.2 (C-10´), 30.0 (C-11´), 27.2 (C-17), 26.1 (C-10), 17.6 (C-8), 16.5 (C-8´), **HPLC:** 18.37 min (method: 2).

(*S*)-2-(Ethoxycarbonylamino)-3,3-dimethylbutanoic acid (22)

To a suspension of *L-tert.*-leucine **(18)** (1.50 g, 11.43 mmol) in dioxane (7.5 mL) was added 2M NaOH (18 mL) and ethyl chloroformate (2.36 g, 21.73 mmol). After stirring at 60°C for 12h the reaction mixture was allowed to cool to rt and extracted with CH_2Cl_2 (40 mL). The aqueous layer was acidified to pH=3 with 1M HCl and extracted three times with ethyl acetate (40 mL). The combined organic layers were washed with brine, dried over Na_2SO_4, filtered and concentrated *in vacuo* to give 2.29 g (99%) of **22** as a colourless rubber. **^{1}H NMR** (300 MHz, D4-MeOH) ppm δ: = 4.10 (tt, ^{3}J = 5.3 Hz, ^{3}J = 4.6 Hz, 2H, H-4), 4.00 (s, 1H, H-2), 1.31-1.19 (m, 3H, H-5), 1.01 (s, 9H, H-9). **^{13}C NMR** (75 MHz, D4-MeOH) ppm δ: = 174.7 (C-1), 158.9 (C-3), 63.9 (C-2), 62.1 (C-4), 34.9 (C-6), 27.1 (C-7), 14.5 (C-5).

***L*-tert.-Leucinemethylamide (21)**

Acetyl chloride (1.77 g, 22.56 mmol) was added to a solution of **22** (2.29 g, 11.29 mmol) in toluene (20 mL). After stirring at 110°C for 6h the reaction mixture was allowed to cool to rt and concentrated *in vacuo*. The residue was solved in an etheral methylamide (1.00 mmol methylamide hydrochloride, 1.00 mmol KOH, in 1.3 mL Et_2O) solution (80 mL) and kept at 1°C for 12h. The reaction mixture was filtrated, the residue dissolved in Et_2O and precipitated with petroleum ether to give 1.22 g (75%) of **21** as a colourless solid. **^{1}H NMR** (300 MHz, D4-MeOH) ππμ δ: = 6.77 (br.s, 1H, NH), 3.07 (s, 1H, H-3), 2.81-2.69 (m, 1H, H-1), 1.98-1.86 (m, 2H, NH_2), 0.93 (s, 9H, H-5).

JBC Papers in Press. Published on October 29, 2009 as Manuscript M109.059394
The latest version is at http://www.jbc.org/cgi/doi/10.1074/jbc.M109.059394

The disintegrin and metalloproteinase 17 (ADAM17) mediates inflammation-induced shedding of syndecan-1 and -4 by lung epithelial cells

Jessica Pruessmeyer[1,2], Christian Martin[1], Franz M. Hess[1], Nicole Schwarz[1], Sven Schmidt[1], Tanja Kogel[1,2], Nicole Hoettecke[3], Boris Schmidt[3], Antonio Sechi[4], Stefan Uhlig[1], Andreas Ludwig[1,2]

[1] Institute of Pharmacology and Toxicology, Medical Faculty, RWTH Aachen University, Aachen, Germany; [2] Interdisciplinary Center for Clinical Research Biomat., Medical Faculty, RWTH Aachen University, Aachen; Germany; [3] Clemens Schöpf-Institute of Chemistry and Biochemistry, Technische Universität Darmstadt, Darmstadt, Germany; [4] Institute for Biomedical Engineering – Cell Biology, Medical Faculty, RWTH Aachen University, Aachen, Germany

Running head: Syndecan shedding by ADAM17

Address correspondence to: Andreas Ludwig, Institute of Pharmacology and Toxicology, RWTH Aachen University, Pauwelsstr. 30, 52074 Aachen, Germany; Phone: +49 241 8035771, Fax: +49 241 8082716, E-Mail: aludwig@ukaachen.de

Syndecans are cell surface proteoglycans that bind and modulate various proinflammatory mediators and can be proteolytically shed from the cell surface. Within the lung, syndecan-1 and -4 are expressed as transmembrane proteins on epithelial cells and released in the bronchoalveolar fluid during inflammation. We here characterize the mechanism leading to the generation of soluble syndecan-1 and -4 in cultured epithelial cells and murine lung tissue. We show that the bladder carcinoma epithelial cell line ECV304, the lung epithelial cell line A459 and primary alveolar epithelial cells express and constitutively release syndecan-1 and -4. This release involves the activity of the disintegrin-like metalloproteinase ADAM17 as demonstrated by use of specific inhibitors and lentivirally transduced shRNA. Stimulation of epithelial cells with PMA, thrombin or proinflammatory cytokines (TNFα/ IFNγ) led to the downregulation of surface-expressed syndecan-1 and -4 which was associated with a significant increase of soluble syndecans and cell-associated cleavage fragments. The enhanced syndecan release was not related to gene induction of syndecans or ADAM17, but rather due to increased ADAM17 activity. Soluble syndecan-1 and -4 were also released into the bronchoalveolar fluid of mice. Treatment with TNFα/IFNγ increased ADAM17 activity and syndecan release in murine lungs. Both constitutive and induced syndecan shedding was prevented by the ADAM17 inhibitor. ADAM17 may therefore be an important regulator of syndecan functions on inflamed lung epithelium.

Introduction

Syndecans are a family of cell surface proteoglycans that play regulatory roles in wound healing, inflammation, angiogenesis and neuronal patterning. There are four members of the syndecan family (syndecan-1, -2, -3 and -4) each consisting of an ectodomain carrying heparan sulphate or chondroitin sulphate rich glucosaminoglycan chains, a transmembrane domain and a short cytoplasmic tail (1). Syndecan-1 is predominantly found on endothelial and epithelial cells while syndecan-4 is ubiquitously expressed (2). Syndecans are also released as soluble variants that have been found in various body fluids including serum of cancer patients, wound fluid or bronchoalveolar fluid of inflamed lungs (3-7).

Recent research with syndecan-1$^{-/-}$ and syndecan-4$^{-/-}$ mice has demonstrated that syndecans play an important role in the regulation of inflammation and wound healing (1). Syndecans act as coreceptors modulating binding and signaling of cytokines, chemokines and adhesion molecules. Syndecan-1 deficiency results in increased

acute lung inflammation. Syndecan-1 cleavage by matrix metalloproteinase 7 (MMP7) helps to establish a gradient for the chemokine KC guiding transepithelial migration of neutrophils into the airway (8). These activities can be partially reversed by soluble syndecans competing with transmembrane syndecans for their extracellular ligands (9).

Soluble syndecans are generated by proteolytic shedding at the cell surface (4;10;11). A basal shedding activity results in the constitutive release of syndecans by cultured cells. Cell simulation with PMA, thrombin or proinflammatory cytokines enhances the shedding (4;12;13). Matrix metalloproteinases including MMP7, MMP9 and MT-MMP1 were found to be capable of cleaving syndecans (8;11;12;14). However, it remains unclear whether other members of the metalloproteinase family would contribute to syndecan shedding under physiological and pathophysiological conditions. Especially, the disintegrin and a metalloprotease 10 (ADAM10) and the closely related protease ADAM17 appear to be likely candidates for syndecan shedding because they are coexpressed with syndecans in various cell types including epithelial cells (15) and are responsible for constitutive or inducible shedding of several epithelial surface molecules including TNFα, transmembrane chemokines, E-cadherin and junctional adhesion molecule A (16-19). Although it has been proposed that ADAM17 could be a physiologically relevant syndecan sheddase, its involvement in the release of soluble syndecan has not been directly studied.

We here characterize the shedding mechanism leading to the generation of soluble syndecan-1 and -4 by epithelial cells *in vitro* and *in vivo*. We demonstrate that epithelial cells shed syndecan-1 and -4 in a constitutive and inducible fashion. Pharmacologic and genetic evidence is provided that constitutive and induced shedding of both syndecans is critically mediated by ADAM17. Finally, we demonstrate that soluble syndecan-1 and -4 are released into the bronchoalveolar fluid of murine lungs treated with proinflammatory cytokines and that this release is effectively blocked by inhibition of ADAM17. ADAM17 may therefore be an important regulator of syndecan functions on inflamed lung epithelium.

Material and Methods

Recombinant proteins, antibodies, fluorescent dyes, inhibitors

Mouse monoclonal antibodies to syndecan-1 (DL-101, IgG1) and syndecan-4 (5G9, IgG2a) and goat polyclonal antibody to murine syndecan-4 (N-19) were from Santa Cruz Biotechnology (Santa Cruz, USA). Rat monoclonal antibody to murine syndecan-1 (281-2, IgG2a) was from BD Bioscience (San Jose, USA). Human IFNγ and human TNFα were from Peprotech (Hamburg, Germany). Murine IFNγ and murine TNFα, mouse monoclonal antibodies against human ADAM10 and ADAM17, respectively, mouse IgG_{2b} and IgG_1 isotype controls, recombinant catalytic domain of ADAM17, and normal rabbit IgG were from R&D Systems (Wiesbaden, Germany). PE-conjugated or POD-conjugated secondary antibodies were from Jackson (Newmarket, UK). Mouse monoclonal antibody to ß-actin was from Abcam (Cambridge, USA). The ELISA for mouse albumin was from Bethyl Laboratories (Montgomery, USA). The metalloproteinase inhibitors GW280264 and GI254023 were synthesized and assayed for inhibition of recombinant human ADAM17 and ADAM10 as described (16;20). The metalloproteinase inhibitors TMI-1 and TMI-2 were synthesized and characterized by Wyeth Research, (Cambridge MA, USA) (21). The γ-secretase-inhibitor DAPT (N-[N-(3,5-difluorophenacetyl-L-alanyl)]-S-phenylglycine *t*-butyl ester) was from Calbiochem (Darmstadt, Germany). Goat anti-mouse IgG conjugated to Alexa Fluor 594 and goat anti-rabbit IgG conjugated to Alexa Fluor 488 were from Molecular Probes/Invitrogen (Karlsruhe, Germany). Trap6 was from Sigma (Munich, Germany).

DNA constructs

Short hairpin RNA (shRNA) targeting ADAM10 and ADAM17 was inserted into the lentiviral expression vector pLVTHM (22) using *Mlu*I and *Cla*I. The targeting sequences were gacatttcaacctacgaat for ADAM10 mRNA

and aggaaagccctgtacagta for ADAM17 mRNA. A sequence of ccgtcacatcaattgccgt served as scramble control. To form the shRNA all sequences were separated by a noncomplementary spacer (ttcaagaga) from their corresponding reverse complement sequence.

The cDNA of syndecan-1 and -4 was amplified by PCR and inserted into pcDNA3.1+ using *EcoR*I and *Xho*I. For generation of syndecan-1-2Z expression vector, syndecan-1 cDNA was amplified without stop codon and inserted upstream to 2Z-His cDNA in pcDNA3.1+ using *Kpn*I and *Not*I (23). All sequences were verified by sequencing.

Cell culture and transfection

The alveolar lung carcinoma epithelial cell line A549 was obtained from the DSMZ (Braunschweig, Germany) and cultured in M199 medium or DMEM medium with 10% FCS and antibiotics. Primary human alveolar epithelial cells were obtained from PromoCell (Heidelberg, Germany) and cultured in supplemented growth medium according to manufacturer's instructions. The human bladder carcinoma epithelial cell line ECV304 and the human embryonic kidney cell line HEK293 were cultured as described (24).

Transient transfection was carried out with lipofectamine (Invitrogen, Karlsruhe, Germany) according to manufacturer's instructions. Recombinant lentiviruses were produced by transient transfection of 293T packaging cells according to standard protocols (25). In brief, subconfluent 293T cells were cotransfected with 10 µg of the specific pLVTHM-plasmid, 7.4 µg of pCVM-ΔR8.74 and 2.6 µg of pMD2G-VSVG using calcium phosphate precipitation. The medium was changed after 24 h, and the lentivirus containing supernatants were harvested after another 48 h of incubation. To transduce ECV304 cells $1x10^5$ cells were seeded into six-wells and after 24 h, 20% of the culture medium was replaced by culture supernatant containing lentivirus. To enhance the efficiency of transduction polybrene (8 µg/ml, Sigma) was added. After 48 h, the cells were transduced for a second time.

Syndecan cleavage assays

Cells were grown in 6-well dishes to 80-90% confluence in fully supplemented medium for 48 hours. Cells were washed once with sterile PBS and received 1000 µl of serum-free medium with GI254023 (10 µM), GW280264 (10 µM) or dimethylsulfoxide (DMSO). After 1 h, the cells were stimulated with PMA (100 ng/ml), trap-6 (5 µM) or TNFα/IFNγ (both 10 ng/ml), for the indicated periods of time. Digestion of cells with recombinant ADAM17 catalytic domain (5 ng/ml) was performed in serum-free DMEM supplemented with antibiotics for 3h at 37°C. For analysis of shed syndecan conditioned media were harvested, supplemented with a protease inhibitor mixture (Complete, Roche, Manheim Germany), cleared by high speed centrifugation and analyzed by dot blotting (see below). For analysis of syndecan surface expression cells were scraped off in 1 ml ice-cold PBS and examined by flow cytometry (see below).

Dot blotting for syndecan-1 and -4

Conditioned media were diluted in blotting buffer (0.15 M NaCl buffered to pH 4.5 with 50 mM sodium acetate, and with 0.1% Triton X-100), and applied to cationic polyvinylidine difluoride–based membrane (Hybond-N^+, Amersham) under vacuum in an immunodot apparatus (Slot blot, Amersham , Freiburg, Germany). By acidifying the samples in blotting buffer, only highly anionic molecules in the conditioned media, such as proteoglycans, are retained by the cationic Immobilon-N membrane. The membranes were washed twice with blotting buffer, blocked for 1 h with PBS supplemented with 0.5% BSA, 3% non-fat dry milk and 0.5% Tween 20 (all from Sigma). Human syndecans were detected by incubating membranes overnight at 4°C with anti-syndecan-1 mAb DL-101 (0,6 µg/ml) or anti-syndecan-4 5G9 (0,6 µg/ml) followed by incubation with POD-coupled goat anti-mouse (diluted 1:20.000 in PBS-T). For murine syndecans, mAb 281-2 to murine syndecan-1 (1 µg/ml) and goat polyclonal antibody against murine syndecan-4 (1 µg/ml), followed by the appropriate POD-coupled goat anti-rat and rabbit anti-goat antibodies (diluted 1:20.000 in PBS-T) were

used. After addition of chemiluminescence substrate (ECL advanced, Amersham), signals were recorded and quantified using a luminescent image analyzer LAS3000 and Multi Gauge 3.0 software (Fujifilm, Tokyo, Japan).

Western Blotting
Samples were subjected to SDS-polyacrylamide gel electrophoresis under reducing conditions using 10% Tris-glycine gels. Proteins were transferred onto polyvinylidene difluoride membranes (Hybond-P, Amersham) that were probed with normal rabbit IgG (0.5 µg/ml) followed by incubation with POD-coupled goat anti-rabbit IgG (see above). Equal loading and transfer of proteins to the membrane was verified by detection of β-actin using a specific monoclonal antibody.

Flow cytometric analysis
Cells were analyzed for syndecan expression by staining with anti-syndecan-1 mAb DL-101, anti-syndecan-4 5G9. Isotype controls for mouse IgG1 and mouse IgG2a, respectively, were used in parallel. Lentivirally transduced ECV304 cells were assessed for down-regulation of the respective target protein using mouse monoclonal antibodies against ADAM10 and ADAM17 (1 µg/ml and 5 µg/ml resp.) and a PE-conjugated anti-mouse antibody (1:10,000) (18). The fluorescence signal was then analyzed by flow cytometry (Guava EasyCyte Mini, Guava Technologies, Hayward, USA).

RT- PCR
The mRNA expression levels of syndecan-1, syndecan-4, ADAM10 and ADAM17 were quantified by real-time PCR and normalized to the mRNA expression level of glyceraldehyde-3-phosphate dehydrogenase (GAPDH). RT-PCR analysis was performed as described (26). Briefly, RNA was extracted using RNeasy Kit (Qiagen, Hilden, Germany) and quantified by spectrophotometry (NanoDrop, Peqlab, Erlangen, Germany). RNA (1 µg) was reverse transcribed using RevertAid First Strand cDNA Synthesis Kit (Fermentas, St Leon-Rot, Germany) in 20 µl volume according to manufacturers' protocols. PCR reactions were then performed in triplicates of 20 µl volume containing 1 µl of cDNA template, 10 µl 2x LightCycler SYBR Green I Master mix (Roche) and 0,5 µM forward and reverse primer. Following primers were used: syndecan-1 forward, ggctgtagtcctgccagaag; syndecan-1 reverse tctgtgtggggagtgtgaag; syndecan-4 forward, tcgatccgagagactgaggt; syndecan-4 reverse, ccagatctccagagccagac; adam10 forward, tccacagcccattcagcaa, adam10 reverse, gcgtctcatgtgtcccatttg; adam17 forward, gaagtgccaggaggcgatta; adam17 reverse, cgggcactcactgctattacc, GAPDH forward, ccagtgagcttcccgttca; GAPDH reverse, cagaacatcatccctgcctcta. All PCR reactions were run on a LightCycler 480 System (Roche) with 40 cycles of 10 s denaturation at 95°C, followed by 20 s annealing at 55°C and 15 s amplification at 72°C. Standard curves were determined for each gene of interest with serial dilutions of its cDNA inserted in pcDNA3.1. Data were obtained as threshold cycle CT value and calculated as delta CT value as follows: $\Delta CT = CT_{\text{gene of interest}} - CT_{GAPDH}$.

ADAM17 activity assay
Lysates of cultured cell lines (70,000 cells) or lung tissue (3 mg) were prepared and analyzed for ADAM10/17 activity using a fluorogenic peptide-based assay kit from R&D Systems following the manufacturer's instructions. The enzymatic activity was expressed in relation to a serially diluted standard of recombinant ADAM17 run in parallel.

Animals
C57/BL 6 N female mice (20–25 g) with an age of 9-10 weeks were obtained from Janvier (Le Genest-Saint-Isle, France) and used as lung donors.

Intranasal administration of inhibitors in mice and bronchoalveolar lavage
Mice were anesthetized with Ketamin/Xylazin (27 mg and 430 mg/kg body weight). Five minutes after anesthesia, mice were intranasally treated with GW280264, GI254023 (30 µg/kg each) or DMSO control (0.6%) in 50 µl PBS. After 30 min, the mice were awake again and no direct effect of the inhibitors on the mice was observed. After 4 h

of inhibitor treatment, animals were sacrificed and lungs were lavaged three times with a total volume of 1 ml of PBS.

Isolated perfused lungs

One hour after intranasal application of inhibitors, mice were anesthetized with Nembutal (3.5 g Pentobarbital/kg BW). Preparation and perfusion (1 mL·min^{-1} non-recirculating RPMI 1640 medium supplemented with hydroxyethyl starch) of mouse lungs through the pulmonary artery was performed as described previously (27). Briefly, anaesthetised animals were positioned in an open tempered (37°C) chamber and intubated. The abdomen and chest were opened to expose the heart and lungs. The left atrium and pulmonary artery were cannulised and perfusion was started. Lungs (n=3 per group) were then intratracheally challenged with TNFα/IFNγ (5 and 20 µg/kg, respectively, in 50 µl of PBS) or vehicle control. The lungs were perfused and ventilated for 4 h under baseline conditions with an end-inspiratory pressure of 8 cm H_2O and an end-expiratory pressure of 3 cm H_2O, resulting in a tidal volume of 200 µl as measured by numerical integration of airflow velocity. The lungs were then disconnected, the left lung was lavaged with 500 µl PBS and the lung tissue and the bronchioalveolar lavage (BAL) fluid were frozen immediately in liquid nitrogen and kept at -80°C.

Statistics

Data were statistically analyzed using one-way ANOVA and subsequent group comparisons. Where required, p-values were adjusted by the Bonferroni procedure (GraphPad Prism 5.01, GraphPad Software, San Diego, USA).

Results

Shedding of syndecan-1 and -4 by epithelial cells involves ADAM17

Syndecan-1 and -4 are both highly expressed on the surface of ECV304 cells (bladder carcinoma epithelial cell line) and A549 cells (alveolar lung cancer epithelial cell line). Dot blot analysis of culture supernatants revealed that both cell lines release increasing amounts of soluble syndecan-1 and -4 over time (Figure 1A). In the presence of the dual ADAM17 and ADAM10 inhibitor GW280264 (16;20) the release of both syndecans was profoundly reduced (Fig 1B). Similar results were obtained with the commercially available metalloproteinase inhibitor TAPI-1. Moreover, the dual ADAM17 and MMP inhibitor TMI-1 as well as the selective ADAM17 inhibitor TMI-2 (21) reduced the production of soluble syndecan-1 and -4 (suppl. Fig. 1). By contrast, the inhibitor GI254023 blocking ADAM10 but not ADAM17 (16;20) only had a minor effect. Flow cytometry analysis revealed that inhibition of syndecan release by GW280264 was associated with an increased surface expression of syndecan-1 and -4 (Fig 1C). These findings suggest that ADAM17 could be involved in the release of syndecans by the epithelial cell lines.

To confirm that ADAM17 is capable of mediating syndecan cleavage we added the recombinant catalytic domain of ADAM17 to ECV304 and A549 cells and found enhanced release of syndecan-1 and -4 (Fig 2A). To further examine the role of ADAM17 in the generation of soluble syndecan, expression of ADAM10 and ADAM17 was silenced by lentivirally transduced shRNA. Downregulation of ADAM10 and ADAM17 on the stably transduced ECV304 cells was confirmed by flow cytometry (Fig 2B). Reduction of ADAM17 expression was associated with suppression of syndecan release while silencing of ADAM10 had no effect (Fig 2C). These results show that endogenous ADAM17 is critical for the generation of soluble syndecan-1 and -4.

Inducible shedding of syndecan-1 and -4 is mediated by ADAM17

Cell stimulation with PMA, thrombin or proinflammatory cytokines has been reported to induce the release of syndecans (4;12;13). In line with this, stimulation of epithelial cells with PMA or the thrombin receptor agonist trap6 leads to a rapid release of soluble syndecans (Fig. 3A and suppl. Fig.2) while the combination of TNFα and IFNγ required a longer stimulation period to induce an increase of soluble syndecans in the conditioned media (Fig 3A). The stimulation of syndecan release by PMA or TNFα/IFNγ was associated with a reduction of syndecan surface expression (Fig

3B) suggesting that cell stimulation led to enhanced shedding of syndecan-1 and -4. Again this inducible syndecan shedding was effectively blocked by the metalloproteinase inhibitor TAPI-1 or the combined ADAM17/ADAM10 inhibitor GW280264 but not by the ADAM10 inhibitor GI254023 (Fig 4A and B). Moreover, specific downregulation of ADAM17 led to reduced syndecan release while silencing of ADAM10 had no effect (Fig 5A).

To exclude the possibility that the induced syndecan release would be influenced by increased gene expression, syndecan-1 and syndecan-4 mRNA was quantified by RT-PCR analysis. These studies showed that cytokine stimulation for 24h did not increase expression of syndecan-1 and -4 (Fig 5B). Moreover, the cytokine-induced increase in proteolytic shedding was not associated with increased mRNA expression or surface expression of ADAM17 as demonstrated by RT-PCR analysis and flow cytometry (Fig 5B and C). An activity assay for ADAM17 using a fluorogenic peptide, however, revealed that cytokine stimulation of the epithelial cell lines led to increased activity of the protease (Fig 5D). Therefore, enhanced syndecan shedding should be the result of increased ADAM17 activity induced by the proinflammatory cytokines.

Syndecan shedding generates a C-terminal fragment

Syndecan shedding has been found to occur at a single site proximal to the cell membrane (10) and should not only release the N-terminal ectodomain but also generate a C-terminal cleavage fragment (CTF) containing the transmembrane domain. For other shedding substrates including notch, E-cadherin, CX3CL1, CXCL16 and CD44, CTFs have been found to undergo intramembraneous cleavage via γ-secretase (23;28-30). To study the generation and turn over of syndecan CTFs, we fused the C-terminus of syndecan-1 and -4 to a 2Z-His-tag which is readily detected via its high affinity interaction with the F_c-part of IgG (23). Upon transfection of the tagged constructs, soluble syndecan-1 and -4 were released into the conditioned media. This was increased by PMA and blocked by the inhibitor GW280264, as expected (Fig. 6A). Western blot analysis using rabbit IgG for detection of the tagged proteins revealed the presence of the three different protein bands in HEK293 cells transfected with syndecan-1-2Z-His, and two different protein bands in HEK293 cells transfected with the syndecan-4-2Z-His, but none of the proteins was detected in wt-HEK293 cells transfected with an empty control vector (Fig. 6A). The smallest protein bands of syndecan-1-2Z-His and syndecan-4-2Z-His migrated at approximately 25 kDa and slightly above. These proteins most likely represented cleavage products, consisting of the 17 kDa tag and syndecan CTFs. The generation of these fragments was considerably enhanced when shedding was induced by PMA, but reduced when shedding was blocked with GW280264 (Fig. 6A).

Treatment with the γ-secretase inhibitor DAPT had no effect on the release of soluble syndecans (Fig. 6B). Interestingly, the inhibitor led to a profound increase of the 25 kDa CTFs without affecting the expression of non-cleaved syndecan. However, when shedding of syndecans was blocked by inhibition of ADAM17 no such accumulation was seen upon treatment with the γ-secretase inhibitor. These findings suggest that ADAM17 is relevant for the release of syndecans and the generation of cellular cleavage fragments that undergo further proteolytic degradation potentially by γ-secretase.

Syndecan shedding in the lung

Since soluble variants of syndecan-1 and -4 have been found in the bronchoalveolar fluid (8), we questioned whether the generation of soluble syndecans in the lung would involve a mechanism similar to that found in cell lines. First, we examined primary human alveolar epithelial cells for the presence and shedding of syndecans. Release of syndecan-1 and -4 was blocked by combined inhibition of ADAM17 and ADAM10 but not by inhibition of ADAM10 only (Fig. 7A). As seen for the epithelial cell lines shedding of both syndecans by primary alveolar epithelial cells was enhanced by PMA or proinflammatory

cytokines and blocked by the ADAM10/17 inhibitor. Again inhibition of shedding was associated with increased surface expression whereas stimulated shedding was linked to decreased surface expression of syndecan-1 and 4 (suppl. Fig. 3).

To demonstrate syndecan shedding *in vivo*, mice were intranasally treated with either GW280264 or GI254023 and analyzed for the presence of soluble murine syndecan-1 and -4. In these experiments, the level of soluble syndecans was markedly reduced by the dual ADAM10/17 inhibitor GW280264 but not by the ADAM10 inhibitor GI254023, suggesting that syndecans in the lung undergo proteolytic shedding via ADAM17 (Fig. 7B). Moreover, when isolated perfused mouse lungs were challenged by intratracheal administration of TNFα and IFNγ, levels of syndecan-1 and -4 in the bronchoalveolar fluid were profoundly increased. Again, this increase was suppressed by the ADAM10/17 inhibitor (Fig. 7C). As seen for cultured epithelial cell lines, cytokine treatment of the murine lungs led to a marked increase of ADAM17 activity without affecting mRNA expression of the protease (Fig. 7D).

Discussion

In the present study we have investigated the proteolytic release of soluble syndecan-1 and -4 ectodomains from epithelial cells. By pharmacologic inhibition as well as by transcriptional silencing we have identified ADAM17 as an important sheddase on epithelial cells responsible for the conversion of syndecan-1 and -4 into soluble ectodomains and cell-associated C-terminal trunk molecules. In particular, ADAM17 mediates not only constitutive shedding by epithelial cells but also shedding in response to inflammatory stimuli such as PMA, thrombin or IFNγ/TNFα. Also in intact lungs constitutive and stimulated release of syndecans was sensitive to ADAM17 inhibition. Collectively, these findings suggest a critical role of ADAM17 in the constitutive and regulated shedding of syndecan-1 and -4 in the alveolar space.

Since the discovery of soluble syndecans metalloproteinases have been implicated in the proteolytic release of soluble ectodomains from transmembrane syndecans. Syndecan shedding is effectively suppressed by the broad spectrum metalloproteinase inhibitor batimastat which blocks the proteolytic activity of MMPs as well as ADAMs (31). To date, syndecan shedding activity has been mostly reported for members of the MMP family. MMP9 has been found to mediate chemokine-induced shedding of syndecan-1 and -4 by HeLA-cells (12). Endogenous MT1-MMP has been implicated in syndecan-1 shedding by mammary fibroblasts (14) and overexpression of this protease enhances syndecan-1 shedding by HEK293T cells (11). MMP7-deficient mice were found to shed less syndecan-1 into the bronchoalveolar fluid of bleomycin-treated mice, and addition of recombinant MMP7 to cultured murine mammary gland cells or mouse myeloma cells increased syndecan-1 shedding (8). These data indicate that different MMPs are capable of shedding syndecans which may depend on the cell type and stimulatory conditions. Apart from the observation that ADAM12 can interact with syndecans (32) the role of ADAMs as syndecan sheddases has not yet been investigated directly. Interestingly, TIMP-3 but not TIMP-1 was found to suppress syndecan shedding (11;13). TIMP3 not only blocks a number of MMPs but also ADAM17 while TIMP-1 inhibits a number of MMPs and ADAM10 but not ADAM17 (33;34). From these inhibition studies an involvement of ADAM17 appears possible. In fact, our study demonstrates that ADAM17 is the most relevant sheddase for syndecan-1 and -4 in epithelial cells. Since the inhibitor TMI-2 which blocks ADAM17 but not MMP7, MMP9 and MT1-MMP1 (21) is an effective inhibitor of syndecan shedding in epithelial cells a contribution of MMPs appears unlikely.

Shedding via ADAM17 has been reported for numerous other proteins, all belonging to the class of type 1 transmembrane molecules with a single transmembrane domain (19). ADAM17 mediates their shedding proximal to the cell membrane and in many cases and this requires no specific cleavage site (35). Several ADAM17-mediated cleavage events can be

activated by PMA, ionomycin, chemokines or cytokines (35). While PMA-induced cleavage is a very rapid event, cleavage stimulated by IFNγ and TNFα requires a longer time period. In a previous study we have reported that TNFα/IFNγ-induced shedding of the junctional adhesion molecule JAM-A in endothelial cells does not require enhanced biosynthesis or surface expression of the ADAM17, but rather involves an altered activity of the protease (18). Our present data indicate that syndecan shedding in epithelial cells is associated with changes in ADAM17 activity but not with regulation of its expression level. The mechanism of how cytokines trigger ADAM17 activity leading to enhanced shedding of JAM-A and syndecans remains to be identified.

Cleavage by ADAM17 or ADAM10 leads to the generation of C-terminal cleavage fragments that contain the transmembrane domain and therefore reside in the cell membrane. In the case of several shedding substrates the membrane associated CTFs are removed from the cell membrane by intramembraneous cleavage via the γ-secretase complex which contains the protease presenilin (23;28-30). For Notch this process plays an essential role for intracellular signaling and it's function in transcriptional regulation (28). Interestingly, also syndecans undergo sequential cleavage by ADAMs and γ-secretase and future studies need to investigate a potential role of this process in syndecan-mediated outside-in signal transduction such as activation of PKC isoforms and rac1 (36).

Syndecan ectodomains have been found in blood serum, wound fluid and bronchoalveloar fluid. Especially under pathologic conditions such as lung inflammation or leukemia, levels of soluble syndecans can be considerably increased (3-7). Recent research has provided increasing evidence for the involvement of syndecan in cell migration (11), cancer cell proliferation (14), transepithelial efflux of neutrophils into inflamed lung (8), but also in epithelial regeneration (37), resolution of inflammation (38), resistance to bacterial sepsis (39) and wound repair (9). How syndecan shedding influences all these different processes, remains unclear. In general, these activities may be explained by a reduction in transmembrane syndecans or an increase in soluble syndecans. On the one hand reduced syndecan surface expression may curtail presentation of chemokines, growth factors, or antimicrobial peptides as well as diminished outside-in signaling via syndecans. Soluble syndecans on the other hand could either act as antagonists by sequestration of chemokines or as agonists by a yet undefined mechanism (1). Our study indicates that ADAM17 mediates constitutive and inflammation- related syndecan-1 and -4 shedding from lung epithelial cells into the alveolar space. ADAM17 may therefore contribute to a dysregulated balance of transmembrane and soluble syndecan functions in the inflamed lung. Further research will have to clarify whether inhibitors of ADAM17 can be used to limit syndecan shedding to interfere with neutrophil recruitment and infections in the inflamed lung.

Acknowledgement

We thank Melanie Esser and Nadine Ruske for technical assistance. We thank Dr. Yuhua Zhang and Dr. Stanley F. Wolf, (Wyeth Research) for providing the inhibitors TMI-1 and TMI-2. This work was supported in part by IZKF BioMAT. of the RWTH Aachen, and by SFB 542 projects A12 and C16.

Reference List

1. Bartlett, A. H., Hayashida, K., and Park, P. W. (2007) *Mol Cells.* **24,** 153-166
2. Kim, C. W., Goldberger, O. A., Gallo, R. L., and Bernfield, M. (1994) *Mol Biol Cell.* **5,** 797-805
3. Seidel, C., Sundan, A., Hjorth, M., Turesson, I., Dahl, I. M., Abildgaard, N., Waage, A., and Borset, M. (2000) *Blood.* **95,** 388-392
4. Subramanian, S. V., Fitzgerald, M. L., and Bernfield, M. (1997) *J Biol Chem.* **272,** 14713-14720
5. Joensuu, H., Anttonen, A., Eriksson, M., Makitaro, R., Alfthan, H., Kinnula, V., and Leppa, S. (2002) *Cancer Res.* **62,** 5210-5217
6. Hasegawa, M., Betsuyaku, T., Yoshida, N., Nasuhara, Y., Kinoshita, I., Ohta, S., Itoh, T., Park, P. W., and Nishimura, M. (2007) *Respirology.* **12,** 140-143
7. Penc, S. F., Pomahac, B., Winkler, T., Dorschner, R. A., Eriksson, E., Herndon, M., and Gallo, R. L. (1998) *J Biol Chem.* **273,** 28116-28121
8. Li, Q., Park, P. W., Wilson, C. L., and Parks, W. C. (2002) *Cell.* **111,** 635-646
9. Elenius, V., Gotte, M., Reizes, O., Elenius, K., and Bernfield, M. (2004) *J Biol Chem.* **279,** 41928-41935
10. Wang, Z., Gotte, M., Bernfield, M., and Reizes, O. (2005) *Biochemistry.* %**20;44,** 12355-12361
11. Endo, K., Takino, T., Miyamori, H., Kinsen, H., Yoshizaki, T., Furukawa, M., and Sato, H. (2003) *J Biol Chem.* **278,** 40764-40770
12. Brule, S., Charnaux, N., Sutton, A., Ledoux, D., Chaigneau, T., Saffar, L., and Gattegno, L. (2006) *Glycobiology.* **16,** 488-501
13. Fitzgerald, M. L., Wang, Z., Park, P. W., Murphy, G., and Bernfield, M. (2000) *J Cell Biol.* **148,** 811-824
14. Su, G., Blaine, S. A., Qiao, D., and Friedl, A. (2008) *Cancer Res.* **68,** 9558-9565
15. Dijkstra, A., Postma, D. S., Noordhoek, J. A., Lodewijk, M. E., Kauffman, H. F., ten Hacken, N. H., and Timens, W. (2009) *Virchows Arch.* **454,** 441-449
16. Hundhausen, C., Misztela, D., Berkhout, T. A., Broadway, N., Saftig, P., Reiss, K., Hartmann, D., Fahrenholz, F., Postina, R., Matthews, V., Kallen, K. J., Rose-John, S., and Ludwig, A. (2003) *Blood* **102,** 1186-1195
17. Abel, S., Hundhausen, C., Mentlein, R., Schulte, A., Berkhout, T. A., Broadway, N., Hartmann, D., Sedlacek, R., Dietrich, S., Muetze, B., Schuster, B., Kallen, K. J., Saftig, P., Rose-John, S., and Ludwig, A. (2004) *J Immunol.* **172,** 6362-6372
18. Koenen, R. R., Pruessmeyer, J., Soehnlein, O., Fraemohs, L., Zernecke, A., Schwarz, N., Reiss, K., Sarabi, A., Lindbom, L., Hackeng, T. M., Weber, C., and Ludwig, A. (2009) *Blood.* **113,** 4799-4809
19. Pruessmeyer, J. and Ludwig, A. (2009) *Semin Cell Dev Biol.* **20,** 164-174
20. Ludwig, A., Hundhausen, C., Lambert, M. H., Broadway, N., Andrews, R. C., Bickett, D. M., Leesnitzer, M. A., and Becherer, J. D. (2005) *Comb.Chem.High Throughput.Screen.* **8,** 161-171
21. Zhang, Y., Hegen, M., Xu, J., Keith, J. C., Jr., Jin, G., Du, X., Cummons, T., Sheppard, B. J., Sun, L., Zhu, Y., Rao, V. R., Wang, Q., Xu, W., Cowling, R., Nickerson-Nutter, C. L., Gibbons, J., Skotnicki, J., Lin, L. L., and Levin, J. (2004) *Int.Immunopharmacol.* %**20;4,** 1845-1857
22. Wiznerowicz, M. and Trono, D. (2003) *J Virol.* **77,** 8957-8961
23. Schulte, A., Schulz, B., Andrzejewski, M. G., Hundhausen, C., Mletzko, S., Achilles, J., Reiss, K., Paliga, K., Weber, C., John, S. R., and Ludwig, A. (2007) *Biochem.Biophys.Res.Commun.* **358,** 233-240
24. Hundhausen, C., Schulte, A., Schulz, B., Andrzejewski, M. G., Schwarz, N., von Hundelshausen, P., Winter, U., Paliga, K., Reiss, K., Saftig, P., Weber, C., and Ludwig, A. (2007) *J Immunol.* **178,** 8064-8072

25. Salmon, P. and Trono, D. (2006) *Curr.Protoc.Neurosci.* **Chapter 4:Unit 4.21.,** Unit
26. Scholz, F., Schulte, A., Adamski, F., Hundhausen, C., Mittag, J., Schwarz, A., Kruse, M. L., Proksch, E., and Ludwig, A. (2007) *J Invest Dermatol.* **127,** 1444-1455
27. Held, H. D. and Uhlig, S. (2000) *Am.J Respir.Crit Care Med.* **162,** 1547-1552
28. de Strooper, B., Annaert, W., Cupers, P., Saftig, P., Craessaerts, K., Mumm, J. S., Schroeter, E. H., Schrijvers, V., Wolfe, M. S., Ray, W. J., Goate, A., and Kopan, R. (1999) *Nature.* **398,** 518-522
29. Maretzky, T., Reiss, K., Ludwig, A., Buchholz, J., Scholz, F., Proksch, E., de Strooper, B., Hartmann, D., and Saftig, P. (2005) *Proc.Natl.Acad.Sci.U.S.A* **102,** 9182-9187
30. Okamoto, I., Kawano, Y., Murakami, D., Sasayama, T., Araki, N., Miki, T., Wong, A. J., and Saya, H. (2001) *J Cell Biol.* **155,** 755-762
31. Holen, I., Drury, N. L., Hargreaves, P. G., and Croucher, P. I. (2001) *Br J Haematol.* **114,** 414-421
32. Iba, K., Albrechtsen, R., Gilpin, B., Frohlich, C., Loechel, F., Zolkiewska, A., Ishiguro, K., Kojima, T., Liu, W., Langford, J. K., Sanderson, R. D., Brakebusch, C., Fassler, R., and Wewer, U. M. (2000) *J Cell Biol.* **149,** 1143-1156
33. Amour, A., Slocombe, P. M., Webster, A., Butler, M., Knight, C. G., Smith, B. J., Stephens, P. E., Shelley, C., Hutton, M., Knauper, V., Docherty, A. J., and Murphy, G. (1998) *FEBS Lett.* **435,** 39-44
34. Amour, A., Knight, C. G., Webster, A., Slocombe, P. M., Stephens, P. E., Knauper, V., Docherty, A. J., and Murphy, G. (2000) *FEBS Lett.* %**19;473,** 275-279
35. Black, R. A., Doedens, J. R., Mahimkar, R., Johnson, R., Guo, L., Wallace, A., Virca, D., Eisenman, J., Slack, J., Castner, B., Sunnarborg, S. W., Lee, D. C., Cowling, R., Jin, G., Charrier, K., Peschon, J. J., and Paxton, R. (2003) *Biochem.Soc.Symp.* 39-52
36. Bass, M. D., Roach, K. A., Morgan, M. R., Mostafavi-Pour, Z., Schoen, T., Muramatsu, T., Mayer, U., Ballestrem, C., Spatz, J. P., and Humphries, M. J. (2007) *J Cell Biol.* **177,** 527-538
37. Chen, P., Abacherli, L. E., Nadler, S. T., Wang, Y., Li, Q., and Parks, W. C. (2009) *PLoS.One.* **4,** e6565
38. Hayashida, K., Parks, W. C., and Park, P. W. (2009) *Blood.*
39. Hayashida, K., Chen, Y., Bartlett, A. H., and Park, P. W. (2008) *J Biol Chem.* **283,** 19895-19903

Figure legends

Figure 1: Release of syndecan-1 and -4 by epithelial cell lines.

A) Serum-free media from cultured ECV304 cells and A549 cells were harvested after the indicated time periods and blotted onto nitrocellulose at pH 4.5. Membranes were then probed with monoclonal antibodies to syndecan-1 or -4, respectively. B) ECV304 and A549 cells were incubated in presence of the metalloproteinase inhibitors GI254023, GW280264 and TAPI-1 (10 µM each) or DMSO control (0.1%) for 16 h and subsequently conditioned media were analyzed for the presence of syndecan-1 and -4 by dot blotting. A representative dot blot is shown. For statistical analysis the signal intensities were quantified by densitometry and calculated as means and SD from three independent experiments. Asterisks indicate statistically significant differences ($p<0.05$) compared to DMSO control. C) ECV304 and A549 cells were incubated in the absence or presence of GW280264 (10 µM) and subsequently cells were analysed for surface expression of syndecan-1 and -4 by flow cytometry

Figure 2: Constitutive syndecan shedding by ADAM17.

A) ECV304 and A549 cells were treated with recombinant catalytic domain of ADAM17 (5 ng/ml for 3 h) or left untreated and subsequently analyzed for the release of syndecan-1 and -4. B and C) ECV304 cells were lentivirally transduced with scramble shRNA or specific shRNA for ADAM10 or ADAM17. Stably transduced cells were then analyzed for ADAM10 and ADAM17 surface expression by flow cytometry using ADAM10- and ADAM17-specific monoclonal antibodies and the respective isotype controls (B). The release of soluble syndecan-1 and -4 was analyzed by dot blotting and subsequent denstitometric quantification (C). Bar charts indicate means and SD from three independent experiments. Asterisks indicate statistically significant differences compared to the controls ($p<0.05$).

Figure 3: Induced shedding of syndecan-1 and -4 by epithelial cell lines.

A) ECV304 and A549 cells were treated with PMA (100 ng/ml) or a combination of TNFα and IFNγ (both 10 ng/ml) for the time periods indicated and were subsequently assayed for release of syndecan-1 and -4 by dot blotting. B) ECV304 and A549 cells were treated with PMA for 2 h or a combination of TNFα and IFNγ for 24 h or left untreated and subsequently analysed for surface expression of syndecan-1 and -4 by flow cytometry. Data are shown as representative dot blots and histograms of three independent experiments.

Figure 4: Inhibition of induced syndecan release.

ECV304 and A549 cells were treated with PMA (100 ng/ml) for 2 h (A) or a combination of TNFα and IFNγ (both 10 ng/ml) for 16 h (B) in the presence of metalloproteinase inhibitors GI254023, GW280264 or TAPI-1 (10 µM each) or DMSO control (0.1%) and subsequently the release of syndecan-1 and -4 was quantified by dot blotting and densitometry. Data are shown as representative dot blots and means and SD from three independent experiments. Asterisks indicate statistically significant effects of inhibitor treatment ($p<0.05$).

Figure 5: Induced syndecan shedding by ADAM17.

A) ECV304 cells were lentivirally transduced with scramble shRNA or specific shRNA for ADAM10 or ADAM17. Stably transduced cells were stimulated with IFNγ/TNFα (both 10 ng/ml) in the absence or presence of metalloproteinase inhibitors GI254023 and GW280264 (10 µM each) and conditioned media were then analyzed for soluble syndecan-1 and -4. B) ECV304 and A549 cells were left unstimulated or stimulated with IFNγ/TNFα for 16 h and subsequently mRNA expression of syndecan-1 and -4 was analyzed by RT-PCR. C-E) ECV304 and A549 cells were left unstimulated or stimulated with IFNγ/TNFα for 16 h. ADAM10 and ADAM17 mRNA expression was then quantified by RT-PCR (C). Surface expression of ADAM17 was analyzed by flow cytometry (D). ADAM17 activity in cell lysates was measured by cleavage of a fluorogenic substrate using a standard of recombinant human ADAM17 run in parallel (E). Data are shown as dot blots representative for three independent experiments. Bar charts indicate means and SD from three independent experiments. Asterisks indicate statistically significant differences compared to the control ($p<0.05$).

Figure 6: Detection of C-terminal cleavage fragments of syndecan-1 and -4.

A) HEK293 cells were transfected with syndecan-1-2Z-His, syndecan-4-2Z-His or transfected with control vector pcDNA3.1 (+) and treated with PMA (100 ng/ml) or DMSO for 2 h in the absence or presence of metalloproteinase inhibitors GI254023 or GW280264. Subsequently, conditioned media were analyzed for the presence of released syndecan ectodomains by dot blotting. The cell lysates were subjected to SDS-PAGE and Western blotting using rabbit IgG for detection of the 2Z-Tag. B) HEK293 cells expressing syndecan-1-2Z-His or syndecan-4-2Z-His were exposed to metalloproteinase inhibitors GI254023 and GW280264 (10 µM) or γ-secretase inhibitor DAPI (5 µM) or DMSO control for 16 h. Subsequently, soluble and cell- associated syndecans were analyzed by dot blot analysis of the conditioned media and Western blotting of the cell lysates, respectively. Asterisks indicate statistically significant differences compared to the control ($p<0.05$).

Figure 7: Syndecan release by lung epithelial cells *in vitro* and *in vivo*.

A) Primary human alveolar epithelial cells were treated with PMA (100 ng/ml) or DMSO for 2 h or stimulated with IFNγ/TNFα (each 10 ng/ml) or vehicle control for 16 h in the presence or absence of metalloproteinase inhibitors (GI254023 and GW280264, 10 µM) and subsequently conditioned media were investigated for soluble syndecan-1 and -4. Data are shown as dot blot analysis of three independent experiments. B) Mice (n=3 for each group) were intranasally treated with metalloproteinase inhibitor GW280264, GI254023 (30 µg/kg each) or vehicle control for 4 h, sacrificed and analyzed for the presence of syndecan-1 and -4 in the lung fluid obtained from bronchoalveolar lavage (BAL). C) Mice were intranasally treated with metalloproteinase inhibitor GW280264 or vehicle control for 1 h. Afterwards, perfused lungs were treated intratracheally with a combination of IFNγ/TNFα (20 and 5 µg/kg, respectively) or vehicle control (n=3 for each group) and ventilated for 4 h. Subsequently, BAL fluid was analyzed for released syndecan-1 and -4. Data are shown as dot blots and means and SD of densitometric measurements. Statistically significant effects induced by IFNγ /TNFα and the inhibitor are indicated by crosses and asterisks, respectively ($p<0.05$). D) *Ex vivo* perfused murine lungs (n=3) were treated intratracheally with a combination of IFNγ/TNFα (20 and 5 µg/kg, respectively) or PBS and subsequently lung lysates were analyzed for ADAM17 activity using a fluorogenic substrate and for ADAM17 mRNA expression by RT-PCR, respectively. Asterisks indicate statistically significant differences ($p<0.05$).

Figure 1

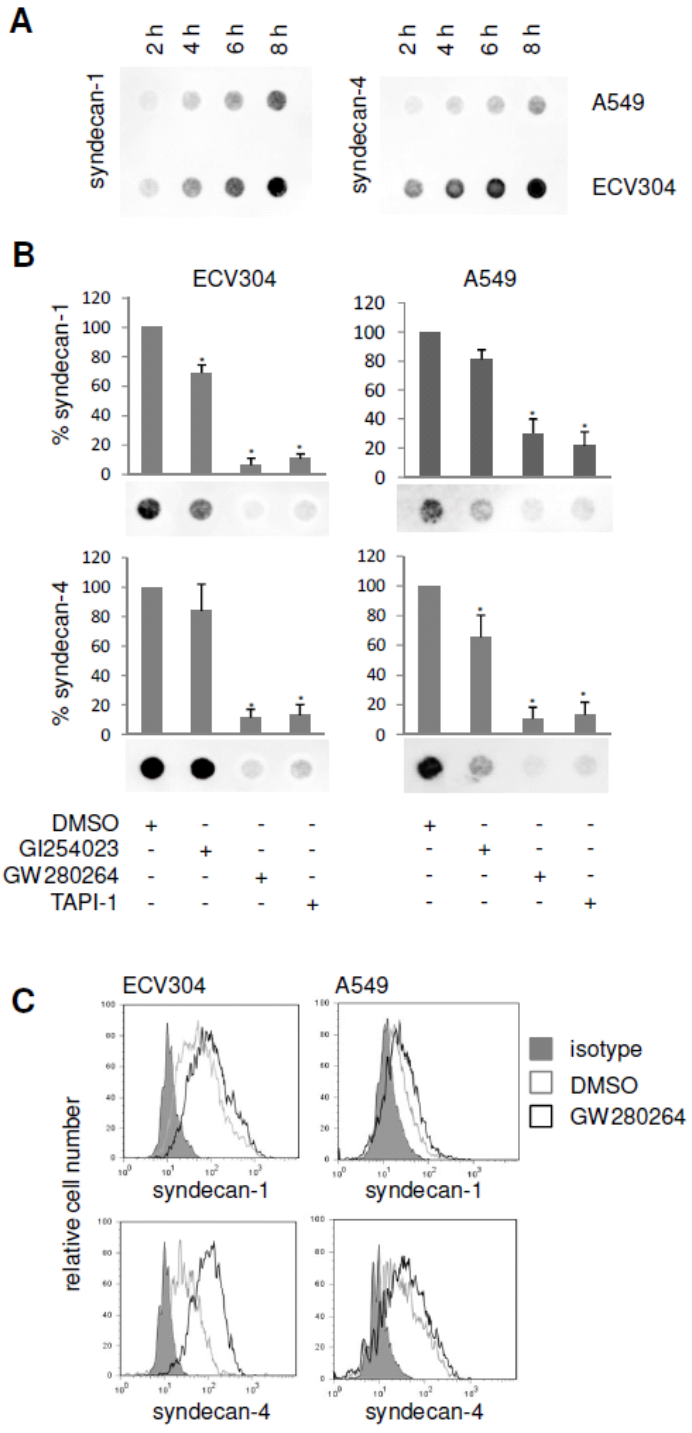

The Journal of Biological Chemistry
ASBMB
jbc

Figure 2

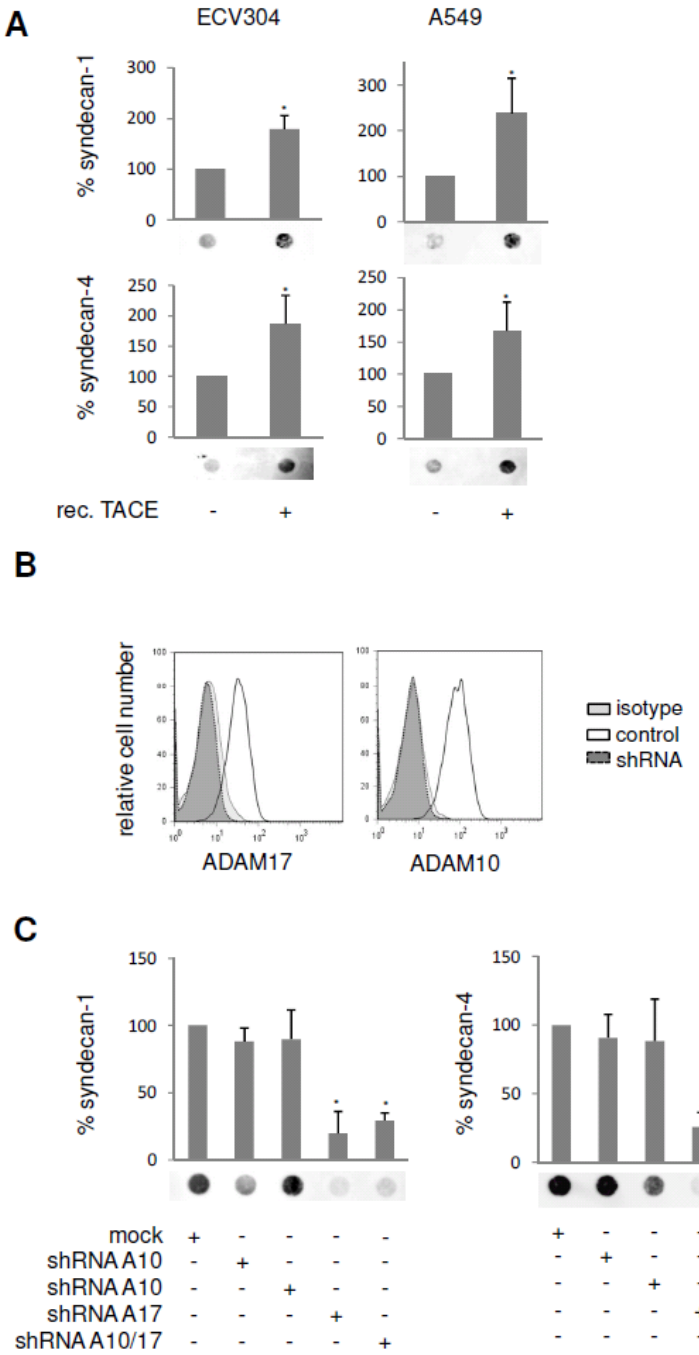

Figure 3

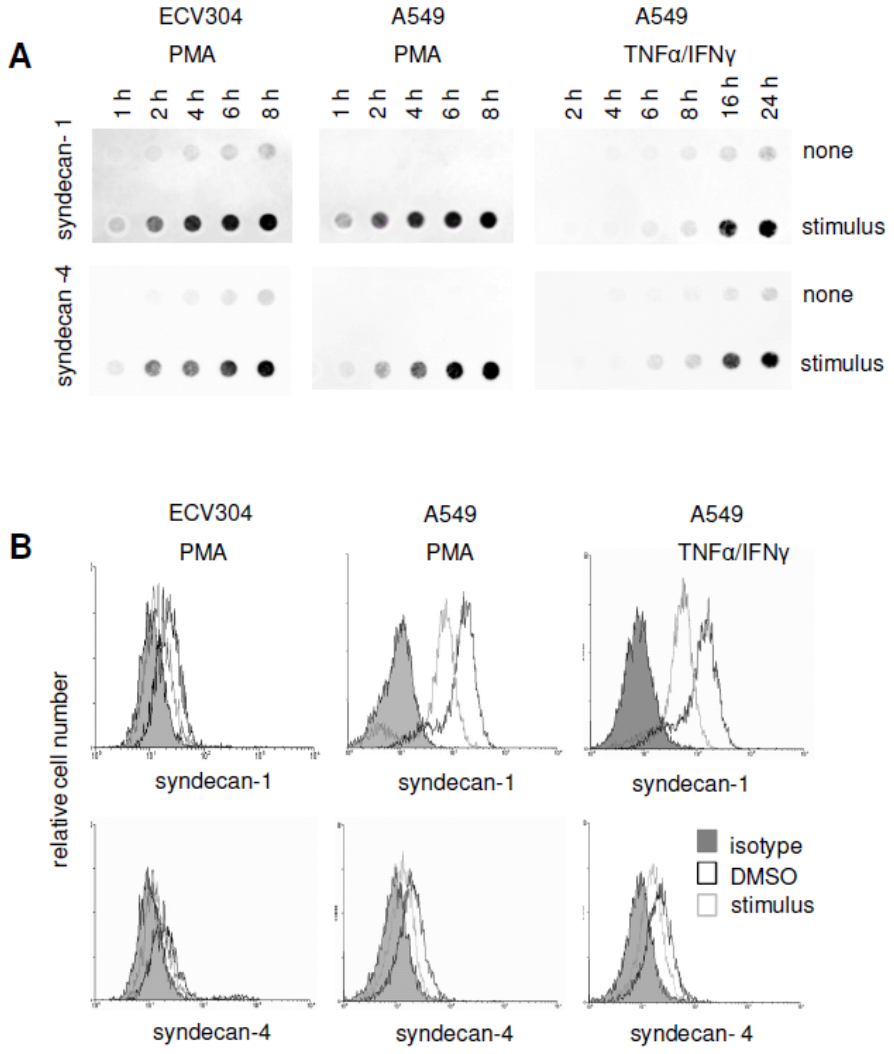

The Journal of Biological Chemistry
ASBMB
jbc

Figure 4

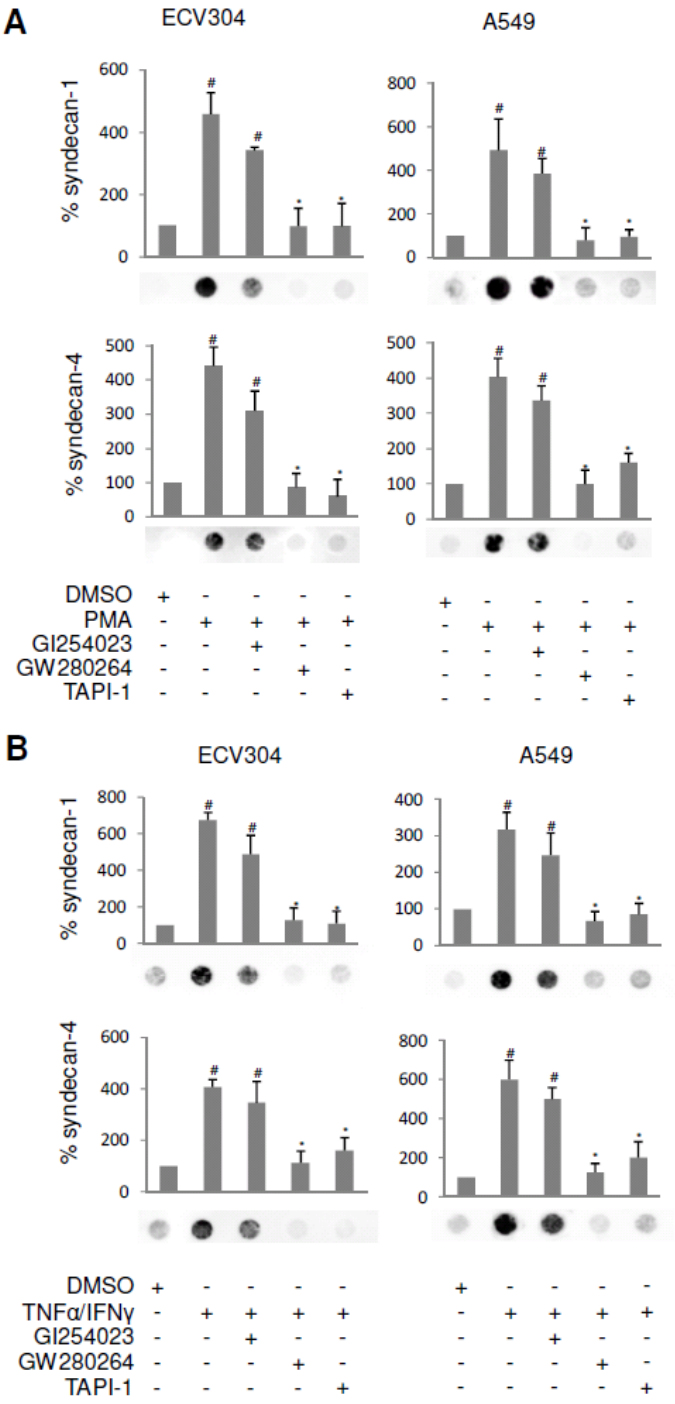

Figure 5

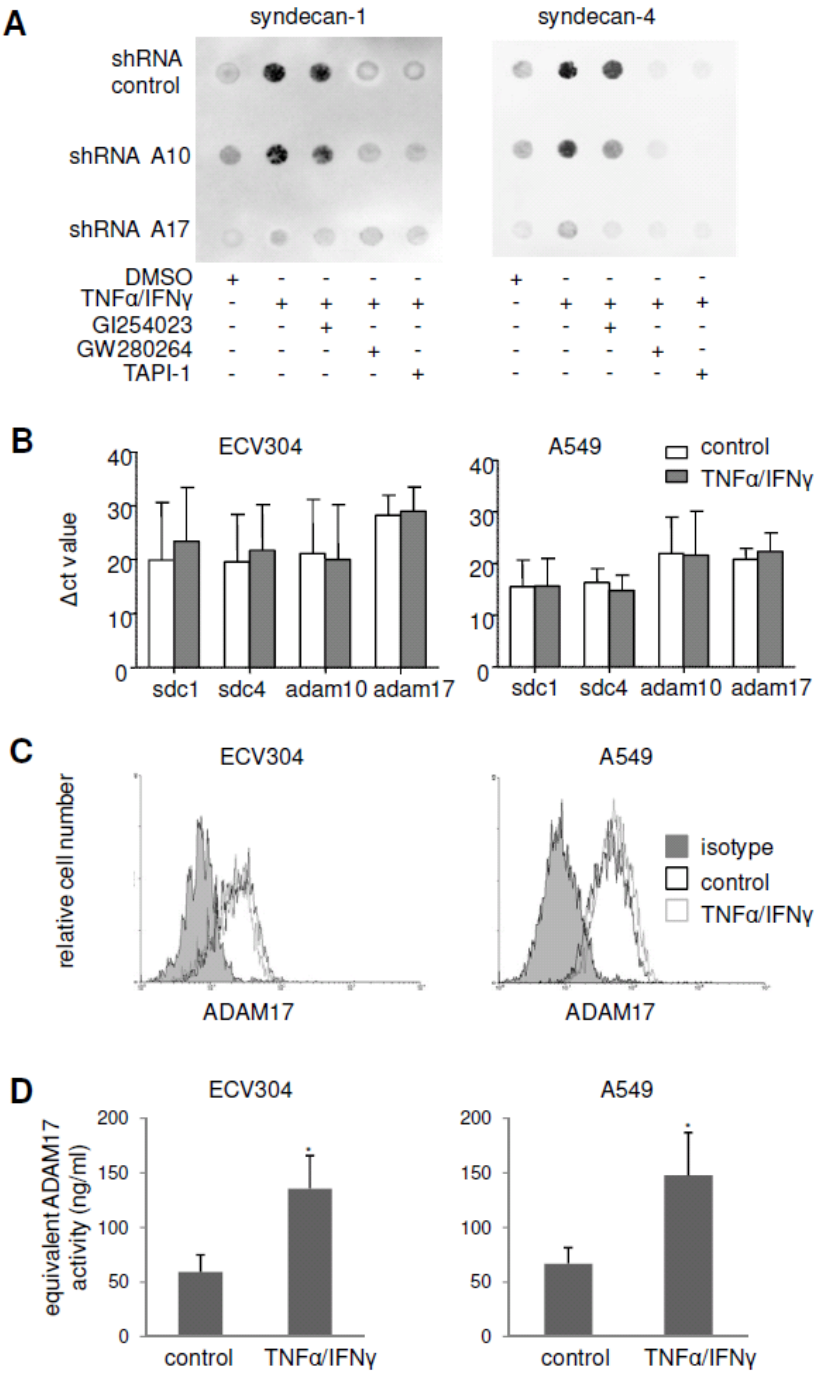

Figure 6

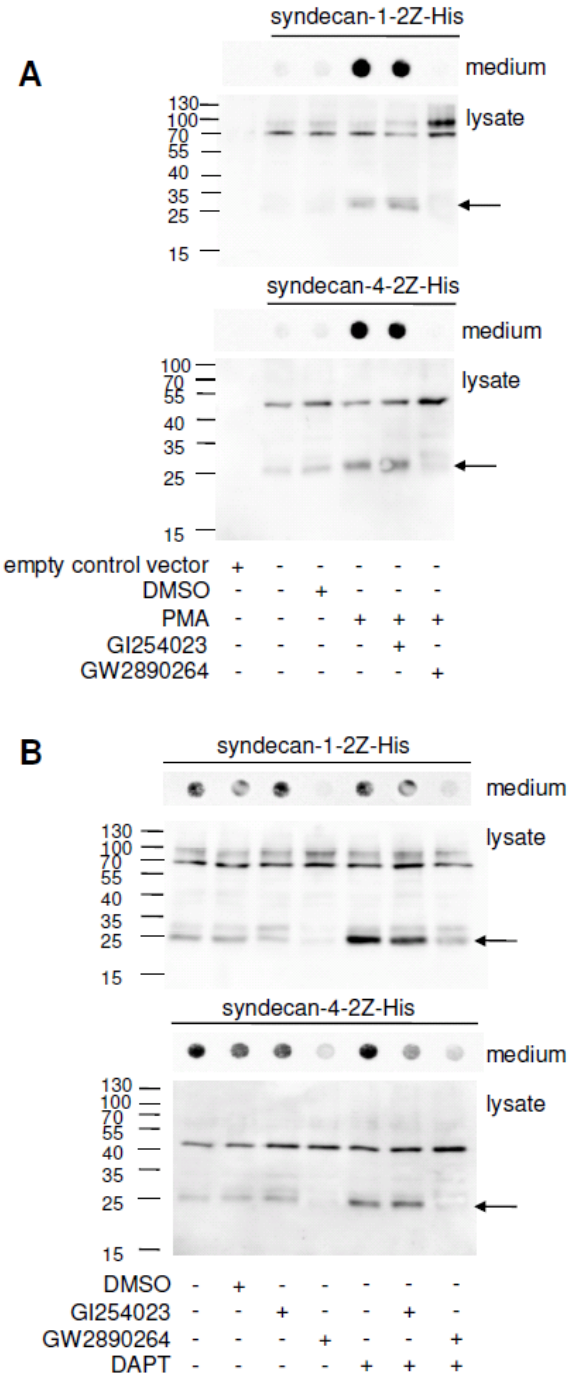

Figure 7

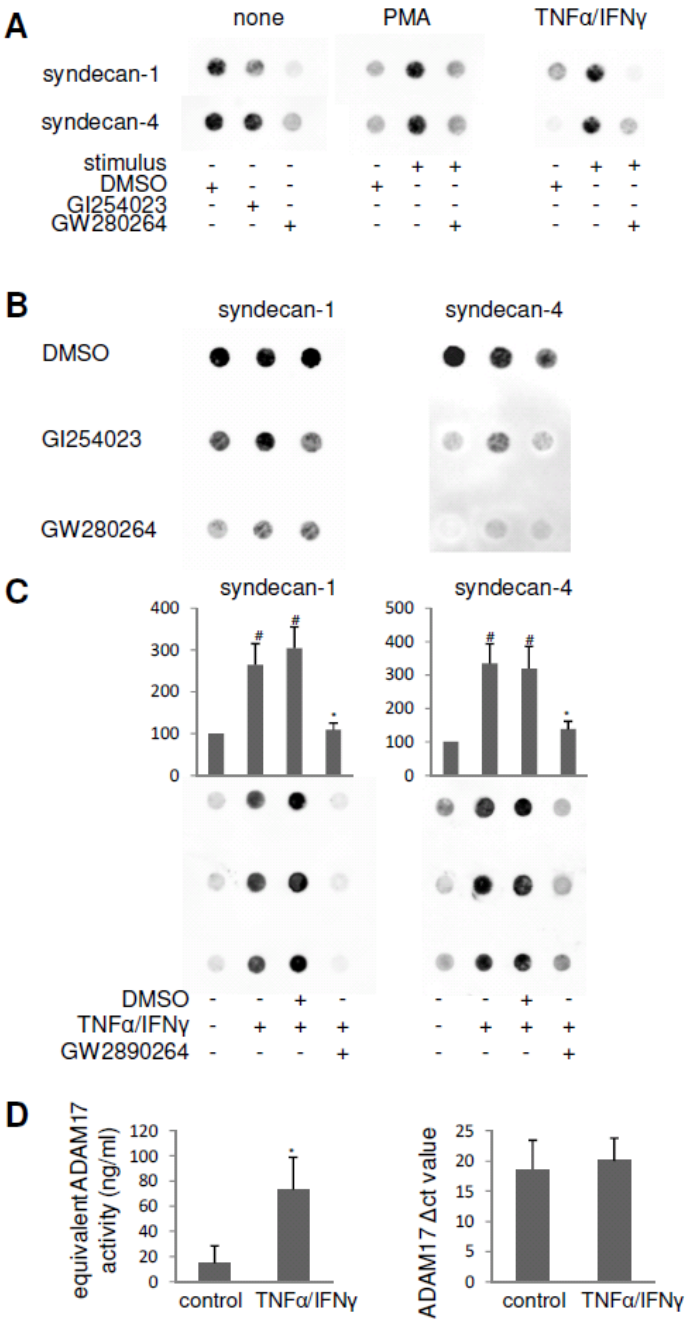

4 Zusammenfassung

In dieser Arbeit wurden die zwei notwendigen funktionellen Gruppen für die Aktivität von γ-Sekretase Modulatoren mit einem Carbazol-Grundgerüst untersucht: der lipophile Rest, am Carbazol-Stickstoff und die Carbonsäurefunktion der Seitenkette. Es wurde ein Modell entwickelt, welches die modulatorischen Eigenschaften der auf NSAID-basierenen GSMs erklärt: Die Carbonsäurefunktion interagiert mit einer Aminosäure (vermutlich Lysin^{624}) auf dem Substrat C99. Dieses Lysin liegt direkt am Membrandurchtritt vor einem GxxxG-Motiv, über welches ein C99-Dimer bilden kann. Der lipophile Rest scheint als Membrananker zu agieren, welcher die Orientierung des GSM sicherstellt und die Bildung des C99-Dimers über das GxxxG-Motiv in der Membran verhindert. Es wird vermutet, dass die Ausbildung dieses Dimers mit der Erhöhung der $A\beta_{42}$-Sekretion assoziiert ist.

Durch die Variation des lipophilen Restes wurde die Vermutung, dass dieser als Membrananker fungiert, gefestigt. Durch Einführung von rigiden linearen lipophilen Resten wurde die modulatorische Aktivität gesteigert, da die Einlagerung in die Membran erleichtert wird. Weitere Untersuchungen der Seitenkette zeigten die Notwendigkeit eines aziden H-Atoms, das anscheinend in einem pKa-Bereich zwischen 7-15 liegen muss um noch modulatorische Eigenschaften zu besitzen. Dieses azide H-Atom muss außerdem über einen Linker von 2-3 Atomen mit dem Carbazol-Grundgerüst verbunden sein. Zusätzlich konnte ein mögliches Prodrug-System über Esterfunktionen identifiziert werden, welches noch weiter untersucht werden muss. Bezüglich der Bindungsstelle unserer GSMs wurde die Vermutung gefestigt, dass die Carbonsäurefuktion mit der basischen Aminosäure Lysin an der Position 624 des Substrates C99 wechselwirkt. Durch diese Wechselwirkung wird die Dimerisierung des Substrates verhindert, welche vermutlich mit der Erhöhung der $A\beta_{42}$-Sekretion assoziiert ist.

Ferner konnte durch eine Struktur-Aktivitäts-Analyse ein direkter Einfluss der Casein Kinase 1 auf die γ-Sekretase ausgeschlossen werden.

Abschließend gelang eine Optimierung der Synthese des ADAM10 Inhibitors GI254023X, in verbesserter Gesamtausbeute zusammen mit einfacheren Detektion bei 254 nm statt 220 nm.

5 Ausblick

Eine Substitution des Carbazol-Grundgerüstes an dem unsubstituierten Phenylring stellt eine gute Möglichkeit dar, die Größe der Bindungstasche zu bestimmen. Ziel dieser Untersuchung ist es ein Derivat zu identifizieren, welches optimal in die Bindungstasche passt und Interaktionen mit dieser zur Folge hat, wie z.B. Wasserstoffbrücken-Bindungen. Eine verbesserte Interaktion mit der Bindungstasche sollte eine Steigerung der modulatorischen Aktivität der GSMs zur Folge haben, vielleicht sogar bis in den nanomolaren Bereich.

Ein Austausch des planaren Carbazol-Grundgerüstes (**42**), welches eine Ringgrößenkombination von 6-5-6 aufweist, hin zu einer 6-6-6 oder 6-7-6 Kombination wie im 9,10-Dihydroakridin (**43**) oder Iminodibenzyl (**45**) sowie der Einbau von weiteren Heteroatomen (**44**) ließe einen Rückschluss auf die geometrische Anordnung der essentiellen Substituenten, der Carbonsäure und des lipophilen Restes, zueinander zu (Abb.26)

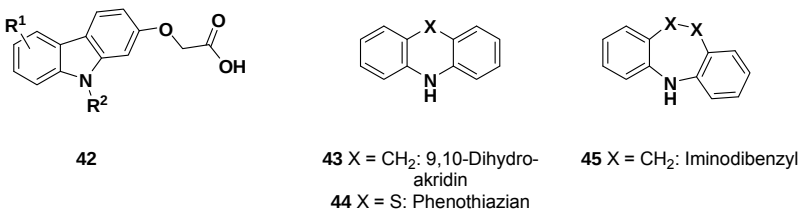

42 **43** X = CH_2: 9,10-Dihydro-akridin **44** X = S: Phenothiazian **45** X = CH_2: Iminodibenzyl

Abb. 26 Übersicht der weiterer Derivatisierungen für GSMs.

Nach der Lipinsky-Regel, der *Rule of Five*, sind die in dieser Arbeit synthetisierten GSMs als nicht *drug-like* einzuordnen. Durch den langen lipophilen Rest sind diese Verbindungen zu unpolar (clogP > 5), um bioverfügbar zu sein. Die Carbonsäure verleiht diesen GSMs einen amphiphilen Charakter was zu einer Micellenbildung führen könnte. Da diese Carbonsäure tragenden GSMs trotzdem die Blut-Hirn-Schranke überwinden können, scheint dies durch einen spezifischen Transporter zu erfolgen. Diesen zu identifizieren wäre eine gute Möglichkeit den Transportmechanismus über die Blut-Hirn-Schranke aufzuklären. Ein Kandidat ist der MCT1-Transporter, der auf den Transport von ansonsten nicht hirngängigen Carbonsäure-tragenden Substanzen über die Blut-Hirn-Schranke spezialisiert ist. Auch die Identifizierung der Bindungsstelle erfordert noch weiterer Untersuchungen. C*ross-linking* Experimente mit einem geringeren Abstand zwischen der vermeintlichen Interaktionsstelle, der Carbonsäure und der photoreaktiven Gruppe von <10Å könnten unser postuliertes Modulationsmodell bestätigen.

Es wurde in dieser Arbeit ein Einfluss der Casein Kinase 1 auf die γ-Sekretase Aktivität ausgeschlossen; ebenso eine direkte Inhibtion der γ-Sekretase durch IC261. Durch

Identifizierung des Inhibitions-Mechanismus könnten eventuell weitere γ-Sekretase-regulierende Stoffwechselwege identifiziert werden, welche in der AD-Forschung Anwendung finden könnten.

Die verbesserte Synthese des ADAM10 Inhibitors GI254023X gelang in dieser Arbeit ausgehend von chiralen Ausgangsverbindungen. Eine Veränderung der Syntheseschritte bis zum ersten *Building Block* (**50**) durch den Einsatz von achiralen Ausgangsprodukten, wie in Abb. 27 vorgeschlagen, würde den Zugang zu diesem Inhibitor vereinfachen und die Syntheseroute von 9 auf vier Schritte verkürzen.

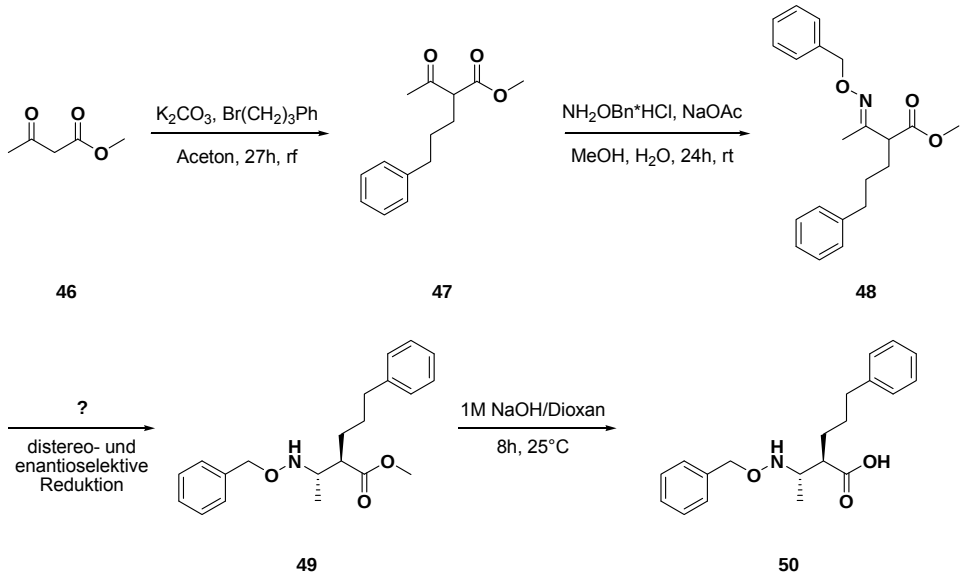

Abb. 27 Synthese des ersten *Building Blocks* (**50**) in der Synthese des ADAM10 Inhibitors aus achiralen Ausgangsprodukten.

Ziel dieser Route ist es das Benzyl-geschütze Oxim **48** zu generieren, welches in einer diastereo- und enantioselektiven Reduktion das gewünschte1*S*-2*R*-konfigurierte Produkt **49** liefert. Die Herausforderung hierbei ist die Identifizierung eines chiralen Liganden oder Reagenzes, so dass **49** diastereoselektiv mit sehr gutem Enantiomerenüberschuss generiert wird und ohne Aufreinigungsschritte weiter zu **50** umgesetzt werden kann.

6 Literaturverzeichnis

[1] S. Baumann, N. Hoettecke, R. Narlawar, B. Schmidt, *Med. Chem. Alzheimer's Dis.* **2008**, 193-224.

[2] N. Hoettecke, S. Baumann, *Bioforum* **2008**, *31*, 32-34.

[3] N. Höttecke, S. Baumann, A. Taghavi, H. A. Braun, B. Schmidt, *Frontiers in Medicinal Chemistry* **2009**, *4*, 730-766.

[4] B. Schmidt, H. A. Braun, R. Narlawar, *Curr. Med. Chem.* **2005**, *12*, 1677-1695.

[5] S. Parvathy, E. H. Karran, A. J. Turner, N. M. Hooper, *FEBS Lett.* **1998**, *431*, 63-65.

[6] D. Beher, J. D. Wrigley, A. P. Owens, M. S. Shearman, *J. Neurochem.* **2002**, *82*, 563-575.

[7] W. T. Kimberly, M. J. LaVoie, B. L. Ostaszewski, W. Ye, M. S. Wolfe, D. J. Selkoe, *PNAS* **2003**, *100*, 6382-6387.

[8] M. S. Wolfe, *Biochemistry* **2006**, *45*, 7931-7939.

[9] B. De Strooper, *Neuron* **2003**, *38*, 9-12.

[10] A. L. Brunkan, A. M. Goate, *J. Neurochem.* **2005**, *93*, 769-792.

[11] G. Yu, F. Chen, M. Nishimura, H. Steiner, A. Tandon, T. Kawarai, S. Arawaka, A. Supala, Y. Q. Song, E. Rogaeva, E. Holmes, D. M. Zhang, P. Milman, P. Fraser, C. Haass, P. St George-Hyslop, *Acta Neurol. Scand. Suppl.* **2000**, *176*, 6-11.

[12] W. T. Kimberly, W. Xia, T. Rahmati, M. S. Wolfe, D. J. Selkoe, *J. Biol. Chem.* **2000**, *275*, 3173-3178.

[13] W. G. Annaert, L. Levesque, K. Craessaerts, I. Dierinck, G. Snellings, D. Westaway, P. S. George-Hyslop, B. Cordell, P. Fraser, B. De Strooper, *J. Cell Biol.* **1999**, *147*, 277-294.

[14] G. Thinakaran, D. R. Borchelt, M. K. Lee, H. H. Slunt, L. Spitzer, G. Kim, T. Ratovitsky, F. Davenport, C. Nordstedt, M. Seeger, J. Hardy, A. I. Levey, S. E. Gandy, N. A. Jenkins, N. G. Copeland, D. L. Price, S. S. Sisodia, *Neuron* **1996**, *17*, 181-190.

[15] D. Selkoe, R. Kopan, *Annu. Rev. Neurosci.* **2003**, *26*, 565-597.

[16] T. Sato, T. S. Diehl, S. Narayanan, S. Funamoto, Y. Ihara, B. De Strooper, H. Steiner, C. Haass, M. S. Wolfe, *J. Biol. Chem.* **2007**, *282*, 33985-33993.

[17] G. Yu, M. Nishimura, S. Arawaka, D. Levitan, L. Zhang, A. Tandon, Y. Q. Song, E. Rogaeva, F. Chen, T. Kawarai, A. Supala, L. Levesque, H. Yu, D. S. Yang, E. Holmes, P. Milman, Y. Liang, D. M. Zhang, D. H. Xu, C. Sato, E. Rogaev, M. Smith, C. Janus, Y. Zhang, R. Aebersold, L. S. Farrer, S. Sorbi, A. Bruni, P. Fraser, P. St George-Hyslop, *Nature* **2000**, *407*, 48-54.

[18] W. P. Esler, C. Das, W. A. Campbell, W. T. Kimberly, A. Y. Kornilova, T. S. Diehl, W. Ye, B. L. Ostaszewski, W. Xia, D. J. Selkoe, M. S. Wolfe, *Nat. Cell Biol.* **2002**, *4*, E110-111; author reply E111-112.

[19] S. Zhou, H. Zhou, P. J. Walian, B. K. Jap, *Biochemistry* **2007**, *46*, 2553-2563.

[20] W. P. Esler, W. T. Kimberly, B. L. Ostaszewski, T. S. Diehl, C. L. Moore, J. Y. Tsai, T. Rahmati, W. Xia, D. J. Selkoe, M. S. Wolfe, *Nat. Cell Biol.* **2000**, *2*, 428-434.

[21] C. Goutte, M. Tsunozaki, V. A. Hale, J. R. Priess, *PNAS* **2002**, *99*, 775-779.

[22] H. Steiner, E. Winkler, D. Edbauer, S. Prokop, G. Basset, A. Yamasaki, M. Kostka, C. Haass, *J. Biol. Chem.* **2002**, *277*, 39062-39065.

[23] R. Francis, G. McGrath, J. Zhang, D. A. Ruddy, M. Sym, J. Apfeld, M. Nicoll, M. Maxwell, B. Hai, M. C. Ellis, A. L. Parks, W. Xu, J. Li, M. Gurney, R. L. Myers, C. S. Himes, R. Hiebsch, C. Ruble, J. S. Nye, D. Curtis, *Dev. Cell* **2002**, *3*, 85-97.

[24] W. J. Luo, H. Wang, H. Li, B. S. Kim, S. Shah, H. J. Lee, G. Thinakaran, T. W. Kim, G. Yu, H. Xu, *J Biol Chem* **2003**, *278*, 7850-7854.

[25] J. Eder, U. Hommel, F. Cumin, B. Martoglio, B. Gerhartz, *Curr. Pharm. Des.* **2007**, *13*, 271-285.

[26] V. K. Lazarov, P. C. Fraering, W. Ye, M. S. Wolfe, D. J. Selkoe, H. Li, *PNAS* **2006**, *103*, 6889-6894.
[27] M. S. Brown, J. Ye, R. B. Rawson, J. L. Goldstein, *Cell* **2000**, *100*, 391-398.
[28] T. Ogura, K. Mio, I. Hayashi, H. Miyashita, R. Fukuda, R. Kopan, T. Kodama, T. Hamakubo, T. Iwatsubo, T. Tomita, C. Sato, *Biochem. Biophys. Res. Commun.* **2006**, *343*, 525-534.
[29] S. Zhou, H. Zhou, P. J. Walian, B. K. Jap, *PNAS* **2005**, *102*, 7499-7504.
[30] S. F. Lichtenthaler, R. Wang, H. Grimm, S. N. Uljon, C. L. Masters, K. Beyreuther, *PNAS* **1999**, *96*, 3053-3058.
[31] C. Esh, L. Patton, W. Kalback, T. A. Kokjohn, J. Lopez, D. Brune, A. J. Newell, T. Beach, D. Schenk, D. Games, S. Paul, K. Bales, B. Ghetti, E. M. Castano, A. E. Roher, *Biochemistry* **2005**, *44*, 13807-13819.
[32] L. M. Munter, P. Voigt, A. Harmeier, D. Kaden, K. E. Gottschalk, C. Weise, R. Pipkorn, M. Schaefer, D. Langosch, G. Multhaup, *Embo J.* **2007**, *26*, 1702-1712.
[33] P. Kienlen-Campard, B. Tasiaux, J. Van Hees, M. Li, S. Huysseune, T. Sato, J. Z. Fei, S. Aimoto, P. J. Courtoy, S. O. Smith, S. N. Constantinescu, J. N. Octave, *J. Biol. Chem.* **2008**, *283*, 7733-7744.
[34] M. Vooijs, E. H. Schroeter, Y. Pan, M. Blandford, R. Kopan, *J. Biol. Chem.* **2004**, *279*, 50864-50873.
[35] R. Kopan, M. X. Ilagan, *Nat. Rev. Mol. Cell Biol.* **2004**, *5*, 499-504.
[36] D. M. Barten, V. L. Guss, J. A. Corsa, A. Loo, S. B. Hansel, M. Zheng, B. Munoz, K. Srinivasan, B. Wang, B. J. Robertson, C. T. Polson, J. Wang, S. B. Roberts, J. P. Hendrick, J. J. Anderson, J. K. Loy, R. Denton, T. A. Verdoorn, D. W. Smith, K. M. Felsenstein, *J. Pharmacol. Exp. Ther.* **2005**, *312*, 635-643.
[37] H.-K. Wong, T. Sakurai, F. Oyama, K. Kaneko, K. Wada, H. Miyazaki, M. Kurosawa, B. De Strooper, P. Saftig, N. Nukina, *J. Biol. Chem.* **2005**, *280*, 23009-23017.
[38] T. A. Comery, R. L. Martone, S. Aschmies, K. P. Atchison, G. Diamantidis, X. Gong, H. Zhou, A. F. Kreft, M. N. Pangalos, J. Sonnenberg-Reines, J. S. Jacobsen, K. L. Marquis, *J. Neurosci.* **2005**, *25*, 8898-8902.
[39] A. F. Kreft, R. Martone, A. Porte, *J. Med. Chem.* **2009**, *52*, 6169-6188.
[40] H. Li, M. S. Wolfe, D. J. Selkoe, *Structure* **2009**, *17*, 326-334.
[41] P. Osenkowski, H. Li, W. Ye, D. Li, L. Aeschbach, P. C. Fraering, M. S. Wolfe, D. J. Selkoe, *J. Mol. Biol.* **2009**, *385*, 642-652.
[42] D. Pissarnitski, *Curr. Opin. Drug Discov. Devel.* **2007**, *10*, 392-402.
[43] B. Schmidt, S. Baumann, H. A. Braun, G. Larbig, *Curr.Top. Med. Chem.* **2006**, *6*, 377-392.
[44] P. C. Fraering, M. J. LaVoie, W. Ye, B. L. Ostaszewski, W. T. Kimberly, D. J. Selkoe, M. S. Wolfe, *Biochemistry* **2004**, *43*, 323-333.
[45] A. Y. Kornilova, C. Das, M. S. Wolfe, *J. Biol. Chem.* **2003**, *278*, 16470-16473.
[46] B. Zhao, M. Yu, M. Neitzel, J. Marugg, J. Jagodzinski, M. Lee, K. Hu, D. Schenk, T. Yednock, G. Basi, *J. Biol. Chem.* **2008**, *283*, 2927-2938.
[47] A. Weihofen, M. K. Lemberg, E. Friedmann, H. Rueeger, A. Schmitz, P. Paganetti, G. Rovelli, B. Martoglio, *J. Biol. Chem.* **2003**, *278*, 16528-16533.
[48] M. S. Shearman, D. Beher, E. E. Clarke, H. D. Lewis, T. Harrison, P. Hunt, A. Nadin, A. L. Smith, G. Stevenson, J. L. Castro, *Biochemistry* **2000**, *39*, 8698-8704.
[49] J. L. Castro Pineiro, A. L. Smith, G. I. Stevenson, (Merck Sharp + Dohme Limited, UK). WO20010166564, **2001**.
[50] J. E. Audia, T. E. Mabry, J. S. Nissen, S. L. McDaniel, in *PCT Int. Appl.*, (Elan Pharmaceuticals, Inc., USA; Eli Lilly and Company). WO9932453, **1999**.
[51] H. F. Dovey, V. John, J. P. Anderson, L. Z. Chen, P. de Saint Andrieu, L. Y. Fang, S. B. Freedman, B. Folmer, E. Goldbach, E. J. Holsztynska, K. L. Hu, K. L.

Johnson-Wood, S. L. Kennedy, D. Kholodenko, J. E. Knops, L. H. Latimer, M. Lee, Z. Liao, I. M. Lieberburg, R. N. Motter, L. C. Mutter, J. Nietz, K. P. Quinn, K. L. Sacchi, P. A. Seubert, G. M. Shopp, E. D. Thorsett, J. S. Tung, J. Wu, S. Yang, C. T. Yin, D. B. Schenk, P. C. May, L. D. Altstiel, M. H. Bender, L. N. Boggs, T. C. Britton, J. C. Clemens, D. L. Czilli, D. K. Dieckman-McGinty, J. J. Droste, K. S. Fuson, B. D. Gitter, P. A. Hyslop, E. M. Johnstone, W. Y. Li, S. P. Little, T. E. Mabry, F. D. Miller, J. E. Audia, *J. Neurochem.* **2001**, *76*, 173-181.

[52] T. A. Lanz, C. S. Himes, G. Pallante, L. Adams, S. Yamazaki, B. Amore, K. M. Merchant, *J. Pharmacol. Exp. Ther.* **2003**, *305*, 864-871.

[53] A. Capell, H. Steiner, M. Willem, H. Kaiser, C. Meyer, J. Walter, S. Lammich, G. Multhaup, C. Haass, *J. Biol. Chem.* **2000**, *275*, 30849-30854.

[54] B. K. Hadland, N. R. Manley, D.-M. Su, G. D. Longmore, C. L. Moore, M. S. Wolfe, E. H. Schroeter, R. Kopan, *PNAS* **2001**, *98*, 7487-7491.

[55] A. Geling, H. Steiner, M. Willem, L. Bally-Cuif, C. Haass, *EMBO Rep.* **2002**, *3*, 688-694.

[56] T. A. Lanz, J. D. Hosley, W. J. Adams, K. M. Merchant, *J. Pharmacol. Exp. Ther.* **2004**, *309*, 49-55.

[57] G. T. Wong, D. Manfra, F. M. Poulet, Q. Zhang, H. Josien, T. Bara, L. Engstrom, M. Pinzon-Ortiz, J. S. Fine, H. J. Lee, L. Zhang, G. A. Higgins, E. M. Parker, *J. Biol. Chem.* **2004**, *279*, 12876-12882.

[58] F. Panza, V. Solfrizzi, V. Frisardi, C. Capurso, A. D'Introno, A. M. Colacicco, G. Vendemiale, A. Capurso, B. P. Imbimbo, *Drugs Aging* **2009**, *26*, 537-555.

[59] H. Fuwa, Y. Takahashi, Y. Konno, N. Watanabe, H. Miyashita, M. Sasaki, H. Natsugari, T. Kan, T. Fukuyama, T. Tomita, T. Iwatsubo, *ACS Chemical Biology* **2007**, *2*, 408-418.

[60] G. M. Rishton, D. M. Retz, P. A. Tempest, J. Novotny, S. Kahn, J. J. S. Treanor, J. D. Lile, M. Citron, *J. Med. Chem.* **2000**, *43*, 2297-2299.

[61] A. F. Kreft, D. C. Cole, K. R. Woller, J. R. Stock, G. Diamanitis, D. M. Kurbrak, K. M. Kutterer, W. J. Moore, D. S. Casebier, (Wyeth, John, and Brother Ltd., USA; Arqule, Inc.). WO2002057252, **2002**, p. 133 pp.

[62] A. W. Konradi, M. N. Mattson, C. M. Semko, X. M. Ye, (Elan Pharmaceuticals, Inc., USA). WO2007024651, **2007**, p. 102 pp.

[63] S. Bowers, A. W. Garofalo, R. K. Hom, A. W. Konradi, M. N. Mattson, M. L. Neitzel, C. M. Semko, A. P. Truong, J. Wu, Y.-Z. Xu, (Elan Pharmaceuticals, Inc., USA). WO2007022502, **2007**, p. 141 pp.

[64] M. Neitzel, (Elan Pharmaceuticals, Inc., USA). WO2006078753, **2006**, p. 111 pp.

[65] J. Netzer William, F. Dou, D. Cai, D. Veach, S. Jean, Y. Li, G. Bornmann William, B. Clarkson, H. Xu, P. Greengard, *PNAS* **2003**, *100*, 12444-12449.

[66] P. C. Fraering, W. Ye, M. J. LaVoie, B. L. Ostaszewski, D. J. Selkoe, M. S. Wolfe, *J. Biol. Chem.* **2005**, *280*, 41987-41996.

[67] S. Cheng, D. D. Comer, L. Mao, G. P. Balow, D. Pleynet, (Neurogenetics, Inc., USA). WO 2004110350, **2004**, p. 178 pp.

[68] A. Fisher, N. Bar-Ner, Y. Karton, (Israel Institute for Biological Research, Israel). WO2003092580, **2003**, p. 102 pp.

[69] A. Caccamo, S. Oddo, L. M. Billings, K. N. Green, H. Martinez-Coria, A. Fisher, F. M. LaFerla, *Neuron* **2006**, *49*, 671-682.

[70] www.torreypinestherapeutics.com.

[71] N. Shimomura, S. Yoshikawa, Y. Hisatake, A. Imai, (Eisai R & D Management Co., Ltd., Japan). WO2008140111, **2008**, p. 29pp.

[72] D. Beher, M. Bettati, G. D. Checksfield, I. Churcher, V. A. Doughty, P. J. Oakley, A. Quddus, M. R. Teall, J. D. Wrigley, (Merck Sharp & Dohme Limited, UK). WO 2005013985, **2005**, p. 74 pp.
[73] P. Blurton, F. Burkamp, I. Churcher, T. Harrison, J. Neduvelil, (Merck Sharp & Dohme Limited, UK). WO2006008558, **2006**, p. 58 pp.
[74] F. Wilson, A. Reid, V. Reader, R. J. Harrison, M. Sunose, R. Hernandez-Perni, J. Major, C. Boussard, K. Smelt, J. Taylor, A. Leformal, A. Cansfield, S. Burckhardt, (Cellzome A.-G., Germany). WO2006045554, **2006**, p. 57 pp.
[75] N. Ramsden, F. Wilson, (Cellzome A.-G., Germany). WO2006048219, **2006**, p. 35 pp.
[76] D. Pratico, J. Q. Trojanowski, *Neurobiol. Aging* **2000**, *21*, 441-445.
[77] P. L. McGeer, E. G. McGeer, *Arch. Neurol.* **2001**, *58*, 1790-1792.
[78] S. Weggen, J. L. Eriksen, P. Das, S. A. Sagi, R. Wang, C. U. Pietrzik, K. A. Findlay, T. E. Smith, M. P. Murphy, T. Bulter, D. E. Kang, N. Marquez-Sterling, T. E. Golde, E. H. Koo, *Nature* **2001**, *414*, 212-216.
[79] J. L. Eriksen, S. A. Sagi, T. E. Smith, S. Weggen, P. Das, D. C. McLendon, V. V. Ozols, K. W. Jessing, K. H. Zavitz, E. H. Koo, T. E. Golde, *J. Clin. Invest.* **2003**, *112*, 440-449.
[80] L. Gasparini, L. Rusconi, H. Xu, P. del Soldato, E. Ongini, *J. Neurochem.* **2004**, *88*, 337-348.
[81] Y. Takahashi, I. Hayashi, Y. Tominari, K. Rikimaru, Y. Morohashi, T. Kan, H. Natsugari, T. Fukuyama, T. Tomita, T. Iwatsubo, *J. Biol. Chem.* **2003**, *278*, 18664-18670.
[82] D. Beher, E. E. Clarke, J. D. J. Wrigley, A. C. L. Martin, A. Nadin, I. Churcher, M. S. Shearman, *J. Biol. Chem.* **2004**, *279*, 43419-43426.
[83] T. Morihara, T. Chu, O. Ubeda, W. Beech, G. M. Cole, *J. Neurochem.* **2002**, *83*, 1009-1012.
[84] S. Weggen, J. L. Eriksen, S. A. Sagi, C. U. Pietrzik, T. E. Golde, E. H. Koo, *J. Biol. Chem.* **2003**, *278*, 30748-30754.
[85] G. P. Lim, F. Yang, T. Chu, P. Chen, W. Beech, B. Teter, T. Tran, O. Ubeda, K. H. Ashe, S. A. Frautschy, G. M. Cole, *J. Neurosci.* **2000**, *20*, 5709-5714.
[86] B. P. Imbimbo, *J. Alzheimer's Dis.* **2009**, *17*, 757-760.
[87] T. L. Kukar, T. B. Ladd, M. A. Bann, P. C. Fraering, R. Narlawar, G. M. Maharvi, B. Healy, R. Chapman, A. T. Welzel, R. W. Price, B. Moore, V. Rangachari, B. Cusack, J. Eriksen, K. Jansen-West, C. Verbeeck, D. Yager, C. Eckman, W. Ye, S. Sagi, B. A. Cottrell, J. Torpey, T. L. Rosenberry, A. Fauq, M. S. Wolfe, B. Schmidt, D. M. Walsh, E. H. Koo, T. E. Golde, *Nature* **2008**, *453*, 925-929.
[88] R. Narlawar, B. I. Perez Revuelta, C. Haass, H. Steiner, B. Schmidt, K. Baumann, *J. Med. Chem.* **2006**, *49*, 7588-7591.
[89] R. Narlawar, B. I. Perez Revuelta, K. Baumann, R. Schubenel, C. Haass, H. Steiner, B. Schmidt, *Bioorg. Med. Chem. Lett.* **2007**, *17*, 176-182.
[90] S. Mochizuki, Y. Okada, *Cancer Sci.* **2007**, *98*, 621-628.
[91] T. G. Wolfsberg, P. Primakoff, D. G. Myles, J. M. White, *J. Cell Biol.* **1995**, *131*, 275-278.
[92] J. W. Fox, J. B. Bjarnason, *Methods Enzymol.* **1995**, *248*, 368-387.
[93] M. S. Rosendahl, S. C. Ko, D. L. Long, M. T. Brewer, B. Rosenzweig, E. Hedl, L. Anderson, S. M. Pyle, J. Moreland, M. A. Meyers, T. Kohno, D. Lyons, H. S. Lichenstein, *J. Biol. Chem.* **1997**, *272*, 24588-24593.
[94] F. X. Gomis-Ruth, L. F. Kress, W. Bode, *Embo J.* **1993**, *12*, 4151-4157.
[95] E. Lolis, G. A. Petsko, *Annu. Rev. Biochem.* **1990**, *59*, 597-630.

[96] R. A. Black, C. T. Rauch, C. J. Kozlosky, J. J. Peschon, J. L. Slack, M. F. Wolfson, B. J. Castner, K. L. Stocking, P. Reddy, S. Srinivasan, N. Nelson, N. Boiani, K. A. Schooley, M. Gerhart, R. Davis, J. N. Fitzner, R. S. Johnson, R. J. Paxton, C. J. March, D. P. Cerretti, *Nature* **1997**, *385*, 729-733.
[97] E. A. Clark, J. S. Brugge, *Science* **1995**, *268*, 233-239.
[98] R. O. Hynes, *Cell* **1992**, *69*, 11-25.
[99] J. Pruessmeyer, A. Ludwig, *Semin. Cell Dev. Biol.* **2009**, *20*, 164-174.
[100] J. Walter, C. Kaether, H. Steiner, C. Haass, *Curr. Opin. Neurobiol.* **2001**, *11*, 585-590.
[101] M. Sastre, J. Walter, S. M. Gentleman, *J. Neuroinflammation* **2008**, *5*, 25.
[102] F. Fahrenholz, S. Gilbert, E. Kojro, S. Lammich, R. Postina, *Ann. N.Y. Acad. Sci.* **2000**, *920*, 215-222.
[103] Y. Avramovich, T. Amit, M. B. Youdim, *J. Biol. Chem.* **2002**, *277*, 31466-31473.
[104] C. B. Xue, X. He, R. L. Corbett, J. Roderick, Z. R. Wasserman, R. Q. Liu, B. D. Jaffee, M. B. Covington, M. Qian, J. M. Trzaskos, R. C. Newton, R. L. Magolda, R. R. Wexler, C. P. Decicco, *J. Med. Chem.* **2001**, *44*, 3351-3354.
[105] S. L. Parsons, S. A. Watson, R. J. Steele, *Eur. J. Surg. Oncol.* **1997**, *23*, 526-531.
[106] A. Ludwig, C. Hundhausen, M. H. Lambert, N. Broadway, R. C. Andrews, D. M. Bickett, M. A. Leesnitzer, J. D. Becherer, *Comb. Chem. High Throughput Screen* **2005**, *8*, 161-171.
[107] J. S. Fridman, E. Caulder, M. Hansbury, X. Liu, G. Yang, Q. Wang, Y. Lo, B. B. Zhou, M. Pan, S. M. Thomas, J. R. Grandis, J. Zhuo, W. Yao, R. C. Newton, S. M. Friedman, P. A. Scherle, K. Vaddi, *Clin. Cancer Res.* **2007**, *13*, 1892-1902.

Lebenslauf:

Persönliches

Name	Nicole Höttecke
Adresse	Pankratiusstrasse 65
	64289 Darmstadt
Telefon	0049/61511544467
Mobil	0049/17620329457
E-Mail	nicole@hoettecke.net

Nationalität	Deutsch
Geburtstag	30.04.1982 in Lippstadt
Sprachen	Deutsch (Muttersprache), Englisch (sehr gut)

Promotion

10.2006-12.2009	Beginn der Promotion bei Prof. Dr. Schmidt, Technische Universität Darmstadt mit dem Thema „Entwicklung und Synthese von γ-Sekretase-Modulatoren zur Behandlung von Morbus Alzheimer“
04.2008 - 09.2008	Kooperation mit der RWTH Aachen bei PD Dr. Andreas Ludwig im Rahmen des DFG-Projektes LU869/4-1 „*Shedding* proinflammatorischer Mediatoren durch die Metalloproteinasen ADAM10 und ADAM17 bei der entzündlichen Leukozytenrekrutierung“
04.2008	Praktikum bei der Firma Hoffmann-LaRoche in Basel (Schweiz) im Rahmen einer Kooperation auf dem Gebiet der Alzheimer-Forschung (Pharma Research Basel Discovery- Neuroscience)

Studium

10.2001	Beginn des Studiums der Biochemie an der Ernst-Moritz-Arndt-Universität Greifswald
09.2004	Vordiplom: „Gut“ (1.9), organische Chemie: „Sehr gut“ (1.0), andere „Gut“
02.2005 – 03.2005	Betriebspraktikum in der Abteilung „Thrombose & Angiogenese“ der Firma Sanofi-Aventis in Frankfurt am Main
09.2005	Diplomprüfungen: Organische Chemie: „Sehr gut“ (1.3), Pharmazeutische Biologie: „Gut“ (2.3), Biochemie: „Gut“ (2.3)
10.2005	Diplomarbeit im Fachbereich Organische Chemie im Arbeitskreis von Prof. Langer an der Universität Rostock mit dem Thema: „Synthese antibiotisch aktiver 2-Vinyl-chroman-4-one“, Note:1.0
09.2006	Abschluss des Studiums der Diplom-Biochemie zum Ende des 10. Fachsemesters, Note: „Sehr Gut“ (1.5)

Schulbildung

1988	Einschulung in der Paul-Gerhard-Schule Rüthen
1989 – 1992	Nikolaus Grundschule Rüthen
1992 – 2001	Friedrich-Spee-Gymnasium Rüthen
1996	Teilnahme an einem Englandaustausch nach Dereham
1999 – 2001	Aktive Teilnahme in einer Theatergruppe des Gymnasiums, sowohl auf der Bühne als auch in der Organisation
06.2001	Erhalt der allgemeinen Hochschulreife (Abitur) Note: 2.5

Kenntnisse / Fähigkeiten

Grundlagen der medizinalchemischen Forschung: Optimierung einer Leitstruktur, Auswertung von Struktur-Aktivitäts-Untersuchungen, biochemische Untersuchungsmethoden (Western Blot, ELISA)

Sehr gute theoretische und praktische Kenntnisse der organischen Synthesechemie (insbesondere Heterocyclenchemie, asymmetrische Synthese und Medizinalchemie) und gängiger analytischer Methoden (NMR, IR, MS, HPLC, LC, LCMS, DC).

Erfahrungen in der Handhabung von Schlenck-Techniken und metallorganischer Verbindungen.

Führungserfahrung durch Betreuung von Praktikanten sowie Bachelor-, Diplom- und Examensarbeiten.

Sehr gute Kenntnisse von MS/Mac-Office-Anwendungen (Word, Excel, PowerPoint), chemischen Datenbanken (SciFinder, Beilstein Online) sowie ChemDraw und IsisDraw.

Referenzen

Promotion	Prof. Boris Schmidt, TU Darmstadt, Petersenstr. 22, 64287 Darmstadt Tel: 06151-163075
Diplom	Prof. Peter Langer, Universität Rostock, Albert-Einstein-Str. 3a, 18059 Rostock Tel: 0381-4986410

Publikationsliste:

Nicole Hoettecke, Sven Rotzoll, Uwe Albrecht, Michael Lalk, Christine Fischer, Peter Langer *Bioorganic & Medicinal Chemistry* **2008**, *16*, 10319–10325.
"Synthesis and antimicrobial activity of 2-alkenylchroman-4-ones, 2-alkenylthiochroman-4-ones and 2-alkenylquinol-4-ones."

Nicole Höttecke, Christine Fischer, Helmut Reinke, Peter Langer, *Zeitschrift für Naturforschung B*, **2009**, *64b*, 699-706.
„Synthesis of Bicyclic Salicylates by [3+3] cyclization of 1,3-Bis(Silyl Enol Ethers) with Cyclic 3-(Silyloxy)alk-2-en-1-ones."

Stefanie Baumann, Nicole Höttecke, Robert Schubenel, Karlheinz Baumann, Boris Schmidt *Bioorg. Med. Chem. Lett.* **2009**, *19*, 6986-6990.
"NSAID-derived γ-secretase modulators. Part III: Membrane anchoring."

Jessica Pruessmeyer, Christian Martin, Franz M. Hess, Nicole Schwarz, Sven Schmidt, Tanja Kogel, Nicole Hoettecke, Boris Schmidt, Antonio Sechi, Stefan Uhlig, Andreas Ludwig *J. Biol. Chem.* accepted 29.10.2009. (http://www.jbc.org/cgi/doi/10.1074/jbc.M109.059394)
"The disintegrin and metalloproteinase 17 (ADAM17) mediates inflammation-induced shedding of syndecan-1 and -4 by lung epithelial cells."

Nicole Höttecke, Andreas Ludwig, Sabine Foro, Boris Schmidt *Neurodegener. Dis.*, Zur Publikation angenommen: 09.12.09. "Improved synthesis of the ADAM10 inhibitor GI254023X."

Nicole Höttecke, Miriam Liebeck, Karlheinz Baumann, Robert Schubenel, Edith Winkler, Harald Steiner, Boris Schmidt *ChemMedChem*, eingereicht: 02.12.09. "Inhibition of γ-secretase by the CK1 inhibitor IC261 does not depend on CK1."

Nicole Höttecke, Matthias Gralle, Maria Angela C. Dani, Karlheinz Baumann, Fred Wouters, Christian Czech, Boris Schmidt *Nature Chem. Biol.*, eingereicht. "The Modulation of Aβ production involves dimerization of APP."

Buchkapitel:

Stefanie Baumann, Nicole Höttecke, Boris Schmidt, "γ-Secretase as a target for AD", *in* Medicinal Chemistry of Alzheimer Disease, ed. A. Martinez, Research Signpost, **2008**.

Nicole Höttecke, Stefanie Baumann, Ali Taghavi, Hannes A. Braun and Boris Schmidt, "Drug Development and Diagnostics for Alzheimer's Disease Up to 2008", *in* Frontiers in Medicinal Chemistry Vol. 4, Ed.: Atta-ur-Rahman, A.B. Reitz, pp. 730-766, Bentham Books **2009**.

Übersichtsartikel:

Nicole Höttecke, Stefanie Baumann *Bioforum* **2008**, *6*, 32-34.
"Alzheimer-Demenz: Ein Pla(qu)e mit Hoffnung auf Besserung?"

Poster:

Stefanie Baumann, Nicole Höttecke, Daniel Kieser, Boris Schmidt, "TIC Taβ Tau – Asystematic approach to protein aggregation with small molecules."
Gesellschaft Deutscher Chemiker Wissenschaftsforum, 16.-19. September 2007, Ulm.

Stefanie Baumann, Nicole Hoettecke, Rajeshwar Narlawar, Thomas Kukar, Todd E. Golde, Karlheinz Baumann, "Mapping the binding site of γ-secretase modulators by small (and not so small) organic molecules"
Alzheimer´s Association, 26.-31. Juli 2008, Chicago, USA.

Boris Schmidt, Andrea Zall, Daniel Kieser, Nicole Hoettecke, Karlheinz Baumann, „Replacement of a carboxylic acid by isosteres on a carbazolic scaffold provides γ-secretase modulators"
Gesellschaft Deutscher Chemiker Wissenschaftsforum, 31. August-02. September 2009, Frankfurt am Main.

Boris Schmidt, Andrea Zall, Daniel Kieser, Nicole Hoettecke, Karlheinz Baumann, „Carboxylic acid isosteres linked on a carbazolic scaffold as γ-secretase modulators"
ChemBioNet, 30. Novermber-01. Dezember 2009, Frankfurt am Main.

Nicole Höttecke
Pankratiusstr. 65
64289 Darmstadt

16.12.2009

Eidesstattliche Erklärung

Ich erkläre hiermit an Eides Statt, dass ich meine Dissertation selbständig und nur mit den angegebenen Hilfsmitteln angefertigt habe.

Nicole Höttecke

Nicole Höttecke
Pankratiusstr. 65
64289 Darmstadt

16.12.2009

Erklärung

Ich erkläre hiermit, noch keinen Promotionsversuch unternommen zu haben.

Nicole Höttecke